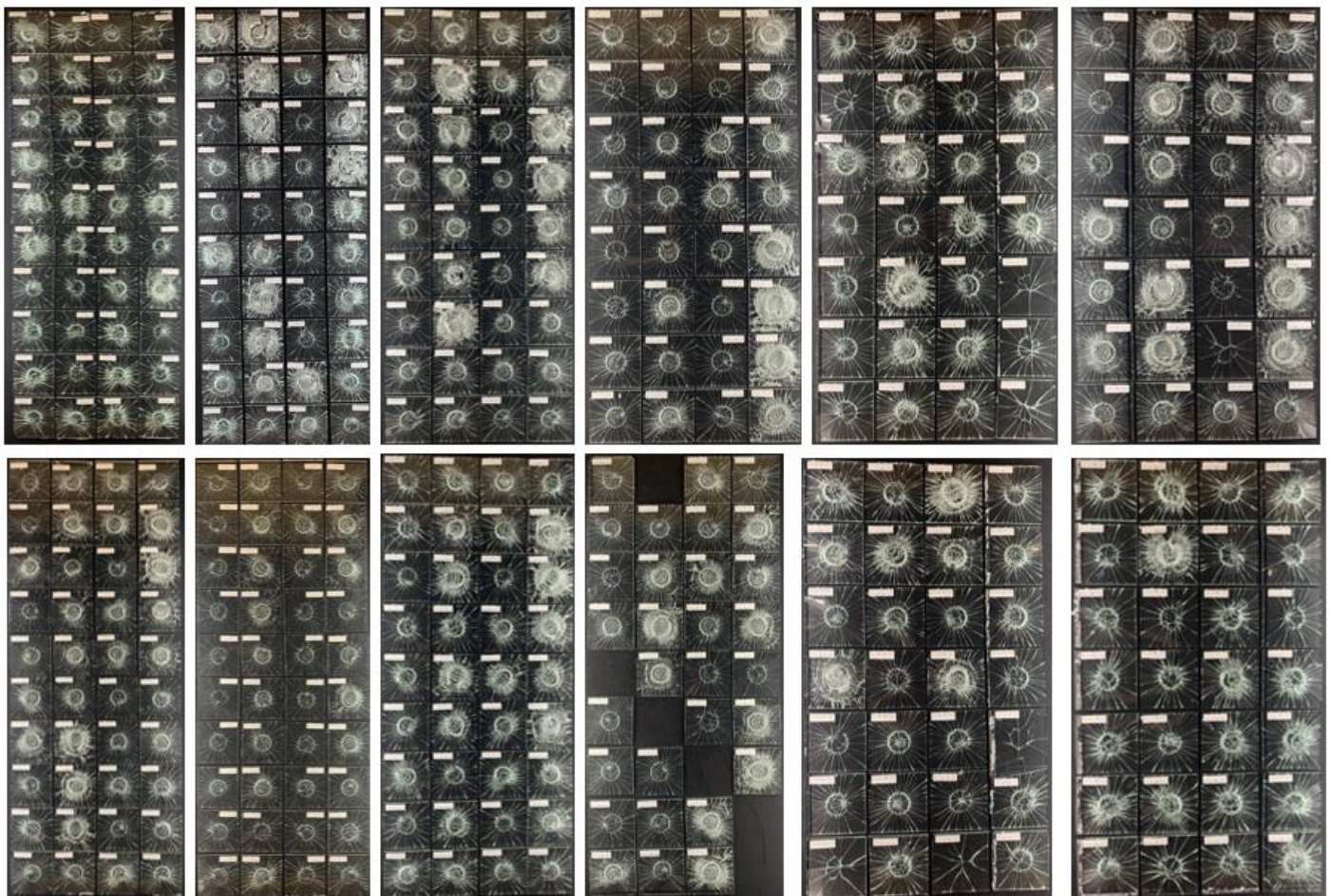


STRENGTH OF NATURALLY AGED INSULATED GLASS UNITS DETERMINED BY EXPERIMENTAL TESTING

GLASS REUSE



NIELS STUURSTRAAT

GLASS REUSE

STRENGTH OF NATURALLY AGED INSULATED GLASS UNITS DETERMINED BY EXPERIMENTAL TESTING

By

Niels Stuurstraat

in partial fulfilment of the requirements for the degree of

Master of Science
in Civil Engineering

at the Delft University of Technology

Supervisor:	Prof. dr. ir. P.C. Louter	TU Delft
Thesis committee:	Ir. C. Noteboom	TU Delft
	Prof. dr. M. Overend	TU Delft
Lab assistants:	Ir. P.A. De Vries	TU Delft
	J. Hermsen	TU Delft
	F.J.P. Schilperoort	TU Delft

Acknowledgements

This thesis was written as part of the Civil Engineering master's programme at Delft University of Technology.

I would like to express my gratitude to all of those who have helped me in completing this master thesis.

Firstly, I would like to thank my main supervisor, Prof.dr.ir. Christian Louter for his pleasant guidance and help during all stages of the project. The other members of the committee, ir. Chris Noteboom, who provided feedback on interim reports, and Prof. Mauro Overend, with their knowledge and insights, were also very helpful in the way this thesis came about.

Next, my appreciation for the help of the lab staff who helped me with the practical work during the research: ir. Peter de Vries, John Hermsen, and Fred Schilperoort. Knowing the safety rules in the lab and their help in preparing the experiment and explaining the necessary measuring devices were necessary to carry out the research properly. Small problems were solved quickly, and the cooperation was experienced as pleasant.

I would like to thank GSF Glasgroep for making the weathered glass available to TU Delft so that this research could be carried out. The cooperation with the Hogeschool van Amsterdam, where research is being conducted on insulation values of naturally aged glass, was found to be pleasant and very instructive, due to a number of consortium meetings where I was allowed to present the progress of my research on the strength of weathered glass. Insights from the glass industry were very informative and useful.

N. Stuurstraat
Delft, December 2023

Abstract

The reuse of insulating glass plays a crucial role in promoting sustainability and circularity within the construction sector. CO₂ emissions must be reduced according to the Climate Agreement. Reusing materials can help achieve this goal. Reusing glass without reheating it can provide environmental and cost benefits, making it a suitable option.

In this study, 36-year-old insulating glass panels (double-glazing) from an apartment building in Amstelveen have been tested for strength through destructive testing. This is done to see what the strength of the glass is after the glass has been in the building for 36 years and has been exposed to opportunities for damage. Various patterns of damage on both the interior and exterior side of the glass panels from an insulated glass unit affects the strength that can eventually be assigned to the glass. The aim of this thesis is to be able to show whether and how insulated glass units can be reused and what the strength is of naturally aged glass after a certain lifetime.

From six insulated glass units obtained, specimens measuring 150mm x 150mm are extracted and tested for strength using a Coaxial Double Ring test. Prior to the destructive tests, a number of specimens were viewed under the Keyence VHX 7000 digital microscope to see how the damages are and whether they vary between the four sides of an insulated glass unit. This revealed that the outer side of the outer panel (side #1) contains the most and homogeneous damage. Weathering, especially rain and wind, which can bring sand particles, for example, create homogeneous damage on the glass surface. The entire surface is exposed to this type of weathering. The outer side of the inner panel (side #4) also contained quite a lot of damage from probably cleaning and (human) touching. Despite the fact that the inner sides of both panels (the sides in the cavity, side #2 and #3) theoretically had little potential for weathering, damage could also be seen on these, although it was more localised, meaning it probably occurred during the production process or preparation of the specimens for this experiment.

During the Coaxial Double Ring tests, 406 specimens were tested for strength. The strengths of the specimens ranged from 16.8 MPa to 243.7 MPa, with an average strength of 67.5 MPa. The average strengths of side #2 and #3 (sides in the cavity) are slightly higher than those of side #1 and #4 (outer sides), between 9% and 17%. A tin-tester was used to determine which side of each specimen was the tin-side prior to the strength tests, to include this in the analysis of the results. The specimens tested on the tin-side were found to be on average much weaker than the specimens tested on air-sides. The average measured strength of the air-side is 31% higher than that of the tin-side. In a number of tests carried out with new glass, this large difference is already present, while literature states that the difference in strength between the air- and tin-sides can be considered marginal.

Fracture statistics were used to analyse the data and find a strength for each series tested. This was done using Weibull theory. The two-parameter Weibull distribution has proven to be very conservative at low failure probabilities, resulting in a very low design strength (failure probabilities of 0.8% and 0.12%) for a series of specimens when there is a large spread in data. The spread in data was often of greater influence than the values of the measured strengths. As a result, the design strengths for series tested on the air-side were usually lower than specimens tested on the tin-side, while the average strength measurements were actually higher. The greater variation in strengths of specimens coming

from the inner side #2 and #3 results in lower design strengths than the outer sides (#1 and #4), which contain more (homogeneous) damage. The values of design strengths of the naturally aged glass tested were almost always lower than the design strength of new glass according to current standards. The design strengths of new glass are 22.5 MPa according to NEN2608 and 25.0 MPa according to EN16612. When looking at how many specimens failed at stresses lower than these values, there are only three and six respectively. So, there are very few spots in 36-year-old glass that are weaker than the design strength that can be assumed according to NEN2608 or EN16612. These lowest values are not consistently found in specimens tested on either the air-side or the tin-side, so based on this study, the influence of this can be ruled out. By this means, a more realistic and less conservative option seems to be to take the strength of the weakest specimen in a test series and then assign it to the entire panel from which that test series comes.

Reuse options are discussed in the final section of this thesis. Using a number of common glass structures, it explains the ways in which weathered glass can or cannot be reused and in what function. How the results obtained can be handled and used is a point of discussion, as the values are not always representative of the strength of the entire glass panel. Further research will have to show whether the current design standards and the parameters used in them are well chosen or whether they should be different for used glass. For example, use a lower material factor of 1.35 instead of 1.6 – 1.8 when calculating the design strength or use a higher failure probability than 0.0012 to determine design strength in a Weibull distribution. The efficiency and effectiveness of the method used can also be optimised in further research.

Contents

Acknowledgements.....	iii
Abstract.....	v
Contents.....	vii
List of tables.....	xi
List of figures.....	xiii
Nomenclature.....	xvii
1. Introduction.....	1
1.1 Motivation.....	1
1.2 Problem statement.....	2
2. Theoretical Background.....	3
2.1 Introduction.....	3
2.2 History of glass.....	3
2.2.1 General.....	3
2.2.2 IGU.....	4
2.3 Production process of glass.....	5
2.4 Insulated Glass Unit.....	7
2.5 Strength of glass.....	10
2.5.1 Characteristic strength.....	10
2.5.2 Actual strength.....	11
2.6 Statistics of glass.....	13
2.7 Recycling of glass.....	14
2.8 Reuse of glass.....	16
3. Weathering and glass deterioration.....	19
3.1 Introduction.....	19
3.2 Temperature.....	20
3.3 Acidity (pH).....	21
3.4 Air pollution.....	21
3.5 Humidity.....	22
3.6 UV radiation.....	23
3.7 Human damaging.....	23
3.8 Other causes.....	25
4. Experimental investigation.....	27
4.1 Introduction.....	27
4.2 Test specimens.....	27
4.3 Setup.....	29

4.4 Dimensions	31
4.5 Specimen preparation.....	32
4.6 Microscopy examination.....	37
4.6.1 Side #1	39
4.6.2 Side #2	40
4.6.3 Side #3	41
4.6.4 Side #4	42
4.6.5 Strongest vs weakest	43
4.7 Tin- and air-side	45
4.8 Prestress measuring.....	46
4.9 CDR tests	48
4.9.1 Machine.....	49
4.9.2 Procedure	50
4.9.3 Results.....	53
4.10 Discussion.....	55
5. Failure Analysis	57
5.1 Introduction.....	57
5.2 Fractographic analysis	57
5.3 Statistical processing of the results	61
5.4 Sides comparison	64
5.5 Effect of tin- and air-side	66
5.5.1 All data.....	66
5.5.2 Sides comparison	70
5.5.3 Low values influence	75
5.6 Effect of location.....	78
5.6.1 IGU orientation	78
5.6.2 Specimen location.....	80
5.7 New glass comparison	84
5.8 Goodness of fit.....	87
5.9 Discussion.....	88
6. Reuse opportunities.....	91
6.1 Introduction.....	91
6.2 Design strength of reused glass.....	91
6.3 Reuse.....	98
6.3.1 Entire IGU.....	99
6.3.2 Hybrid	99
6.3.3 Single glazing.....	100

6.3.4 Smaller panels	101
6.3.5 Lamination	103
7. Discussion	107
8. Conclusion	111
9. Recommendations for further research	115
References	119
Appendix A	125
SCALP measurements	125
Appendix B	127
Dimensions measurements.....	127
Appendix C	141
Microscopy examination photos	141
Appendix D	149
Overview CDR test results.....	149
Appendix E	151
Python script	151
Appendix F.....	153
Additional Weibull plots.....	153
Appendix G.....	165
All CDR test results	165
Appendix H.....	175
Characteristic and design strengths (load duration of 5 seconds).....	175
Appendix I	179
Normal distribution values.....	179

List of tables

Table 1. Lower limit bending strength per glass type (Veer, 2007).	11
Table 2. Characteristic bending strength per glass type (prCEN/TC250-1, 2018).	11
Table 3. Factors for determining the strength.	12
Table 4. Embodied energy and carbon building materials (Hoogerwaard, n.d.).	15
Table 5. CO ₂ emission and saving potential (Nußholz et al., 2020).	16
Table 6. Overview of the IGUs received.	29
Table 7. Verification of dimensions of specimens and rings according to ASTM C1499-09.	32
Table 8. Overview of the specimens number and dimensions of each testing series.	36
Table 9. List of microscopically examined specimens.	38
Table 10. Overview of tin- and air-sides of the IGUs.	46
Table 11. Prestress for each panel.	48
Table 12. Summary of the CDR test results (load duration of 60 sec).	54
Table 13. Average failure stresses of specimens per IGU (load duration of 60 sec).	54
Table 14. Fracture origin locations for the different series.	58
Table 15. Fracture origin location for air- and tin-side.	58
Table 16. Weibull parameters and characteristic values for each series.	63
Table 17. Design strength for Dutch and European design standard.	92
Table 18. Load distribution example of lamination glass with three layers with different thicknesses.	104
Table 19. Prestress measurements.	125
Table 20. Dimensions specimens from panel 1-out.	128
Table 21. Dimensions specimens from panel 1-in.	129
Table 22. Dimensions specimens from panel 2-out.	130
Table 23. Dimensions specimens from panel 2-in.	131
Table 24. Dimensions specimens from panel 3-out.	132
Table 25. Dimensions specimens from panel 3-in.	133
Table 26. Dimensions specimens from panel 4-out.	134
Table 27. Dimensions specimens from panel 4-in.	135
Table 28. Dimensions specimens from panel 5-out.	136
Table 29. Dimensions specimens from panel 5-in.	137
Table 30. Dimensions specimens from panel 6-out.	138
Table 31. Dimensions specimens from panel 6-in.	139
Table 32. Characteristic values IGU 1.	149
Table 33. Characteristic values IGU 2.	149
Table 34. Characteristic values IGU 3.	149
Table 35. Characteristic values IGU 4.	150
Table 36. Characteristic values IGU 5.	150
Table 37. Characteristic values IGU 6.	150
Table 38. All test results.	166
Table 39. 2PW and Normal distribution – Side #1.	179
Table 40. 2PW and Normal distribution – Side #2.	179
Table 41. 2PW and Normal distribution – Side #3.	180
Table 42. 2PW and Normal distribution – Side #4.	180

List of figures

Figure 1. Circular process of the use of glass.	1
Figure 2. Obsidian (Geology Page, 2019).	3
Figure 3. Glassblowers (Taylor & Hill, 2011).	3
Figure 4. Drawn glass (Tresinie, 2023).	4
Figure 5. Float glass production process (Float Glass Process, n.d.).....	6
Figure 6. Tin bath (D&O, 2021).	6
Figure 7. Breakage pattern of different glass types (Peerless Products Inc., 2020).	7
Figure 8. IGU (Glazcon, 2018).	8
Figure 9. U-factor for different gases.	9
Figure 10. Weibull probability plot example (Datsiou & Overend, 2018).	14
Figure 11. Glass reuse cycle (Nußholz et al., 2020).	17
Figure 12. Neat lattice structure (Canrinus-Moezelaar, 2017).	19
Figure 13. SiO ₄ -tetrahedron (Muller, 2015).	19
Figure 14. Damage example thermal breakage (Glasschades, 2006).	20
Figure 15. pH-silica dissolution correlation diagram (Papadopoulos & Drosou, 2012).	21
Figure 16. Electron micrographs of soda-lime glass before and after weathering at a relative humidity of 98% and temperature of 50 °C (53000x).	22
Figure 17. Damage caused by penetrating moisture (Glasschades, 2006).	23
Figure 18. Damage caused by cleaning (Glasschades, 2006).	24
Figure 19. Damage caused by transportation (Glasschades, 2006).	25
Figure 20. Damage caused by grinder tips (Glasschades, 2006).	25
Figure 21. The apartment building.....	28
Figure 22. Spacer info.....	28
Figure 23. Section and perspective view of basic fixturing and the test specimen for equibiaxial testing.	30
Figure 24. 4-point system.	30
Figure 25. Moment distribution of 4-point system.	30
Figure 26. Separating the panels.	33
Figure 27. From one IGU to two separate panes.	34
Figure 28. Cutting process.	34
Figure 29. Specimen preparation.	35
Figure 30. Manually applying foil to specimens.	36
Figure 31. Keyence VHX7000 digital microscope.	37
Figure 32. Microscopy examination side #1.....	39
Figure 33. Microscopy examination side #2.....	40
Figure 34. Microscopy examination side #3.....	41
Figure 35. Microscopy examination side #4.....	42
Figure 36. Microscopy examination strongest specimen 4-in #3 5.3 (x20).....	43
Figure 37. Microscopy examination weakest specimen 6-out #2 4.2 (x20).....	43
Figure 38. Big damage on 6-out #2 4.2 (x1000).....	44
Figure 39. Tin-side detector.....	45
Figure 40. Tin- and air-side determination (Garibaldi Glass, 2021).....	45
Figure 41. Stress gradient glass.	46

Figure 42. Setup prestress measuring with SCALP-05.	47
Figure 43. Used software and machine for the CDR tests.	49
Figure 44. Testing procedure.	52
Figure 45. Fracture origin location.	59
Figure 46. Extreme values fracture origins.	60
Figure 47. Examples of unclear location of fracture origin.	60
Figure 48. Excel file to receive scale and shape parameter.	62
Figure 49. Weibull probability distribution: All sides.	65
Figure 50. Weibull probability distribution: Air-side vs tin-side.	67
Figure 51. Weibull probability distribution: All sides – only tin-side.	68
Figure 52. Weibull probability distribution: All sides – only air-side.	69
Figure 53. Weibull probability distribution: Air-side vs tin-side - #1.	71
Figure 54. Weibull probability distribution: Air-side vs tin-side - #2.	72
Figure 55. Weibull probability distribution: Air-side vs tin-side - #3.	73
Figure 56. Weibull probability distribution: Air-side vs tin-side - #4.	74
Figure 57. Weibull probability distribution: All values - without 5% lowest.	76
Figure 58. Weibull probability distribution: All values - without 10% lowest.	77
Figure 59. Weibull probability distribution: West- vs east-orientated.	79
Figure 60. Edge- and mid-specimens.	80
Figure 61. Weibull probability distribution: Edge- vs mid-specimens.	81
Figure 62. Weibull probability distribution: All sides - only mid-specimens.	82
Figure 63. Weibull probability distribution: All sides - only edge-specimens.	83
Figure 64. Weibull probability distribution: Old vs new glass - data Irene.	85
Figure 65. Weibull probability distribution: Old vs new glass - data Thijs.	86
Figure 66. Goodness of fit of the test data to the three probability distributions	88
Figure 67. Characteristic strength of all series for $P_f=0.05$ and load duration of 5 seconds.	93
Figure 68. Design strength of all series for $P_f=0.0012$ and load duration of 5 seconds.	93
Figure 69. Design strength of all series obtained from characteristic strength with $\gamma_{m,A} = 1.15$ and load duration of 5 seconds.	94
Figure 70. Weibull probability distribution: Air-side vs tin-side (5 sec).	95
Figure 71. Weibull probability distribution: All sides (5 sec)	96
Figure 72. Weibull probability distribution: All data (5 sec).	97
Figure 73. Reuse options.	98
Figure 74. Average strengths of the specimens coming from the panels.	102
Figure 75. Smaller panel options.	103
Figure 76. Stress distribution laminated glass (Kuntsche et al., 2019).	105
Figure 77. Laminated glass options.	105
Figure 78. Bimodal Weibull distribution (Ballarini et al., 2016).	108
Figure 79. Bilinear Weibull distribution (Ballarini et al., 2016).	108
Figure 80. Weibull probability distribution: Old vs New (Thijs) glass (5 sec) – Bimodal flow.	109
Figure 81. Lowest measured strength of each series, load duration of 60 seconds.	109
Figure 82. Microscopic photos side #1, magnification 20x.	141
Figure 83. Microscopic photos side #1, magnification 50x.	142
Figure 84. Microscopic photos side #2, magnification 20x.	143
Figure 85. Microscopic photos side #2, magnification 50x.	144
Figure 86. Microscopic photos side #3, magnification 20x.	145
Figure 87. Microscopic photos side #3, magnification 50x.	146
Figure 88. Microscopic photos side #4, magnification 20x.	147
Figure 89. Microscopic photos side #4, magnification 50x.	148
Figure 90. Python script to extract information from Excel data.	151

Figure 91. Weibull probability distribution: All sides IGU 1.....	153
Figure 92. Weibull probability distribution: All sides IGU 2.....	154
Figure 93. Weibull probability distribution: All sides IGU 3.....	155
Figure 94. Weibull probability distribution: All sides IGU 4.....	156
Figure 95. Weibull probability distribution: All sides IGU 5.....	157
Figure 96. Weibull probability distribution: All sides IGU 6.....	158
Figure 97. Weibull probability distribution: Edge- vs mid-specimens air-side.....	159
Figure 98. Weibull probability distribution: Edge- vs mid-specimens tin-side.....	160
Figure 99. Weibull probability distribution: Old vs New (Irene) glass (5 sec) – Bimodal flow.	161
Figure 100. Weibull probability distribution: Old vs New (Irene) glass (5 sec) – 2PW.	162
Figure 101. Weibull probability distribution: Old vs New (Thijs) glass (5 sec) – 2PW.	163
Figure 102. Characteristic strength of all series for $P_f=0.05$ and load duration of 5 seconds.....	175
Figure 103. Design strength of all series obtained from the characteristic strength with $\gamma_{m,A} = 1.15$ and load duration of 5 seconds.	175
Figure 104. Characteristic strength of all sides for $P_f=0.05$ and load duration of 5 seconds.....	176
Figure 105. Design strength of all sides for $P_f=0.0012$ and load duration of 5 seconds.	176
Figure 106. Characteristic strength new and old glass for $P_f=0.05$ and load duration of 5 seconds.	177
Figure 107. Design strength new and old glass for $P_f=0.0012$ and load duration of 5 seconds.	177

Nomenclature

Abbreviations

Abbreviation	Definition
2PW	Two-parameter Weibull
AD	Anderson Darling goodness of fit test
AR	As Received glass
BLW	Bilinear Weibull
BMW	Bimodal Weibull
CDF	Cumulative Distribution Function
CDR	Coaxial Double Ring test
GHG	Greenhouse Gasses
IGU	Insulated Glass Unit
IR	Inside Loading Ring
LR	At Loading Ring
MLE	Maximum Likelihood Estimation
NA	Naturally Aged glass
ND	Not Detectable
OR	Outside Loading Ring
SCG	Subcritical Crack Growth
WLR	Weighted Least Squares Regression

Symbols

Symbol	Definition
A	Surface area
D	Test specimen diameter for circular test specimens
D_L	Loading ring diameter
D_S	Supporting ring diameter
F	Breaking load
$f_{b;k}$	Design strength
$f_{g;k}$	Characteristic strength
$f_{m;t;u;d}$	Tensile strength
h	Test specimen thickness
k	Weibull modulus
k_A	Size effect factor
k_e	Edge quality factor
k_{mod}	Load duration modification factor
k_{sp}	Surface treatment factor
k_z	Glass zone factor
l	Length of specimen's edges
n	Stress corrosion constant
<i>n</i>	Number of specimens
p_{AD}	Anderson Darling goodness of fit value
P_f	Probability of failure
t_f	Failure time
t_{ref}	Reference time for equivalent failure stress
β	Shape factor of the Weibull distribution
$\gamma_{m;A}$	Glass material factor
$\gamma_{m;V}$	Glass prestress factor
δ	Displacement
E	Young's modulus
θ	Scale parameter of the Weibull distribution
λ	Fracture stress of a specimen at a probability of 63.2%.
ν	Poisson's ratio
σ	Stress rate
σ_f	Failure stress
$\sigma_{f,eq}$	Equivalent failure stress

1. Introduction

1.1 Motivation

Since 1952, float glass as it is known today has been used in the building industry. Increasingly, an entire facade of a building is made of glass because it looks modern and transparent. In fact, in buildings today, an average of 48% of the facade is made of glass. There are already some buildings with 100% glass facades. So, in this industry, glass usage is of a high order. The downside of the large number of construction projects at this time, is the fact that of today's total greenhouse gases, between 30% and 40% come from the construction industry. Furthermore, 35% of total European waste comes from the construction industry. These high numbers make it a challenge for contemporary engineers to find sustainable solutions to relieve the earth of waste and greenhouse gases from this industry.

Glass is still the most commonly used material in facades today. Increasingly, glass is also used as structural elements, but this is still only a small part of total glass use in buildings. Because many buildings are being renovated and built these days, the demand for new glass is very high. Old glass panels no longer meet certain requirements and are being replaced by new panels. The old panels increase the in growing glass waste. Waste glass is much recycled or remelted into new glass panels. Remelting costs a lot of energy because of the high temperature at which it has to be done, which in turn leads to high CO₂ emissions. Recycling glass saves the raw materials used in producing new glass, but in terms of emissions, there is thus little difference. So, the challenge is to also reduce the process of recycling when it comes to glass, and to investigate the extent to which used glass is suitable to be reused for new purposes, without reheating in other words. The glass that is reused still have to meet the current requirements, to provide a safe and sustainable solution. The linear model is shown in Figure 1 below has thus already been made circular by recycling. This apparent circularity, because a lot of emissions still occur, should be replaced in the future as much as possible by the step of reusing ('Reuse'), after which the 'Disposal' step is immediately followed by use in a new function. This really keeps away from waste and emission leakage.

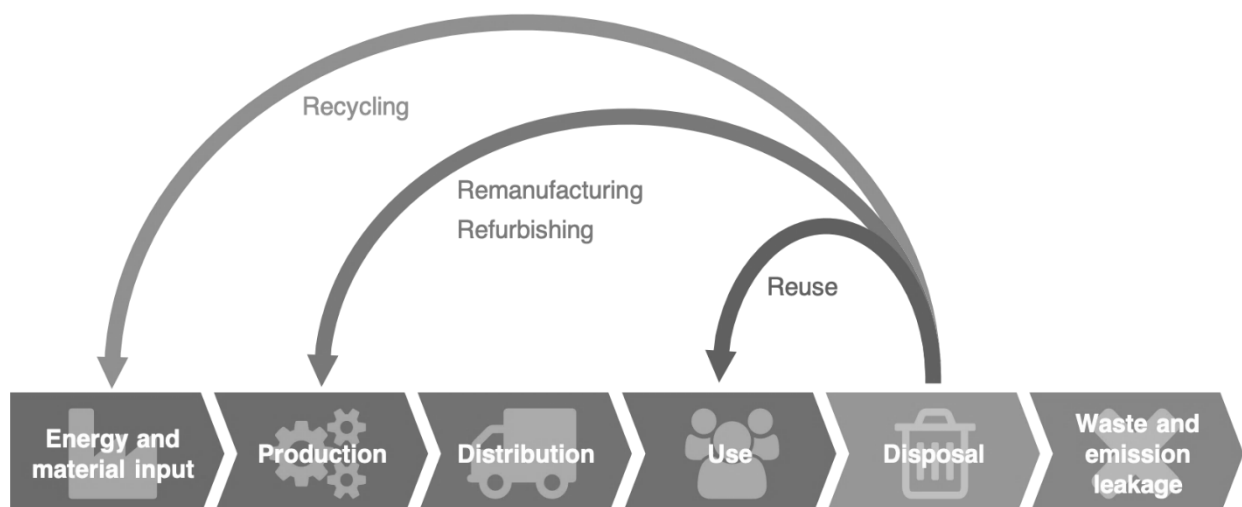


Figure 1. Circular process of the use of glass.

1.2 Problem statement

The definition of the problem is that due to high energy costs and the emission of a lot of CO₂, the current approach to producing glass could be a lot more sustainable. To address this, reusing glass becomes an interesting solution. The problem is that it is difficult to estimate how the properties of glass change with ageing and weathering. Therefore, the aim of this research is to be able to estimate this. Experimental tests of several small samples of naturally aged insulated glass units will be used to see to what extent the properties of the glass deteriorate during its lifetime. A study is also being carried out on the causes on which defects occur in/on the glass during its lifetime. The interesting thing about double glazing is to investigate the surface strengths and external appearances of different sides of the glass panel.

For this study, naturally aged glass is tested for strength. Weathering or naturally aged glass refers to glass that has been in use for a certain number of years. A strength of these double-glazed panes is attached by means of tests and fracture statistics. With these results, different variables can be compared, allowing conclusions to be drawn for the obtained panes. The main question formulated in this research is as follows:

How does weathering of double glazing affect the strength of glass?

Because double glazing has four sides, two of which are on the side of the (air) cavity, the results of the tests are distinguished from each other during the examination. Thus, a microscope is used to get a general view of the damages contained in the IGUs. The influence of the air- and tin-side is also considered, which has to do with the manufacturing process. Looking at differences in results of strength and damages of the different sides are part of the sub-questions of the research, formulated below:

- *What are the differences in appearance between the different sides of the two panes?*
- *What are the differences between the strengths of the two panes and both sides?*
- *What is the influence of the air- and tin-sides of the glass?*
- *What are the possibilities of continuing with used glass?*

The ultimate goal of this research is to find out how strong double-glazed panels still are after being in use for a certain period of time. Using the data, is it possible to predict what the strength will be after a certain number of years of use? Going forward, options can be given for reusing panels from an old IGU so that it meets current, possibly modified, standards in terms of strength.

Based on this research, additional data is also obtained that can be used and compared with previous research on naturally aged glass. Similarly, certain results were compared with those of new glass tested by Irene Sofokleous and Thijs van der Linden, who carried out similar tests and obtained results.

2. Theoretical Background

2.1 Introduction

The first chapter highlights the theoretical background of issues applicable to this study. To explain the behaviour of glass, a certain prior knowledge is required. In the first place, the first section (Section 2.2) briefly discusses the history of glass, showing how and when glass was discovered. Then, Section 2.3 explains how glass is produced and what substances glass is made of. Different types of glass will pass by here. It then zooms in on a particular glass application, namely the insulating glass unit (IGU). This will be discussed in a little more detail in Section 2.4, as this type of glass is being tested for this study. It matters to have enough knowledge of the glass being tested so that ambiguities can be avoided. After it is clear where glass comes from and how we obtain contemporary glass panes, the theoretical strength of it will be looked at in Section 2.5. This is done using current standards. Because glass is an unpredictable material in terms of strength, Section 2.6 talks about the statistics behind the strength of glass. How likely is the glass to fail under a given stress? Statistics predicts an answer to this question. Furthermore, opportunities in recycling and reusing are being looked at. It looks at how and whether this happens in today's construction and glass industries, and where opportunities lie for the future. This can be read in the final Sections 2.7 and 2.8.

2.2 History of glass

2.2.1 General

The oldest glass objects found date from around 3500 B.C. (Springer Handbook of Glass, 2019). These were found in Egypt and eastern Mesopotamia (current Syria). Small opaque pearls have been found at these sites. This is the oldest found glass made by humans, but there is also a form of natural glass, which is as old as the earth itself. For example, lava from volcanoes contains a substance that looks like glass, namely obsidian. Obsidian is an igneous rock that occurs as a natural glass, formed by the rapid cooling of viscous lava from volcanoes. Obsidian is very rich in silica (about 65 to 80 per cent). This heating and rapid cooling is also done with the glass of our time. Furthermore, obsidian is an opaque substance that does allow light to pass through. This natural form of glass is thought to have been used by humans as a cutting tool even as early as the Stone Age. Man-invented glass may have been discovered by chance. For instance, layers of glass have been found on pottery. This glaze-like



Figure 2. Obsidian (Geology Page, 2019).



Figure 3. Glassblowers (Taylor & Hill, 2011).

layer was created because grains of sand were mixed in high concentration with water, after which the pottery was baked in a hot kiln. This created a glassy layer on the pottery.

Shortly before the beginning our era, the technique of glass blowing was discovered, after which the very first flat glass was produced around the year zero. This was done by the Romans, who made small sheets of glass by pouring out molten glass mass on a stone table. It was also the Romans who introduced glass into architecture, with the discovery of clear glass (using manganese oxide) in Alexandria around the year 100 A.D. Windows made of cast glass sheets, of an admittedly poor optical quality, were used in the most important buildings and luxurious villas in Pompeii, among others (Stichting Vlakglas Recycling Nederland, n.d.).



Figure 4. Drawn glass (Tresinie, 2023).

For many centuries after this, glass production slowly developed, with the glass-blowing technique being the most commonly used technique for making glass panes. Raw materials were melted in a furnace and a blowpipe was then used to make glass objects and windows. It was only in the 19th century, the century of great industrial progress, that glass production was taken over by the larger factories, leaving the old-fashioned craft of glass blowing in the background. There were more possibilities in terms of size, and the quality of glass in terms of light transmission also improved a lot. Around 1845, it was possible to manufacture large panes of glass. So, this is less than 200 years ago. Another century later, in 1952, the current method of producing flat glass was invented by British manufacturer Pilkington. This method is called the float glass method. More about the production process of float glass in Section 2.3.

2.2.2 IGU

It took hundreds of years before there was a development in the field of new glass construction. Until 1865, the use of single-pane glass was the standard, the function of glass being to let in light and block wind. The insulating effect of single glazing was hardly there. From 1865, this changed when an American engineer and inventor Thomas Stetson mounted two single-glass panes against each other. He found out that when the moist air between the panes was replaced by dry air, an insulating effect was created, and heat loss was reduced. The first IGU was a reality. Yet it still took some time before insulated glass hit the market. In fact, it did not appear on the commercial market until 1950, under the name Thermopane, which was coined by Charles D. Haven and John Hopfield. So, with the help of Libbey Owens Ford company - a national glass supplier for automobile manufacturers and commercial building, it entered the market in the 1950s (*How Insulated Glass Changed Architecture | All-West Glass, 2022*).

From 1948, double-glazing was increasingly used in the Netherlands, where the layer of air between the two panes of glass provided a somewhat (sound) insulating effect. After the 1973 oil crisis, insulation became increasingly popular (Stichting Vlakglas Recycling Nederland, n.d.). Double-glazing and insulation materials were increasingly developed and used more often. Nowadays, there are many different types of glass and different constructions of glass sheets to achieve a construction. For instance, certain coatings or noble gas fillings are often used between two or even three panes of glass to optimise sound and heat insulation.

2.3 Production process of glass

Because the behaviour of glass is going to be described, the raw materials of glass are discussed and also how these raw materials are formed into glass panes. Float glass will be considered here, as this is the type of glass being investigated in this study. The reason it is called float glass is made clear below.

The raw materials from which glass is produced are sand, soda and chalk. The most common constituent of sand is silica (silicon dioxide, or SiO_2), usually in the form of quartz. Yield soda ash is an alkali whose active ingredient is sodium carbonate (Na_2CO_3). And the final main raw material is chalk, which is a form of limestone (CaCO_3). The most common type of glass in windows is soda-lime glass. This consists of the following ingredients and corresponding proportions in accordance with material code ISO 16293-1:20 (*iTeh Standards*, 2008):

▪ silicon dioxide	(SiO_2)	69 % to 74 %
▪ sodium oxide	(Na_2O)	5 % to 14 %
▪ calcium oxide	(CaO)	10 % to 16 %
▪ magnesium oxide	(MgO)	0 % to 6 %
▪ aluminium oxide	(Al_2O_3)	0 % to 3 %
▪ others		0 % to 5 %

As mentioned earlier, there will be zoomed in at the production process of float glass. This process was invented in 1952 by Alastair Pilkington. He was a British inventor and entrepreneur who thus became best known for inventing and perfecting the float glass process for the commercial production of flat glass (Sir Alastair Pilkington, n.d.). The reason it is such a well-known invention is the fact that he found way to make glass panes with a perfectly flat surface. This was obtained by pouring molten glass onto a bath of molten tin. This molten glass came from a melting furnace of about 1500 degrees. Below this, flat glass cullet is often added, in addition to the usual raw materials, to enable a lower melting point. In fact, this glass cullet need only soften. This ultimately costs less energy and money. The molten glass is thus then poured into a bath of tin. Because tin has a higher density than the molten glass (7300 and 2500 kg/m^3 , respectively), the glass floats on the tin. Hence the name float glass, because it floats, as it were, on the bath of tin (Figure 6). Because the molten tin has a perfect flat surface, so does the glass lying on top of it. Because of the surface tension, the top of the glass also has a flat surface. The cast glass, which comes out of the melting furnace, has a temperature of around 1000 degrees when it comes into contact with the tin. Because the melting point of tin is 232 degrees, tin is therefore also in a liquid state. When the glass leaves the tin bath, it is actually ready. After that, it only needs to be carefully and quietly cooled and (at the end) cut. The total production line is about 350 metres long. The thickness of the glass sheet can vary between 0.4 and 25 mm (Stichting Vlakglas Recycling Nederland, n.d.-b). Currently, about 90% of all glass is made using this method. Figure 5 shows a schematic representation of the processes that take place to eventually obtain float glass.

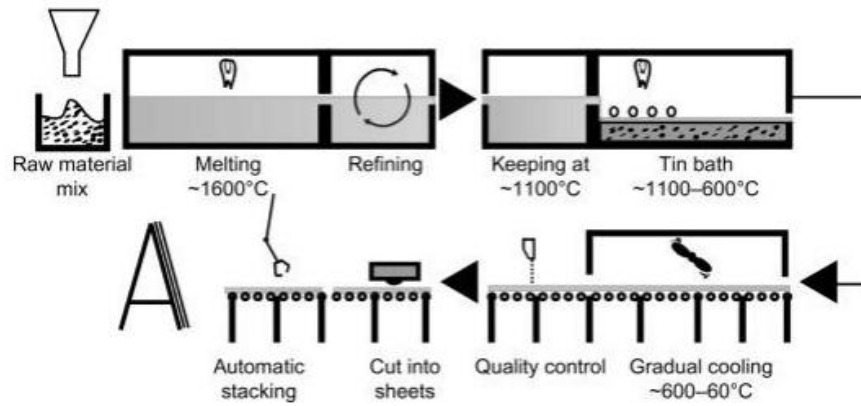


Figure 5. Float glass production process (Float Glass Process, n.d.).

A consequence of production via this method is the fact that one side of the glass may contain traces of tin, while the other side does not. The so-called tin-side and air-side. The tin-side is actually a smoother surface compared to the air-side on a microscopic level (Garibaldi Glass, 2021). There are different ways to find out what the tin-side is of a glass plate is. This is discussed further in Chapter 4.

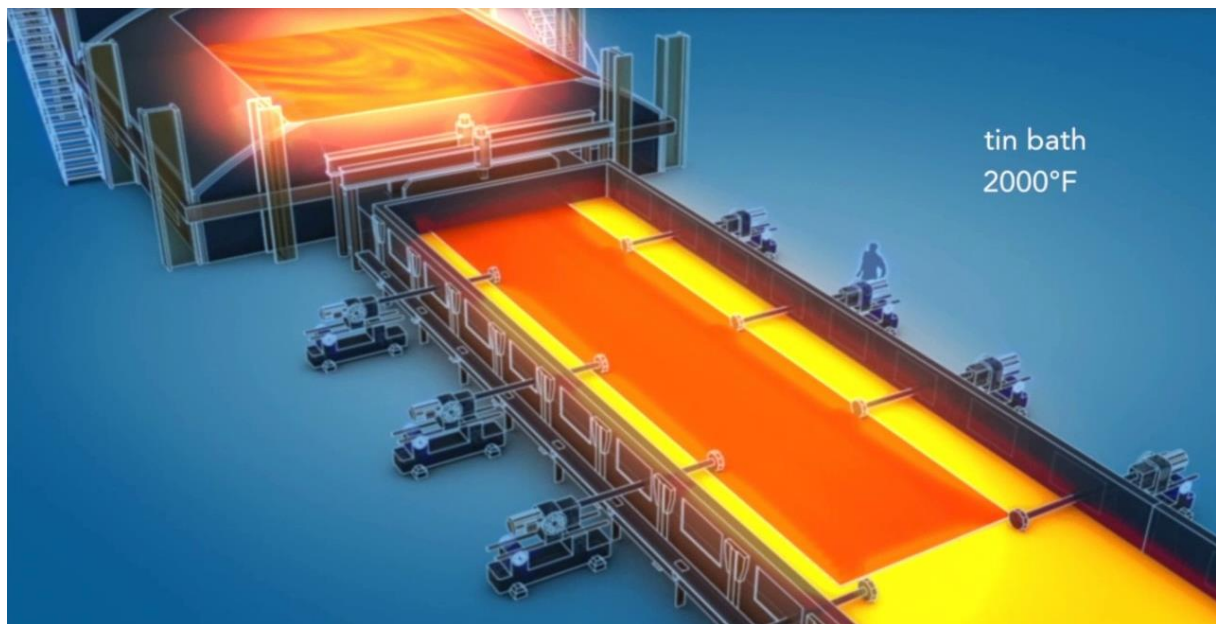


Figure 6. Tin bath (D&O, 2021).

A step further into the manufacturing process of glass, three different commonly used processes are briefly explained so that it can be seen how small differences in the process can make a lot of difference in the behaviour of glass. The three types of glass are annealed, tempered and heat-strengthened glass. Annealed glass (AN) is the product that forms when going through the normal manufacturing process of float glass. This process is characterised by the slow cooling process. When safety of glass is a strong requirement, this glass is not recommended, unless it is laminated. This is because large, sharp shards can form when it collapses. This glass is often used for doors and windows, with two or three layers of glass and a plastic interlayer providing laminated glass to ensure a stronger and more reliable

glass construction. Annealed glass is often chosen when an economical choice is desired. Exceptions to this do exist. Laminated annealed glass is very safe though, with one consequence being that it no longer becomes the most inexpensive choice. Annealed glass is sometimes used in more expensive projects because it has the best optical quality, as toughened glass has some distortion due to the tempering process.

Tempered glass is also called toughened glass. Because the float glass obtained from the production process is heated to 700 degrees again, after which the glass is cooled more quickly. This results in a higher surface compression because the surface cools faster than the interior layers. As a result, this glass is around four to five times stronger than normal annealed glass. When tempered glass fails due to, it does not do so in large sharp shards, but in lots of less sharp, small fragments (Figure 7). Tempered glass is often used when safety is a high requirement.

Heat-strengthened glass (HS) is made in the same way as tempered glass, only the cooling process is slower. This leads to lower surface compression. It is about two times stronger than annealed glass. The collapse pattern is more similar to annealed glass than tempered glass, which is why this glass is often used in places where it is a requirement that it stays in place, when it breaks. Another advantage over tempered glass, is the fact that there is less distortion, making the clarity of the glass better (Products, 2019).



Figure 7. Breakage pattern of different glass types (Peerless Products Inc., 2020).

2.4 Insulated Glass Unit

Insulated glass units are tested for the study. In this section, the different components of an IGU are outlined, after which variations on IGUs are also considered. Consider different types of IGUs, with variations of thickness, cavity filling and materials.

Both sides of both glass panes will be tested for strength, where it can be seen what the behaviour of these used panes is. An IGU thus contains two panes of glass with an inert gas between them. This gas layer ensures that the heat transfer is diffused, making the window more energy efficient. Windows are often a major source of heat loss in a house, but a house without windows is also undesirable. Nowadays, most homes and buildings contain double-glazed windows. Because an IGU is a type of structure made up of several parts, it is therefore called a 'unit', rather than a glass panel. The main components of an IGU can be seen in Figure 8 are briefly explained below:

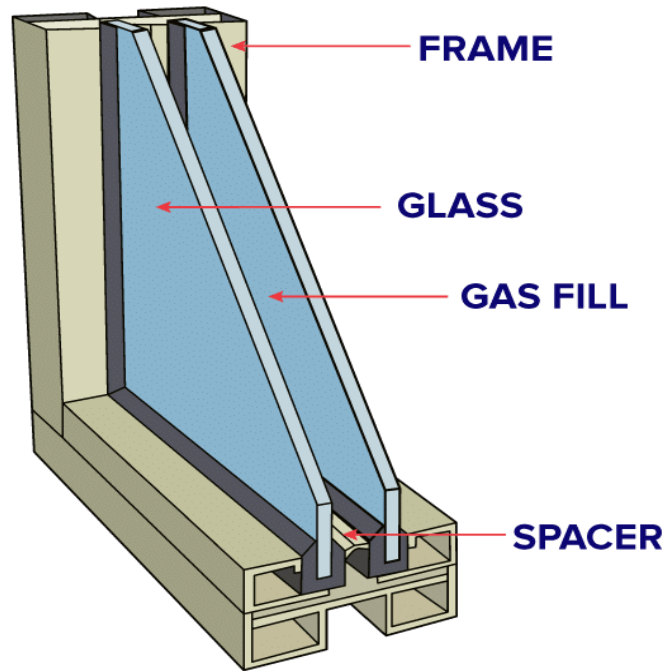


Figure 8. IGU (Glazcon, 2018).

- Glass: different types of glass can be used in an IGU. For example, laminated glass or tempered glass when safety is a high requirement. There are also IGUs where three glass panes are used, when, for example, soundproofing or heat insulation is of great importance. The more and the thicker glass is (usually) more expensive, but more efficient.
- Spacer: To keep the glass panes apart, a spacer is needed. A spacer's job is also to ensure that moisture does not get between the two glass panes. Spacers are often made of aluminium, stainless steel, or a silicone material.
- Window frame: to prevent heat losses, the frame in which the glass panes are fixed is also a determining factor.
- Gas: The gas used to provide better insulation is between the two glass panes. Commonly used gases are argon, krypton, xenon or just air. The first three gases mentioned are less conductive than air, so the U-factor is lower. The U-Factor measures how well the window insulates. While the U-Factor can take any value, in general for windows it ranges from 0.20 to 1.20. The lower the U-Factor, the better the window insulates (DOE Logo Flatten-2, n.d.). Figure 9 is a graph showing the difference in U-factor of different gases (air, argon and krypton). The x-axis shows the gap dimension between the two glass panes. The glass spacing given in inches, where 1 inch equals 2.54 cm.

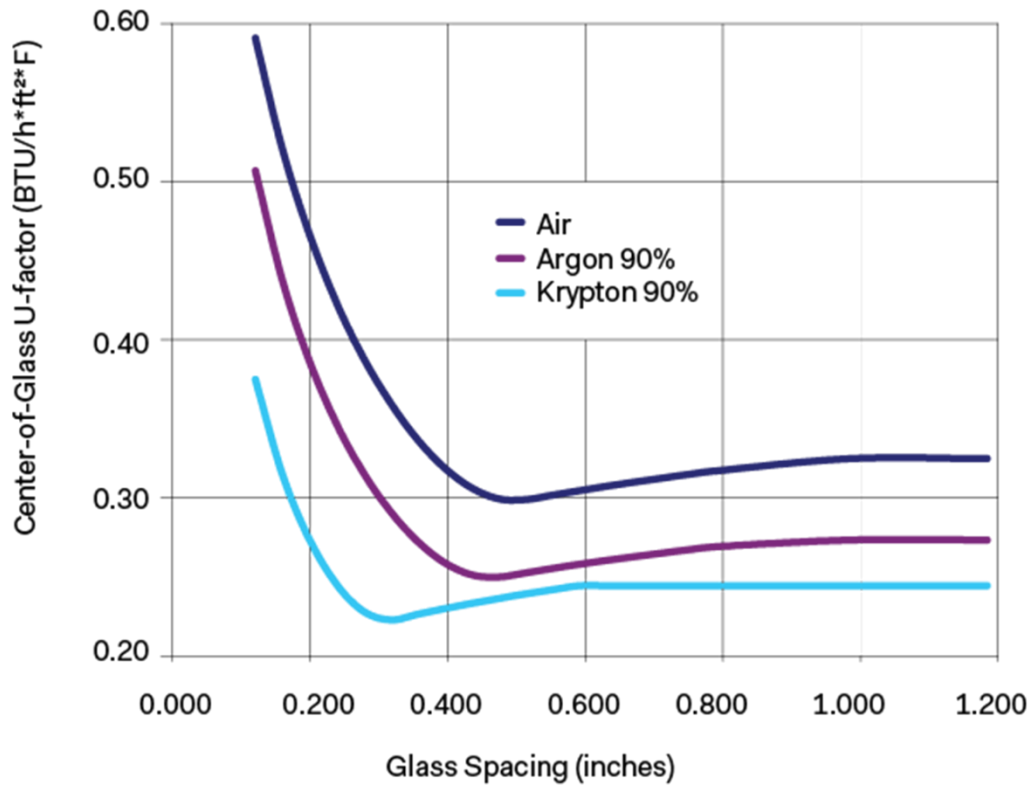


Figure 9. U-factor for different gases.

So, the main components of an IGU are the glass itself, the spacer, the frame, and the gas in the cavity. Because people today are capable of inventing all sorts of things, there are therefore also many variations in this.

First, the glass itself. The most common form of an IGU is with two panes, but a triple glass unit is also sometimes chosen, although to a lesser extent. The thickness of the panes normally varies between 2 and 8 mm. The type of glass can also vary, considering annealed, heat-treated, tempered or laminated glass. To take one step further in the options available today, the glass can also be coated with different types of coatings (Low-E), colours (tints), or patterns. Low-E glass is a microscopic coating, not an insulator. Low-E stands for low emissivity, means that it reflects heat off a window and back inside the home (Barton, 2022). For this study, double glass units of annealed glass were used, and has no coating, colour, or pattern (*INSULATED GLASS UNITS -TYPES AND OPTIONS* | *Advanced Window Corp*, n.d.).

Next, another part of the IGU, the spacer, or structure that maintains the space between the two or more glass panes. Different materials and technologies have been developed over the years for using the spacer. The material determines the amount of heat and cold that is able to pass through the glass. Generally, spacers are divided into two groups, namely aluminium and warm edge spacers. Aluminium spacers are the most widely used in recent decades and have a basic level of performance. Aluminium is a structurally strong material and a very efficient conductor of heat. This means that aluminium spacers allow indoor heat to easily escape outside. Moreover, due to the aluminium, cold glass edges create a temperature difference between the centre of the glass and the edges. However, this does make IGUs susceptible to condensation. As energy consumption requirements for IGU seals became more stringent, other spacer solutions were considered. Spacers with warm edges made of materials with low conductivity were introduced. This performs better than traditional aluminium spacers. These

warm edge spacers proved to be an innovative solution, as it both prevents heat loss through windows, improving energy efficiency, and greatly reduces the problem of condensation (Risle, 2020). This better performance automatically leads to a more costly alternative. Three examples of warm-edge spacers are:

- stainless steel: have only one-tenth the thermal conductivity of aluminium and improve resistance to condensation;
- plastic-metal hybrid: typically made of plastic materials combined with metal fillings;
- flexible: have been developed using pliable, flexible thermoplastic or silicone-based materials.

The lifetime of an IGU is often limited by the design and manufacturing quality of the edge sealing system. The sealing makes sure the insulated air doesn't escape from the cavity. The most common used sealant in IGUs is butyl sealant. A distinction is made between primary sealing and secondary sealing. This double sealing system make up about 90% of the European insulated glass market. Primary sealing serves as a barrier to prevent moisture ingress and also to minimise the loss of energy-saving inert gases from the IGU. Secondary sealants adhere to the spacer and seal the edge of the IGU against moisture ingress and protect the unit from gases exiting and entering the internal structure (Van Den Bergh et al., 2013).

Lastly, the cavity between the glass panes. When an IGU is filled with gas, this means that the air in the cavity has been replaced by and filling gas. The three gases used to fill the cavity are, as previously mentioned, argon, krypton and xenon. These gases are less conductive than air, which causes the thermal conductivity to be reduced, or in other words to obtain a lower U-value of the structure. As shown in Figure 9, the U-values of krypton and argon are lower than those of air at the same cavity thickness. Xenon is the best choice when it comes to heat-loss prevention, because the gas is much heavier than the other two gasses, make it even harder for heat to escape. Krypton gas is the densest gas and can be used well with thinner IGUs, for example in triple-pane construction, where cavity thicknesses are often minimal (Haglin, 2021). When looking at costs, it is clear to see that with better performance (less heat loss), the price goes up. Argon is thus the cheapest option, followed by krypton and xenon is the most expensive option as filling for the cavity (KLG Glass, 2019).

2.5 Strength of glass

Glass is a special material, and difficult to compare with other materials such as steel and concrete. This is mainly because damage to glass has a huge impact on the strength it ultimately has. The method of loading also affects the strength. Because this can differ for each glass panel, therefore, practically speaking, the strength of each glass panel also differs from each other. Because of this, it has always been a challenging process to identify the strength of glass.

2.5.1 Characteristic strength

Theoretically, the strength of glass has a relationship of the bond energy between the atoms. The energy to detach these atoms is around 25-30 GPa. So, this is pure glass, without load and/or damage from production, transport, cutting or by weathering, for example. In practice, the strength of glass is therefore ten or even a hundred times lower (Ivanovna Min'ko & Mikhailovich Nartsev, 2013). So actually, this theoretical strength can be forgotten immediately. The compression strength of glass is much higher than its tension strength. The compression strength of glass is around 21000 N/mm²,

while the tension strength is at most 100 N/mm². The compression strength is difficult to measure, because in experimental tests a tensile force always occurs somewhere in the glass at the moment you collapse the glass specimen, so the glass never reaches the theoretical compression strength (Vander Werf, n.d.). Ultimately, the 5%-fractile bending strength (characteristic value) of annealed glass according to European standards is $f_{g,k} = 45$ N/mm², which is the same as 45 MPa. The design strength will therefore be even lower, because a partial safety factor is added over this. As mentioned earlier, increasing strength can be done through the tempering process. This increases the characteristic bending strength according to European standards to $f_{g,k} = 70$ and 120 MPa for heat and thermally toughened glass, respectively.

2.5.2 Actual strength

The actual strength can be obtained by doing experiments. By repeating this often, a bending strength of the glass can be found out. Because there is always variation in the results, the following values were measured as lower limits for the bending strength. This lower limit means that 99.99% of the specimens have a higher strength than this value. The lower limit bending strength values for the different glass types are shown in Table 1. Lower limit bending strength per glass type (Veer, 2007).

Table 1. Lower limit bending strength per glass type (Veer, 2007).

Glass type	Lower limit bending strength (MPa)
Annealed	20
Heat-strengthened	40
Fully tempered	80

So, these values are a lower limit, so the average strength measured in experiments will be a lot higher, for all glass types. Destructive tests of glass give typical strength values between 30 to 100 MPa and according to measurements referred to in the EU standard EN16612 (2019).

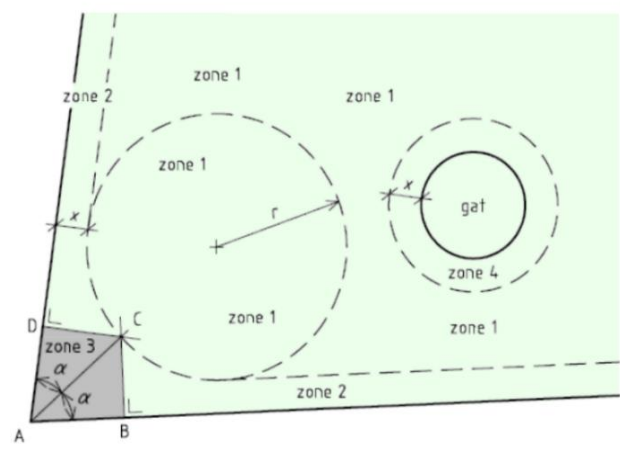
The characteristic value for the bending strength from the European standards is the following:

Table 2. Characteristic bending strength per glass type (prCEN/TC250-1, 2018).

Glass type	Characteristic bending strength (MPa)
Annealed	45
Heat-strengthened	70
Fully tempered	120

Another way to find out the strength of glass is to use the formula from the Dutch design code NEN2608. This formula consists of a number of factors that influence the strength of the glass. These constants are briefly explained in Table 3, followed by the formulae to calculate the theoretical strength of glass (NEN2608, 2014).

Table 3. Factors for determining the strength.

Name	Symbol	Value															
Size effect	k_A	In general: $k_A = 1$ If point load is present or whether there is a nonlinear calculation: $k_A = 1.644 * A^{-\frac{1}{25}}$ with A in mm ²															
Edge quality	k_e	<table border="1"> <thead> <tr> <th>Glass type</th> <th>Loaded out of pane</th> <th>Loaded in pane</th> </tr> </thead> <tbody> <tr> <td>Annealed</td> <td>0.8</td> <td>0.8</td> </tr> <tr> <td>Heat-strengthened (HS)</td> <td>1</td> <td>0.8</td> </tr> <tr> <td>Fully toughened (FT)</td> <td>1</td> <td>1</td> </tr> </tbody> </table>	Glass type	Loaded out of pane	Loaded in pane	Annealed	0.8	0.8	Heat-strengthened (HS)	1	0.8	Fully toughened (FT)	1	1			
Glass type	Loaded out of pane	Loaded in pane															
Annealed	0.8	0.8															
Heat-strengthened (HS)	1	0.8															
Fully toughened (FT)	1	1															
Surface quality	k_{sp}	<table border="1"> <thead> <tr> <th>Glass type or surface</th> <th>Loaded out of pane</th> </tr> </thead> <tbody> <tr> <td>Float glass</td> <td>1</td> </tr> <tr> <td>Patterned glass</td> <td>0.8</td> </tr> <tr> <td>Enamelled surface (frit)</td> <td>0.78</td> </tr> </tbody> </table>	Glass type or surface	Loaded out of pane	Float glass	1	Patterned glass	0.8	Enamelled surface (frit)	0.78							
Glass type or surface	Loaded out of pane																
Float glass	1																
Patterned glass	0.8																
Enamelled surface (frit)	0.78																
Load duration	k_{mod}	$k_{mod} = \left(\frac{5}{t}\right)^{\frac{1}{c}}$ with c = 16, and t = load duration time [seconds]															
Glass zone factor	k_z	<table border="1"> <thead> <tr> <th>Glass type</th> <th>Zone 1</th> <th>Zone 2</th> <th>Zone 3</th> <th>Zone 4</th> </tr> </thead> <tbody> <tr> <td>Heat-strengthened (HS)</td> <td>1</td> <td>1</td> <td>consider without prestress</td> <td>1</td> </tr> <tr> <td>Fully toughened (FT)</td> <td>1</td> <td>0.9</td> <td>consider without prestress</td> <td>0.9</td> </tr> </tbody> </table> <p>- Zone 1: center zone of pane - Zone 2: edge zone of pane For heat strengthened glass: $x = 1.5 \times t_{glass\ plate}$ For fully toughened glass: $x = 1 \times t_{glass\ plate}$ - Zone 3: corner zone of pane, determined by: $r = 2 + \sqrt{2} \times t_{glass\ plate}$ - Zone 4: zone around holes, defined by x as mentioned above for heat-strengthened and fully toughened glass.</p> 	Glass type	Zone 1	Zone 2	Zone 3	Zone 4	Heat-strengthened (HS)	1	1	consider without prestress	1	Fully toughened (FT)	1	0.9	consider without prestress	0.9
Glass type	Zone 1	Zone 2	Zone 3	Zone 4													
Heat-strengthened (HS)	1	1	consider without prestress	1													
Fully toughened (FT)	1	0.9	consider without prestress	0.9													
Glass characteristic value bending strength	$f_{g;k}$	$f_{g;k} = 45 \text{ N/mm}^2$															
Glass prestress	$f_{b;k}$	Float glass – heat strengthened: $f_{b;k} = 70 \text{ N/mm}^2$ Float glass – fully tempered: $f_{b;k} = 120 \text{ N/mm}^2$															
Glass material factor	$\gamma_{m;A}$	$\gamma_{m;A} = 1.8$ (or 1.6 if wind load is normative)															
Glass prestress factor	$\gamma_{m;V}$	$\gamma_{m;V} = 1.2$															

The formulae needed to calculate the strengths are shown in formula (1) and (2).

- Tensile strength of annealed glass:

$$f_{mt;u;d} = \frac{k_A * k_e * k_{mod} * k_{sp} * f_{g;k}}{\gamma_{m;A}} \quad (1)$$

- Tensile strength of prestressed glass (heat strengthened or fully tempered):

$$f_{mt;u;d} = \frac{k_A * k_e * k_{mod} * k_{sp} * f_{g;k}}{\gamma_{m;A}} + \frac{k_e * k_z * (f_{b;k} - k_{sp} * f_{g;k})}{\gamma_{m;V}} \quad (2)$$

Because prestressed glass (heat strengthened or fully tempered) will not be used in this study, formula (2) will not be used. However, it is significant to understand how many factors affect the particular types of glass.

This research will show that several small specimens are cut from the same glass panel, measuring different strengths. This is expected to fall in the given range, with strengths depending on the degree to which the glass has been stressed and to what extent it has been deteriorated and damaged. A deep crack or scratch can greatly affect the strength. More on this in the next chapter.

2.6 Statistics of glass

As already made clear in the previous chapter, it is a matter of statistics when glass collapses. The probability of glass failing at a certain stress can be calculated, but there is no certainty that it will happen exactly then. The occurrence of a crack at the site of maximum stress is difficult to predict exactly where and when this will happen. A Weibull analysis is widely approved when it comes to describing and predicting brittle failure. This analysis assumes that something fails at the weakest point of a given body. In the case of glass, this is well linked to the presence of a critical crack or scratch. Because different types of glass also have different types of flaws, it remains a challenge to predict the behaviour of glass through a theoretical probability density function.

In probability theory and statistics, the Weibull distribution (named after the Swedish civil engineer and applied mathematician Waloddi Weibull) is a continuous probability distribution. The most commonly used formula for calculating probability is the two-parameter Weibull distribution (2PW) (Schenkelberg, 2021):

$$P_f = 1 - e^{-\left(\frac{x}{\lambda}\right)^k} \quad (3)$$

Here ‘ P_f ’ is the probability of failure, ‘ x ’ is the applied stress, and ‘ k ’ is a constant called the Weibull modulus. The Weibull modulus is a dimensionless parameter of the Weibull distribution which is used to describe variability in measured material strength of brittle materials.

If $k < 1$, the distribution is decreasing, meaning that the failure or event becomes more likely over time. If $k = 1$, the Weibull distribution is equivalent to the exponential distribution, meaning the probability of failure or event remains constant over time. If $k > 1$, the distribution is increasing, meaning that the failure or event becomes less likely as time passes.

The ‘ λ ’ is another constant called the characteristic strength of the specimen which is determined by the fracture stress of the specimen at a probability of 63.2%. If the applied stress (x) then equals the

characteristic strength (λ), P_f equals 0.632, or 63.2%. The Weibull distribution shows in graphic form a straight line with slope k and $x = \lambda$ at the probability of 63.2%. A Weibull plot should look like the one in Figure 10, in which an almost straight line can be drawn through the data points. For glass, this is actually never the case. This is because multiple competing causal factors control failure in glass (Veer, 2007).

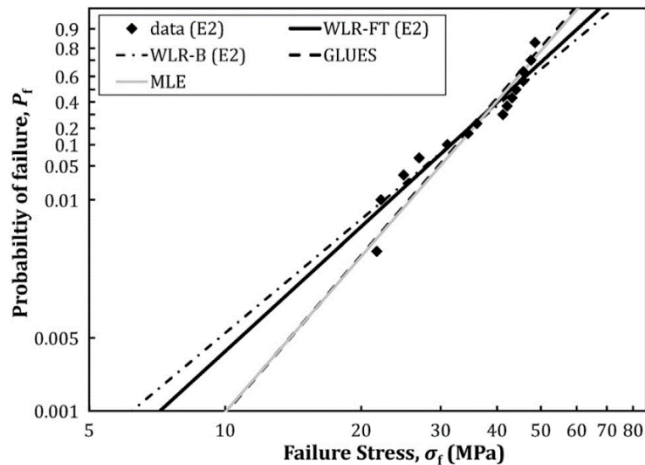


Figure 10. Weibull probability plot example (Datsiou & Overend, 2018).

There are often some data points that are far from the trend line. Often it is the low values in the Weibull plots of glass that make the linear trend break. This is therefore because some glass specimens contain large scratches or cracks, causing them to collapse faster than expected. The higher the failure rate of the glass, the more it behaves according to the predictable values of the Weibull plot. With anomalous data points, it can be questioned whether a linear trend is always the best approximation of the probability density. It may also be the case that certain implausible values or invalid test values should not be included in the Weibull plot, to get a better result and thus prediction. When processing the results of the experiment, it can be considered whether a linear gradient fits the results, or whether perhaps a different gradient of the trend line better represents the situation. For example, a linear gradient with a kink or a curve.

2.7 Recycling of glass

When looking at which sector is responsible for most greenhouse gas (GHG) emissions, it is the construction sector. Various sources indicate that 30 to 40% of all GHG emissions come from the construction sector. Think mainly of the production of materials, emissions from transport to and from the construction site and from work on the construction site itself. Because GHG are a cause of climate change, there are opportunities for the construction sector to improve on this. This can be done mainly by reusing materials, so that depleting raw materials are not needed and emissions from the production of materials can be reduced. This is different from reuse, where a product (or parts of a product) is reused without separating it into raw materials. In recycling, raw materials can therefore be separated. Zooming in on the use of glass in buildings, an average of 48% of a building's facade is now made of glass, with skyscrapers sometimes even consisting of a facade with 100% glass use. With an increasing understanding of how to improve the thermal insulation of glass in recent years, the use of glass has gained a better position as an important construction material for low-energy buildings (Glass for

Europe, 2023). As mentioned earlier, resource depletion is a reason to look more towards recycling materials. For instance, even the raw materials of glass are limited (sand, lime or calcium carbonate and soda ash), making recycling of products increasingly urgent.

Glass recycling already happens frequently. When recycling flat glass, the main focus is on the origin and state of the glass cullet. These glass cullets can be added to the production process. A distinction is made between three different types of glass cullets (Flat Glass Recycling, n.d.):

- internal cullets: from cutting waste in the factory itself (75 - 80%);
- pre-consumer cullets: cuttings from subsequent manufacturing processes (20 - 25%);
- end-of-life products: glass from old car windows or an old window (0 - 5%).

By adding glass cullet in the manufacturing process, the furnace temperature can be reduced from 1600 to about 1150 degrees Celsius. This reduces energy requirements and CO₂ emissions. Every 10 per cent of recycled cullet can achieve a 2 - 3 per cent reduction in energy consumption. Viewed differently, 1.1 tonne of cullet can save 1.3 tonnes of raw materials (Flat Glass Recycling, n.d.). Furthermore, between 250 and 300 kg of CO₂ emissions can be avoided per tonne of recycled glass. The latter in particular contributes to reducing GHG emissions. When looking at the embodied carbon and embodied energy of glass compared to steel and concrete, it becomes clear that these are quite high values, and they come close to the values of steel. These values can be seen in Table 4. Embodied energy is the sum of all energy required to produce goods or services, considered as if that energy were contained in the product itself. Embodied carbon refers to the GHG arising from the manufacturing, transportation, installation, maintenance, and disposal of the building material.

Table 4. Embodied energy and carbon building materials (Hoogerwaard, n.d.).

	Embodied energy (MJ/kg)	Embodied carbon (kgC/kg)
Float glass	15 – 15.9	0.232
Reinforced concrete	1.39	0.057
Steel	24.6	0.466

That there is still a battle to be won in the field of float glass recycling is the fact that only 15% of float glass is used in the production of new float glass (Hoogerwaard, n.d.). In Europe, this percentage is slightly higher, where float factories work with around 25% recycled cullet. This does mean that 85% of float glass is still produced with the higher-temperature furnaces that use more energy and emit more CO₂. It is not that that glass is no longer recycled. Much of the float glass is used in the glass container industry. Container glass manufacturers specialise in the production of glass for food and beverages, including cooking sauces, jams, preserves, water, oil and vinegar. This is where some 72% of float glass goes. The remaining 12% is mainly used in the production of glass fibres.

The reason why not all cullet originating from float glass can be used in the production process for new float glass is contamination. Consider, for example, colour change of the glass due to contamination. Contamination can also affect the melting of glass and disturb it. Finally, contaminated used glass can also have a negative effect on the lifetime of glass furnaces.

When zooming in on insulating glass or IGU, it can be concluded that this does represent an environmentally conscious way of producing glass. In fact, insulating glass saves nine times more CO₂ than is released during its manufacture. Recycling an IGU is almost the same as normal float glass, except that first the glass has to be separated from the sealant and the aluminium spacer.

The reason that glass recycling is discussed in more detail is the fact that this research will look at used glass. The idea is that this glass will be reused, which is different from recycling. However, to achieve a particular goal, it is useful to know how glass is recycled, and to know that it saves energy and CO₂

emissions but is still much more than when float glass is reused 1-to-1, without using cullet to produce 'new' float glass anyway. The next section goes into more detail about glass reuse, whether and how it is already being done and how it can be done more and better.

2.8 Reuse of glass

Another way to be environmentally conscious about material use, apart from recycling, is to reuse materials. This looks similar, but in reuse, the material is not modified and used in the same state for a new purpose. So, this is another step further and better when it comes to minimising waste from old structures. There is also no need to reuse raw materials, which reduces their depletion. Furthermore, glass is prefabricated, so there is less waste on the construction site. Finally, there is less waste in the factory itself, or in other words fewer internal cullets. When considering CO₂ emissions and the energy required to produce glass, it is progress when materials are reused. When recycling glass, it is often reheated, which, although less than the glass production process, still emits CO₂ and requires energy to heat the glass. When reusing glass 1-to-1, heating is not necessary, and the CO₂ emissions released in the process are also not an issue. When looking at numbers when it comes to CO₂ emissions, this can be seen in Table 5. It shows how much CO₂ is emitted by both new (primary-based) and reused (secondary-based) glass. Reused glass does have some CO₂ emissions, due to transport and possible production of a new window frame, for example. It can be seen that 77% of CO₂ emissions are thus saved by reusing the used glass (Nußholz et al., 2020).

Table 5. CO₂ emission and saving potential (Nußholz et al., 2020).

<i>Type</i>	Windows
Primary based product (t CO ₂ -eq)	72.5
Secondary based product (t CO ₂ -eq)	16.5
Carbon saving potential (t CO ₂ -eq)	56
Carbon saving potential (%)	77

Material reuse stands as one of the most promising clean-energy solutions for reducing GHG emissions in the EU construction sector (Ritzen et al., 2019). Yet it is not as easy as it seems. There are several reasons why reusing materials in the construction industry is still quite rare. Some of the barriers are technical barriers, logistical barriers, cost and liability. Technical barriers mean that used glass panes no longer always provide the performance and quality that it had at the beginning of its lifetime. Think of usage damage or damage that can occur during the deconstruction process. Another thing that comes into play in the deconstruction process are the practicalities of economic 'scrapping'. It is often cheaper to throw everything against the ground, thus destroying all the material, than to more carefully and slowly dismantle parts of a structure for reuse. Reusing an IGU also involves other technical aspects, in terms of performance and quality. For instance, certain films used in an IGU can become opaque when in contact with moisture and/or incompatible components. This is another example where reusing an IGU is thus hampered. An IGU has an expected lifespan of 20 to 25 years, and a guaranteed lifespan of 10 years. Beyond these technical hurdles that arise when glass may be reused, logistical issues may also arise. Consider the distance a glass panel would have to travel to be reused. Transportation also costs energy and money. This does not always outweigh the benefit gained from it when this glass panel is reused. It has already been said, but the cost involved in something is often still the biggest reason for doing or not doing something. So, if it is more expensive to reuse a glass panel in another building than to produce a new panel, reusing this material remains a discussion. Reuse can be seen in

direct system reuse or disassembly and component reuse. The difference is that an IGU, for example, can be reused in its entirety (direct system reuse), but components of an IGU, for example a glass panel, can also be disassembled for reuse (component reuse) (Hartwell et al., 2021). Some things still need to be done before a used glass panel is used in a new function. These include possibly cutting the glass panel, or producing a new frame that is mounted around the panel. Often, a second layer is also added to meet energy efficiency standards. An overview into the steps glass goes through before it can be reused is shown in Figure 11.

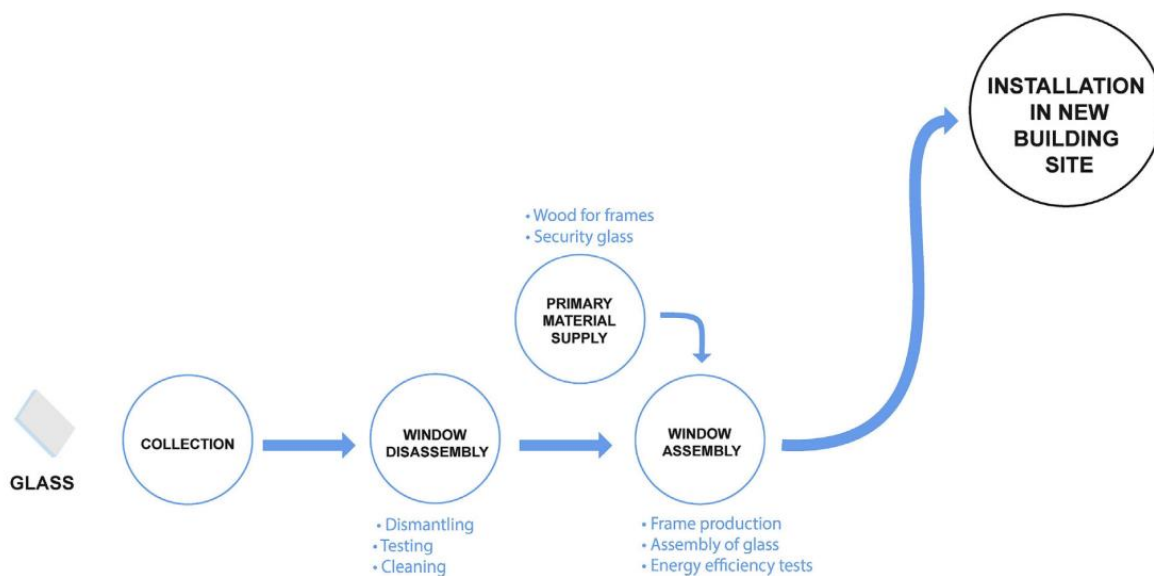


Figure 11. Glass reuse cycle (Nußholz et al., 2020).

For reuse to yield financial benefits and become price-competitive with linear products, processes and inputs must be carefully managed to ensure that the additional costs of recovery production processes outweigh the potential cost savings of using secondary materials. The more processes and material inputs required for a reused product, the less likely it is to become price-competitive due to the potential cost savings from cheaper secondary materials.

This study looks at whether used glass in a building is still useable enough in terms of strength, or the quality and performance, to be reused in some way. By checking this and coming up with possible solutions on how, in this case, double-glazing can be reused in an efficient way. This is to make it attractive for new projects to consider reusing ban materials, to ensure a cleaner construction industry as an end goal.

3. Weathering and glass deterioration

3.1 Introduction

The chemical composition of glass is the key factor in the interaction of glass with the environment. Under certain exposure conditions its optical properties, chemistry and structure are modified by different weathering processes.

Unlike most materials, glass is highly resistant to corrosion and can, in a sense, be considered corrosion-resistant. Nevertheless, glass can be negatively affected by the environment it is in. It is also referred to as glass corrosion, which basically means that a material is affected by external or internal factors leading to a certain degree of loss of aesthetics, functionality, structure or shape. The chemical composition of glass plays a significant role here. Under certain conditions, it can be affected, which can, for example, change the optical properties of glass. Causes for the degradation of glass properties are discussed in this chapter. The causes that damage glass in one way or another vary widely. Damage can be caused by human activity, but polluted air or UV radiation, for example, can also affect glass properties. There will be looked at these causes so that explanations can be given for any weathering found in the glass used for this study.

As mentioned above, the chemical composition of glass is briefly explained again for helping to understand different types of glass weathering. Glass consists mainly of the substance silica or silicon dioxide (SiO_2). The chemical structure of SiO_2 is like a tetrahedral SiO_4 structure (see Figure 13). Each acid atom is connected to two silica atoms and therefore only half counts. A 2D schematisation of the atomic structure is shown in Figure 12. A network of atoms emerges, with the particles closely packed together and trapped in a neat lattice.

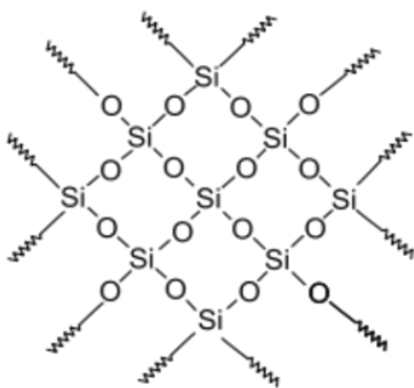


Figure 12. Neat lattice structure (Canrinus-Moezelaar, 2017).

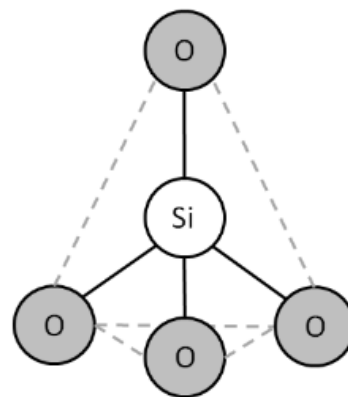


Figure 13. SiO_4 -tetrahedron (Muller, 2015).

When windows are installed in a building, home or other function, it has to deal with the environment. The environment at a site can vary during its lifetime. These environmental parameters are divided into five different categories, each of which is explained, indicating how and to what extent it can affect the glass.

These categories are:

- temperature
- acidity (pH)
- air pollution
- humidity
- UV radiation
- other causes

Each environmental influence is briefly described below, explaining its impact on the glass.

3.2 Temperature

That temperature (changes) affects the properties and behaviour of glass can already be seen in the various manufacturing processes. Different rates of cooling and/or heating is a crucial factor in obtaining the different types of glass. With a sudden temperature change, thermal stress is generated, which can result in thermal shock fracture. When a hot glass specimen is suddenly cooled - for example, by immersing it in ice water - a large amount of tension can be created in the outer layers as they shrink relative to the inner layers. This tension can lead to cracks. In this case, it is about large temperature changes. With small and gradual temperature changes, such as those that occur during the transition from day to night, the risk of cracking is much less. Hasselman et al. (1976) predicted the thermal fatigue life of soda lime silica glass from a slow or subcritical crack growth (SCG) concept. A conclusion is that the thermal fatigue life is approximately proportional to the critical temperature change ΔT -n, where n represents a crack growth exponent in the SCG law, by assuming that the crack length at failure is sufficiently larger than the initial one (Papadopoulos & Drosou, 2012).

Another way float glass can crack is temperature differences within the glass pane. Consider a bright sun, shadows, a hot or dark-coloured object close to the window, or something stuck or painted on the glass, such as a sticker or window decoration. When a sheet of glass is heated unevenly, tensions are created between the differently heated glass areas. Because glass has a thermal conductivity coefficient

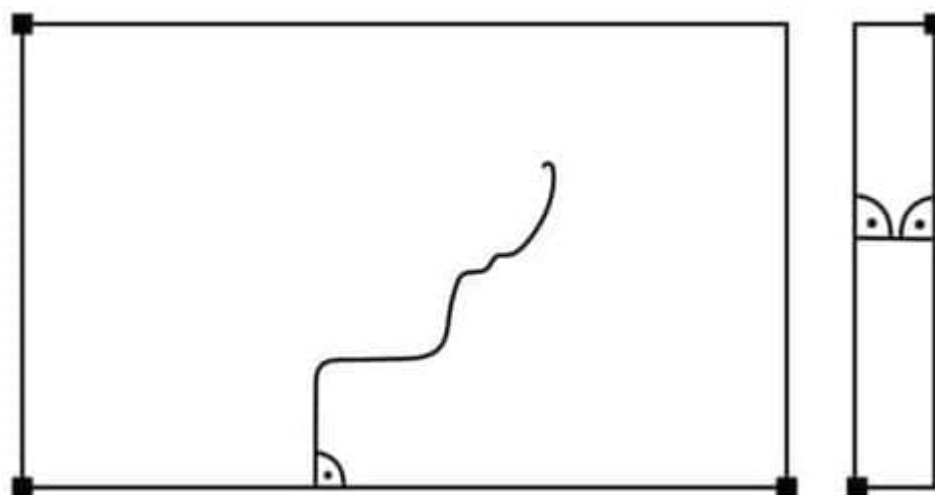


Figure 14. Damage example thermal breakage (Glasschades, 2006).

of only 0.8 - 0.9 W/mK, rapid temperature equalisation is not possible. By comparison, steel and aluminium have a thermal conductivity coefficient of 50 and 237 W/mK, respectively. Because the frame (and also a spacer in double-glazing) is made of a different material than the glass, and therefore has a different thermal conductivity, this can cause large temperature differences within the glass construction (glass, frame, spacer). When a temperature difference within the same glass sheet is high enough, it can lead to thermal glass breakage. A normal thermal fracture starts from the edge and has a directional change (kink) at the cold/warm zone. An example of a thermal fracture is shown in Figure 14. It depends on the size of the micro-cracks in the glass how large the temperature difference has to be for the glass to break. The deeper the cracking is, the smaller the temperature difference leading to breakage. Cracks of 0.02 to 0.08 mm combined with temperature differences of 30 to 60 °C can already lead to thermal glass breakage (*Glasschades*, 2006).

3.3 Acidity (pH)

The acidity of the environment the glass is in can also affect its properties. The pH value indicates how 'acidic' the environment is. If the pH value is higher than 7, it is 'base' or 'alkaline', and if it is lower than 7, it is 'acidic'. When the value is 7, it is considered a neutral environment, such as pure water. When pH rises to values above 7, the mechanism changes and shifts (gradually) to congruent dissolution. Congruent dissolution is the transition from a solid substance to a liquid of the same composition. The dissolution of, in this case, silica is increasing exponentially after treating the glass with a solution which has a higher pH than 7 (Figure 15) . The glass structure is severely affected in this scenario as the fragments of the network are lost. The formation of craters and pits of different size, depth and degree of interconnection can be observed with equipment such as a microscope (Papadopoulos & Drosou, 2012).

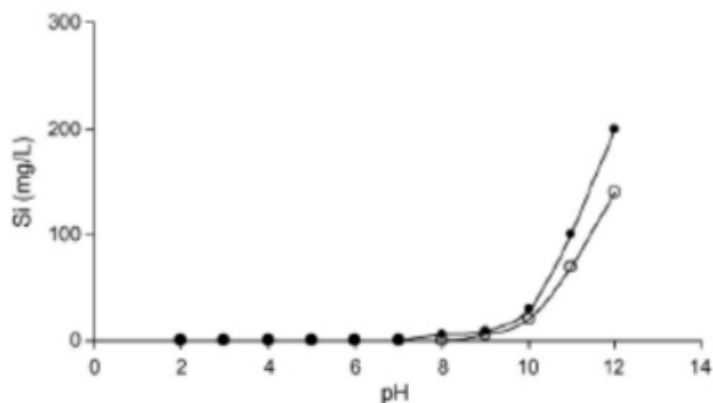


Figure 15. pH-silica dissolution correlation diagram (Papadopoulos & Drosou, 2012).

3.4 Air pollution

Bad air quality can also cause weathering and glass deterioration. The composition of polluted air can cause the glass to deteriorate and have faster rates of corrosion. For instance, studies have been done that concluded that 1 ppm NO (nitrogen monoxide) or 5 ppm SO₂ (sulphur dioxide) accelerates the rate at which glass corrodes by about a factor of 3, compared to the same glass at the same temperature and humidity in clean air in a laboratory. These substances are found, for example, in smog, which is

temporarily highly polluted air. Especially in warm and sunny climates and close to polluting places, such as cars and factories, smog occurs regularly. In glasses not subject to cracking, the leaching of alkali ions from the surface of the glass results in a depleted region which behaves as a diffusion barrier. However, cracking provides access to a fresh surface in which the process can begin again. So, when glass is exposed to the substances that react with it, and cracks form, this is a repeated process. Because there are cracks, there is always a new piece of glass which reacts again with the contaminants. As a result, polluted air therefore affects the degree and rate of corrosion of glass. This can be considered during experiments if large cracks are found before specimens are brought to failure (Papadopoulos & Drosou, 2012).

3.5 Humidity

In general, glass can be hydrated and then recrystallised when in direct contact with water (Papadopoulos & Drosou, 2012). Recrystallisation is the ordering of the amorphous atomic structural state of a glass system from a randomly ordered network to a well-ordered periodic crystalline structure. Recrystallisation causes a layer of elements from the glass matrix, usually alkalis and alkaline earth elements, to form at certain spots on the glass. The glass surface is affected in this way and a pitting-like surface appears. Figure 16 shows what weathering looks like at a relative humidity (RH) of 98%. After research, it has been seen that an increase in ambient relative humidity has a greater effect on the hydration rate than levels of SO₂ and NO. Furthermore, the study also showed that the relationship between the hydration rate and the time needed to hydrate to a certain depth is inversely

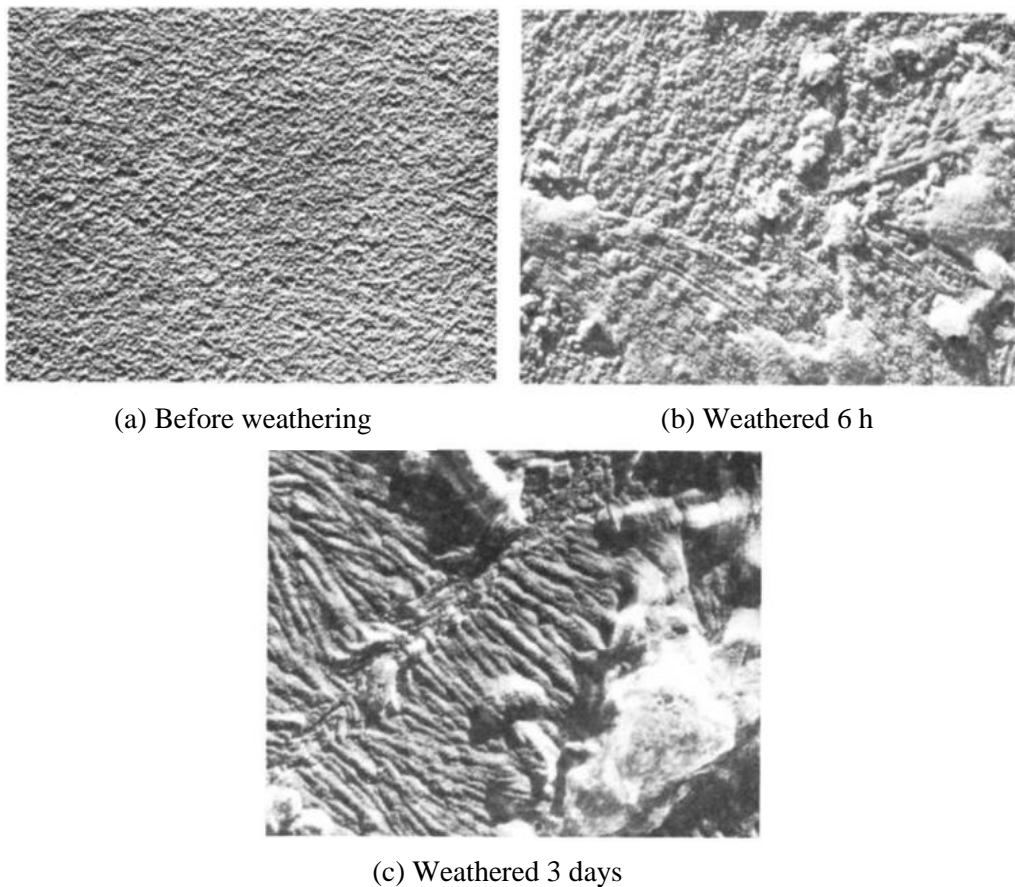


Figure 16. Electron micrographs of soda-lime glass before and after weathering at a relative humidity of 98% and temperature of 50 °C (53000x).

quadratic. So, when the hydration rate increases by a factor of 10, the time the glass takes to decay decreases by a factor of 100 (Cummings et al., 1998). So high humidity can quickly cause additional damage is pre-existing cracks or scratches (Walters & Adams, 1975). All this indicates that during the study, it is necessary to measure temperature and relative humidity in the room where the experiment is conducted. This allows any differences in results to be explained by the relative humidity.

Long-term moisture on the glass surface can cause a damage pattern on the glass. This patches of leached spots on the surface may be distributed all over the pane and often look like spouts of water droplets. This type of damage is therefore often seen on the outside of a window, rarely on the inside. Figure 17 shows an example of this type of damage (Glasschades, 2006).

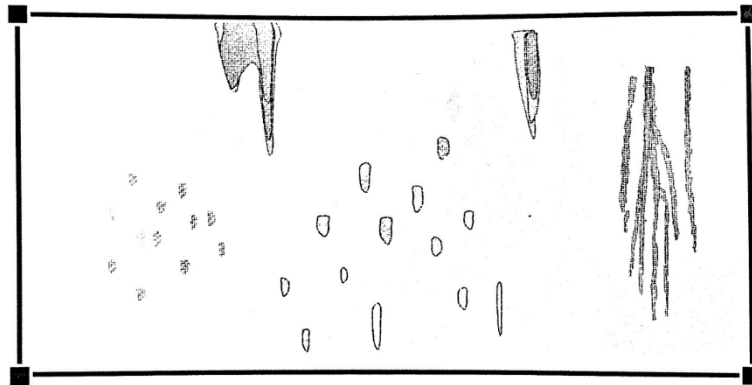


Figure 17. Damage caused by penetrating moisture (Glasschades, 2006).

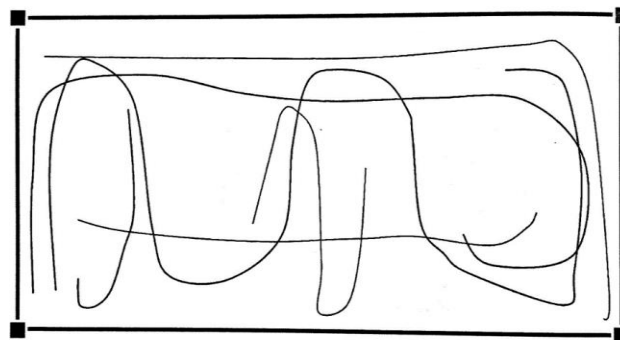
3.6 UV radiation

There are two different ways in which UV radiation affects when it comes to the properties of glass. The first is simple, which is the fact that UV radiation promotes the formation of Si-ions (Papadopoulos & Drosou, 2012). Because these are ions with a lower valence (the ability to form bonds), this disrupts the atomic structure and thus results in cracks in the glass. Secondly, UV radiation can trigger a chemical reaction with organic contaminants on the glass surface, such as air pollution or (excrement of) insects or animals, oxidising these residues. This oxidation process thus requires sunlight, but also (rain) water to oxidise and wash away the organic contaminants. The photocatalytic reaction created by the presence of sunlight thus causes a chemical reaction on/in the glass which can damage it. This also makes UV radiation a component that can be considered in research.

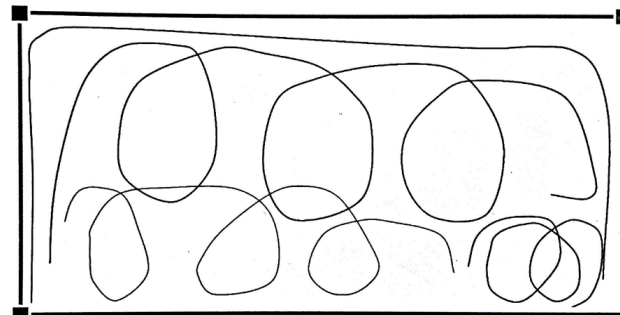
3.7 Human damaging

Another cause of weathering of glass is done by humans themselves. Consider any touching of glass by humans. It can cause very small scratches that at a later stage can grow into deeper scratches or even cracks. Windows near or in doors often suffer this kind of damage, because this glass is simply touched more often than windows over doors or other places where people cannot reach as easily. Another way windows can be damaged is by cleaning them. By sweeping a cloth over a window, we (humans) see the glass become clean, as the dirt is wiped off. When wiping this muck off, there is a chance that small particles/grains will be scraped across the glass, which can cause small scratches. These scratches are often not visible to the naked eye but can be mapped with a microscope. In Figure 18, some examples of patterns of cleaning damage can be seen.

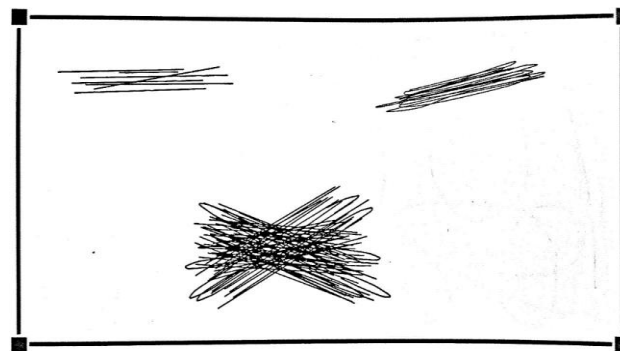
Grains of sand can also cause relatively deep scratches that greatly affect the strength of the glass. During tests on the bending tensile strength of new glass, values of up to 200 MPa have been found, eight times higher than NEN2608 prescribes. This is also the reason why tests of windows for load-bearing strength, for example on the building site, only tell something about that window at that moment. Such a test is therefore not representative for the other windows, where one grain of sand can be the cause of a completely different outcome of a strength test (Kruijs, n.d.). Other causes of human damage to glass include pushing flower boxes or furniture against it. All these innocent human actions can affect the properties and performance of the glass. Another extreme which fortunately is less common is vandalism. Vandalism cause glass, despite often still being in good condition, to suddenly fail, with reuse often no longer an option. Thus, human activity also damages glass. Small scratches from cleaning and window cleaning, for instance, can affect the properties measured. Any human cause of damage will be reported for this study.



(a) Longitudinally and transversely



(b) Circular



(c) Grouped

Figure 18. Damage caused by cleaning (Glasschades, 2006).

3.8 Other causes

Other causes of damage applicable to this experiment are mainly damages sustained after the windows have been removed from their function. Firstly, consider the dismantling of the windows. This involves mechanics removing the windows from the frames and may cause scratches. Next, the windows are taken from the building and then transported to a storage area. From this storage area, it is transported to the TU Delft basement, in this case, where the IGUs are waiting to be examined. During transport of the IGUs, the occurrence of transport scuffing is quite possible, due to, for example, grains of sand between the windows without separators, strong winds in sandy environments or when travelling behind a sand truck. The pattern of such kind of damage is shown in Figure 19, where it can be seen that a single grain of sand can already cause a substantial scratch with no clear direction. Once arrived in the basement of TU Delft, the plates get dirty and are not conducive to quality. Next, the process of separating and cutting the IGUs is also a source of additional potential damage. 'Sawing through' the IGUs causes the release of the moisture-resistant pellets that can cause scratches on the inside of the IGU. Also, sawing through the hard corners of the IGUs creates dirty air that could cause a chemical reaction with the glass. Cutting the corners with an angle grinder, causes the sparks to hit the glass. This creates a rough glass surface due to metal particles from the grinder. After any removal of these particles, very small craters are left in the glass surface. This leads to a damage pattern as shown in Figure 20. Cutting and breaking the glass panes into usable specimens creates microscopic cracks and notches at the glass edge of the specimens. When the window is loaded, this always creates one of the essential weak points. Because the sides are not loaded in this study, these micro-cracks will have little or no effect on the measured strength of a specimen. In short, the transport, separation, and cutting process is a source of additional damage. This will have to be considered when analysing the specimens and post-test results.

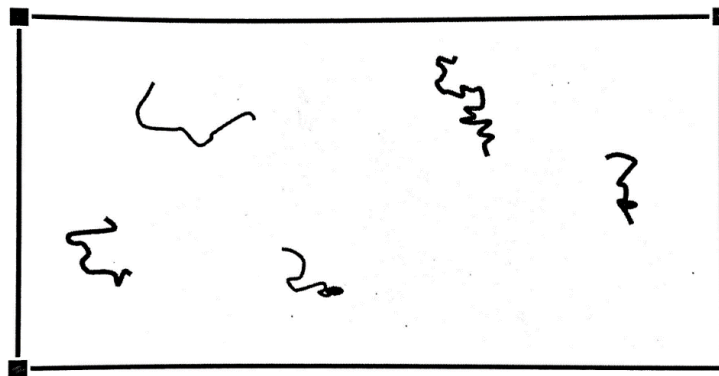


Figure 19. Damage caused by transportation (Glasschades, 2006).

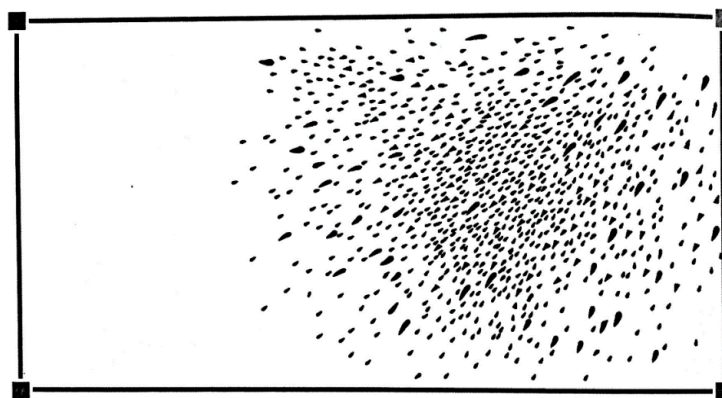


Figure 20. Damage caused by grinder tips (Glasschades, 2006).

4. Experimental investigation

4.1 Introduction

This chapter contains experimental research on used double-glazed units, also called IGUs. First, the background of the glass units needs to be clarified. Consider the duration of use, location and orientation. This is clarified in Section 4.2. Section 4.3 explains the setup of the Coaxial Double Ring (CDR) test, clarifying how and why it is tested. The dimensions of the specimens were then determined to find a proper ratio in the number of specimens tested per series. The dimensions of the specimens used and corresponding checks according to current standards, are the found in Section 4.4. Before the destructive tests can be carried out, the glass panels have to be prepared for this purpose, such as cleaning, cutting, etc. This process is clarified in Section 4.5. Furthermore, the surface condition of all sides of the glass units is examined using a microscope, known as non-destructive testing, which is presented in Section 4.6. Here, the surface damage on the weathered glass is charted. After this, small devices are used to determine the tin- and air-sides of the glass units, and the prestress contained in the glass is also measured. This is further explained in Sections 4.7 and 4.8, respectively. After this is done and the glass is better known, the test procedure is explained, and the main results of the CDR tests can be seen in Section 4.9.

4.2 Test specimens

The examined glass came from an apartment building located on Carmenlaan in Amstelveen, in the Netherlands. The apartment building itself was built in 1965. The insulated glass units themselves came from plastic window frames, installed in 1986, so the glass units are 36 years old when they were received by TU Delft. It is the first generation of double glazing, without coating and with an air cavity. The glass panes in the insulated glass units are annealed glass. It is a tall 11-storey flat, with garages in the plinth and storerooms on the first floor. The 72 flats Carmenlaan (217-359) are on floors 2 to 11. Building type is the cast-building system EBA-II. Eigen Haard is the owner. The renovation project is carried out by contractor Hemubo and GSF Glasgroep is a subcontractor and was responsible for dismantling the glass panels made available for this study. The locations of the glass panels received were a bit confusing. There were some inconsistencies in the attached document and the stickers stuck on the IGUs. For this study, the information that was on the IGUs themselves was chosen as the guide. Eventually, six double-glazed panels became available to test for strength. These units came from four different locations of the building. Two locations in the building provide two IGUs while two spots in the building provide one IGU. A further distinction is that two of the six IGUs received were openable windows (pivot). The other four were fixed.



(a) Location on map



(b) West facade



(c) East facade

Figure 21. The apartment building.

Furthermore, the theoretical thicknesses of the glass were also different from what they were in practice. According to the glass panel report, all IGUs were the same in terms of thickness, namely 5 mm for the outer panel, and 4 mm for the inner panel. This was not actually the case. However, the information on the spacer was the same for each IGU, so it can be assumed that each IGU was produced and installed at the same time. The aluminium spacer listed the supplier (Thermobel ® Glaverbel) and the date of production, 1986 (04 1 86), which can be seen in Figure 22.



(a) Date



(b) Supplier

Figure 22. Spacer info.

A summary of the IGUs received with corresponding location, orientation and thicknesses can be seen in Table 6.

Table 6. Overview of the IGUs

	Name	Floor	Orientation	Dimension height x width (mm)	Thickness outer panel (mm)	Thickness inner panel (mm)	Pivot or fixed
1	Front façade 2 nd floor L 247	2	East	1509 x 656	8	6	Fixed
2	Front façade 2 nd floor R 233	2	East	1509 x 656	5	4	Fixed
3	Back façade 2 nd floor L 247	2	West	1458 x 680	5	4	Fixed
4	Back façade 2 nd floor R 233	2	West	1458 x 680	6	4	Fixed
5	Front façade 9 th floor middle 355	9	East	1075 x 607	6	4	Pivot
6	Back façade 9 th floor middle 355	9	West	1080 x 612	6	8	Pivot

4.3 Setup

To determine the surface bending strength of the obtained glass, the most commonly used method for this purpose is the Coaxial Double Ring test. Here, small specimens are tested for surface bending tensile strength. The advantage of testing small specimens instead of testing the whole glass is the fact that a higher number of tests can be done, resulting in statistically significantly better results.

To set up the CDR test, the American code, namely the ASTM C1499-09 (2013) code for the Coaxial Double Ring test, is followed. This code consists of a step-by-step plan of how to perform the test, as well as a number of checks that are decisive for determining the dimensions of the specimens, as well as the dimensions for the rings that are attached in the designated machine. The setup of the CDR test according to the ASTM code is shown in Figure 23. The inner ring, also called loading ring, and the outer ring, also called supporting ring, can be clearly seen here and the other parts of the test are also indicated here. When a compressive force from the inner ring is applied to the test specimen, a tensile stress is created on the bottom side of the specimen. The highest stress will (theoretically) be within the dimensions of the inner ring. Furthermore, it is recommended that the inner ring is hinged to the machine to ensure that the force is transferred centrally to the specimen.

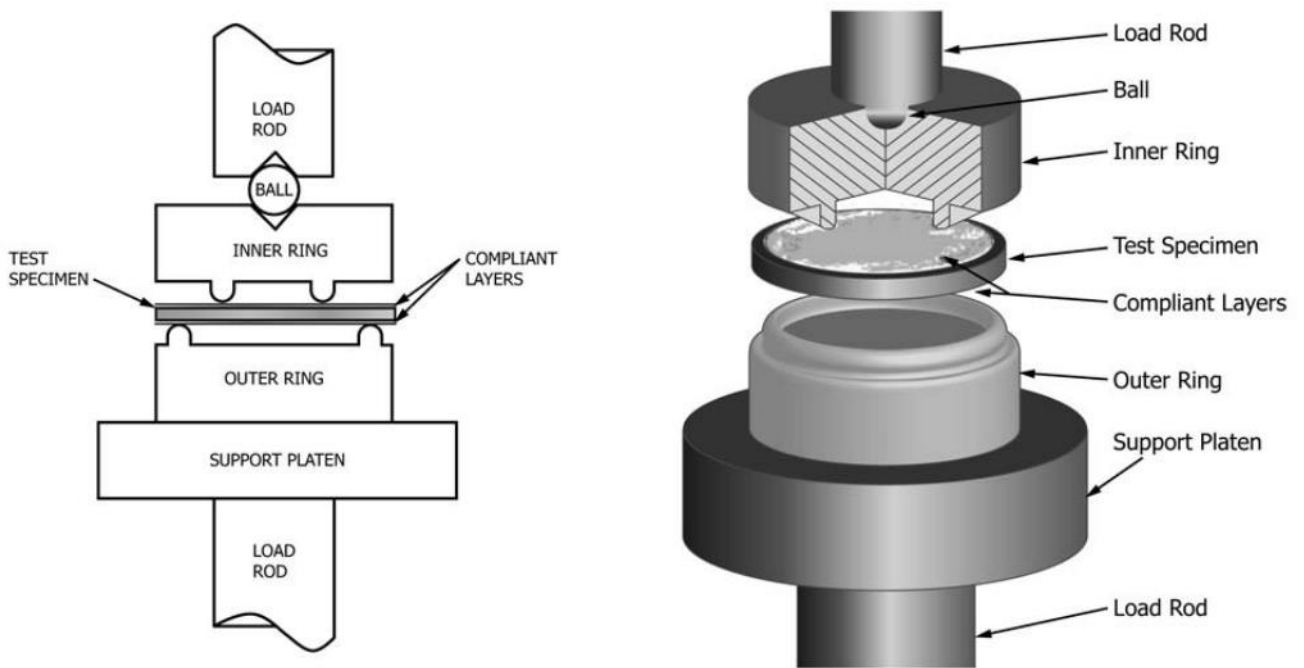


Figure 23. Section and perspective view of basic fixturing and the test specimen for equibiaxial testing.

The principle of this method of testing is to create a homogeneous tensile stress on the glass surface. This homogeneous stress area will theoretically be within the loading (inner) ring at all times. This is because it can be seen as a 4-point bending test performed in a circle. As a result, a circular homogeneous tensile stress can be found within the loading ring, which is the smallest ring and represents the external load, so to speak. Figure 24 and Figure 25 show that inside the loading ring there is a constant moment, which therefore automatically means that the bending stress is also constant in this region. This is only true if the distance of the force 'F' from the supporting point is the same on both sides. The forces 'F' represents the loading ring, the support point represents the outer ring, or supporting ring.

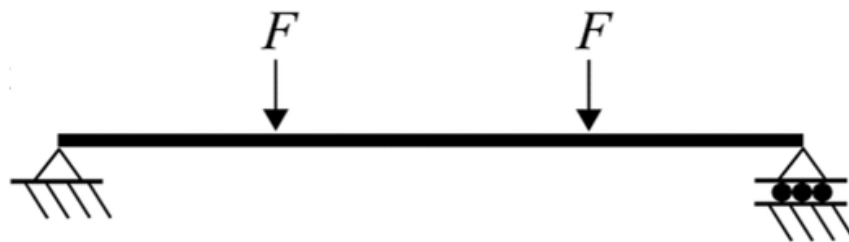


Figure 24. 4-point system.

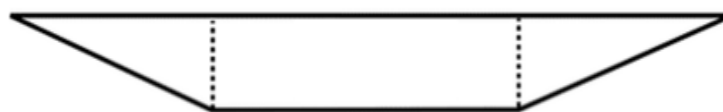


Figure 25. Moment distribution of 4-point system.

4.4 Dimensions

To do the CDR tests, it is necessary to cut the glass panels into smaller specimens. The specimen sizes were determined according to the requirements of the ASTM C1499-09 (2013). Because many things vary in the IGUs obtained, such as the thicknesses, orientation and depth, it was decided to do the size of all specimens the same, so as not to create another additional variable in the study. There are a number of checks prescribed by the ASTM that the dimensions of the specimens, the loading ring and supporting ring of the CDR test must comply with.

In the first check, it is verified whether the dimensions of the supporting ring are proportional to the thickness of the specimen. The relative dimensions should be chosen to ensure that the behaviour is well described by the simple plate theory. This check can be seen in the formula below:

$$\frac{D_s}{10} \geq h \geq \sqrt{\frac{2\sigma_f D_s^2}{3E}} \quad (4)$$

Where:

- h = the test specimen thickness in units mm,
- D_s = the support ring diameter in units mm,
- σ_f = the expected equibiaxial fracture strength in units MPa,
- E = the modulus of elasticity in units MPa.

The following check is to verify the ratio between the size of the specimen and the supporting ring:

$$2 \leq \frac{D-D_s}{h} \leq 12 \quad (5)$$

Where:

- D = the test specimen diameter in units of mm for circular test specimens.

Because rectangular double-glazed panels were obtained, it is impractical to work with circular specimens. Square glass specimens were therefore chosen. For this, the 'D' (equivalent diameter) has to be converted to a value valid for square specimen. The formula for this according to the ASTM C1499-09 is shown in formula (6):

$$D = 0.54(l_1 + l_2) \quad (6)$$

Where:

- l₁ = the length of edge 1,
- l₂ = the length of edge 2.

The edge lengths should be within $0.98 \leq l_1/l_2 \leq 1.02$

Finally, one more check related to the dimensions of the loading and supporting ring. According to the ASTM code for the CDR test, the ratio between the two rings falls between the following values:

$$0.2 \leq \frac{D_L}{D_s} \leq 0.5 \quad (7)$$

Where:

- D_L = the loading ring diameter in units mm.

Using these requirements of the ASTM code for the CDR tests and combined with a desired number of test specimens for the study, a specimen size of 150mm x 150mm was arrived at. At these dimensions, all the above checks satisfy for different thicknesses, and a respectable number of specimens can be extracted from the IGUs used. When larger dimensions are chosen, the maximum number of specimens that can be extracted from an IGU drops rapidly and the study becomes less reliable. According to the code, a minimum of ten test specimens is needed to make a valid statement about the average biaxial flexural strength. Table 7 shows all the checks for the different thicknesses with the dimensions for the specimens as mentioned above. Each column contains a specific thickness. So, there are four glass panes of 4 mm thickness, two panes of 5 mm, four panes of 6 mm and two panes of 8 mm thickness. More on the naming of specimens later in this chapter. As can be seen, each check is satisfactory, and the choice of this dimension can be accepted according to the code.

Table 7. Verification of dimensions of specimens and rings according to ASTM C1499-09.

<i>Series</i>		2-in, 3-in, 4-in, 5-in	2-out, 3- out	1-in, 4-out, 5-out, 6-out	1-out, 6-in
Specimen's thickness	h (mm)	4	5	6	8
Width	l ₁ (mm)	150	150	150	150
Length	l ₂ (mm)	150	150	150	150
Equivalent diameter	D (mm)	162	162	162	162
Expected eq. biaxial strength	σ _f (MPa)	100	100	100	100
Young's Modulus	E (MPa)	70000	70000	70000	70000
Diameter of supporting ring	D _S (mm)	120	120	120	120
Diameter of loading ring	D _L (mm)	60	60	60	60
Verification					
Max specimen's thickness	h _{max} (mm)	12.0	12.0	12.0	12.0
Min specimen's thickness	h _{min} (mm)	4.0	4.0	4.0	4.0
Thickness check		OK	OK	OK	OK
(D-D _S)/h		10.5	8.4	7.0	5.25
Overhang size check (2 ≤ x ≤ 12):		OK	OK	OK	OK
D _L /D _S		0.50	0.50	0.50	0.50
Ratio diameter check (0.2 ≤ x ≤ 0.5):		OK	OK	OK	OK
l ₁ /l ₂		1.00	1.00	1.00	1.00
Ratio edges check (0.98 ≤ x ≤ 1.02):		OK	OK	OK	OK

4.5 Specimen preparation

After determining what the dimensions of the specimens should be, namely 150mm x 150mm x (thickness) mm, the next step is to prepare the specimens. A number of steps precede when a specimen is ready for testing. As shown in Table 6, six IGUs were made available for this study. Because the IGUs consist of two glass panes, the first step is to separate the glass panes. This was done manually with the help of lab assistant John Hermsen. The spacer and sealing hold the two glass panes together, and so the task was to cut them through. This was eventually done in a systematic way, to keep the

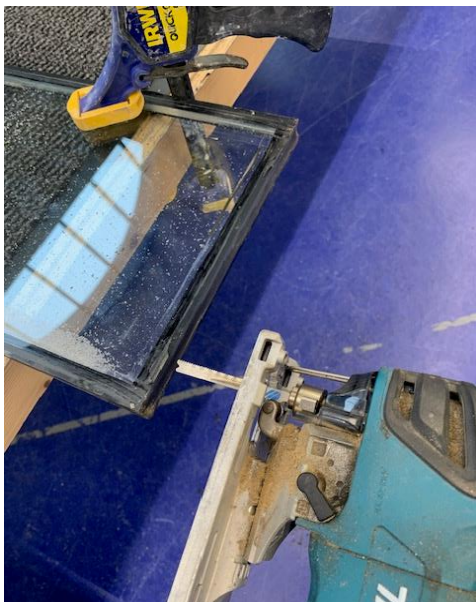
amount of smell, mess and noise as low as possible. Because there was plastic reinforcement in the corners of the IGU, it was necessary to cut the corners with a grinder. This gave a lot of smell, caused by the rubber sealing. Once the corners were cut with the grinder, the edges of the IGU were further cut with a jigsaw. To get properly between the two panes with the saw, a hole was drilled with an electric drill prior to this. All these steps involved trying not to touch the glass on the inside with the grinder, drill and jigsaw. This method of separation is shown in Figure 26. Additional damage to the glass could affect the results of this study, which is not desirable. Minor damage caused by the release of the moisture-resistant granules contained in the spacer is almost impossible to prevent. All the grains are removed after separating the panes and the glass panes are cleaned as best as possible to continue with the cutting process.



(a) Cut corners with grinder



(b) Drill a hole to get between the panels



(c) Cutting the edges with a jigsaw



(d) Release of moisture-resistant granules between panes

Figure 26. Separating the panels.

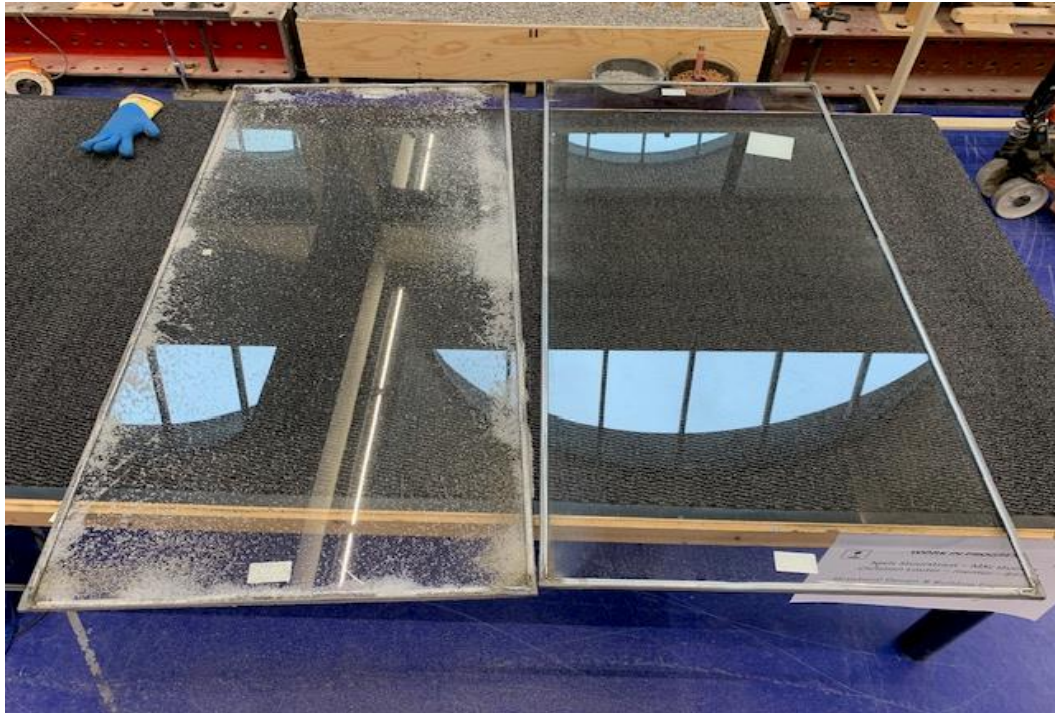
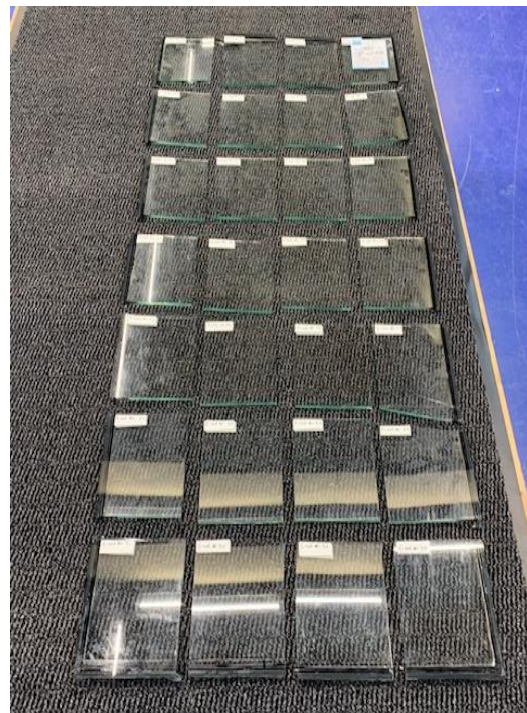


Figure 27. From one IGU to two separate panes.

After all the six IGUs were separated into twelve glass panes (Figure 27), the next step was cutting. The panes were cut into as many 150mm x 150mm specimens as possible. First, horizontal strips were cut, as shown in Figure 28a, then square specimens were cut from them, shown in Figure 28b. The cutting was done with an oil glass cutter and was carried out by me. Because the cut spacer and sealing did remain attached to the glass panes at the edges, breaking, especially the 8 mm thick panes, was sometimes tricky. With a few exceptions, all specimens are neatly 150mm x 150mm.



(a) Horizontal strips



(b) Square specimens

Figure 28. Cutting process.

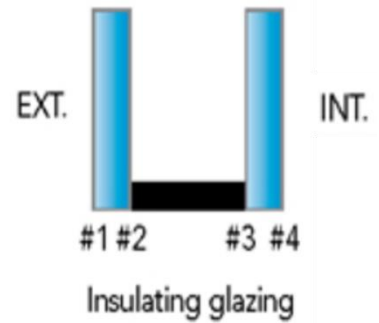
As also mentioned above, the spacer and sealing residue were still attached to the glass plates. To get flat specimens, a knife was used to manually remove the excess remains of the spacer and sealing. How this was done is shown in Figure 29a. It was not possible to remove all residues, such as the bitumen layer under the spacer. This adhesive layer ensures that the spacer stays attached to the glass. The residues were removed as best as possible without damaging the glass. The glue residue remaining on the glass after this is located at the edge of the specimen and it is assumed that this does not affect the results of the tests.



(a) Remove spacer and sealing remain

5-out #2 1.4	5-out #2 1.3	5-out #2 1.2	5-out #2 1.1
5-out #2 2.4	5-out #2 2.3	5-out #2 2.2	5-out #2 2.1
5-out #2 3.4	5-out #2 3.3	5-out #2 3.2	5-out #2 3.1
5-out #2 4.4	5-out #2 4.3	5-out #2 4.2	5-out #2 4.1
5-out #2 5.4	5-out #2 5.3	5-out #2 5.2	5-out #2 5.1
5-out #2 6.4	5-out #2 6.3	5-out #2 6.2	5-out #2 6.1
5-out #2 7.4	5-out #2 7.3	5-out #2 7.2	5-out #2 7.1

(b) Naming of panel 5-out



(c) Different IGU sides

Figure 29. Specimen preparation.

A step that has actually already gone into during the previous steps is the naming of the specimens. During the cutting process, stickers are constantly used to know which glass pane is cut from which IGU. For example, there are 6 IGUs so each sticker starts with a 1, 2, 3, 4, 5 or 6. Thus, it can be found out which IGU the glass pane comes from. Because each IGU consists of two glass panes, each number is followed by '-in' or '-out'. This makes it known whether we are dealing with the inner or outer panel of the IGU in question. The inside panel refers to the panel that is on the interior side of the building, and the outside panel is therefore on the exterior side. A #1, #2, #3 or #4 is then added to the name of a specimen. This indicates which can of the IGU we are dealing with. Side #1 and #2 are on an exterior panel, and #3 and #4 are on an interior panel. This can be seen in Figure 29c. The remainder of the report will often refer to side #1 to #4, thus referring to the sides shown in Figure 29c. Finally, to the name of a specimen comes the location of the specimen in the corresponding glass pane. Figure 29b shows the structure of the naming of a glass pane. It must be said that in this case the numbering of the columns is the other way around in comparison with the other side of IGU 5-out. This is because then the column numbers of IGU 5-out side #1 are the same as IGU 5-out side #2.

In short, the naming of a specimen can be read as follows:

(number of IGU) - (inner/outer panel) (#side) (rownumber.columnnumber)

For example: 5-out #2 4.3 is:

- IGU number 5 (front façade, 9th floor, middle window from nr. 355 (Table 6));
- outer pane;
- side #2;
- row 4;
- column 3.

Table 8 gives an overview of the number of specimens present after all IGUs have been separated, cut and stickered. Since there are six IGUs, this results in twelve glass panes. Because not all panes are the same size, the number of specimens per series is not equal. In the end, there are 406 specimens.

Table 8. Overview of the specimens number and dimensions of each testing series.

<i>Series</i>	Dimensions (mm)	Amount of specimens
1 - out	150x150x8	40
1 - in	150x150x6	40
2 - out	150x150x5	40
2 - in	150x150x4	40
3 - out	150x150x5	34
3 - in	150x150x4	34
4 - out	150x150x6	32
4 - in	150x150x4	34
5 - out	150x150x6	28
5 - in	150x150x4	28
6 - out	150x150x6	28
6 - in	150x150x8	28

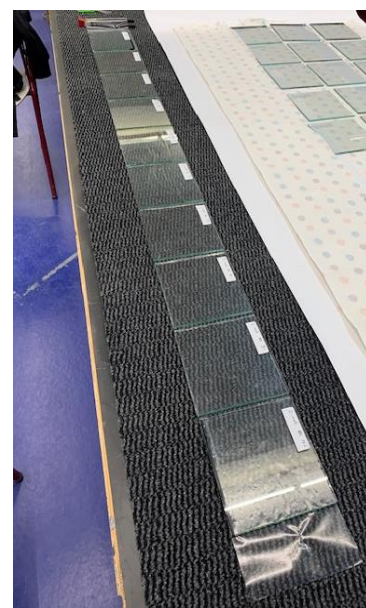


Figure 30. Manually applying foil to specimens.

The final step to be performed before testing can take place is the application of an adhesive foil layer. This is done on the side of the glass of the glass that is not being tested, or the side where compressive stress will occur. This is to prevent the foil from affecting the measured tensile stress when a specimen collapses. The reason a foil has to be applied is the fact that it is desirable that after a specimen collapses, the glass fragments remain in place. Thus, the location of the origin of collapse can be more easily determined. This film was cut into 150mm strips so that it was easy to apply to the specimens. This was also carried out manually. By laying down a strip of the foil, and then placing a number of specimens on it, it is an efficient way of applying foil manually (Figure 30). The foil should be kept tight, to avoid air bubbles and the foil sticking crookedly. Preventing some air between the foil and the specimen is almost impossible when done manually. Ultimately, the influence of air bubbles during testing is assumed to be negligible.

4.6 Microscopy examination

Prior to destructive testing, a number of specimens are studied under the microscope. One reason for this is to see what type and how much damage can be seen on the surface of naturally aged glass. The microscope can be used to measure how big the damages are on or in the surface. Another purpose of the microscopic examination to see differences in surface damage from different sides of the IGU. In advance, it is expected that more and/or different damage will be seen on the outer sides (side #1 and #4) of the IGU than the two sides of the IGU located on the inside, or cavity side (side #2 and #3). Something that can also be linked to this is the fact that the IGUs come from different locations in the building. Consider whether, for example, a west-facing window has different damage than an east-facing window. In short, the goals of viewing a number of specimens with the microscope are:

- the type of damage;
- the size of the damage;
- the differences in damage between different sides.

The way to achieve these goals is through the microscope used, the Keyence VHX7000 digital microscope. This microscope is connected to a monitor that shows live images of what the test specimen what is under the microscope. Various magnifications can be applied, with magnifications ranging from 20x to 3000x being used for this study. The microscope has the ability to zoom in further up to 6000x magnification, but this magnification was not needed for this study. Another specification of the microscope is that it can accurately measure the size of defects, thus knowing how big scratches or craters are in the glass.



Figure 31. Keyence VHX7000 digital microscope.

The choice was made not to view all specimens under the microscope. This is due to the fact that it is not the main purpose of this thesis to view glass under the microscope, but it may help explain results found during CDR testing. Thus, 24 specimens (out of a total 406) were chosen for microscopic examination. From each of the six IGUs obtained, four specimens were picked, with each side of the IGU containing one specimen. For each IGU, a specimen was always chosen that came approximately from the centre of the glass panel. For clarification, Table 9 lists the specimens used for microscopic examination. For each specimen, only the side tested in the CDR test is subjected to the microscopic examination.

Table 9. List of microscopically examined specimens.

IGU	Specimen
1	1-out #1 5.3
	1-out #2 5.2
	1-in #3 5.3
	1-in #4 5.2
2	2-out #1 6.3
	2-out #2 6.2
	2-in #3 6.3
	2-in #4 6.2
3	3-out #1 5.3
	3-out #2 5.2
	3-in #3 5.3
	3-in #4 5.2
4	4-out #1 5.3
	4-out #2 5.2
	4-in #3 5.3
	4-in #4 5.2
5	5-out #1 4.3
	5-out #2 4.2
	5-in #3 4.3
	5-in #4 4.2
6	6-out #1 4.3
	6-out #2 4.2
	6-in #3 4.3
	6-in #4 4.2

The only part of the specimens considered is the part that falls within the loading ring used in the destructive testing. In this case, at the centre of each specimen is a circle with one diameter of 60 millimetres. This is because the highest stress is generated in this area during CDR testing. Despite this, a larger flaw may cause critical defects outside this area. Because these tests are considered invalid, there is no need to map the defects outside the area which falls within the loading ring. This circle cannot be seen in the microscopic photographs. This is because this circle is marked off at the time of the CDR tests, which is after the microscopic examination.

Before the specimens could be put under the microscope, it was necessary to rid them of all unnecessary dirt. This was done with the acetone and a clean cloth, after which, after much effort, the specimens were cleared of all dirt and dust particles. When dirt particles were also seen under the microscope, a damp cotton swab was used to remove the remaining dust particles.

After the specimens were completely clean, the damage was examined for each specimen. To reflect this, a photograph was systematically taken for each specimen at 20x magnification and 50x magnification. After this, each specimen was further zoomed in and searched for the largest defect. These defects were then measured and photographed, at magnifications ranging from 100x to 3000x.

4.6.1 Side #1

Looking at side #1 (outer side of the outer panel), many small pits (pits, small craters) can be seen mainly, with diameters ranging from 23 to 210 micrometres. An example of such a pit is shown in Figure 32 (bottom left). Furthermore, rectilinear scratches were seen on a number of specimens, probably due to window cleaning, as shown in Figure 32 (right picture). Because we are talking about the outside side of the window here, it is to be expected that cleaning scratches could be found here. We also noticed a large scratch in specimen 2-out #1 6.3 (top left), which looks very much like a transport sanding spot, as this scratch seems too large in size for a cleaning damage spot.

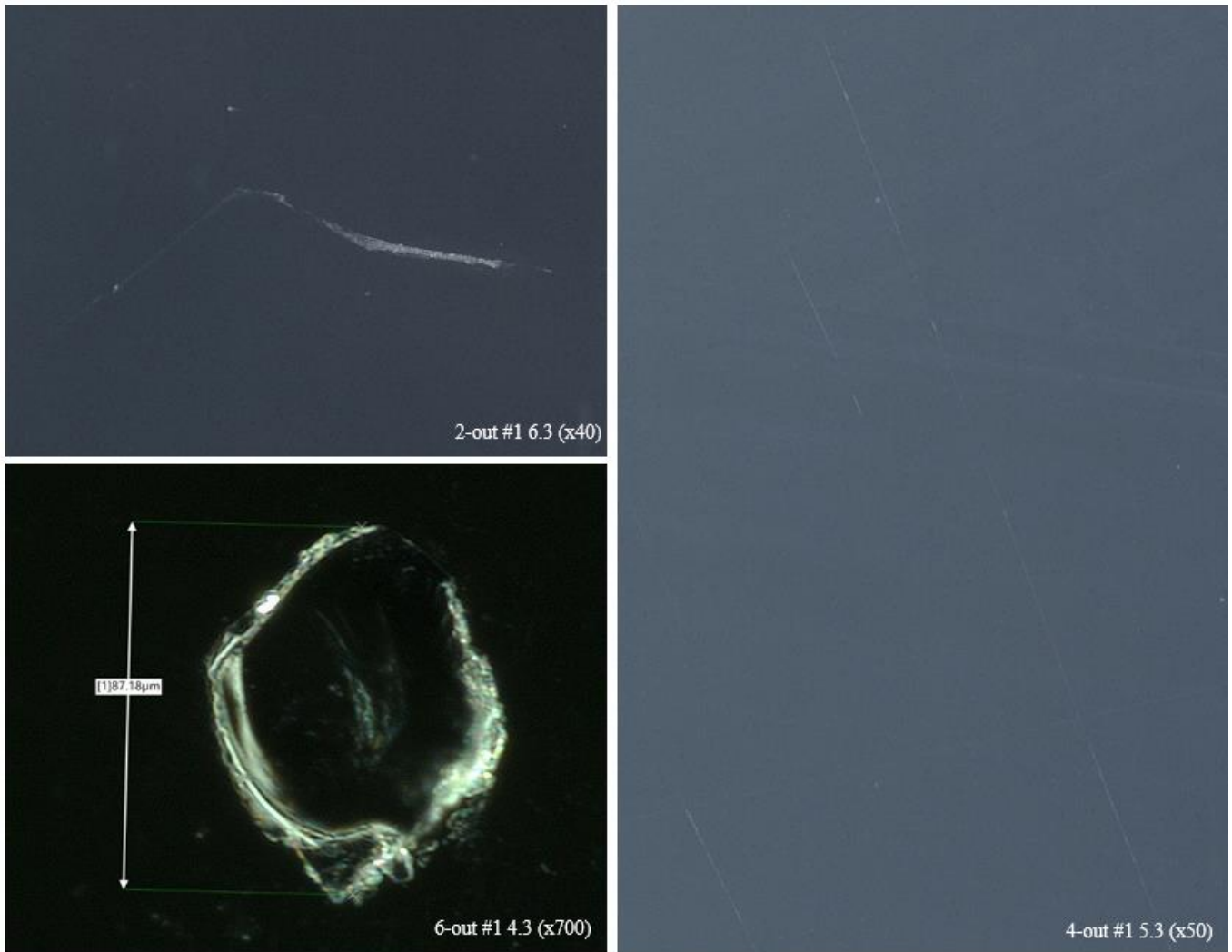


Figure 32. Microscopy examination side #1.

As described earlier, a distinction can be made for side #1 in terms of orientation of the IGU in the building. Because the wind in the Netherlands most often comes from the west and southwest in any month of the year (Infoplaza, n.d.), a window that has side #1 facing southwest might have more damage from, for example, sand particles carried away by the wind or rain. It is known that IGU 1, 2 and 5 are located on the east side, and IGU 3, 4 and 6 on the west side of the building (Table 6). Based on these data and the information from the microscopic examination, it can be concluded that there are no obvious differences in damage pattern between the tested specimens of IGUs 1, 2 or 5 and IGUs 3, 4 or 6. For instance, side #1 of IGUs 1 and 5 are even slightly more damaged than side #1 of IGUs 3

and 4. Because only a few specimens (24 out of a total of 406) were tested under the microscope, no clear conclusion can be drawn from this investigation about the damage pattern related to the orientation in the building. To draw a more reliable conclusion about the damage to an IGU in combination with the orientation of the window in a building, a follow-up microscopy examination should be done, looking at entire panes, rather than just a few specimens.

4.6.2 Side #2

The expectations for side #2 (inner side of the outer panel) are different from that of side #1. Because this side has not been exposed to the environment and (human) touches during its lifetime, different and less damage is expected here. Nevertheless, quite a lot of damage was found here that was also seen on side #1. Here too, although to a slightly lesser extent, damage was found with a diameter almost always around 40 micrometres, as shown in Figure 33 (top left). Furthermore, a damage pattern stood out at specimen 3-out #2 5.2, where it can be clearly seen that the angle grinder did indeed cause

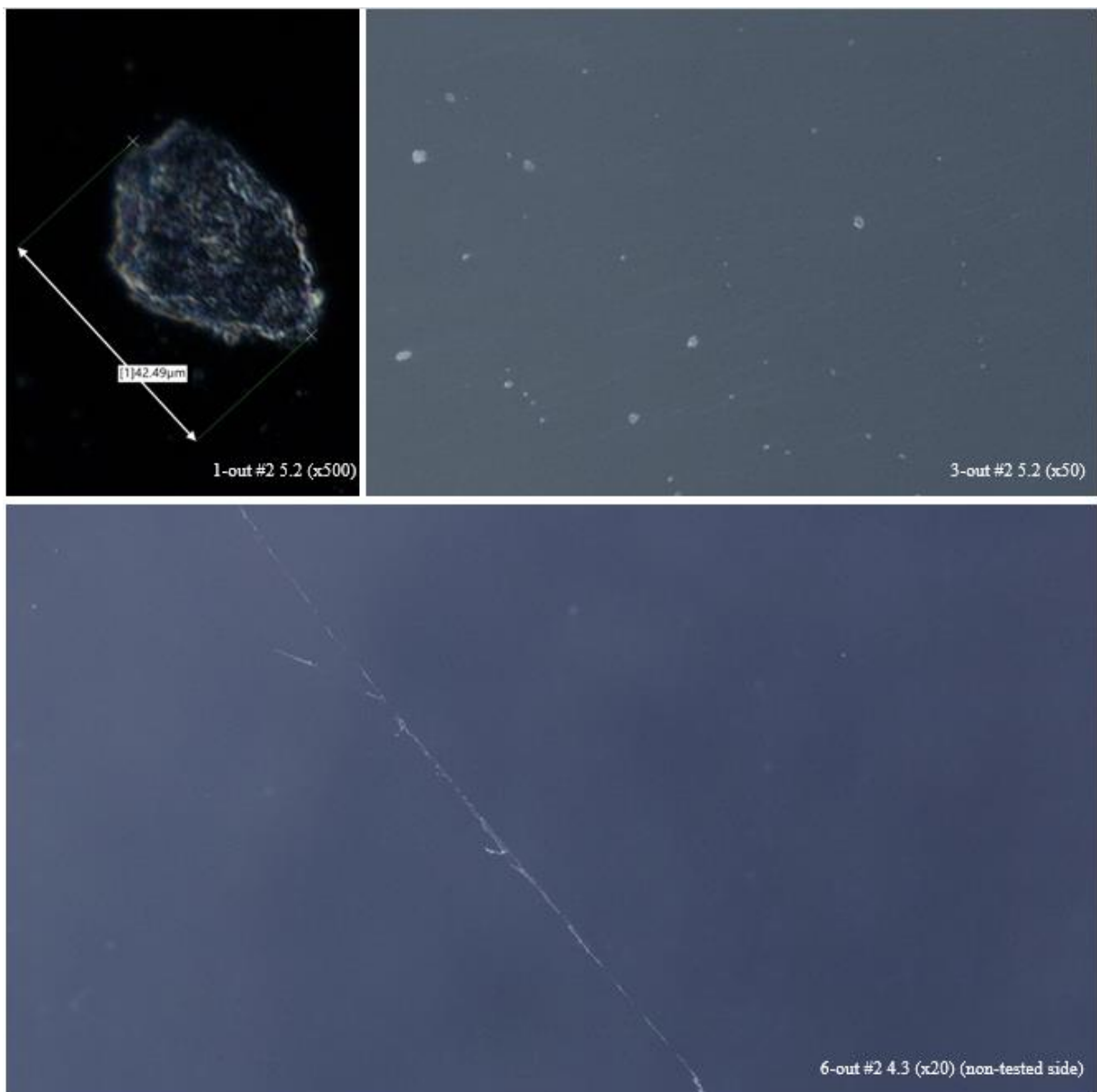


Figure 33. Microscopy examination side #2.

the pattern of damage that occurs according to theory (Glass Damage, 2006) (Figure 33 on the right). It was striking to see how much damage side #2 had compared to side #1. Where you expect to discover almost no damage, the difference in damage with side #1 was actually quite small. Similarly, a large scratch was found (although on the side not being tested), which was thus created before or after the IGU's life stage by probably transporting, as shown in Figure 33 (bottom).

4.6.3 Side #3

For side #3 (inner side of the inner panel), a similar type of damage pattern is expected in advance as for side #2. In general, in terms of numbers, not many damages were visible in the specimens tested on side #3 with the microscope (see Figure 34 in the bottom left). In contrast, the lesions found were quite large and localised. Many large pits (140 to 300 micrometres in diameter) and a number of scratches, as seen in Figure 34. As with side #2, cutting the corners of the IGUs can cause damage due to the sparks caused by the angle grinder. The large pits like Figure 34 (bottom centre), probably have a different cause. The pits or digs were probably caused before or after the life of the IGU, making a tap on the pane with some object during transport the most obvious. With any damage, the cause remains an uncertainty, so too with these relatively large pits.

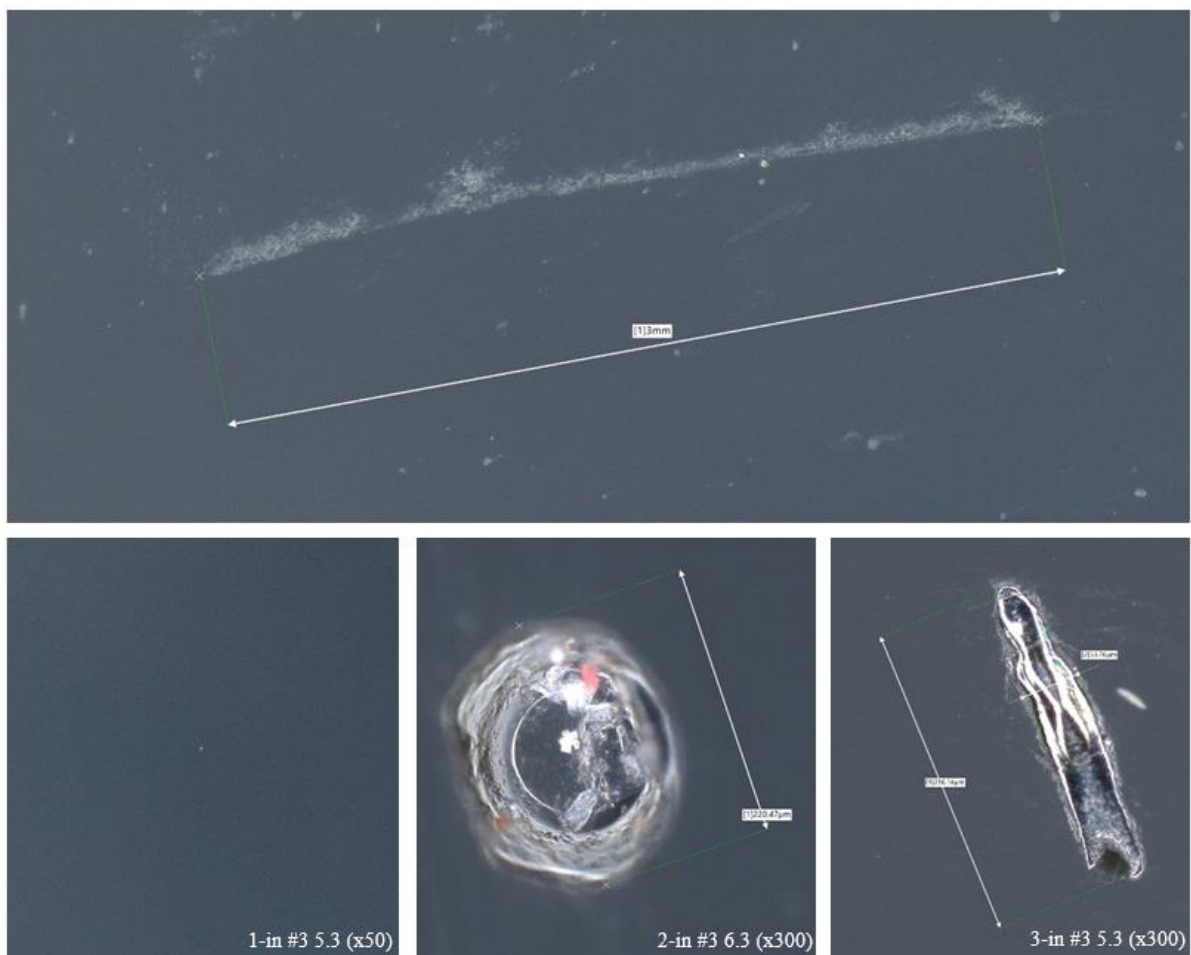


Figure 34. Microscopy examination side #3.

4.6.4 Side #4

Side #4 (inner side of the inner panel) is the side of the IGU that sits on the interior side. It is therefore expected that this side, like side #1, contains cleaning damage. Overall, the tested specimens show quite a lot of different patterns of damage. The number of damages is also quite large compared to side #2 and #3, and similar to side #1. For instance, scratches can be seen, but also localised pits of again around 40 micrometres. The bottom left of Figure 35 shows a probable trace of cleaning damage, with the 'smudge' clearly visible in the damage pattern. A likely explanation for the damage seen in the upper right of Figure 35 is chemical surface damage. This is caused by longer-term action of cement mortar or another grouting material. Cured mortar splashes on the surface can also look like this. Surely it cannot be ruled out either that this damage is due to transport or a contact with some object.



Figure 35. Microscopy examination side #4.

Appendix C shows an overview where all overview images for all sides are shown for both x20 and x50 magnification.

4.6.5 Strongest vs weakest

When looking for the strongest specimen (after all CDR tests were performed) viewed under the microscope, it was found to be specimen 4-in #3 5.3 (121.8 MPa). The weakest specimen viewed under the microscope was specimen 6-out #2 4.2 (39.2 MPa). The damage images of these specimens clearly differed from each other, with a lot more damage seen in this case with strongest specimen than the weakest specimen. Still, the amount of damage is of less importance than the size of the damage, this analysis shows. Figure 36 shows how many small lesions (craters) are present on the strongest specimen. The pits here are almost all between 30 and 40 micrometres in diameter.



Figure 36. Microscopy examination strongest specimen 4-in #3 5.3 (x20)

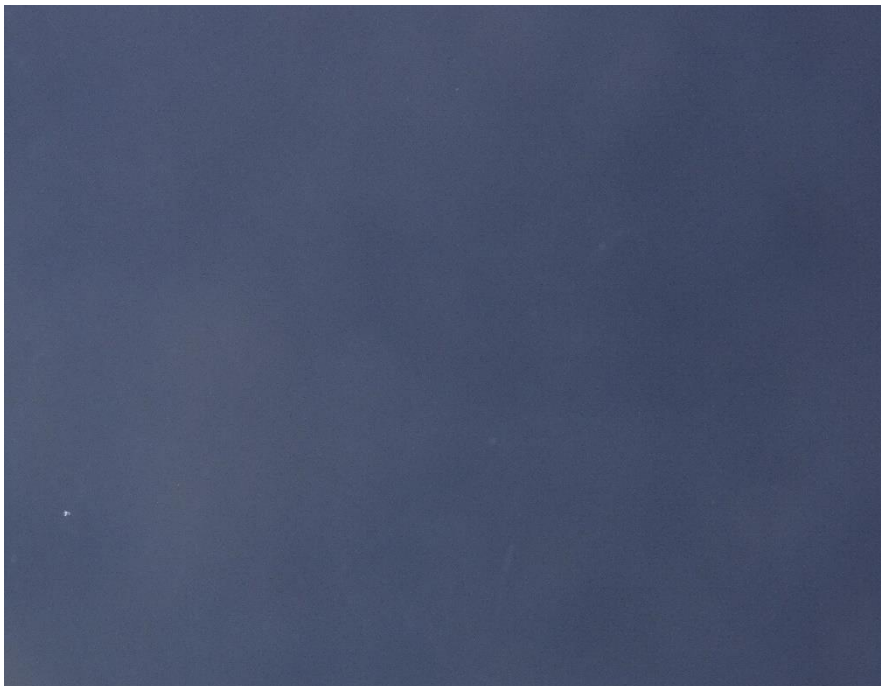


Figure 37. Microscopy examination weakest specimen 6-out #2 4.2 (x20)

The weakest specimen, as can be seen in Figure 37, actually has much less damage at first glance. However, it does have one large pit (bottom left), which determines the strength of the glass panel in this case. This relatively large damage has a diameter of around 120 micrometres and is then of great influence on the measured strength of this specimen. A zoomed-in image of this damage is shown in Figure 38. It thus indicates that more damage does not lead to a weaker specimen, the size of the damage is of greater importance, and largely determines the strength that is measured.

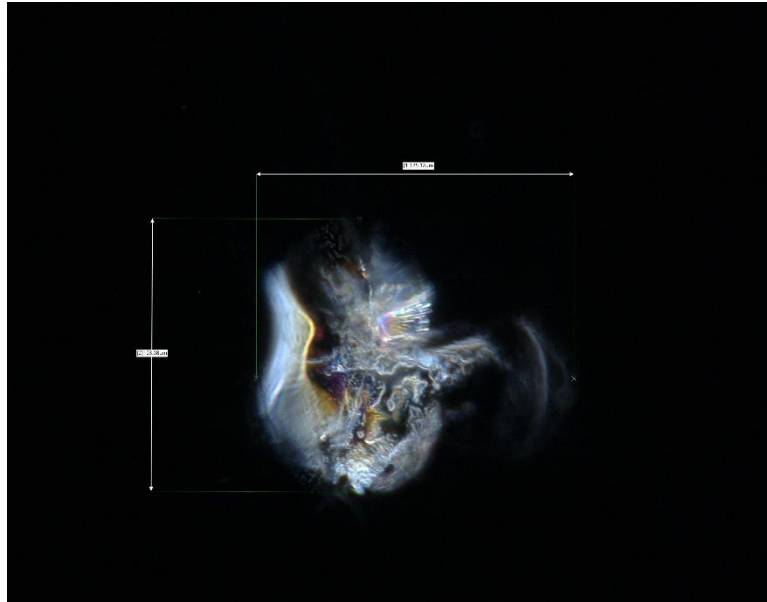


Figure 38. Big damage on 6-out #2 4.2 (x1000)

4.7 Tin- and air-side

During the production process, as mentioned earlier in Chapter 2, the glass is cast on a bath of tin. This leaves residues of tin on one side of the glass, or tin-side. The other side, the side that is on top during production, is called the air-side. There are several ways to determine the tin- and air-sides afterwards. Firstly, this can be done by performing a chemical analysis. This may determine the chemical composition of the glass. It is to be expected that one of the two sides of the glass contains traces of tin. This is the so-called tin-side and this side was therefore in the tin bath during production. Another way of finding out the tin-side, is to use a tin tester, shining a black light on the surface. The device used, CRL Standard Tin Side Detector Model #TS1301, is shown in Figure 39.



Figure 39. Tin-side detector.

The short-wave UV radiation causes the tin to glow with a fluorescent light. When the lamp is shone on the air-side, only the violet UV light is seen. This is because the float glass does not transmit the UV light, and the tin-side is not exposed to the UV radiation. To determine the tin- and air-side of the glass under test, this tin tester was used. So, each glass plate in a dark room tested with the tin tester. It was very clear to see what the tin-side was. This side lit up grey, while the air-side did so much less. This can be clearly seen in Figure 40 (because it was impossible to take a clear picture in the dark room, a picture from another test was used).

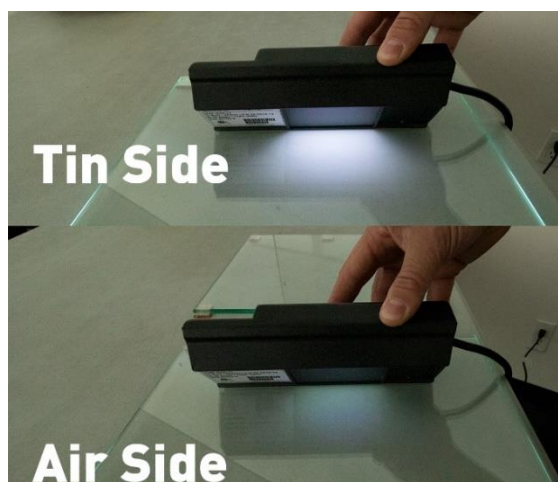


Figure 40. Tin- and air-side determination (Garibaldi Glass, 2021).

One or two specimens per series were then checked on which side is the tin-side. Table 10 gives an overview of which sides are the tin- and air-sides of the received IGUs:

Table 10. Overview of tin- and air-sides of the IGUs.

Number	Name	Tin-side	Air-side
1	Front façade 2 nd floor L 247	#2 & #4	#1 & #3
2	Front façade 2 nd floor R 233	#1 & #3	#2 & #4
3	Back façade 2 nd floor L 247	#1 & #3	#2 & #4
4	Back façade 2 nd floor R 233	#1 & #4	#2 & #3
5	Front façade 9 th floor middle 355	#1 & #4	#2 & #3
6	Back façade 9 th floor middle 355	#2 & #4	#1 & #3

4.8 Prestress measuring

During cooling in the production process of float glass, cold air is blown onto the glass. After this, the outer skin of the glass is cooled while the inner core cools more gradually. As a result, the inner core slowly shrinks, and the outer skin is compressed. This creates a compressive stress on the outer skin and tensile stress in the core. Figure 41 shows a typical stress gradient of a sheet of glass.

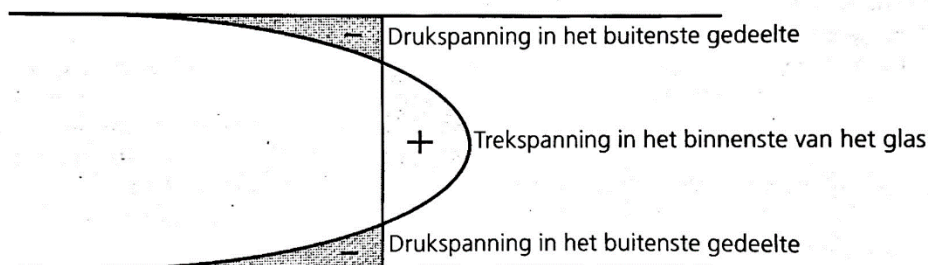
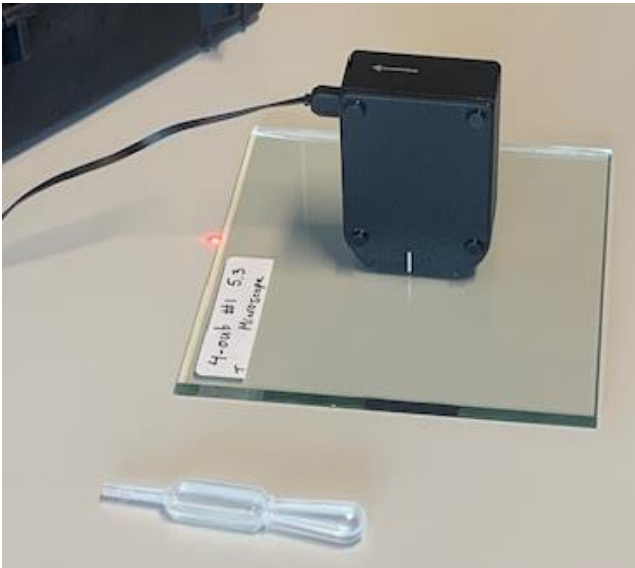
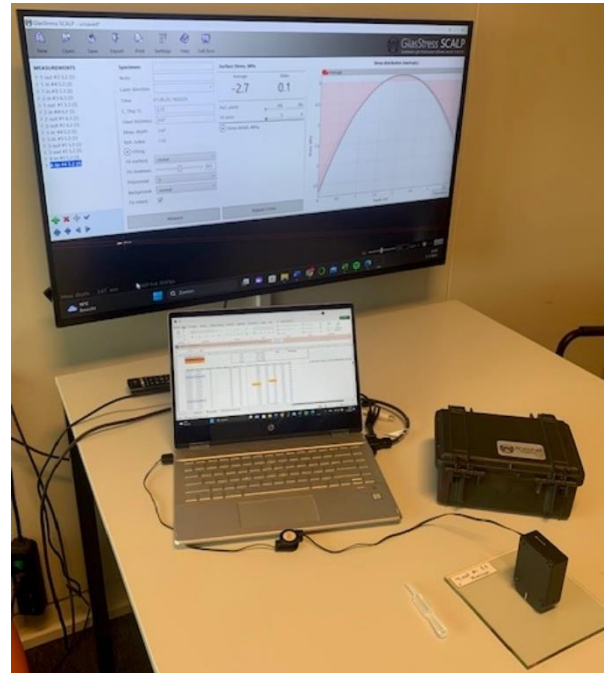


Figure 41. Stress gradient glass.

Because in the tests, the surface loaded on tensile force fails, the prestress from this surface is measured. According to theory, a compressive stress is therefore expected at the outer edge of the glass cross-section. The way this is measured is using a device called the SCALP-05. SCALP-05 is a compact scattered light polariscope for depth wise stress measurement in sheet glass. SCALP uses the scattered light method to determine through the thickness stress distribution (residual and loading stress) in annealed, heat-strengthened and fully tempered flat glass products. Using the SCALP is straightforward. First, the device is connected to a PC. The next step is to clean the glass and add a drop of immersion liquid. Then the SCALP is placed on this spot and click start in the software displayed on the PC. After three seconds, the stress profile is shown on the screen. The figures below are two photos of the setup used to measure prestress in the glass.



(a) SCALP-05 placement on specimen



(b) Setup

Figure 42. Setup prestress measuring with SCALP-05.

For each glass slide obtained, two specimens were chosen to measure with the SCALP. Because twelve glass panes were obtained (six IGUs, i.e. twelve panels), the measurement was performed a total of 24 times. It was assumed that when a certain prestress was measured for a specimen, this value also applies to the rest of the surface of this glass panel. It was thus assumed that there is a homogeneous prestress on the surface of a glass panel. In each case, a specimen was chosen that comes from the centre of a glass panel. Each of the 24 specimens tested was measured five times with the SCALP, to then arrive at an average value for the specimen tested.

Appendix A shows all of the specimens tested and their corresponding measured values. In Table 11 an overview of the sides with corresponding prestresses measured. The values range from -4.57 MPa to -2.53 MPa. As expected, surface compressive stresses were measured everywhere. The software showed that the further into the glass, the smaller the compressive stress becomes, changing to a small tensile stress at the centre, as shown in Figure 42b on the computer screen.

Table 11. Prestress for each panel.

Panel + side	Prestress (MPa)
1-out #1	-4.43
1-out #2	-4.40
1-in #3	-3.61
1-in #4	-3.50
2-out #1	-3.19
2-out #2	-2.53
2-in #3	-3.13
2-in #4	-2.69
3-out #1	-3.17
3-out #2	-3.35
3-in #3	-2.89
3-in #4	-2.70
4-out #1	-3.78
4-out #2	-3.45
4-in #3	-2.54
4-in #4	-2.68
5-out #1	-3.49
5-out #2	-3.67
5-in #3	-2.83
5-in #4	-2.70
6-out #1	-3.56
6-out #2	-3.62
6-in #3	-4.57
6-in #4	-4.51

The values shown above are subtracted from the measured tensile stress which was needed to make the glass break. As a result, the actual tensile stress required to make the glass break is slightly lower than what the CDR test machine measures.

4.9 CDR tests

This section successively describes the procedure of CDR testing and shows the results obtained in summary. The results of CDR tests for all 406 specimens are shown in Appendix D. The tests were conducted at a temperature between 19.4 and 25.2 degrees Celsius. The relative humidity during the tests was minimum 25.0% and maximum 61.5%. Despite these differences, no correlation was found between the measured failure stresses and temperature and/or relative humidity. For this study, the influence of these conditions is therefore disregarded.

4.9.1 Machine

The CDR tests were carried out using Unitronic's machine TC-K5M-F-S, with a range of 5000 kg (50 kN). This machine can perform both pressure and tensile tests on different materials. This machine was located in the steel lab of Civil Engineering at TU Delft. This machine works with a displacement-controlled motor, measuring the force to achieve a given displacement. The linked software gave as output a force-displacement diagram, after which the stress at which the tested specimen failed can be calculated.

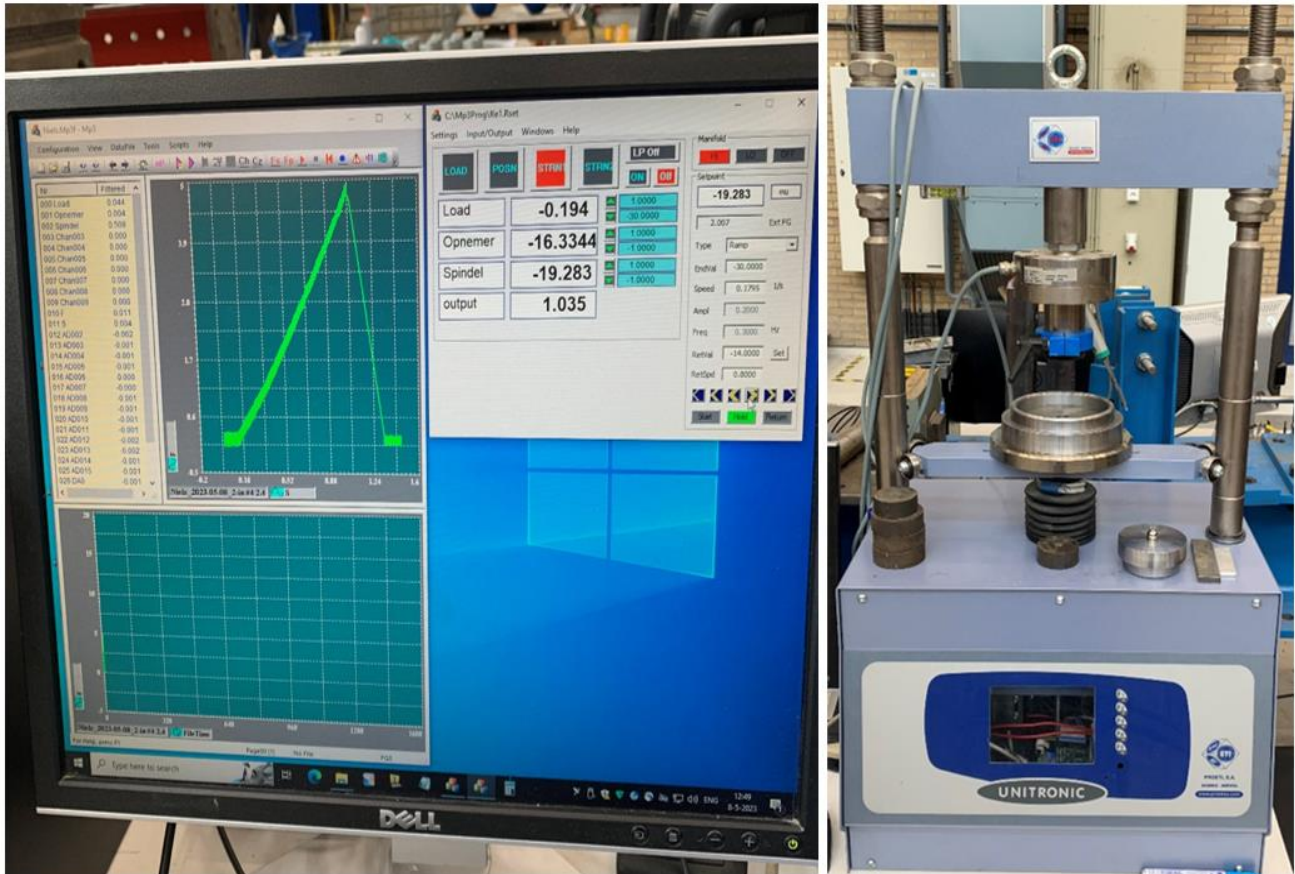


Figure 43. Used software and machine for the CDR tests.

For the tests, the same stress rate is used for each specimen. A stress rate of 20 MPa/s was used for all tests. Because not all specimens have the same thickness, the following formula from the ASTM C1499-09 (2013) standards were used to calculate the displacement rate for all specimens:

$$\delta = \left(\frac{D_s^2}{6 * E * h} \right) * \sigma \quad (8)$$

Where:

- δ = the displacement rate in units of mm/s,
- D_s = diameter of the supporting ring in mm,
- E = the modulus of elasticity in units MPa,
- h = mean thickness of the specimen in mm,
- σ = rate occurring within the test specimen in units of MPa/s (20 MPa/s)

4.9.2 Procedure

The steps taken during testing are briefly explained below. For each specimen, these steps are performed in the same order each time, to obtain the most reliable results possible.

1. Remove name tag

To rule out the possible minimal influence of a sticker on the surface.

2. Put specimen on support ring

Manually, a specimen is placed in the centre of the support ring. The human eye ensures that the specimen is as well centred as possible. To ensure that the support ring always lies the same, a drawn line has been used to ensure that the orientation is always the same.

3. Put loading ring on specimen

After the specimen lies on the support ring, the machine places the loading ring on the surface of the specimen, without applying any force to it. Again, a line was drawn on the loading ring to have the orientation of this ring the same for each test.

4. Rut the rings and specimen 'tight'

Now the glass specimen is fixed, and so there is minimal force on the glass.

5. Mark the rings on the specimen

Fixing the specimen allows the rings to be marked on the glass surface. This is necessary to determine the origin of failure after testing.

6. Set speed (mm/s)

Because it was chosen to load each specimen with the same stress rate of 20 MPa/s, the load rate in mm/s is different for each specimen. This is because the specimens have different thicknesses. The thickness of each specimen is shown in Appendix B.

7. Set variables on 0 (set offset)

After the speed is set, all variables are set to zero. These variables are displacement (mm), force (kN), time (s), temperature (°C) and relative humidity (%).

8. Start measuring

Before pressing on the glass, the measuring equipment is turned on. This is to prevent the machine is already executing a force on the specimen without being measured.

9. Start pressing machine

The machine is switched on and presses the specimen with the input displacement rate in mm/s. The force it takes to affect this displacement is measured.

10. Failure

The specimen breaks or tears.

11. Stop pressing machine

The machine is stopped after failure so that no further pressure is exerted on the glass and no more cracks appear.

12. Stop measuring

Then the measuring equipment is stopped and the position of the pressing device is restored in original. The specimen can now be removed from the machine.

13. Put back sticker on specimen

Finally, the name sticker of the specimen is placed on the tested side.

14. Note location of origin of failure

Finally, it is noted where the origin is of the failure. There are four possibilities:

- IR: inside the loading the ring
- LR: on the loading ring
- OR: outside the loading ring
- ND: not detectable

More on fracture origin location in Section 5.2.

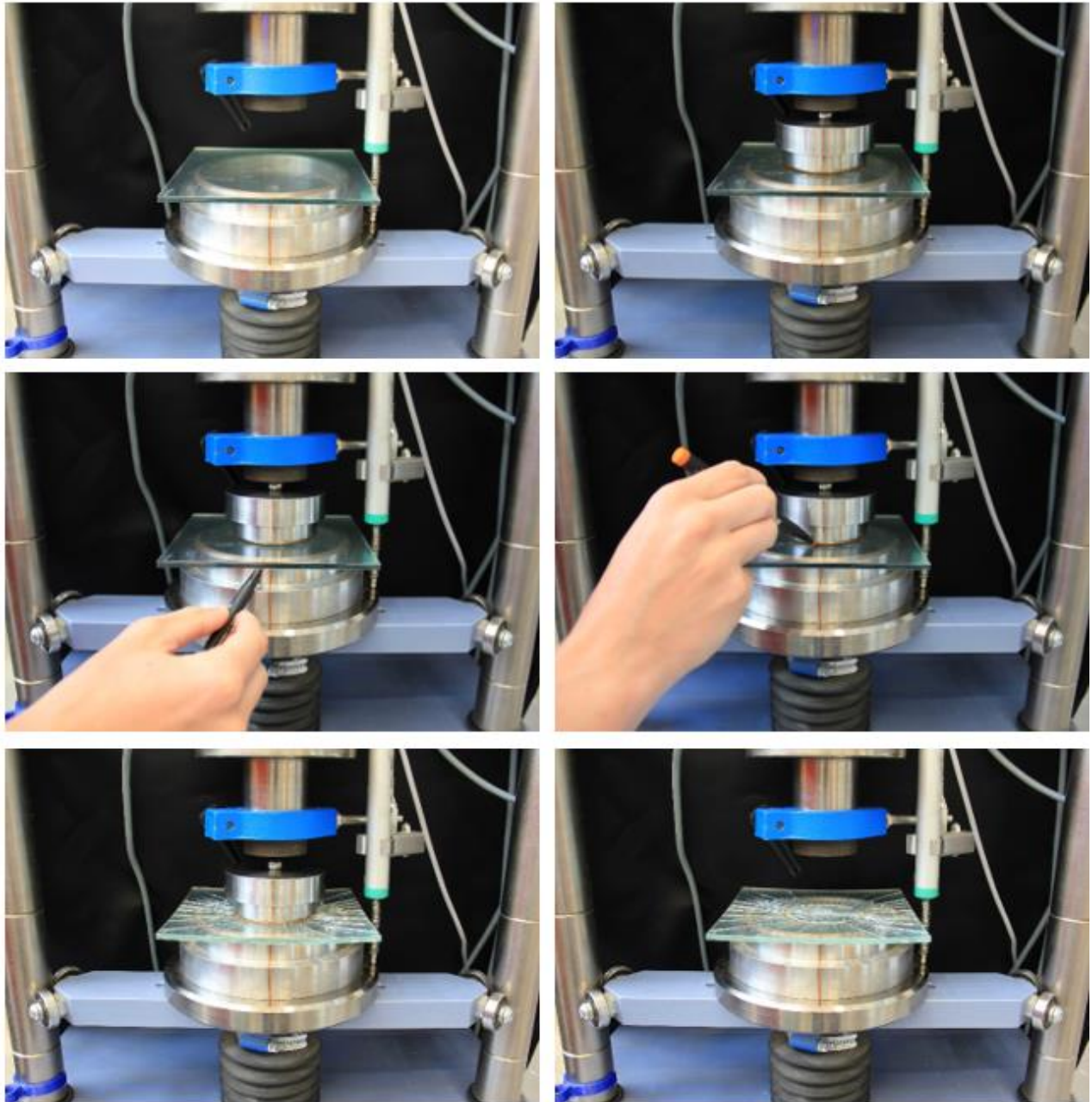


Figure 44. Testing procedure.

After a test, the measurement results can be obtained from an excel file in which every 0.01 seconds the five variables mentioned in step 7 of the procedure are measured. To search for the moment of failure in the excel file, a python script was written that searches for this value. The corresponding displacement, time, temperature and relative humidity are also displayed here. To look for the starting point, or the point when the machine has to apply force to the specimen, we looked at when the measured force is 75 N than the first measured value. At this point, the count of seconds and displacement to failure begins. This was done because there is some noise on the machine, making it difficult to determine the exact time when the machine applied force. This noise was never bigger than 75 N in amplitude, so that's were the 75 kN came from. It turns out that this inaccuracy has virtually no impact on the final breaking force found at the time of failure. The determination of the breaking force also included the weight of the loading ring, as it also acts as a force on the tested glass. The mass of the loading ring, including the small bullet that acted as a hinge in the machine, is 0.9509 kg. The used python file can be seen in Appendix E.

4.9.3 Results

Twelve glass panels from the total six IGUs received were cut into 406 specimens and tested for bending using the CDR test. The breaking load values ranged from 1139 to 17637 N. Because the machine measures a force at which a specimen fails, and not the stress, formula (9) from the ASTM C1499-09 was used to go from breaking load F to failure stress σ_f .

$$\sigma_f = \frac{3F}{2\pi h^2} \left[(1 - \nu) \frac{D_s^2 - D_L^2}{2D^2} + (1 + \nu) \ln \frac{D_s}{D_L} \right] \quad (9)$$

$$D = \frac{L}{0.90961 + 0.12652 \frac{h}{D_s} + 0.00168 \ln \frac{L - D_s}{h}} \quad (10)$$

$$L = 0.5(l_1 + l_2) \quad (11)$$

Where:

- F = breaking load in N,
- h = thickness of specimen,
- ν = Poisson's ratio (0.23 for soda-lime glass (ISO1288-1, 2016)),
- D_s = diameter of supporting ring,
- D_L = diameter of loading ring,
- D = diameter of a circle that expresses the characteristic size of the plate,
- l_1 = length of specimen's edge in dimension x,
- l_2 = length of specimen's edge in dimension y.

The failure stress values ranged from 16.8 to 243.7 MPa. This includes correction for the value of prestress in the surface of the specimens tested. Then each value was rounded to one decimal place. Table 12 shows a summary of the maximum, minimum and mean failure stress, distinguishing between the different sides of an IGU. The standard deviation and time to failure are also shown in this table. On average, side #3 is the side with the highest mean failure stress, and side #1 has the lowest mean value, and can therefore be seen as the weakest side. Prior to testing, it was expected that side #2 and 3 would require higher force to reach failure than side #1 and #4, due to the degree of damage. While this is the case, the differences are quite small. For instance, side #3 is on average 17% and 11% stronger than side #1 and #4, respectively. Side #2 is on average 14% and 9% stronger than side #1 and #4, respectively. What is most striking in this table are the values of the standard deviation, with side #3 in particular showing a very high value. The standard deviation of side #3 is 139% and 79% higher than side #1 and #4, respectively. This therefore means that at side #3, and to a lesser extent at side #2, there is a lot of variation in the measured values. At side #1, this spread in measured values was much less the case, hence the lower standard deviation. A reason for this may be that side #1 and #4 are more evenly damaged by, for example, wind, rain or cleaning damage, so each specimen contains more or less the same type of damage. Side #2 and #3 contain other types of damage, which may be much more localised. One specimen may contain a large scratch or crater, while another specimen from the same pane contains virtually no damage. Appendix D shows an overview showing these values for each IGU separately. This allows the different IGUs to be compared with each other, something that is discussed further in Chapter 5.

Table 12. Summary of the CDR test results (load duration of 60 sec).

<i>IGU</i>	All			
<i>Series</i>	#1	#2	#3	#4
$\sigma_{f,max}$ (MPa)	132.4	143.5	243.7	145.1
$\sigma_{f,min}$ (MPa)	20.5	16.8	30.3	22.2
$\sigma_{f,mean}$ (MPa)	62.2	71.0	72.6	65.2
Standard deviation	17.3	29.9	41.3	23.1
$t_{f,mean}$ (s)	6.5	7.0	5.9	5.6
No. of tests	104	104	97	101

Table 13 shows a summary showing the average strengths distinguishing between the different IGUs. The variation in values is striking, especially for side #2 and #3. For instance, the values of all specimens tested on side #3 vary on average from 48.1 to 133.8 MPa, which is a difference of 85.7 MPa. At side #1, the highest mean value is 66.0 MPa, and the lowest mean value is 54.5 MPa, which is a much smaller difference (11.5 MPa) than at side #3. This again explains the large difference in standard deviation, as shown in Table 12. Several possible causes of this are discussed in the next chapter in more detail.

Table 13. Average failure stresses of specimens per IGU (load duration of 60 sec).

<i>Side</i>	$\sigma_{f,mean}$ (MPa)				<i>All</i>
	#1	#2	#3	#4	
IGU 1	65.2	52.1	93.3	64.7	66.8
IGU 2	66.0	83.6	48.1	71.7	66.3
IGU 3	58.3	98.4	49.7	80.3	71.1
IGU 4	61.2	80.8	76.6	61.1	69.1
IGU 5	54.5	63.6	133.8	60.4	75.9
IGU 6	66.0	51.5	53.6	54.1	56.4
<i>All</i>	62.2	71.0	72.6	65.2	67.5

4.10 Discussion

The preparation for the CDR tests was long and included many parts. The most valuable part of the test preparation, and actually part of the study, was looking at a number of specimens under the microscope. Different types of lesions were detected of different sizes. It was unexpected that side #2 and #3 also contained as much damage as discovered with the microscopic examination. This damage was somewhat more often localised, but no less significant or affecting. The more scattered damage on especially side #1, ensures that the variation in measured strength during the CDR test was the least. Due to the more localised damage of on side #3, for example, the variation in specimen strength was much greater. Side #3 in particular had some very strong specimens, so some specimens had a fragmentation pattern more expected from toughened glass than annealed.

What was further noticed is that there is no consistency in how the air- and tin-sides of a glass panel are always placed on the same side. Thus, the glass panels of an IGU are not assembled using a particular system always the same when it comes to the air- and tin-sides. The results in the next section show the difference in strength between the air- and tin-sides.

Another part before the CDR test was performed is measuring the prestress in the surface. Because this was not done on all specimens, but on only one specimen per glass panel, there may be small error in assuming that the prestress is the same across the entire glass panel. Should this error be there, this a difference is expected to be very small compared to the failure stress to be achieved for the specimens to break. This will hardly affect the obtained results and graphs shown in Chapter 5.

The strengths of the weathered specimens ranged from 16.8 MPa to 243.7 MPa. Interestingly, the weakest specimen was found at side #2, a side containing less damage from weathering than side #1 or #4. A surface flaw caused in some other way most likely caused this low strength. The average strengths of the four sides ranged from 62.2 MPa to 72.6 MPa, and the average strengths of the separate IGUs ranged from 56.4 MPa for IGU 6 (weakest) to 75.9 MPa for IGU 5 (strongest). The average measured strength of all specimens was 67.5 MPa. That there are variations in the different IGUs is no surprise, as certain glass panels may have been treated in a slightly different way during their lifetime and therefore have a slightly higher or lower strength than another IGU. The differences in strength between the four different sides can also be explained by the degree of weathering. Side #1 and #4 are therefore expected to have a slightly lower average strength than side #2 and #3.

Finally, for IGU 6, it was unclear what the inside and outside of the IGU was during its lifetime in the frame. Because it is actually always the case that the outer panel is thicker than the inner panel, it can be assumed that this is also the case here. Nevertheless, it has been decided to assume the outer panel (side #1 and #2) for 6 mm thickness and the inner panel as 8 mm (side #3 and #4). This is because according to GSF (the company that provided the windows for this study), the sticker with information is always stuck on the outer panel, which in this case was on the 6 mm thick panel. Even with the help of microscopic examination, it is not clear what side #1 and side #4 were during the lifetime, because the damage images of the two specimens of these sides of IGU 6 viewed were hardly different from each other.

5. Failure Analysis

5.1 Introduction

In this chapter, the results of the CDR tests shown in Section 4.9.3 are analysed in more detail. First, this is done using fractographic analysis. This analysis is done to determine whether a test is valid or not by looking at the location of the origin of the fracture. Different fracture patterns are shown in this section (Section 5.2). In Section 5.3, the results are processed statistically, using the Weibull distribution, which is the most commonly used distribution function in the field of glass strength. The way in which the Weibull parameters were determined using the data obtained is described. Next, Sections 5.4 to 5.7 show Weibull plots of the results obtained. Each section looks at and analyses a different variable from which conclusions can be drawn. Section 5.4 compares the four different sides of the IGUs. Next, Section 5.5 looks at the influence of the air- and tin-sides of the glass. Herein, specimens tested on the tin-side are compared with specimens tested on the air-side. Section 5.6 focuses on the influence location of the glass panel in the building, also looking at whether it influences where a specific specimen from a panel comes from. This is done to see if there is difference between the strength at the edge or in the centre of a glass panel. Finally, the results of this study with old glass, are compared with other studies where CDR tests have been performed with new (AR) glass. Weibull plots graphically show the strength of old glass in relation to new glass.

5.2 Fractographic analysis

To determine whether a test is valid or not, a fractographic analysis was performed. This analysis determines where the location of the fracture origin is in the tested specimen. When the origin of the fracture is within either or on the loading ring, the test is considered valid. This is therefore within the inner 60 millimetres of the specimen. Another option is that the location of the fracture origin is outside the loading ring. If this is the case, the test is declared invalid, because in these cases the origin is not at the location of the highest stress. Failure of a specimen outside the loading ring can be due to a large defect or scratch outside the loading ring. This causes collapse to occur at that location even at lower stress. Table 14 shows the number of specimens broken per location. A distinction is made here between failure inside the loading ring (IR), on the loading ring (LR), and outside the loading ring (OR). There were also small number of specimens where determination of fracture origin was not possible (ND). These have been added to the specimens that failed outside the ring in the table. In some series, a large number of specimens failed outside the loading ring, for example, at panel 1-in #3 and 4-out #2. It was noticed that the specimens that had the fracture origin outside the loading ring often failed only at high forces. The energy released at these higher forces, often caused the origin to be outside the loading ring. This is the reason why an origin outside the loading ring was more often found at side #2 and #3, because relatively higher failure forces were measured at these sides. It could also be based on the fact that some specimens had some larger defects/damage outside the loading ring, causing these specimens to fail at that location. This cannot be said with certainty because it was not looked at in this experiment.

Table 14. Fracture origin locations for the different series.

Series	IR	LR	OR
1 #1	15	4	1
1 #2	10	7	3
1 #3	7	4	8
1 #4	14	6	1
2 #1	14	4	2
2 #2	13	3	4
2 #3	15	5	0
2 #4	12	5	3
3 #1	12	4	2
3 #2	11	3	4
3 #3	12	1	3
3 #4	8	3	5
4 #1	14	1	3
4 #2	8	4	6
4 #3	10	2	2
4 #4	13	1	2
5 #1	12	1	1
5 #2	12	1	1
5 #3	11	0	3
5 #4	11	2	1
6 #1	12	1	1
6 #2	9	3	2
6 #3	11	3	0
6 #4	8	3	3
Total	274	71	61
% of total	67.5 %	17.5 %	15 %

For series naming, see Table 6.

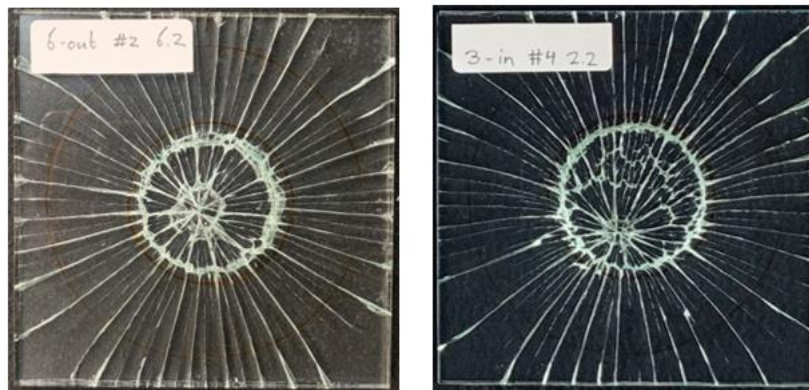
Table 15 distinguishes between the air- and tin-sided specimens in relation to the number of fracture origin locations found after testing. In percentage terms, specimens tested on an air-side had more invalid tests (18.9%) than the tin-side (11.2%). This may be because with the tin-side, failure occurs more often at a lower stress already, in which it more often collapses within the loading ring. At higher stress, the fracture origin is apparently more likely to be outside the loading ring than at lower stress. Nothing can be said about the difference damage pattern between the air- and tin-sides in this statistic, because not systematically the same side is air-side or tin-side every time.

Table 15. Fracture origin location for air- and tin-side.

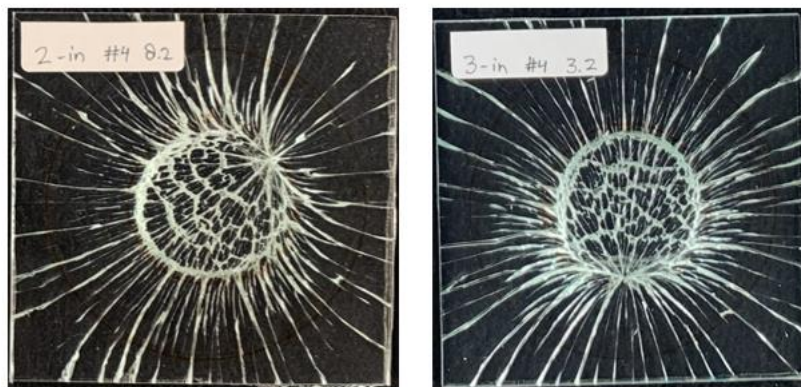
Series	IR	LR	OR	% invalid
Air	130	33	38	18.9 %
Tin	144	38	23	11.2 %

Of the total 406 specimens tested, 274 with the fracture origin within the loading ring. This amounts to 67.5%. The number of specimens that have the origin at the site of the loading ring, also a valid test, are 71 (17.5%). Because the ASTM code does not indicate whether specimens with the origin of fracture in the loading ring are valid or invalid, it was decided to include these tests in the valid tests. This is because at the loading ring, the magnitude of the stress is theoretically as high as in the middle of the homogeneous stress zone, and by including these tests in the results, this gives more values, generating a more reliable study. The remaining 61 specimens failed outside the 60mm loading ring, which falls under invalid tests. This means that 85% (IR + LR) of all tests were found to be valid, and 15% invalid (OR).

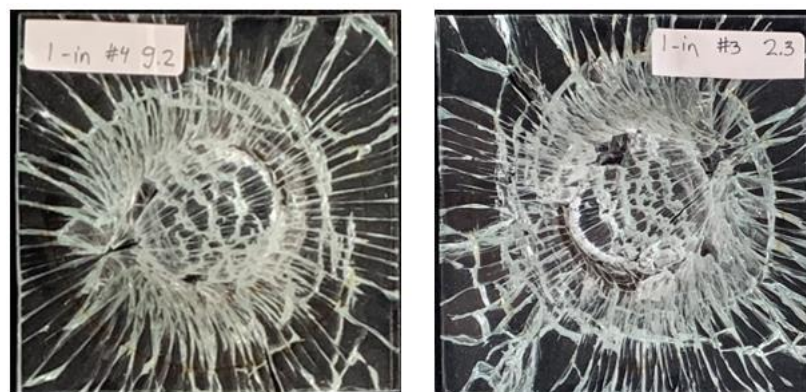
Figure 45 shows typical examples of test specimens with fracture origin inside the loading ring (a), on the loading ring (b) and outside the loading ring (c), from top to bottom.



(a) Inside loading ring



(b) At loading ring



(c) Outside loading ring

Figure 45. Fracture origin location.

Another analysis that can be performed on how specimens fail is to link the measured force required to cause a given failure pattern. Because the machine builds up the force, a higher failure load also involves a large stress that is released during fracture. This causes a denser fracture pattern at higher failure loads than at lower failure loads. The two extremes measured is 20.5 MPa ($F_{\text{breakage}} = 2095.7$ N) as failure stress for the weakest specimen 6-out #1 7.3, and 243.7 MPa ($F_{\text{breakage}} = 10095.3$ N) for the strongest specimen 5-in #3 5.3. Figure 46 shows these specimens after testing. Thus, due to the large difference in accumulated force during the test, there is also large difference in fracture pattern here. It can be said that the higher the accumulated stress, the higher the density of the fracture pattern.

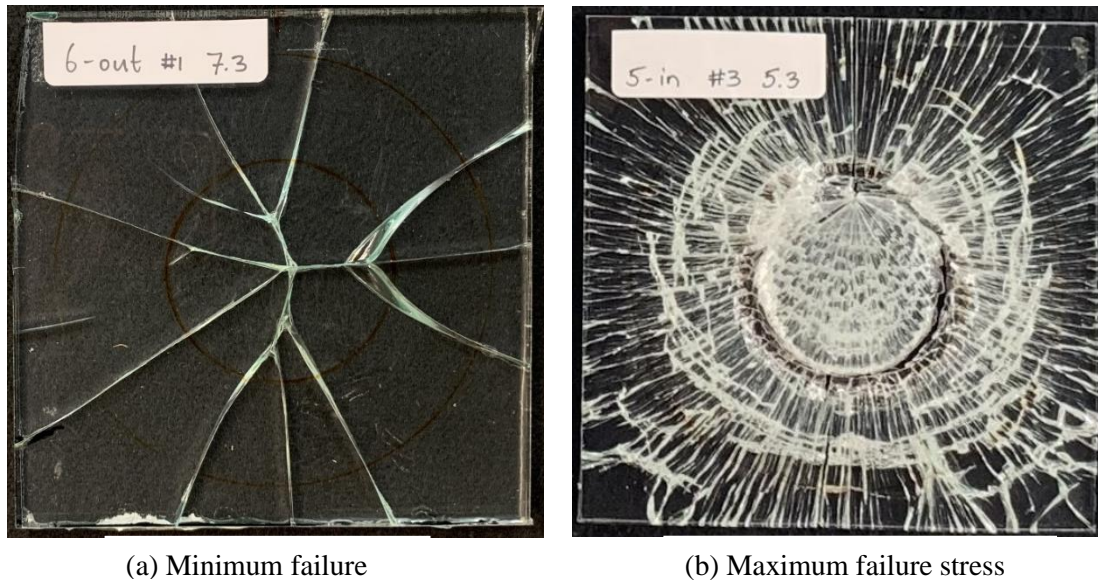


Figure 46. Extreme values fracture origins.

For a number of specimens, it was not clear what the exact origin location was. Often, when specimens were unclear, an origin location from outside the loading ring (OR) was chosen to avoid including invalid specimens in the results. An example of this is shown in Figure 47. It is possible that for the specimens shown, there is more than one fracture origin, because no single clear origin is visible. Due to the high force and high stress released during breakage, the specimens broke into many fragments. These fragmentation patterns might be expected earlier in toughened glass than in the annealed glass tested. The number of specimens where a clear location of the origin could not be established is very few, namely five.

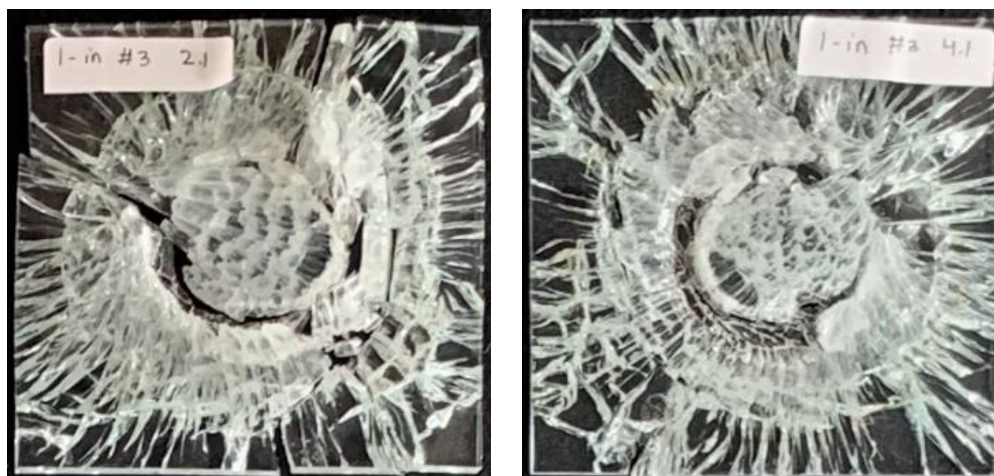


Figure 47. Examples of unclear location of fracture origin.

5.3 Statistical processing of the results

To analyse the data obtained from the CDR tests, the data points are fitted into a graph. As discussed in Section 2.6, this is done using the 2PW distribution. The Weibull distribution is a continuous probability distribution used in statistics to model the time to the occurrence of a particular event or the failure of an object. The Weibull distribution is thus suitable for this study and is more often used when analysing materials and their failure probabilities. The formula for the 2PW distribution can be seen in formula (12). Also, the linearized form (formula (12)) and the formula for the calculation of the equivalent failure stress (formula (13)) can be seen below.

$$P_f(\sigma_{f,eq}) = 1 - \exp \left[- \left(\frac{\sigma_{f,eq}}{\theta} \right)^\beta \right] \quad (12)$$

$$\ln \left[\ln \left(\frac{1}{1-P_f} \right) \right] = \beta * \ln \sigma_{f,eq} - \beta * \ln \theta \quad (13)$$

$$\sigma_{f,eq} = \sigma_f * \left[\frac{t_f}{t_{ref}^{*(n+1)}} \right]^{\frac{1}{n}} \quad (14)$$

Where:

- P_f = Probability of failure,
- $\sigma_{f,eq}$ = equivalent failure stress in MPa for a reference load duration,
- β = shape parameter which describes the scattering of the data,
- θ = scale parameter which indicated stress below of which the 63.2% of the specimens fail,
- σ_f = failure stress in MPa,
- t_f = failure time of each specimen in seconds,
- t_{ref} = equivalent reference time of each specimen in seconds,
- n = stress corrosion constant, for soda-lime glass below 150 °C, a value of 16 can be used (Charles, 1958).

A commonly used value of 60 seconds in the formula of the cumulative damage criterion (formula (14)) was chosen for the reference time (Brown, 1972). Each specimen is converted to an equivalent failure stress with a load duration of 60 seconds. This tackles the influence of load duration of the tests. Another way to do that is to run the tests in a vacuum space, so that environmental influences do not apply. This was not a viable option for this CDR test.

To create Weibull distributions, the shape and scale parameters are needed, as described earlier. For each set of tests, these values are different and must therefore be determined separately for each set. There are several ways to determine these parameters. The three most commonly used ways are the Weighted Least Squares Regression (WLR) method, the Maximum Likelihood Estimation (MLE) and the Method of Moments. For this study, a manual calculation was performed using the WLR method to determine the shape and scale parameters. To find the parameters for a Weibull distribution is based on linear regression. First, note that that the cumulative distribution function of a Weibull distribution can be expressed as in formula (15):

$$F(x) = 1 - e^{-\left(\frac{x}{\theta}\right)^\beta} \quad (15)$$

From which follows:

$$1 - F(x) = e^{-\left(\frac{x}{\theta}\right)^\beta} \quad (16)$$

Then take the natural logarithm from both sides:

$$\ln(1 - F(x)) = -\left(\frac{x}{\theta}\right)^\beta \quad (17)$$

Then multiply both sides by -1 and again take the natural logarithm:

$$\ln(-\ln(1 - F(x))) = \beta \ln x - \beta \ln \theta \quad (18)$$

This can be expressed as a linear equation:

$$y = \beta x' + a \quad (19)$$

Where $y = \ln(-\ln(1-F(x)))$, $x' = \ln(x)$ and $a = -\beta \ln(\theta)$. With this derivation, it has thus been shown that the Weibull parameters can be found via linear regression. This was done manually using Excel. The steps followed in this are briefly explained below. Reference is made to the columns shown in Figure 48 to clarify which steps are required on which to arrive at the shape and scale factors.

1. Collect valid values of the tested series (columns A and B)
2. Sorting values (column C)
3. Taking natural logarithm of these values (column D)
4. Filling in the formula: $F(x)=(i-0.5)/n$ (column E)
5. Fill in the formula: $\ln(-\ln(1-F(x)))$ (column F)
6. Calculate shape factor β (slope of regression line)
7. Calculate scale factor θ (intercept of the regression line)

Equivalent stress	A	B	C	D	E	F		
i	loc	$\sigma_e, 60s$	sort $\sigma_e, 60s$	$\ln(\sigma_f)$	F(x)	$\ln(-\ln(1-F(x)))$		
1	IR	80.6	43	3.7612	0.026316	-3.62428	β	5.371
2	IR	71.1	45.3	3.813307	0.078947	-2.49814	$-\beta \ln(\theta)'$	-22.874
3	IR	67.8	46.2	3.83298	0.131579	-1.95844	θ	70.725
4	IR	84.1	52.8	3.966511	0.184211	-1.5916		
5	IR	90.5	54	3.988984	0.236842	-1.30826	mean	65.2
6	LR	82.5	56	4.025352	0.289474	-1.07368	mean est	65.2
7	IR	59.3	57.2	4.046554	0.342105	-0.87058		
8	IR	52.8	59	4.077537	0.394737	-0.68897	var act.	194.5
9	LR	46.2	59.3	4.082609	0.447368	-0.52245	var est.	195.7
10	IR	43.0	65.7	4.185099	0.5	-0.36651		
11	IR	56.0	67	4.204693	0.552632	-0.21769	R-square	0.940952
12	IR	45.3	67.8	4.216562	0.605263	-0.07307		
13	IR	81.4	71.1	4.264087	0.657895	0.07012		
14	IR	67.0	75.4	4.322807	0.710526	0.214862		
15	IR	75.4	80.6	4.389499	0.763158	0.364894		
16	LR	59.0	81.4	4.399375	0.815789	0.52572		
17	IR	65.7	82.5	4.412798	0.868421	0.707123		
18	LR	57.2	84.1	4.432007	0.921053	0.93176		
19	IR	54.0	90.5	4.50535	0.973684	1.29132		
20	OR							

Figure 48. Excel file to receive scale and shape parameter.

This figure also shows the value of mean, variance and R-squared value. This R-squared value was determined using the R.SQUARE function in Excel. R-squared is a statistical measure in a regression model that determines the proportion of variance in the dependent variable that can be explained by the independent variable. It shows how well the data fit the regression model. This value is always between 0 and 1. The closer the number is to 1, the closer the expectation is to the observed values. In this study, the R-squared values are between 0.792 and 0.975. Thus, at the value of 0.792, it means that 79.2% of the variation in the output can be explained by the input variable.

Using these calculated shape and scale parameters, the mean μ and standard deviation σ can also be determined. A probability of failure was then calculated for each failure stress, which can then be plotted in a Weibull distribution graph. Table 16 shows also values for a probability of failure of 0.008, 0.05 and 0.5, which are commonly used probabilities in the current standards.

Table 16. Weibull parameters and characteristic values for each series.

Series	1 #1	1 #2	1 #3	1 #4	2 #1	2 #2	2 #3	2 #4	3 #1	3 #2	3 #3	3 #4
shape β	5.4	3.3	3.2	3.3	5.1	5.4	7.2	4.9	7.3	3.4	5.4	3.9
scale θ	70.7	58.4	110.2	70.8	71.8	90.7	51.3	78.1	62.1	110.0	53.9	89.1
mean μ	65.2	52.1	98.4	63.3	66.0	83.6	48.1	71.7	58.3	98.4	49.7	80.3
std σ	13.9	19.0	32.4	22.9	15.3	17.7	7.5	17.4	9.1	31.1	10.6	24.8
$\sigma_{f,0.008}$	23.3	18.6	16.8	11.2	28.0	35.1	26.3	32.2	28.0	13.3	19.0	33.6
$\sigma_{f,0.05}$	37.7	28.8	33.0	28.5	40.2	50.0	34.0	45.7	38.3	28.6	28.3	48.3
$\sigma_{f,0.5}$	66.1	50.3	91.4	61.3	66.9	84.8	48.7	71.5	59.1	96.4	47.7	78.0
R^2	0.94	0.79	0.92	0.85	0.85	0.86	0.97	0.95	0.95	0.90	0.95	0.80

Series	4 #1	4 #2	4 #3	4 #4	5 #1	5 #2	5 #3	5 #4	6 #1	6 #2	6 #3	6 #4
shape β	5.8	4.3	2.5	3.2	5.4	2.4	2.3	2.8	2.2	3.0	6.3	3.5
scale θ	66.2	88.9	87.1	68.3	59.1	72.2	152.1	67.9	74.7	58.9	57.7	60.3
mean μ	61.2	80.8	76.6	61.1	54.5	63.7	133.8	60.4	66.0	51.5	53.6	54.1
std σ	12.0	22.5	31.7	21.7	11.5	28.4	61.3	24.3	31.6	13.9	9.8	17.3
$\sigma_{f,0.008}$	23.6	29.1	8.5	12.1	24.1	13.4	8.4	14.7	8.4	18.6	26.8	12.3
$\sigma_{f,0.05}$	34.5	44.6	19.3	22.0	34.0	23.8	27.4	26.1	19.5	29.7	36.0	22.2
$\sigma_{f,0.5}$	59.3	76.6	75.2	58.9	55.2	61.8	123.1	61.6	63.3	52.0	51.8	50.7
R^2	0.92	0.83	0.88	0.93	0.95	0.95	0.88	0.96	0.97	0.86	0.82	0.91

Each series has between eleven and twenty data points, or valid tests. According to the ASTM standard, a minimum of ten tests are required to determine the mean biaxial flexural strength. The mean values for each series are very close to the stress value for a probability of 0.5. This indicates that the shape and scale factor calculations were done correctly and are reliable for graph visualisation with the Weibull plots.

5.4 Sides comparison

The first variable compared is the side of the IGUs tested. Initially, this comparison provides the best answer to the research question, but also to the sub-question on the differences in strength between the different sides of an IGU. Because side #1 and side #4 are exposed to the environment to a different extent than side #2 and #3 during the use phase of an IGU, in addition to different damage pattern, a difference in strength is also expected. Figure 49 shows the Weibull distribution and the values of specific failure probabilities, respectively. Also, the average measured value is shown, to show that the $\sigma_{f,0.5}$, or stress at which 50% of the specimens fail according to the Weibull theory, is not equal to the $\sigma_{f,mean}$, the average measured failure stress. Because the measured failure stresses of side #2 and #3 have a lot more variation than those of side #1 and #4, the reliability of these series is a lot lower. This can be seen from the slope (shape parameter) of the lines in the Weibull plot. The steeper this line runs, the less variation there is in the data, giving a more reliable result. In the figure it is easy to see that the lines that predicted strength of the tested series from the data have different slopes. The lines on side #1 and #4 have a steeper slope than those on side #2 and #3. As a result, despite the higher values for $\sigma_{f,0.5}$ and $\sigma_{f,mean}$ for side #2 and #3, a lower value for both the characteristic strength $\sigma_{f,0.05}$ and the design strength $\sigma_{f,0.008}$ (according to ASTM E1300, 1997) comes out here than for the outer sides of the IGU (side #1 and #4). This raises the discussion whether the Weibull distribution describes the data well at lower probabilities of failure. It seems that it does estimate very conservative values for the low probabilities. These conservative values are, despite this, often used for engineering design purposes. Nevertheless, this method is also used most often in studies or experiments like this one, because, precisely because of this conservative approach, safe margins can be assumed. Looking at the results of the tests of different sides of the IGU, it is thus most striking that side #1, which theoretically has the most damage from weathering (wind, rain, etc.) when an IGU is in a frame, has the highest value for design strength and characteristic strength, despite the lowest value for $\sigma_{f,0.5}$. This indicates little variation in measured failure stresses and thus a fairly even damage pattern across the IGU. This is also true, to a slightly lesser extent, for side #4. In contrast, side #2 and #3 have a large variation in measured failure stresses, which may indicate more localised damage. These damage patterns were discussed earlier in Section 3.7 and Section 3.8. As a result, one specimen fails at a much lower or higher stress than the other, resulting in a more unreliable series. This then leads to the low design and characteristic stress for side #2 and #3.

The reason that the data from side #2 and #3 were not taken together as one large series is the fact that, despite virtually the same potential for damage and conditions, one is still dealing with different glass panels. Side #2 is always of a different glass panel than side #3. As a result, the thickness is almost always different in the case of an IGU, and it may also be the case that the glass panels come from different machines and/or factories and therefore have slightly different properties.

Appendix I, apart from the values of the Weibull distribution used, also gives the values for the $\sigma_{f,0.008}$, $\sigma_{f,0.05}$ and $\sigma_{f,0.5}$ when looking at another distribution function, namely the normal distribution. This is for comparison of the values and may be useful for future research.

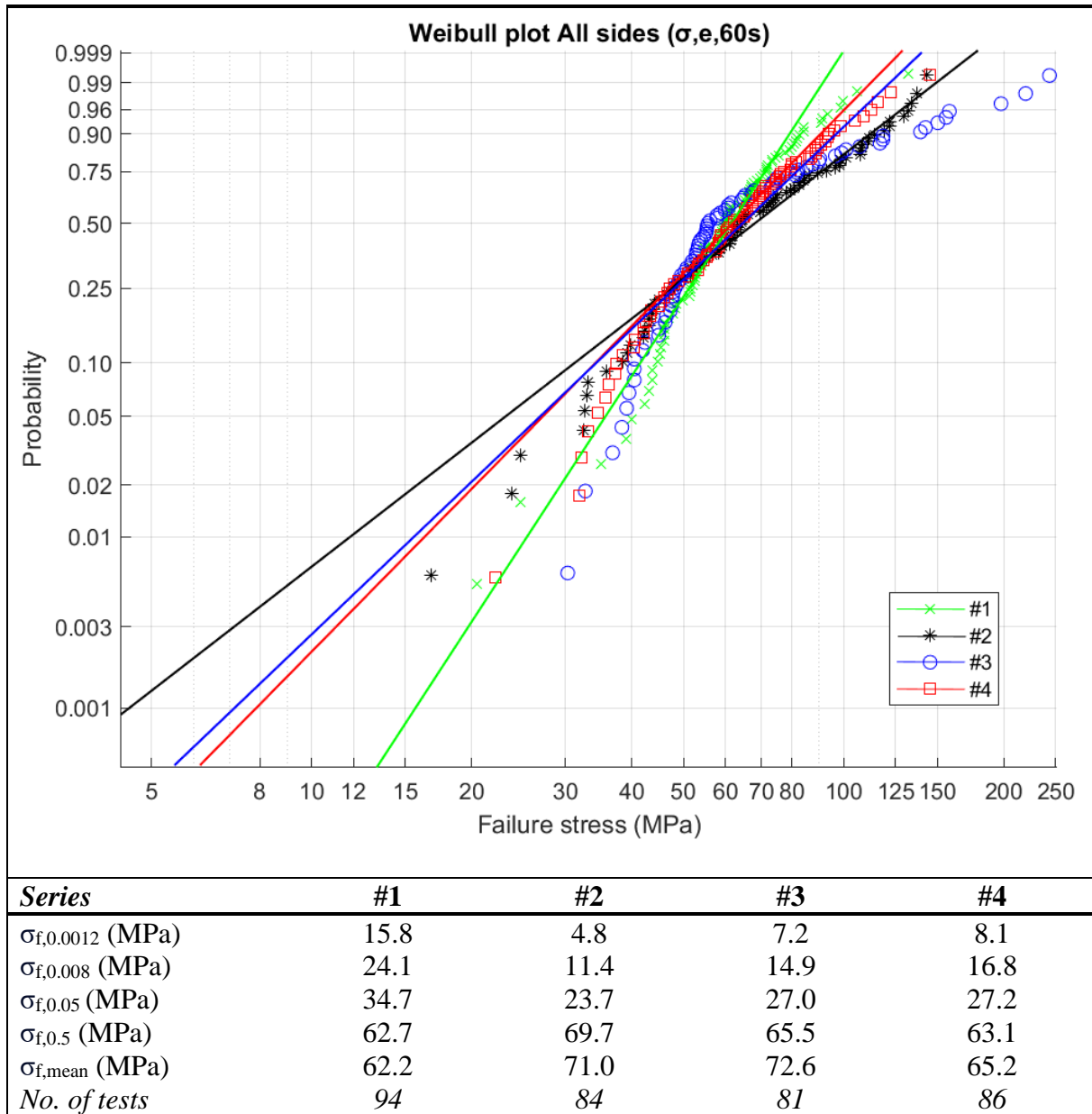


Figure 49. Weibull probability distribution: All sides.

5.5 Effect of tin- and air-side

Section 4.7 demonstrated how it was determined which side of a glass plate is the tin-side and air-side. The side that lies on a bath of tin during the manufacturing process and is then transported over steel rollers is called the tin-side. The other side of the glass, which has only contact with the air, is the air-side. Because tin residues may be found on the tin-side and minor damage may have occurred due to the transport of the glass over the rollers, this section focuses on the differences in strength between the tin-side and air-side.

5.5.1 All data

In existing literature, little attention is paid to the differences in strength between tin- and air-sides, as the differences are said to be marginal. Because it was known for each specimen whether it was tested on the tin- or air-side, this study examined whether these differences were indeed marginal. Out of a total of 345 valid tests conducted, 182 specimens were tested on the tin-side, and 163 on the air-side. Because of this high number, a presentable picture of the difference in results can be shown. The Weibull distribution in Figure 50 shows that there is indeed a difference in result. The $\sigma_{f,0.5}$ of the air-side is a lot higher than that of the tin-side, meaning that theoretically 50% of the specimens tested on air-side only fail at a stress of 75.3 MPa, while for the tin-side this value is 57.3 MPa, which is a difference of 31%. Because of that greater variation in results of the air-side, the line of the Weibull distribution is less steep than that for the tin-side. This may, as in the previous section where side #1, #2, #3 and #4 are compared, indicate a less even damage pattern than for the tin-side. As a result, more variation is found in the results. This leads to the fact that the characteristic strengths $\sigma_{f,0.05}$ are closer together, with the value for air-side being only 9% higher than for the tin-side. On the contrary, at the design strength $\sigma_{f,0.008}$, a slightly higher value is found for the tin-side. The design strength of the tin-side is 8% higher than the design strength of the air-side.

Figure 51 and Figure 52 show plots distinguishing between the tin- and air-sides in addition to the different sides. For with the air-sides, it can be seen that side #2 and #3 have equal steepness, which is expected, and have a lot of variation in data. As a result, the distribution line is less steep than that of side #1 and #4, and low values come out at low failure probabilities. The tin-side shows that for low failure probabilities, side #4 actually gives low values. One cause of this is one very weak specimen compared to the other specimens from side #4. What is also very striking in Figure 51 is the fact that the average strength of the specimens of side #1 and #4 (both 60.4 MPa) is higher than that of side #2 and #3 (51.9 MPa and 48.7 MPa).

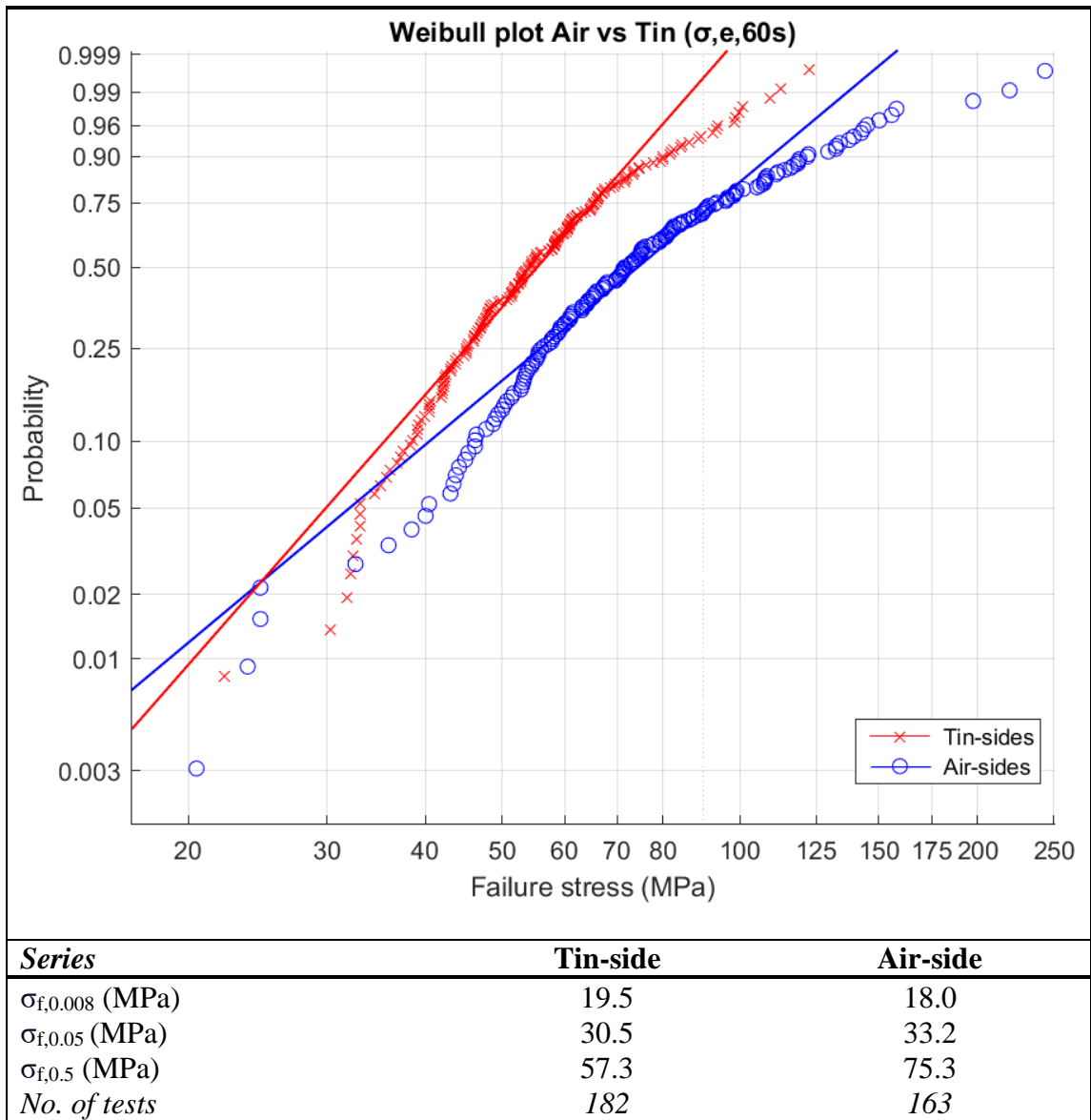
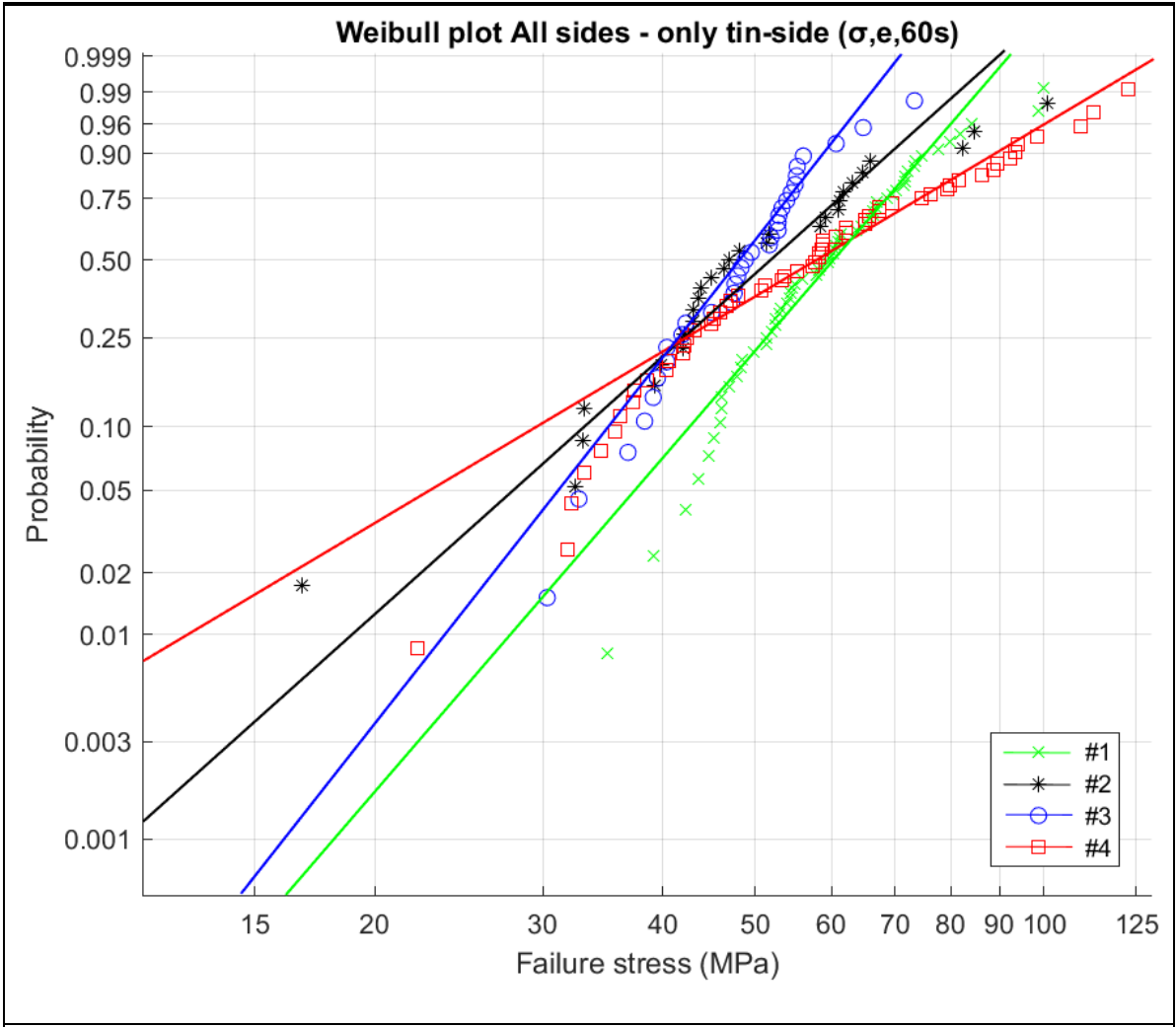
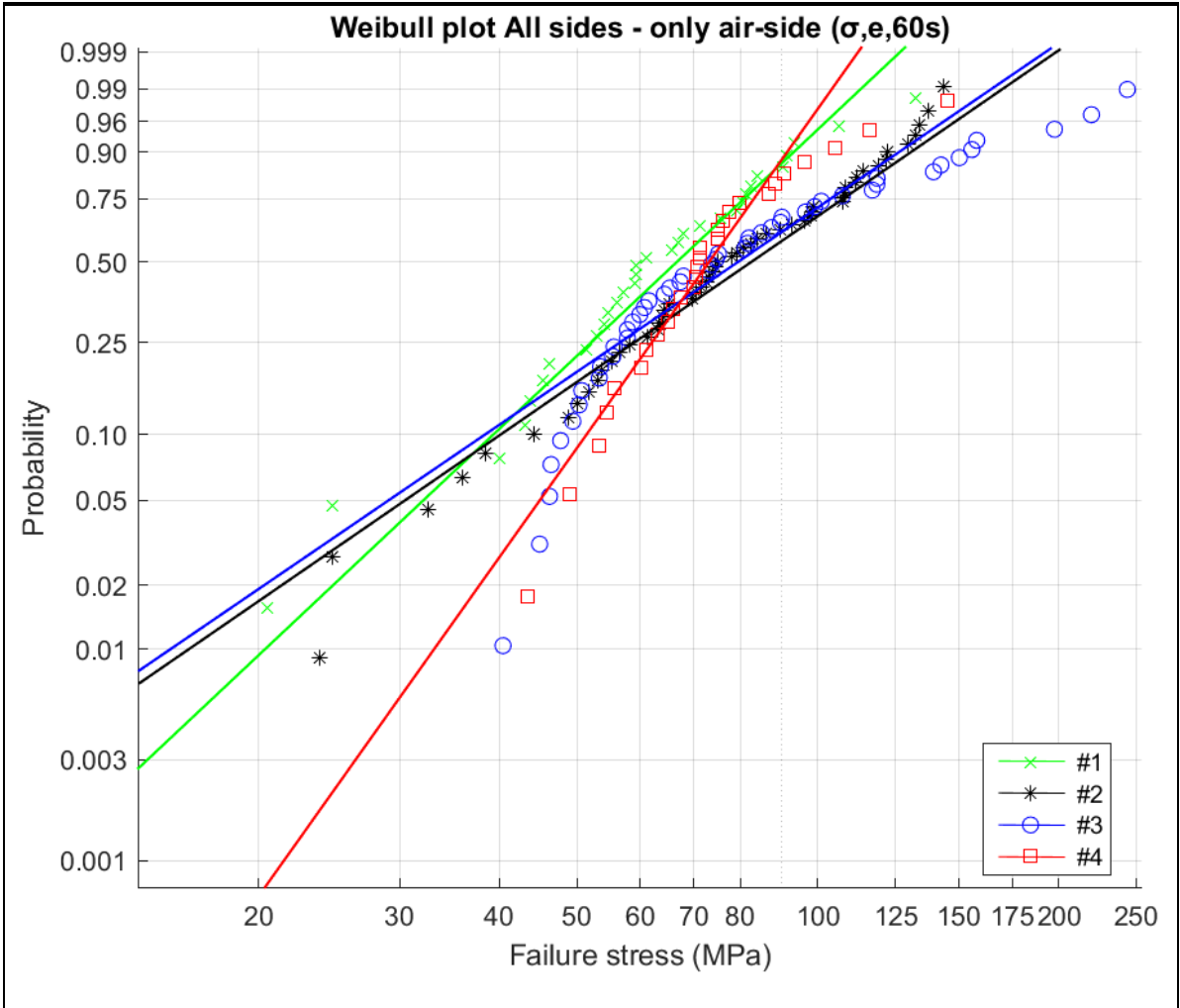


Figure 50. Weibull probability distribution: Air-side vs tin-side.



Series	#1	#2	#3	#4
$\sigma_{f,0.008}$ (MPa)	27.2	17.5	23.9	11.8
$\sigma_{f,0.05}$ (MPa)	38.0	28.2	31.7	24.0
$\sigma_{f,0.5}$ (MPa)	61.2	52.0	49.4	59.1
$\sigma_{f,mean}$ (MPa)	60.4	51.9	48.7	60.4
<i>No. of tests</i>	62	29	33	58

Figure 51. Weibull probability distribution: All sides – only tin-side.

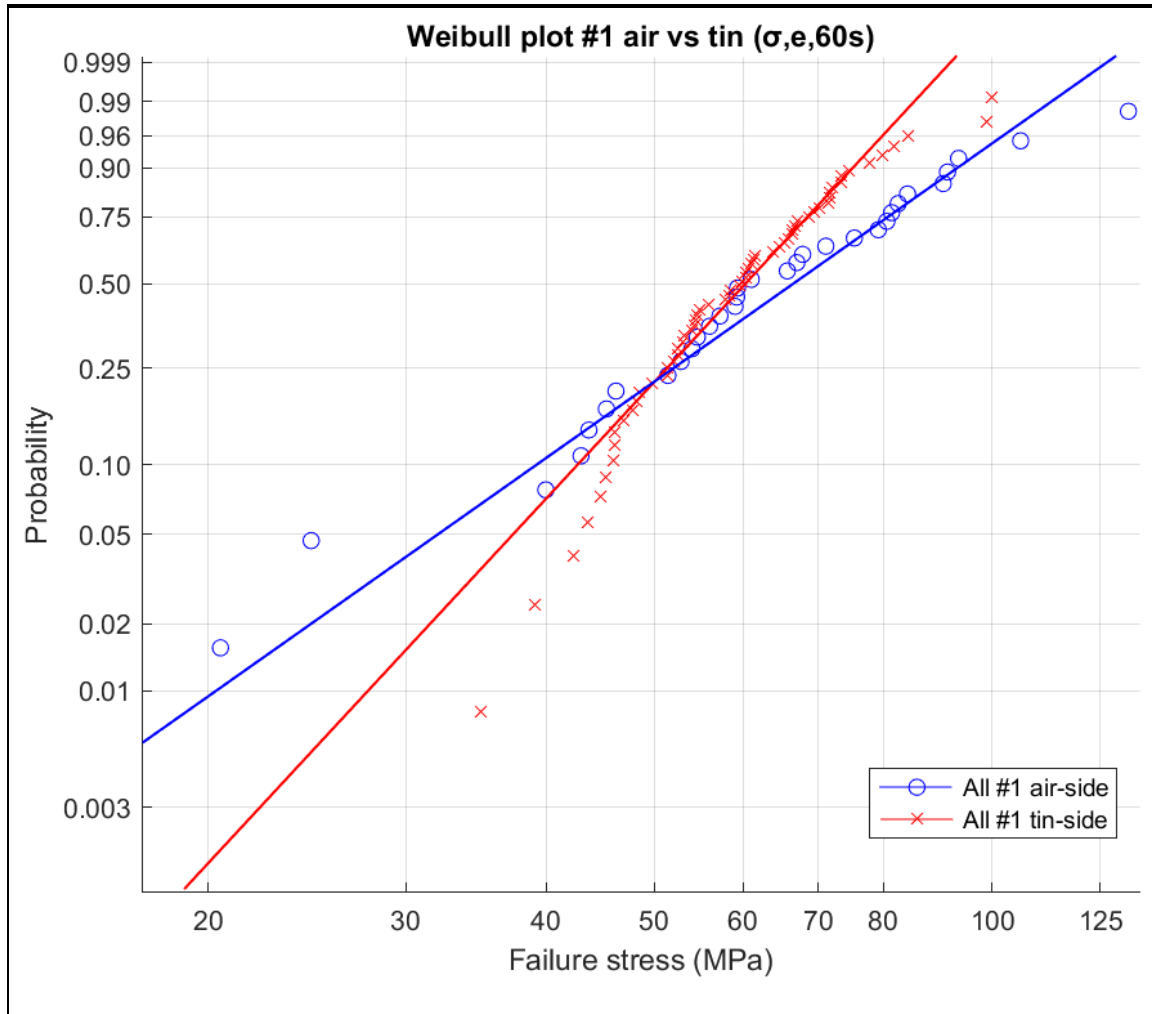


Series	#1	#2	#3	#4
$\sigma_{f,0.008}$ (MPa)	18.3	15.1	14.6	31.3
$\sigma_{f,0.05}$ (MPa)	32.0	30.6	29.1	45.6
$\sigma_{f,0.5}$ (MPa)	67.3	81.3	80.7	73.9
$\sigma_{f,mean}$ (MPa)	65.5	81.1	89.0	75.1
<i>No. of tests</i>	32	55	48	28

Figure 52. Weibull probability distribution: All sides – only air-side.

5.5.2 Sides comparison

In this section, a combination of variables emerges, namely the side of the IGU combined with being a tin- or air-side. Figure 53 to Figure 56 shows the Weibull distributions for side #1, #2, #3 and #4 distinguishing between the tin- and air-sides. The Weibull plots of side #1, #2 and #3 are quite similar to the overall distribution of all sides. Here is the steeper line of the tin-side, which, despite a lower value of $\sigma_{f,0.5}$, gives a higher design strength ($\sigma_{f,0.008}$) for the tin-side than for the air-side. In contrast, this is the opposite for side #4. A reason for this may be that the number of tests of the air-side is quite low (28), reducing the probability of having some outliers among them. For example, the $\sigma_{f,0.5}$ of the air-side of side #4 is not higher than for side #2 and #3, but it has a much higher design strength. Thus, the outliers have a significant impact on the distribution's gradient. In this case, there are no low values among them and so the air-side line at side #4 is very steep. The damage pattern in this series is expected to be almost the same for each specimen, so there is little variation in measured failure stresses. Furthermore, it is noticeable that for side #2 and #3, the $\sigma_{f,0.5}$ (80.3 and 80.1 MPa, respectively) of the air-side is higher than that of the air-side of side #1 and #4 (66.3 and 73.9 MPa, respectively), while the $\sigma_{f,0.5}$ of the tin-side of side #2 and #3 (52.0 and 49.4 MPa, respectively) are actually lower than those of side #1 and #4 (61.3 and 59.1 MPa, respectively). There is no logical explanation for the lower values of $\sigma_{f,0.5}$ for the tin-sides of side #2 and #3 compared to side #1 and #4. Indeed, if it has to do with the way an IGU was separated, or the way the specimens were handled, a lower value is expected at the air-sides as well, rather than only at the tin-sides of side #2 and #3.



Series	Tin-side	Air-side
$\sigma_{f,0.008}$ (MPa)	28.2	16.3
$\sigma_{f,0.05}$ (MPa)	39.0	32.0
$\sigma_{f,0.5}$ (MPa)	61.3	66.3
<i>No. of tests</i>	62	32

Figure 53. Weibull probability distribution: Air-side vs tin-side - #1.

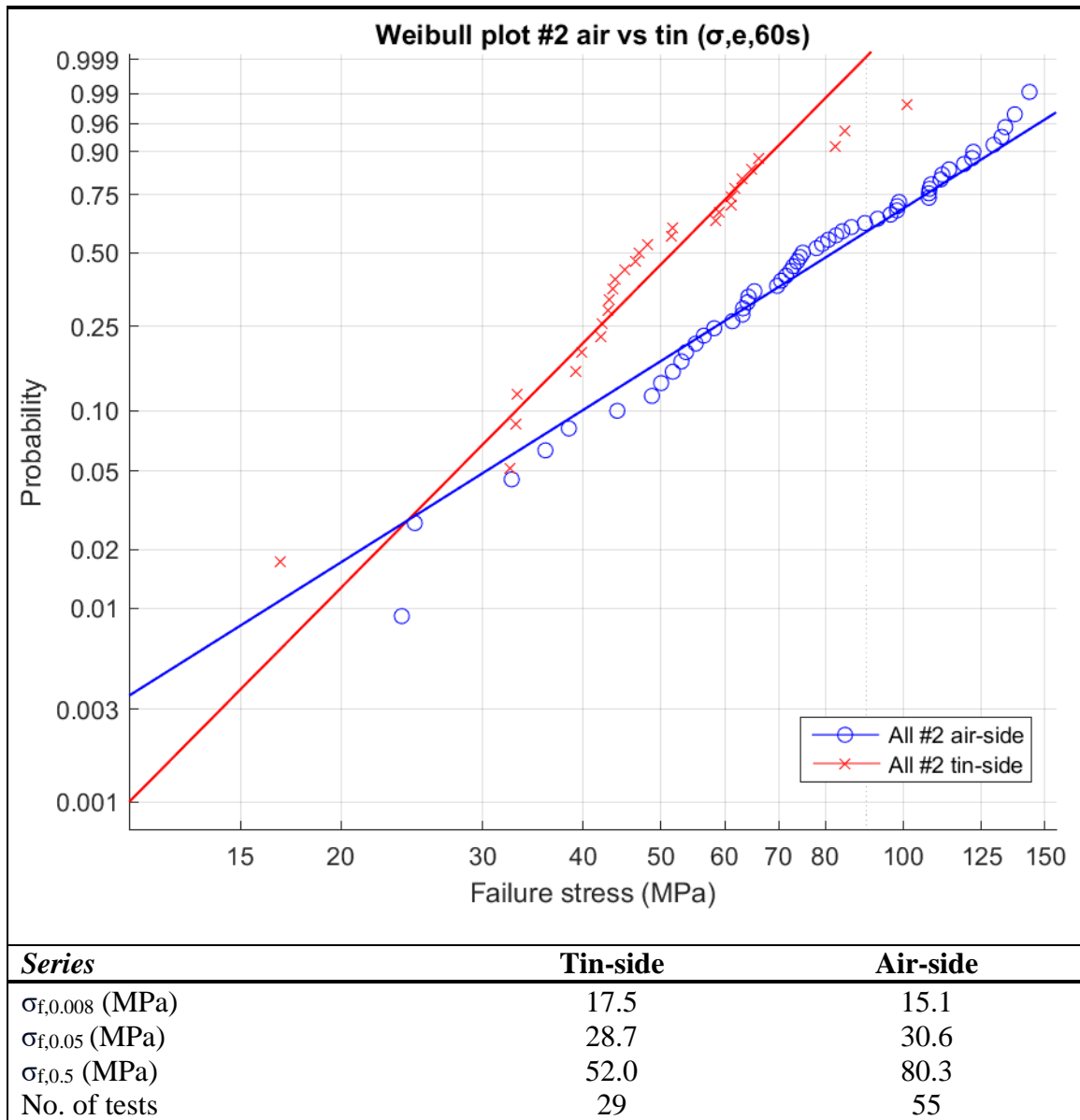
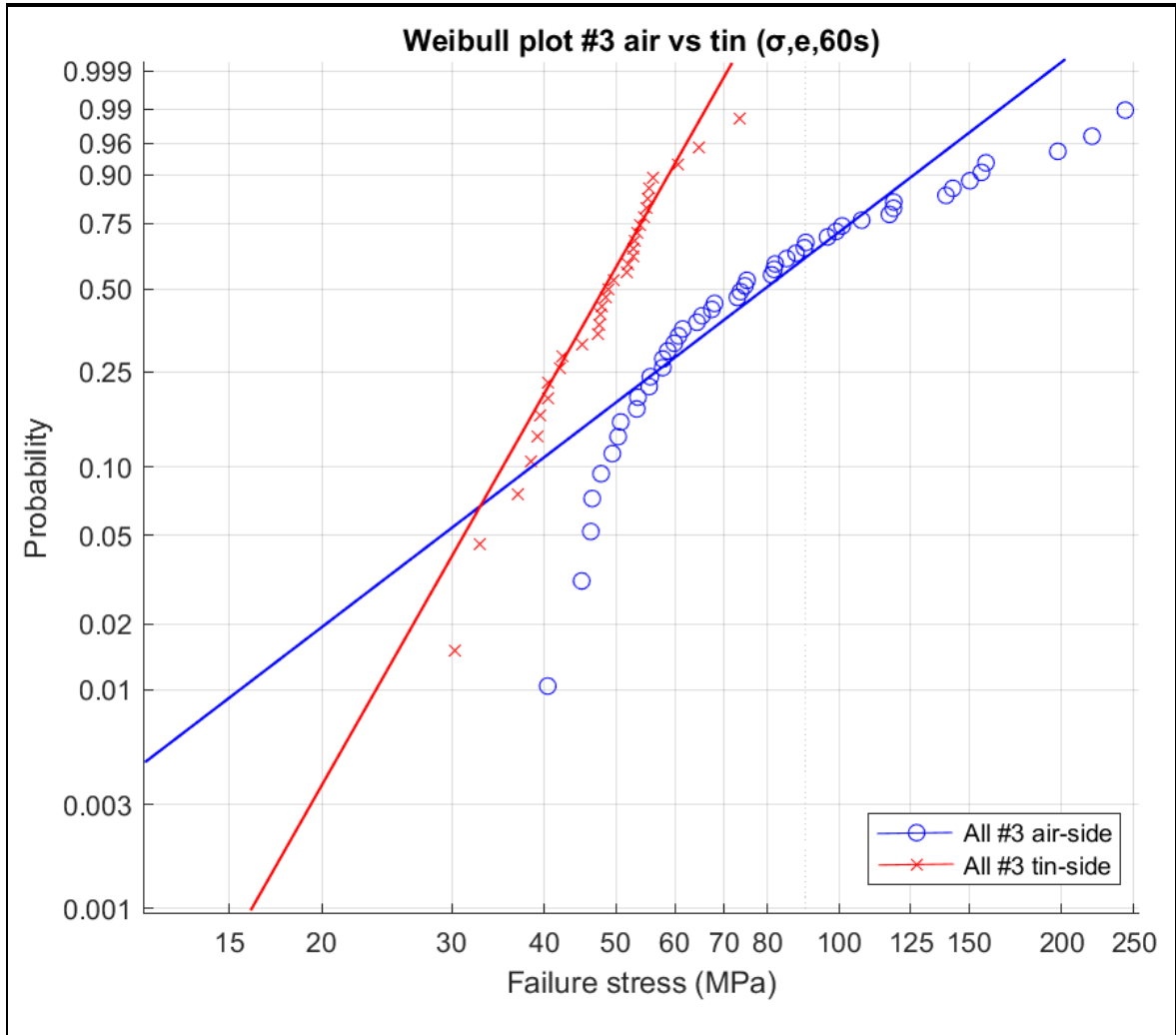
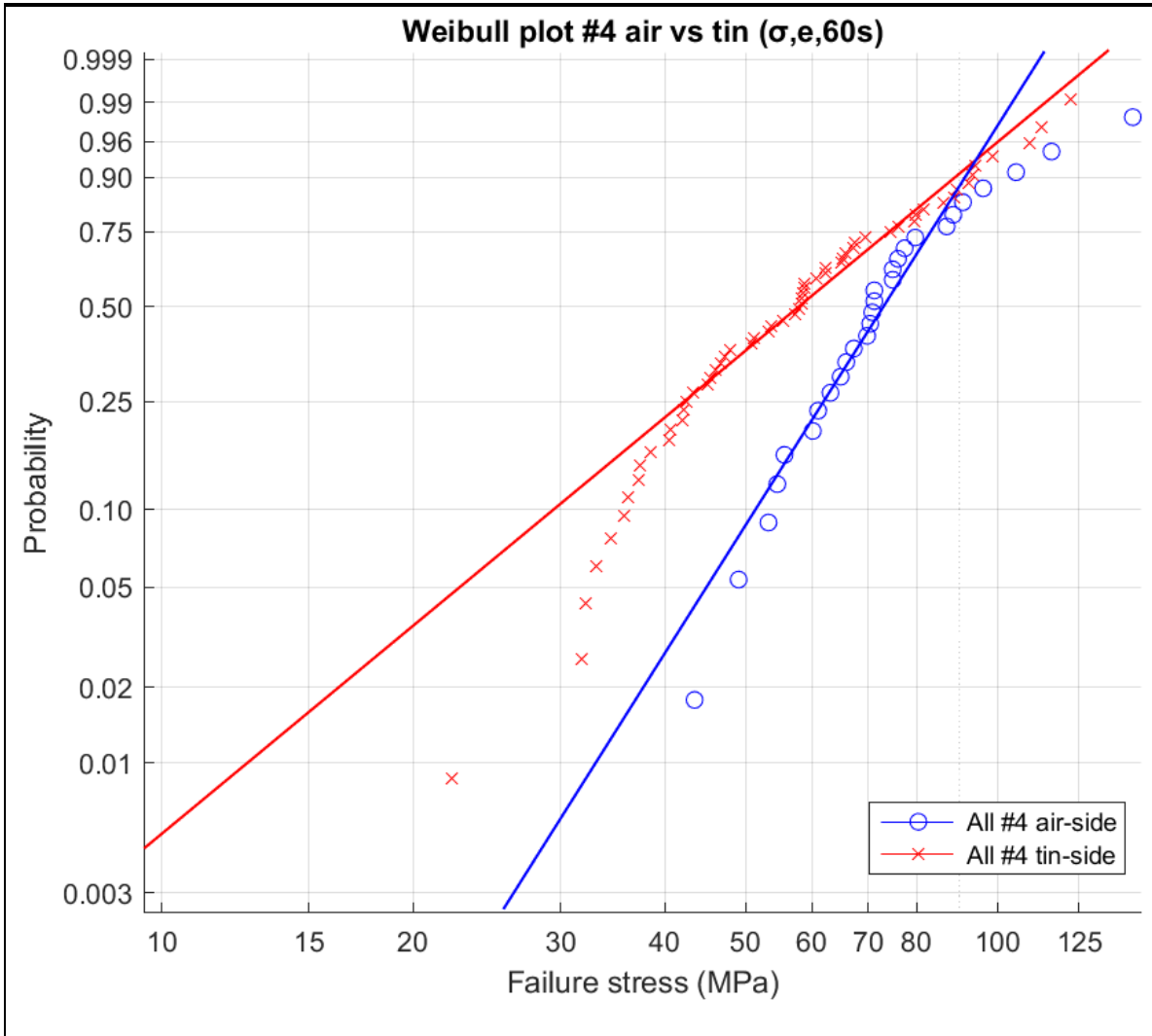


Figure 54. Weibull probability distribution: Air-side vs tin-side - #2.



<i>Series</i>	Tin-side	Air-side
$\sigma_{f,0.008}$ (MPa)	24.9	14.1
$\sigma_{f,0.05}$ (MPa)	33.1	29.3
$\sigma_{f,0.5}$ (MPa)	49.4	80.1
No. of tests	33	48

Figure 55. Weibull probability distribution: Air-side vs tin-side - #3.



Series	Tin-side	Air-side
$\sigma_{f,0.008}$ (MPa)	12.8	31.3
$\sigma_{f,0.05}$ (MPa)	23.5	43.6
$\sigma_{f,0.5}$ (MPa)	59.1	73.9
No. of tests	58	28

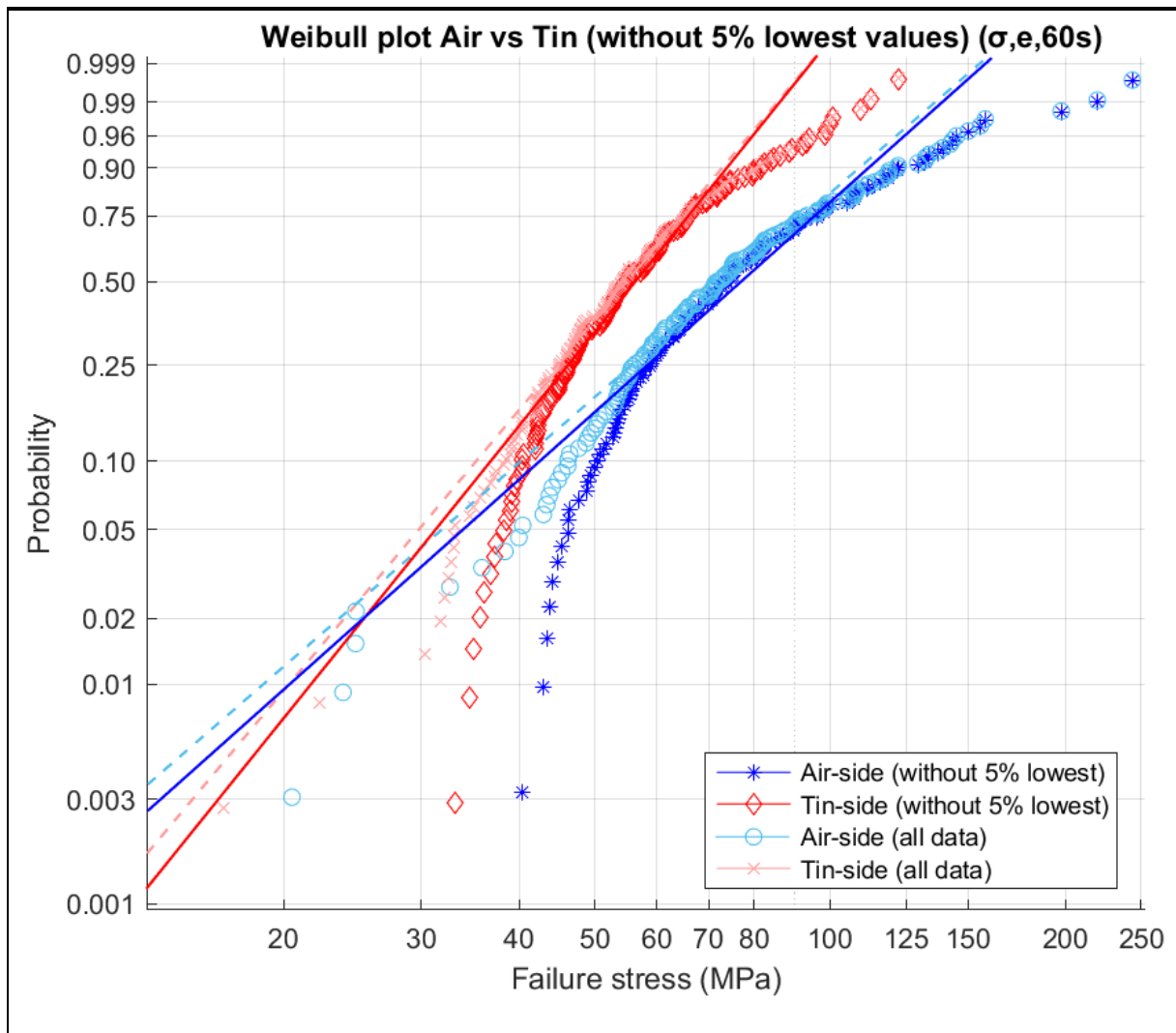
Figure 56. Weibull probability distribution: Air-side vs tin-side - #4.

5.5.3 Low values influence

Because very high and very low values, so-called outliers, have a great influence on the course of the Weibull distribution, a Weibull plot was also made of a comparison between the tin- and air-sides, without the 5% and 10% lowest values of the tin- and air-series. These Weibull distributions are shown in Figure 57 and Figure 58. The purpose of these plots is to show the effect of removing some specimens that succumbed at low failure stress. When it is possible to detect these specimens in advance and possibly already strengthen or repair them, a higher design and/or characteristic strength is found. This may result in a glass panel being able to be treated differently in terms of reuse, rather than just failing to meet current strength requirements.

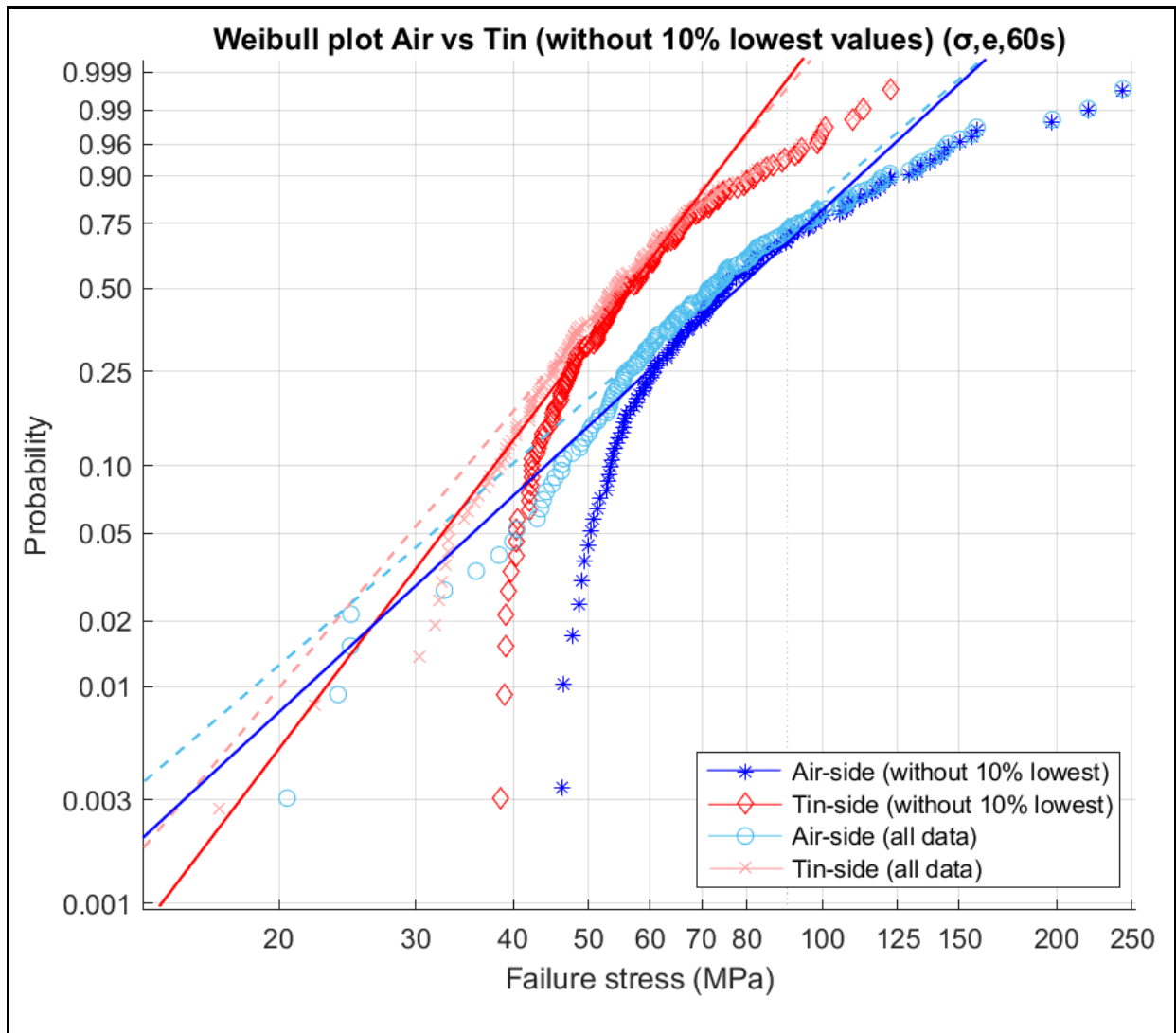
Figure 57 shows what the Weibull plot looks like of both all specimens tested on the tin-side and on the air-side, without including the 5% lowest values. The dotted line represents the distribution as in Figure 50, while the solid line is the distribution without the lowest values. A shift of the lines can be seen here. Thus, the lines become slightly steeper, making the series slightly more reliable, and have a small shift. This shift leads to slightly higher values for the characteristic points $\sigma_{f,0.5}$, $\sigma_{f,0.05}$ and $\sigma_{f,0.008}$. Thus, for the tin-side, these values become 2%, 4% and 13% higher, respectively, and for the air-side, 2%, 6% and 7% higher, respectively. Because the line has a steeper gradient, the relative difference between the characteristic values increases in percentage terms as a lower probability of failure is considered.

In Figure 58, even the 10% lowest values of the respective series are extracted. This causes an even steeper slope and a bigger shift of the Weibull distribution resulting in higher values for the characteristic points. The values of $\sigma_{f,0.5}$, $\sigma_{f,0.05}$ and $\sigma_{f,0.008}$ for the tin-side are 4%, 7% and 19% higher, respectively, and for the air-side are 5%, 12% and 15% higher, respectively, than when all values are included. It shows that when the certain number of weak spots in an IGU (outlier specimens) can be detected and then repaired and/or strengthened, there are significant differences in the result of the Weibull distribution of a series of tests. These weak spots are often caused by somewhat larger scratches or pits. Especially transport and when the glass comes into contact with a hard or sharp object, are most likely the causes of these larger damages to the glass.



<i>Series</i>	Tin-side (-5%)	<i>Tin-side</i>	Air-side (-5%)	<i>Air-side</i>
$\sigma_{f,0.008}$ (MPa)	22.0	19.5	19.2	18.0
$\sigma_{f,0.05}$ (MPa)	31.8	30.5	35.2	33.2
$\sigma_{f,0.5}$ (MPa)	58.5	57.3	78.6	75.3
<i>No. of tests</i>	173	182	155	163

Figure 57. Weibull probability distribution: All values - without 5% lowest.



<i>Series</i>	Tin-side (-10%)	<i>Tin-side</i>	Air-side (-10%)	<i>Air-side</i>
$\sigma_{f,0.008}$ (MPa)	23.3	19.5	20.7	18.0
$\sigma_{f,0.05}$ (MPa)	32.6	30.5	37.1	33.2
$\sigma_{f,0.5}$ (MPa)	59.5	57.3	78.9	75.3
No. of tests	165	182	147	163

Figure 58. Weibull probability distribution: All values - without 10% lowest.

5.6 Effect of location

Because all IGUs are known from which location in the building they originate, there is the possibility of comparing different orientations. Also, during the process of preparing all specimens, it is known where a particular specimen has been in an IGU. Thus, beyond the location of an entire IGU, it is also possible to look at the location of a particular specimen in an IGU. In this section, Weibull distributions are shown where the variable 'location' is central.

5.6.1 IGU orientation

Because the IGUs are not coming out of the building from the same location, the possibility of comparing different orientations has arisen. As shown in Table 6, IGU 1, 2 and 5 are located on the east side of the building, while IGU 3, 4 and 6 are located on the west side. As mentioned earlier in Section 4.6.1, the wind most often comes from a (south) westerly direction. Microscopic examination showed no obvious differences between the IGUs that had side #1 facing east and IGUs that had the outside of the outer panel facing instead west. In advance, the west-oriented IGUs are expected to have some more small scratches that may have been caused by rain and wind, than the east-oriented IGUs. The location of the building from which the IGUs originated is about 25 kilometres distance from the coast, limiting the influence of sand grains carried by the wind. Figure 59 shows the Weibull distribution of both western and eastern oriented IGUs. Here, only side #1 has been considered because it is in contact with environmental factors such as wind and precipitation. As expected, according to these data, the eastern IGUs are less weak than the western IGUs. Thus, values for the $\sigma_{f,0.5}$, $\sigma_{f,0.05}$ and $\sigma_{f,0.008}$ are 6%, 18% and 25% higher for the east-oriented IGUs than for the IGUs on the west side of the building, respectively. Based on these data, it can be concluded that it therefore does matter on which side of the building an IGU is located. Nevertheless, further research is needed to draw better conclusions. For instance, the influence of the tin- and air-sides was not considered in this case, despite in this case the small difference in number of tin-side tests. For the east-facing specimens tested, 19 out of 50 specimens were tested on the tin-side (38%), while for the air-side it was 13 out of 44 (30%). With more tests, more distributions can be made that include tin-side and air-side differences beyond orientation.

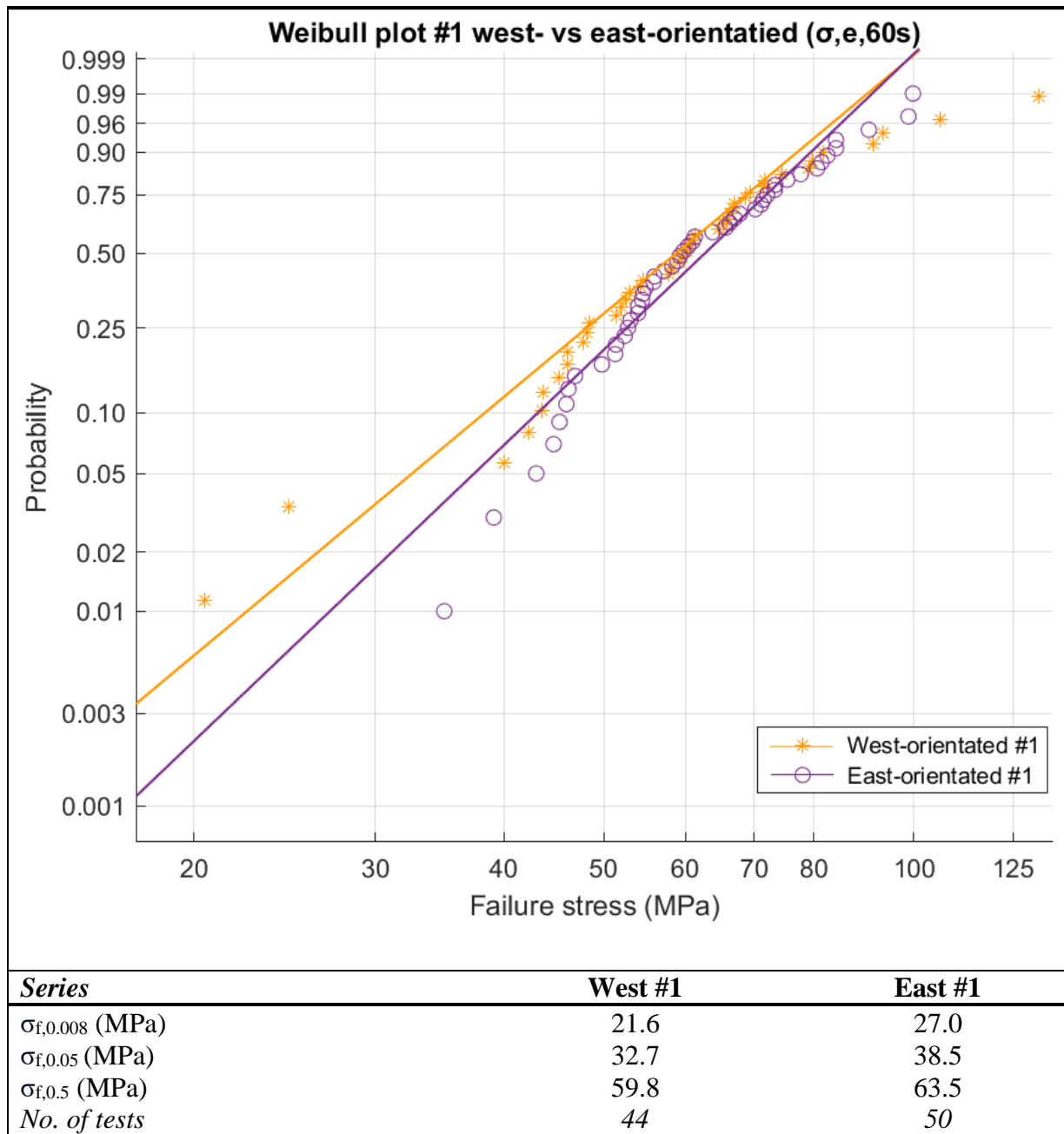


Figure 59. Weibull probability distribution: West- vs east-orientated.

5.6.2 Specimen location

To investigate whether strength differs at certain locations in an IGU, a distinction is made between so-called edge-specimens and mid-specimens. This can be used to investigate whether there is a difference in strength between certain locations in an IGU. The choice of comparing the edge of the IGU with the middle was made because separating the two glass panels of an IGU's may have caused damage that is more severe at the edge than in the middle of a glass panel. The machinery used for this (saw and grinder) may have been in contact with the edge of the glass, or dislodged small pieces that may have caused scratches or small craters. The question sought to be answered is whether the overall treatment of the IGU during its lifetime, i.e. before, during and after its use in the facade, can cause differences in strength between the edge and the centre of a glass panel coming from an IGU. Figure 60 shows which specimens in an IGU are made up for an edge-specimen, and which are made up for a mid-specimen.

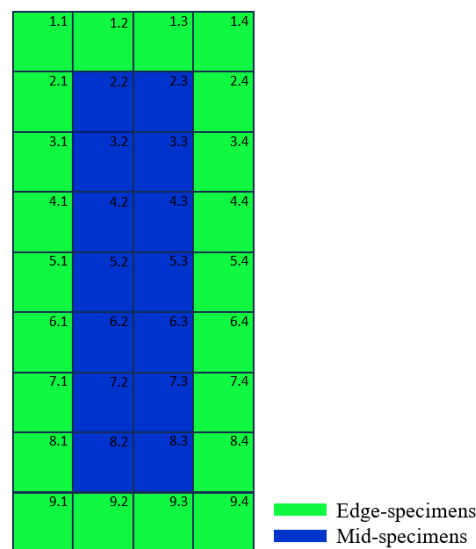
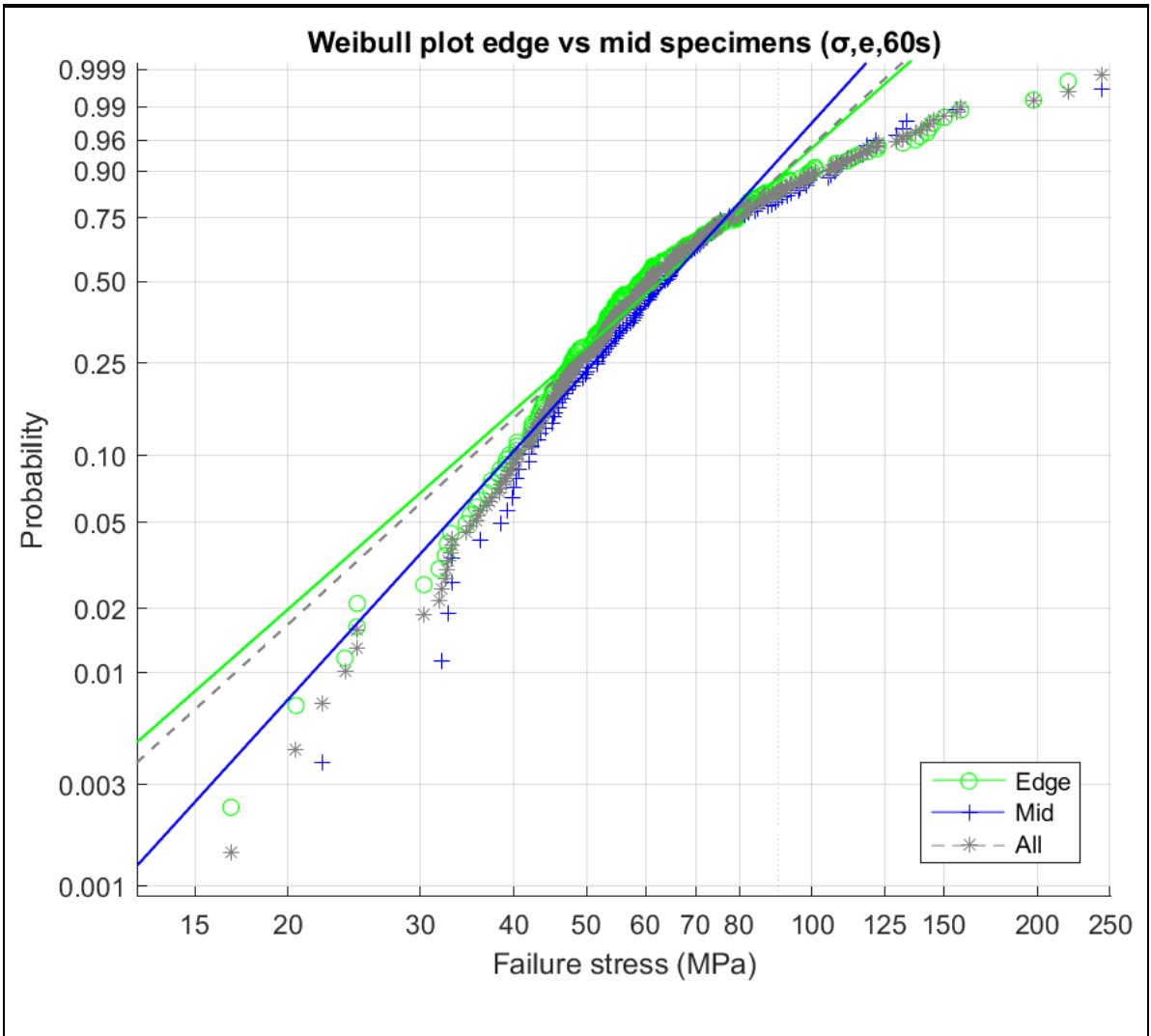


Figure 60. Edge- and mid-specimens.

The Weibull plot in Figure 61 shows distributions for all edge-specimens, all mid-specimens and a light grey dotted distribution line, which are all tested specimens. It can be seen that especially for the characteristic strength $\sigma_{f,0.05}$ and ASTM design strength $\sigma_{f,0.008}$ difference can be seen between the edge and mid-specimens. For instance, these values are 10% and 36% higher for the mid-specimens compared to the edge-specimens, respectively. As mentioned earlier, the Weibull distribution gives somewhat conservative values for lower probabilities of failure, but since a large number of data points (213 edge-specimens and 132 mid-specimens) are used in this case, these values can be assumed to be useful. The variation in results is less for the mid-specimens than for the edge-specimens, so higher design strength is found here. It can be concluded here that the mid-specimens have a higher design strength than the edge-specimens and the middle of an IGU may be slightly more likely to be considered for reuse, when smaller panes are cut out of a large glass panel, for example. Appendix F also provides Weibull plots distinguishing between the air- and tin-side specimens in addition to the mid- and edge-specimens.



<i>Series</i>	Edge	Mid	All
$\sigma_{f,0.008}$ (MPa)	14.6	19.9	15.7
$\sigma_{f,0.05}$ (MPa)	28.3	31.0	29.5
$\sigma_{f,0.5}$ (MPa)	65.6	68.8	66.8
<i>No. of tests</i>	213	132	345

Figure 61. Weibull probability distribution: Edge- vs mid-specimens.

Figure 62 and Figure 63 show Weibull plots of all mid- and edge-specimens, respectively, with the tested side separated. Because the results of the CDR tests of the mid-specimens of side #3 contains a large variation in results, the mid-specimens show that the line for side #3 is less steep than the others, resulting in a low design strength $\sigma_{f,0.008}$. Otherwise, this is the only design strength that is actually lower than for the edge-specimens. So, side #3 seems to be an exception here. Furthermore, it is again clear that for both the mid- and edge-specimens, side #1 has the steepest line and is thus the most 'reliable' series, resulting in a high design and characteristic strength. For side #4, there is little to no difference in the mid and edge specimens, while for side #1 and #2, the mid-specimens give significantly higher values for the characteristic points than the edge-specimens of these sides.

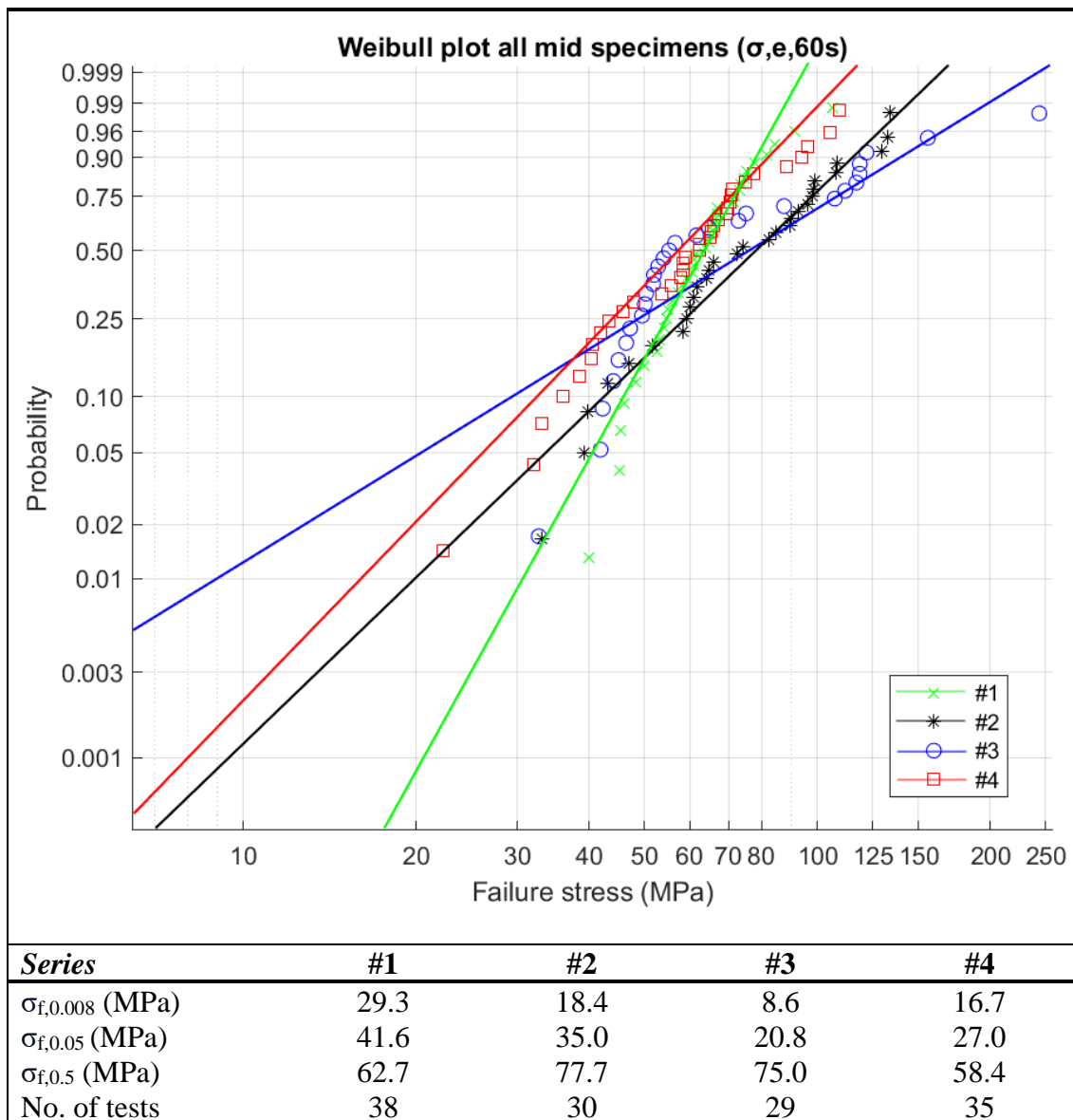


Figure 62. Weibull probability distribution: All sides - only mid-specimens.

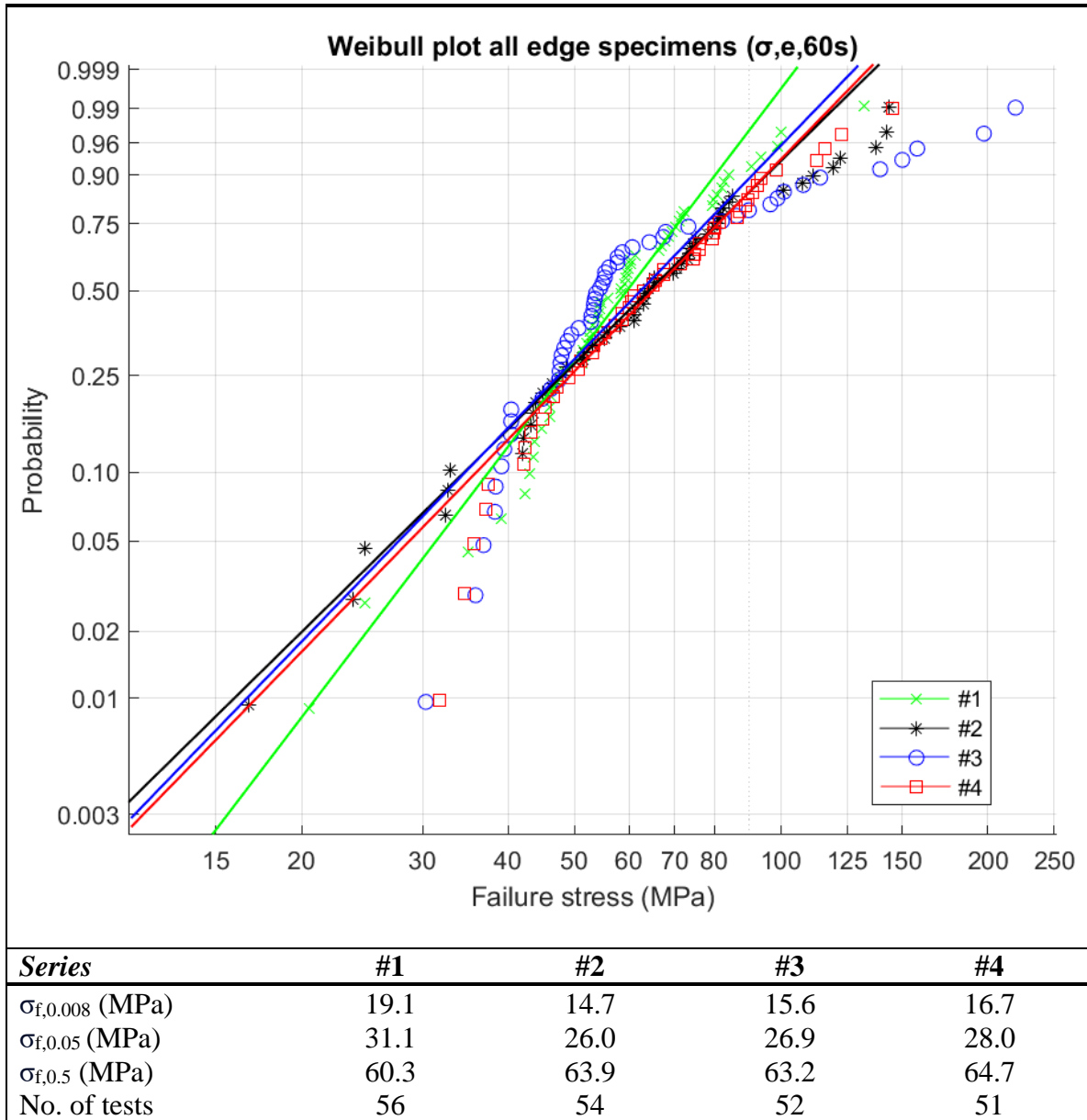


Figure 63. Weibull probability distribution: All sides - only edge-specimens.

5.7 New glass comparison

The difference in strength between the air- and tin-sides, as described in Section 5.5, is significant in the tested (old) glass. The question is whether the difference between the strengths in air- and tin-sides worsens as the glass ages, or is this difference already there with new and unused glass panels? Comparing old and new glass is done by using results from other experiments. For instance, Irene Sofokleous tested both old and new glass with a CDR test for her Master's Thesis (Sofokleous, 2022). The results of the tests with new (AR) glass can then be compared with the results of the CDR tests of old glass from this study. Because the specimens of the new glass had different dimensions at the time of testing, namely 250mm x 250mm and 450mm x 450mm, the values of the equivalent failure stresses cannot be compared one-to-one with the results of the specimens from this study with dimensions of 150mm x 150mm. Using formula (20), the values of the measured failure stresses for new glass with dimensions of 250mm x 250mm and 450mm x 450mm are converted to the same dimensions as the specimens of old glass (150mm x 150mm). After this size conversion, the results can be compared in a more reliable way.

$$\frac{\sigma_{f,A1}}{\sigma_{f,A2}} = \left(\frac{A_1}{A_2}\right)^{\left(\frac{1}{\beta}\right)} \quad (20)$$

Where,

- $\sigma_{f,Ai}$ = the failure stress of the panel,
- A_i = the surface area,
- β = the estimated shape factor of the Weibull distribution ($\beta = 15$ (Shen and WORMER, 1998)).

Figure 64 shows the Weibull distribution of both old (NA) and new (AR) glass, also showing the distinction between air-side and tin-side. For $\sigma_{f,0.5}$, $\sigma_{f,0.05}$ and $\sigma_{f,0.008}$, the tin-side of new glass is 20%, 12% and 9% stronger than the tin-side of old glass, respectively. For the air-side, the new glass is 34%, 42% and 52% stronger, respectively. What is most striking about the characteristic points is the fact that for the $\sigma_{f,0.5}$, or the theoretical value at which 50% of the tested specimens fails, in this case for the tin-side of new glass is lower than for the air-side of old glass. The average measured value ($\sigma_{f,mean}$) of the tin-side of new glass is 72 MPa, while for the air-side of old glass it is 79.4 MPa. It can thus be concluded from the series tested that the average strength of the tin-side of new glass is already lower than that of the air-side of 36-year-old naturally aged glass. Weathering then plays in this case a lesser role than whether a glass panel is tested on the air- or tin-side. Because the slope (shape parameter) of the lines in the Weibull distribution differ little for the different series, it can be questioned how 'clean' and 'undamaged' the as received (new) glass was. Without any small scratches and pits, a steeper line and therefore a more reliable series is expected than is currently the case. Because the data was converted for the dimensions of the specimens, and worked with different machines, different loading and support rings, and different test conditions, it is dangerous to trust this data too completely.

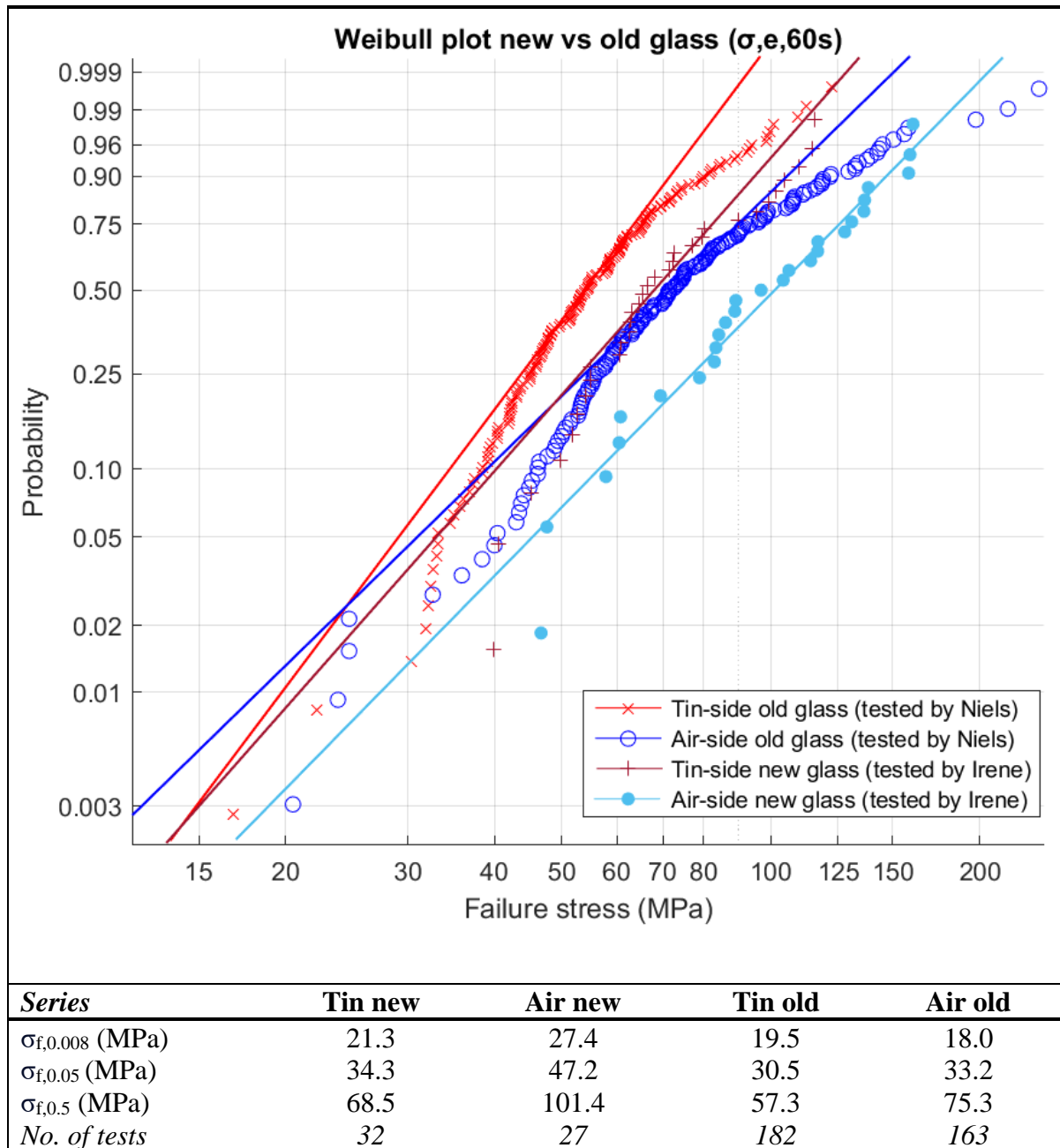


Figure 64. Weibull probability distribution: Old vs new glass - data Irene.

A more reliable comparison can be made with the data obtained from the experiments done by Thijs van der Linden, who for his Bachelor's Thesis tested new glass with the CDR test (Van Der Linden, 2023). In this case, the same machine, loading ring, support ring and specimen dimensions were used. The number of tests is just a bit low (20 tests tin-side, 17 tests air-side), compared to the number of tests done with naturally aged glass. The difference in distributions in this case is much larger than it was with Irene's results. Figure 65 shows the Weibull plots of the new and aged glass, again distinguishing between the air-side and tin-side. For $\sigma_{f,0.5}$, $\sigma_{f,0.05}$ and $\sigma_{f,0.008}$, the tin-side of the new glass tested by Thijs is 44%, 105% and 165% stronger than the tin-side of old glass, respectively. For the air-side, as received glass is 129%, 154% and 176% stronger, respectively. These high values indicate that in this case weathering does play a major role in reducing the strength of the glass. Here, contrary to Irene's data, the tin-side of new glass does have higher values on the characteristic points than the

air-side of old glass, although the average values with 81.3 MPa and 79.4 MPa, respectively, are not far apart. What is striking, however, is the difference in average strength between the air- and tin-sides of new glass. With an average strength of the tin-side of 81.3 MPa and of the air-side of 170.4 MPa, it again becomes clear that the influence of the production process regarding air- and tin-side is very large in this case. Small damages and tin residues that occur on the side of the glass panel that is in the tin bath and transported over the rollers thus, for both new and old glass, affect the strength and distribution course of the Weibull plot.

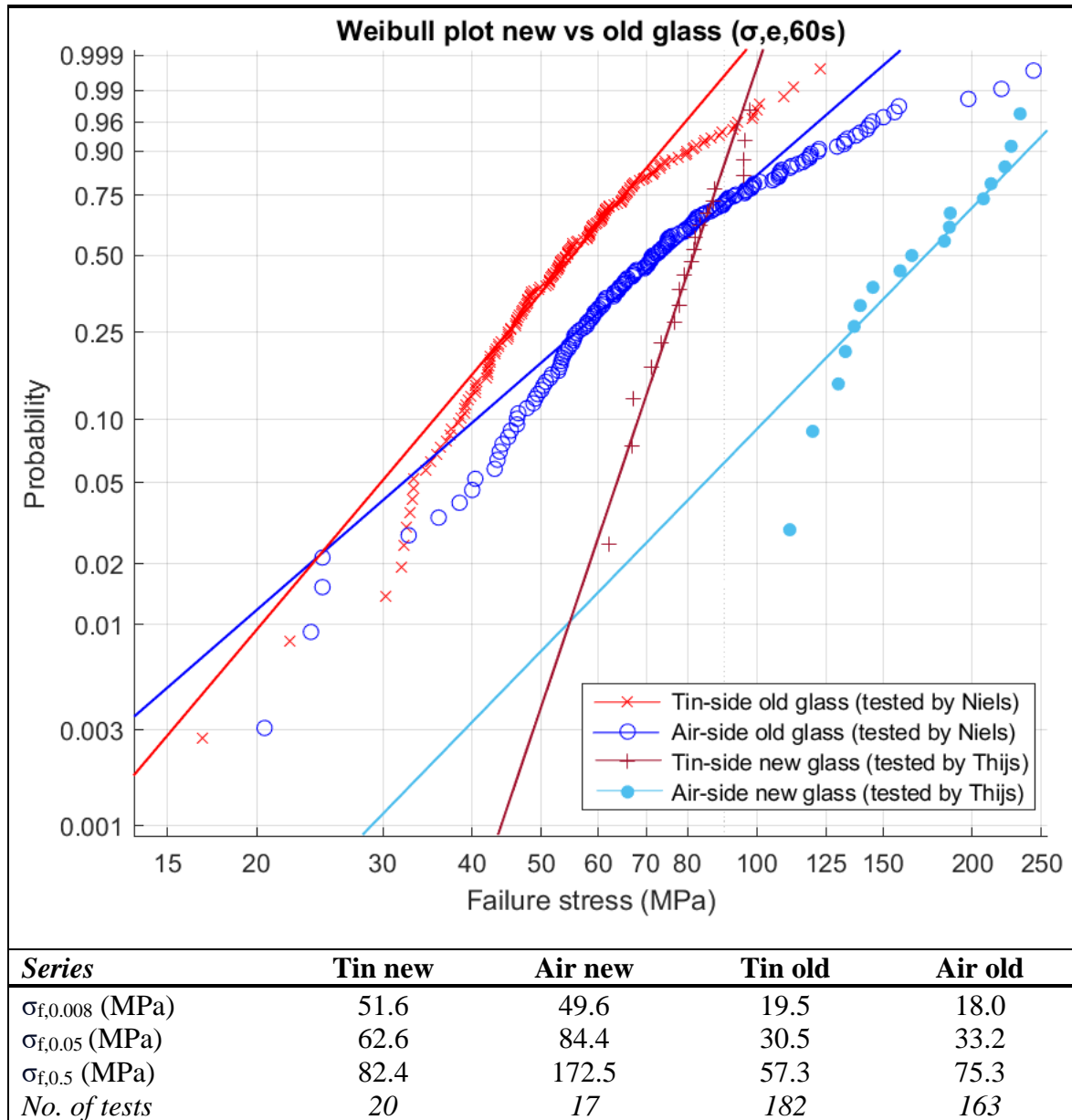


Figure 65. Weibull probability distribution: Old vs new glass - data Thijs.

5.8 Goodness of fit

To investigate whether the 2PW distribution method used properly describes the data, a goodness of fit test was applied. Besides the 2PW, the normal distribution and the lognormal distribution were also included in the goodness of fit test. This is to compare the 2PW used with also commonly used distributions in statistics. The Anderson Darling (AD) method was used for this purpose. This method uses a weight function to give more weight to the data of the upper and lower tail of the CDF (Datsiou and Overend, 2018). The goodness of fit is represented in a p_{AD} -value. This p_{AD} -value is between 0 and 1, where a value of 0 indicates that the data does not follow the chosen distribution function. With a p_{AD} -value of 1, the data follows the chosen distribution perfectly. The probability of rejecting a good fit is chosen before the statistical analysis, and it is called level α . In this project, a value of 0.05 was chosen for the α . This means that when the p_{AD} -value exceeds 0.05, the data is assumed to follow the chosen distribution function at an acceptable level. If $p_{AD} < 0.05$, it can be said that the data does not follow the chosen function well enough. The formulae used to arrive at the p_{AD} -value are shown below in formulae (21), (22) and (23) where n is the number of specimens in the series under study.

$$p_{AD} = \frac{1}{1 + \exp(-0.1 + 1.24 * \ln(AD^*) + 4.48 * AD^*)} \quad (21)$$

Where,

$$AD^* = \left(1 + \frac{0.2}{\sqrt{n}}\right) * AD^2 \quad (22)$$

and

$$AD^2 = -k - \sum_{i=1}^n \frac{(2i-1)}{n} * \left[\ln(P_f(\sigma_i)) + \ln(1 - P_f(\sigma_{n+1-i})) \right] \quad (23)$$

The results can be seen in Figure 66, along with the chosen significance level of 0.05 (horizontal red line). Here it can be seen that for 75% of the tested series, the 2PW has a p_{AD} -value higher than 0.05. For the normal and lognormal distributions, this is even slightly higher, at 79% and 96%, respectively. It is also notable that no clear distinction was found between p_{AD} -values of air -and tin-sides. The high values are not always and air- or tin-side, and this also applies to low values found for goodness of fit. For the new glass tested by Thijs (see right-side of the Figure 66, where also distinction has been made between tin- and air-side), the values of the goodness of fit are a lot lower for the 2PW as for the normal distribution and the lognormal distribution, something that is not always the case with weathered glass. As can be seen in Figure 66, not always the 2PW is the function with the best p_{AD} -value, but it seems to have been sufficient for this study with weathered glass to have used this distribution function.

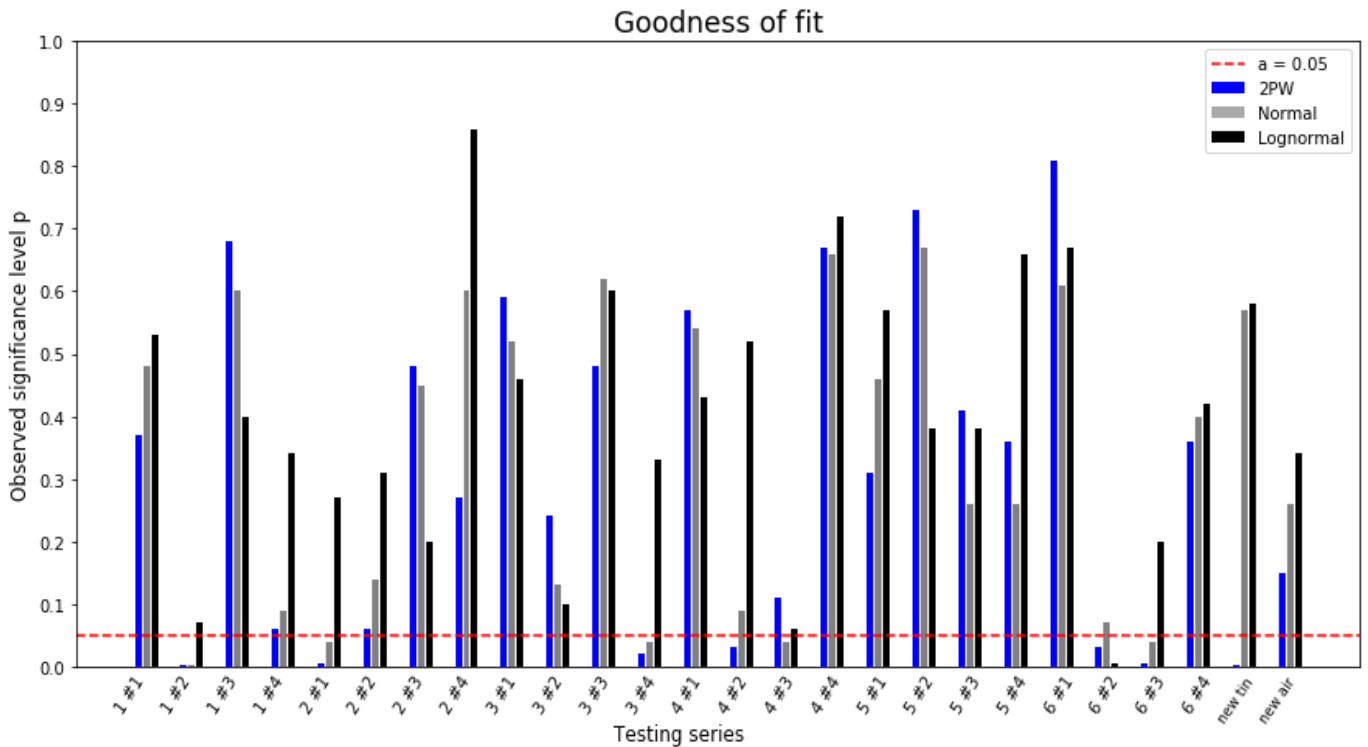


Figure 66. Goodness of fit of the test data to the three probability distributions

5.9 Discussion

Before analysing the results, it was expected, as described in Chapter 4, that the outer sides of both panels (side #1 and #4) would contain more damage than the sides on the inside of an IGU (side #2 and #3). A further distinction was also made between side #1 and #4, with the hypothesis that side #1 was more in contact with effects of the environment, such as precipitation and wind, so a somewhat different damage pattern was expected here than for side #4. Side #2 and #3 received virtually the same treatment during their lifetime, so major differences in strength were not expected here. Again, these hypotheses are generally correct when looking at the whole set of tests. The average strengths of side #2 and #3 are slightly higher than those of side #1 and #4, although the differences are marginal, between 9% and 17%. What is more striking is the fact that in terms of design strength according to the ASTM design code, the stress at which 0.8% of the specimens fail is actually lower for side #2 and #3 than for side #1 and #4. This seems to be due to the fact that the damage pattern is more evenly distributed for side #1 and #4, which means that the measured failure stresses are closer together and thus form a more reliable series. At side #2 and #3, the variation in failure stresses was a lot larger, resulting in a less reliable series of tests and thus a lower design strength.

This immediately raises the issue of whether this design strength according to the ASTM is too conservative. Take side #2, where the weakest of the 84 specimens tested failed at a stress of 16.8 MPa. The design strength of this series is even lower than the weakest specimen at 11.9 MPa. Side #3 is the same case, where the design strength is 8.4 MPa, while the weakest glass specimen only failed at a stress of 30.3 MPa (!). Because the side #3 series also contains specimens with very high values for the failure stress, this makes the stress less reliable, resulting in a lower scale parameter (slope of the line), thus ultimately resulting in a low design strength. This indicates that the way a 2PW

distribution is obtained for low probabilities of failure is very conservative. It seems to describe the data better when there is a kink in the distribution line, for example, or when the line is considered non-linear.

Still, the thing that stands out the most after analysis is the difference in strength ($\sigma_{f,0.5}$) between the air- and tin-side. The average measured strength of the air-side is 31% higher than that of the tin-side. For the new glass tested by Irene and Thijs, the difference in air- and tin-sides was even greater, 48% and 109%, respectively. These large differences are explained by the fact that the tin residue and damage incurred when a sheet of glass passes over a conveyor belt or roll causes a lower strength of one side of the glass. The fact that these differences were so large does raise the question of whether more account should be taken of this during the production of double- or triple-glazing panels, in order to predict in advance, the behaviour and influence of weathering for each side of the glass. Differences in appearance between tin- and air-sides were not considered in the case of this study, as initially only differentiation between different sides of the IGU was made. To see a better difference in damage appearance between the air- and tin-sides, another microscopic examination will have to be carried out, focusing on the variable air- and tin-sides. Again, it is the case that the design strength $\sigma_{f,0.008}$ is very low, especially for the air-side series. Due to the again large variation in values of the air-side, the values for low probabilities of failure seem to be very conservative. As a result, the design strength of the air-side series is even lower than that of the tin-side series, despite the fact that the air-side series also has a large number of high failure stresses.

Despite questioning the credibility of the Weibull distribution in some ways, another way has been found to change the distribution line. Namely, when the 5% or 10% weakest specimens are removed from a series of tests, a more reliable result is obtained, and higher values are found for the characteristic probabilities of failure. The question is how to find the weaknesses in an IGU in advance. In the future, one should be able to map the damages of the entire glass panel, so that research can be used to find out whether the largest damages also cause the weakest spots in the glass panel in question. When this possibility exists, repairing or somehow removing the largest defects in the glass panel can provide higher average, characteristic and design strength. In the case of this study, it has been shown that when strengthening the 10% weakest specimens, this can provide an increase in average strength of about 5%, and for an increase in design strength of up to 19%. This can make the difference between an old glass plate just meeting or just not meeting current standards according to the Eurocode or ATSM.

Because there was an opportunity to see if there is a difference in strength also within a glass panel, edge and mid-specimens were also compared. This was done because it was suspected that the method of separation might have caused more damage to the edge of the glass panels. A roughness was also felt on certain specimens, which was caused by the grinder at the time of cutting the IGU. These were only specimens originating at the edge of the IGU. The results between of the comparison between the edge and mid specimens indicates that a difference was found in strength, where, as expected, the mid specimens had higher strength than the specimens at the edge. It can be valuable to know this, when, for example, smaller panes are extracted from a large glass panel. These tests indicate that in this case, that is in the middle of a glass panel.

The comparison in orientation of the IGU also did not give shocking results. Due to the relationship of wind direction, a slightly lower strength was expected for the west-oriented IGUs. The results showed this expectation to be correct, but more research will need to be done to see if this influence is indeed significant. The distance to the coast, where much sand is carried by the wind, may also be crucial factor in terms of difference in strength between west- and east-oriented IGUs.

The main conclusion from analysing the results is the fact that the air- and tin-side influence is large, and in some cases even greater than 36 years of weathering. Associated conclusion is whether the way they obtained results in this study, via the 2PW distribution, is the best and most reliable way. Especially for low probabilities of failure, this distribution function is known to give very conservative values.

6. Reuse opportunities

6.1 Introduction

The purpose of this chapter is to examine to what extent the strength of old glass panes allows to be reused in the same or new functions. To conduct this examination, the measured strengths, shown in various figures in the previous chapter (Chapter 5), are first compared with the current standards in the field of glass strength. By comparing the measured strengths with values that glass should meet, it can be assessed whether (part of) an IGU can be reused and whether it is justified in terms of strength. The comparison and corresponding conclusions of specimen strengths against glass strength codes and requirements is shown in Section 6.2. A number of options for reusing the IGU are then discussed in Section 6.3. This indicates whether or not the IGU tested are suitable for a particular method of reuse. Herein, five different ways of reuse are distinguished. First, the option of reusing an entire IGU is considered in Section 6.3.1, which is the most sustainable solution. Then there are also other solutions for more sustainable use of materials that are looked at, such as the hybrid IGU (Section 6.3.2), which consists of one new and one old glass panel. Lamination of old glass panels (perhaps together with new panels) of an IGU can also be a way of reuse and is therefore highlighted in Section 6.3.3. The last two possibilities discussed in terms of reuse are using old glass panels from an IGU as single glazing in Section 6.3.4, and using smaller panels taken from or cut out of a used glass panel from an IGU, which is described in Section 6.3.5.

Note that the potential for reuse uses results from the 2PW, so comparing with other survey results using other methods may not give a good impression.

6.2 Design strength of reused glass

The theoretical strength of the tested specimens is based on two different standards, namely the Dutch and the European design codes. These are the Dutch NEN2608 (2014) and the European EN16612 (2019). Table 17 gives an overview of how the theoretical design strength $f_{g,d}$ was determined for both standards. For explanation of the parameters, please refer to Section 2.5.2. The calculation was assumed to be linear and wind load as the normative load. For the k_{mod} at the EN16612, the choice was between short term wind load (5 sec) and long-term wind load (10 min). In this case, the factor for k_{mod} for short term wind load, the value of 1, was used. Furthermore, the tested glass is classified as non-prestressed float glass. As indicated in both standards, the characteristic value for the strength of float glass is set at 45 MPa. This is the so-called 5% risk value, a strength value commonly quoted for construction materials, so also in the case of this study. It was decided to use a value of 1 for the surface factor k_a . When the glass reuse function is known, this factor can be added with the corresponding value for k_A so that the final design strength belongs to the glass surface to be used. So, in this case, the calculation continues with a value of 1 for k_a .

Table 17. Design strength for Dutch and European design standard.

<i>Standard</i>	Formula	k_{mod}	k_{sp}	k_e	k_A	f_{g,k} (MPa)	γ_{m;A}	f_{g,d} (MPa)
NEN2608	$f_{g,d} = k_{mod} * k_{sp} * k_e * k_A * f_{g,k} / \gamma_{m;A}$	1	1	0.8	1	45	1.6	22.5
EN16612	$f_{g,d} = k_{mod} * k_{sp} * k_e * f_{g,k} / \gamma_{m;A}$	1	1	1	-	45	1.8	25

As can be seen, not both values are the same, and the design strength value for the Dutch code is about 11% lower than the value for the European code.

Now that the theoretical values of strength for both standards are known, they can be compared with the results obtained from the CDR tests. As mentioned earlier, for the ASTM standard, the design strength can be obtained when the stress is calculated at a failure probability of 0.8%, or $\sigma_{f,0.008}$. European regulations assign a different failure probability to the design strength, namely the 0.12% probability that a specimen will fail at the design strength. This $\sigma_{f,0.0012}$ is calculated for all test specimens, with the note that in this case, an equivalent load duration of 5 seconds is used, instead of the equivalent load duration of 60 seconds used so far. This causes a different value of $\sigma_{f,eq}$ because in formula (14) the hit changes from 60 to 5 seconds. For the comparison of the characteristic strength of 45 MPa with the $\sigma_{f,0.05}$ as calculated for the different series of tests, also here, the reference load time of 5 seconds is used.

Figure 67 and Figure 68 show how the characteristic and design strengths of the tested series, obtained from the Weibull distributions, relate to the theoretical strengths of the Dutch and European code. To clarify this, a distinction has been made between the air- and tin-sides tested. In terms of characteristic strength $\sigma_{f,0.05}$ and load duration of 5 seconds, it can be seen that only 11 of the total of 24 series tested of between eleven and twenty specimens reached the 45 MPa limit. This is 46% of the series. These series were all tested on the air-side and it can be said that 67% of the tested air-side series meet the theoretical characteristic strength of 45 MPa. For the tin-side, only 25% of the series achieves this value. For the design strength, as mentioned, the load duration reference time also has been reduced to 5 seconds. The stress at a failure probability of 0.12% was calculated and compared with the theoretical design strength of NEN2608 and EN16612, which are shown in Figure 68. It can be seen that eight of the 24 series exceed the design strength of the Dutch code (22.5 MPa), of which there are four to four air-to-tin ratios. This represents a percentage of 33% of the series that still meet the Dutch design strength standard in terms of design strength. As expected, the difference in strength between air- and tin-side at lower failure frequencies is not there as it is with, for instance, the average strengths of series tested on air- or tin-side. Here, only 2 out of 24 series achieve the design strength according to EN16612 of 25.0 MPa, representing 8%. Again, one of the series that has a design strength higher than 25.0 MPa is an air-side, and one series is a tin-side. The percentage of 8% indicates that the tested panels certainly no longer have the strength that new glass should have according to standards.

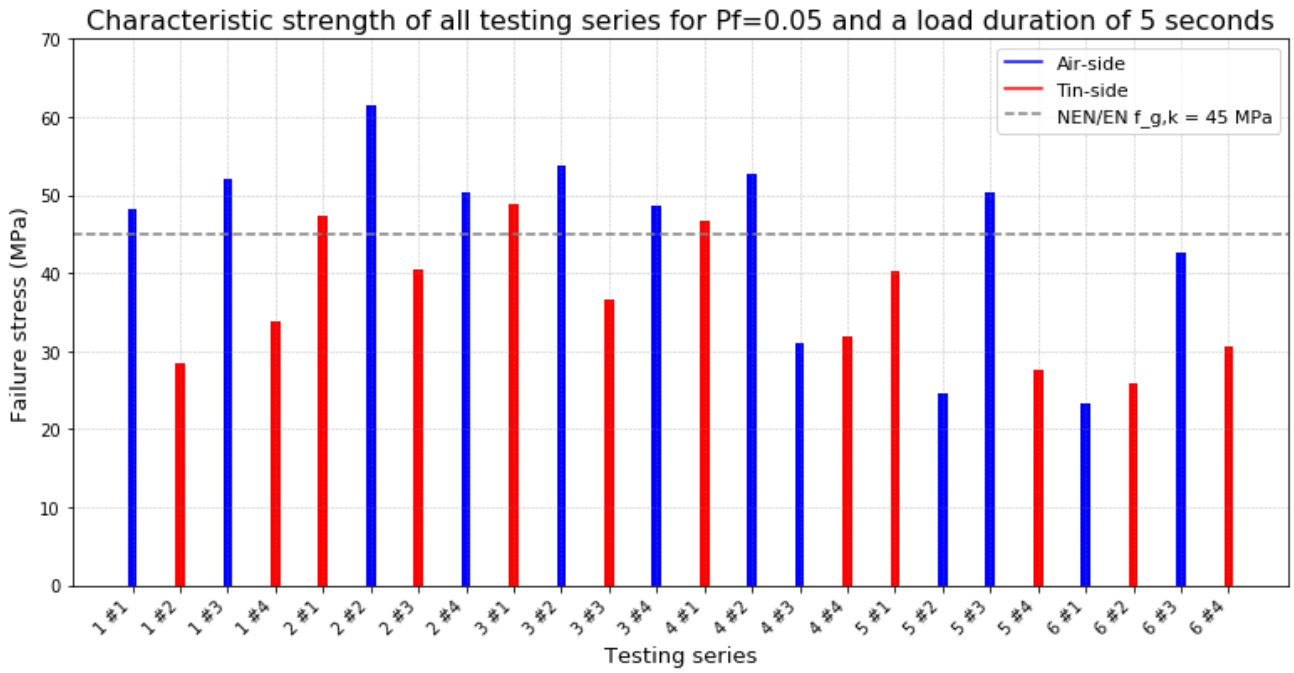


Figure 67. Characteristic strength of all series for $P_f=0.05$ and load duration of 5 seconds.

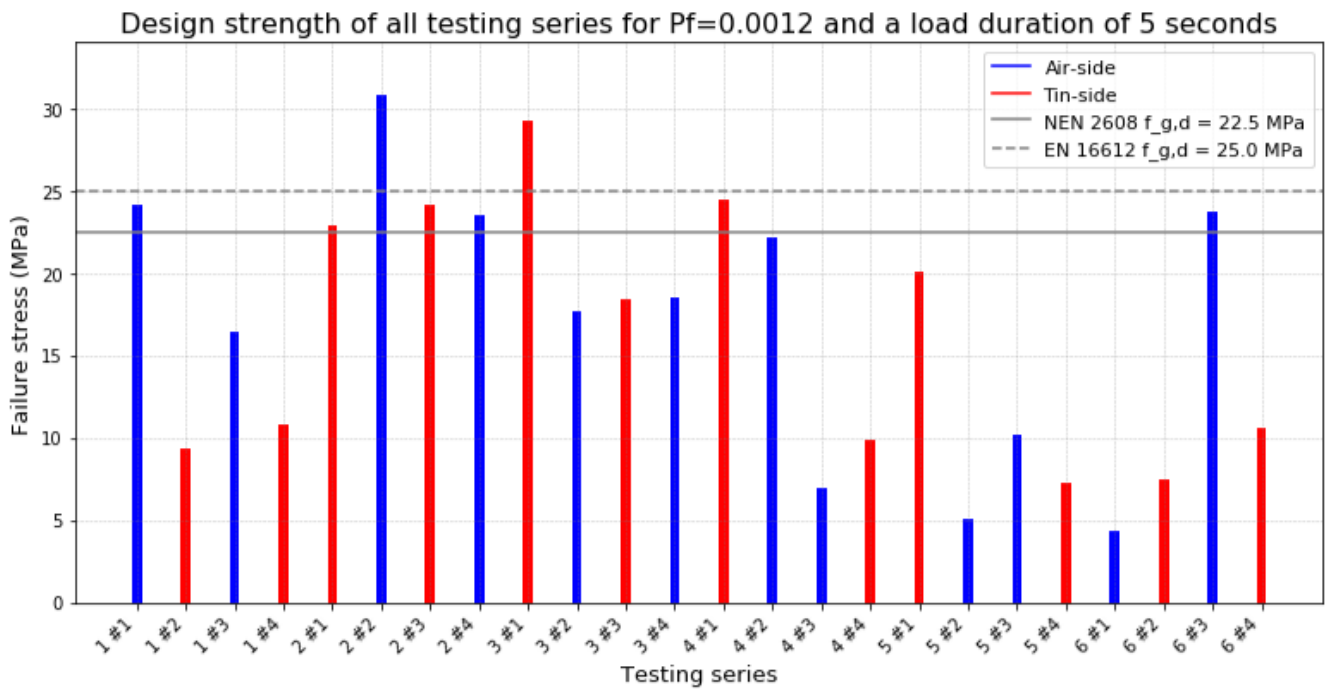


Figure 68. Design strength of all series for $P_f=0.0012$ and load duration of 5 seconds.

The design strength is determined in Figure 68 by reading it from the Weibull distributions of the tested series. Another way to arrive at a design strength is by calculating the design strength from the read characteristic values from the Weibull distributions using the formulas from Table 17. The challenge here is to determine the correct values for the variables within this formula. For example, for glass that has been used for 36 years and performed its function well, is it really necessary to use the high safety factor $\gamma_{m;A}$ of 1.6 or 1.8? For the k_{mod} a value of 1 can be used when it is assumed that wind is the normative load. If, for example, a safety factor of $\gamma_{m;A} = 1.15$ is used and the rest of the parameters in the formula in Table 17 are assumed to be 1, this produces the diagram shown in Figure 69. In this case, the values of the characteristic strength are reduced by a factor of 1.15 to obtain the design strength. It can be seen that the design strength of each series is now a lot higher, which is of course due to the chosen $\gamma_{m;A}$.

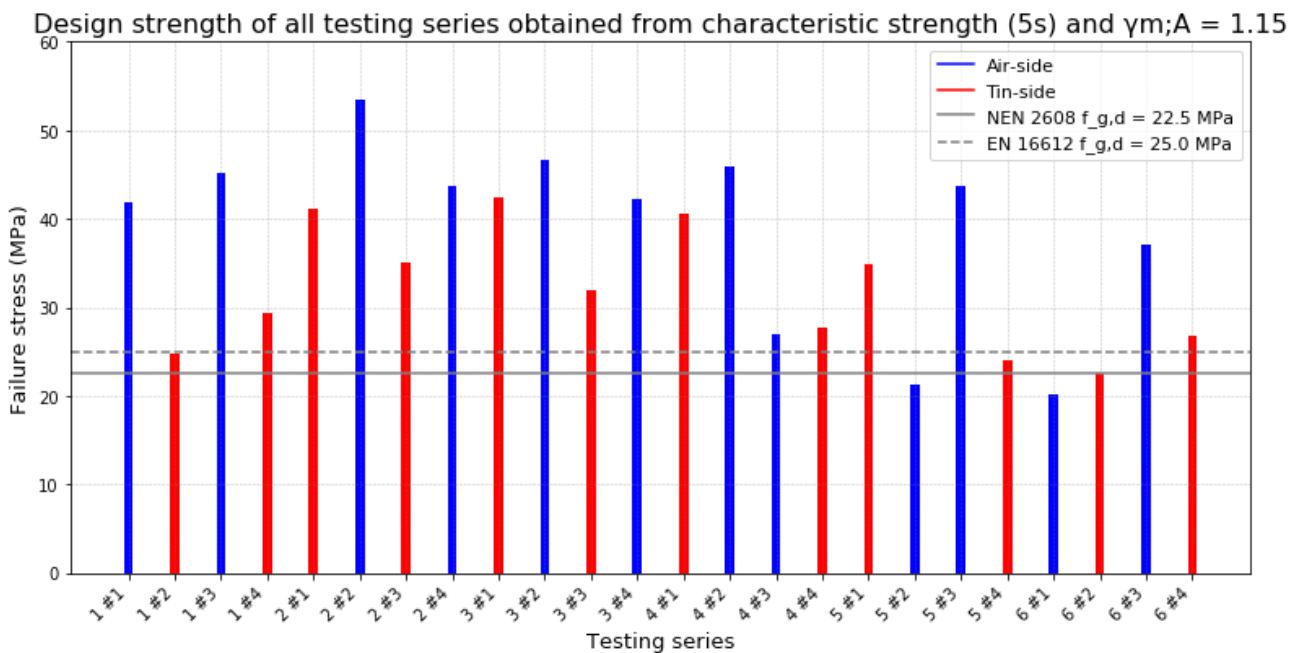


Figure 69. Design strength of all series obtained from characteristic strength with $\gamma_{m;A} = 1.15$ and load duration of 5 seconds.

The question now is whether this value of 1.15 is a valid assumption. This is checked by making a number of Weibull plots in which the load duration is also reduced from 60 to 5 seconds, allowing the results to be compared more reliably with the Dutch and European design standard. As a result, the Weibull distributions change slightly and can be used to tell what a good range for the material factor of used glass is.

The first Weibull distribution made is the comparison between the air- and tin- sides of the tested series. This is shown in Figure 70. The course of the distribution is similar to that of Figure 50. It can also be seen that for the characteristic strength ($\sigma_{f,0.05}$) the value for the tin-side is 36.1 MPa and for the air-side is 39.3 MPa. If it is assumed that a design strength of 25.0 MPa as described in the EN16612 is to be obtained, a range of a material factor can be suggested from this. To reduce the values 36.1 and 39.3 MPa to 25.0 MPa by adding a material factor, it should be between 1.44 ($=36.1/25.0$) and 1.57 ($=39.2/25.0$). This indicates that the material factor of 1.15 may have been an overly optimistic choice when these results are analysed via the 2PW.

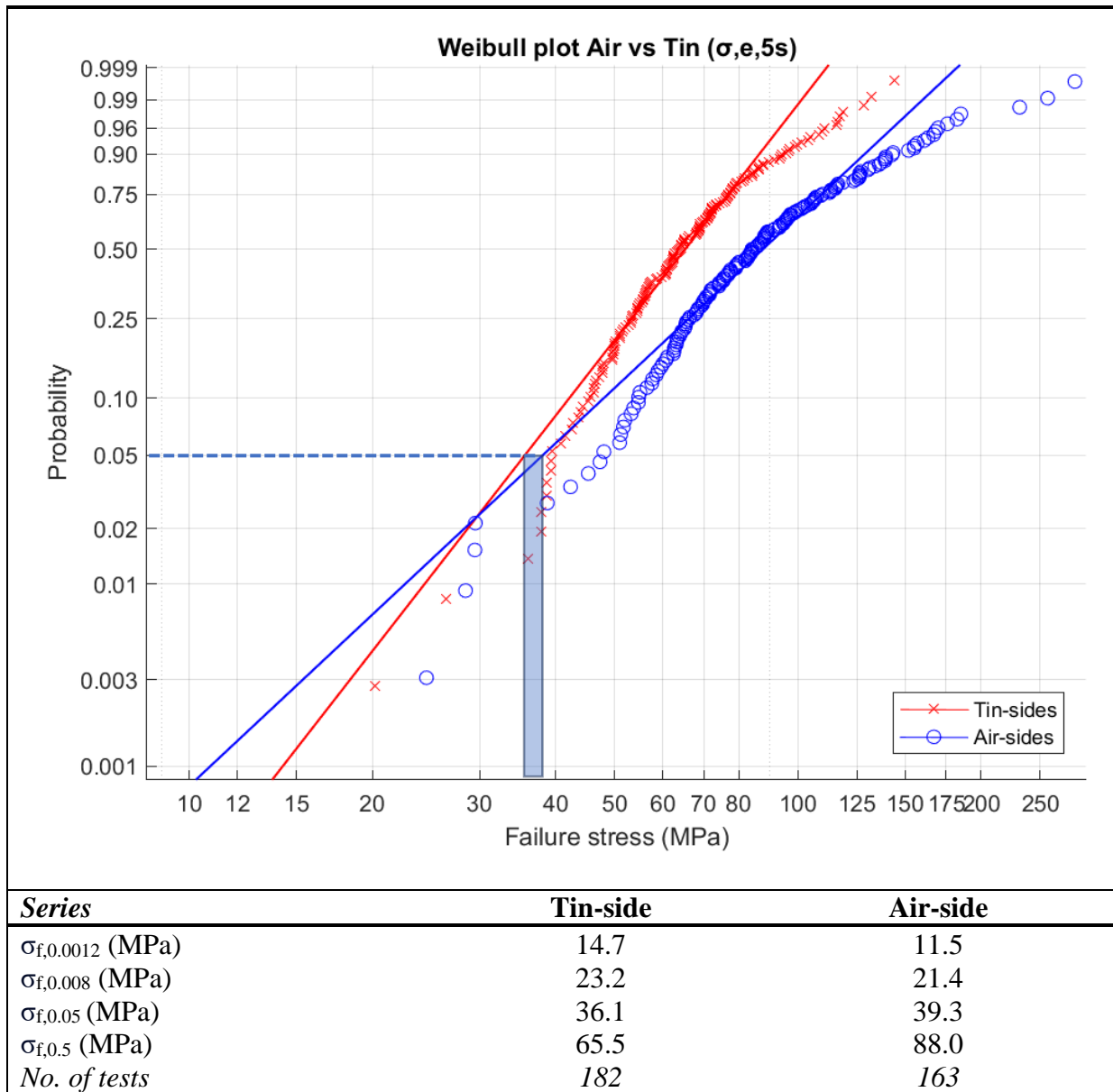


Figure 70. Weibull probability distribution: Air-side vs tin-side (5 sec)

Also, for the Weibull plot comparing the 4 different sides, a new graph was created with 5 seconds load duration instead of the previously used 60 seconds in Figure 49. This new plot can be seen in Figure 71, where also the values are given for the characteristic points, including the $\sigma_{f,0.0012}$, a failure probability that according to EN16612 gives the design strength in the Weibull plot. Now these are very conservative values and again a range of the material factor is considered. Again, assuming a design strength of 25.0 MPa, the material factor, based on the 2PW, can be between 1.18 ($=29.4/25.0$) for side #3 and 1.64 ($=41.1/25.0$) for side #1. In the case a wide range, because the values for the characteristic strength are quite different between the sides.

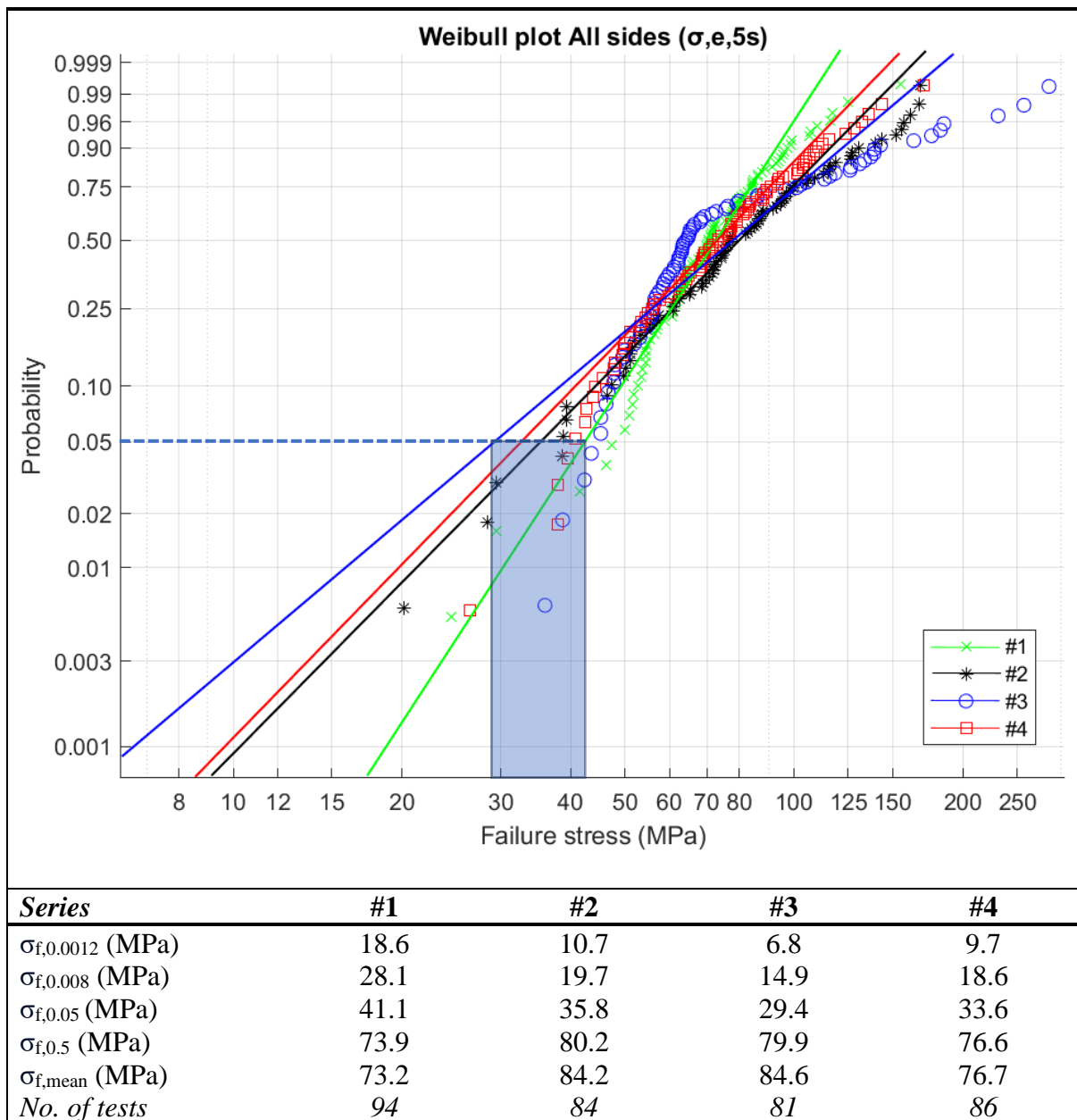


Figure 71. Weibull probability distribution: All sides (5 sec)

To assign a value to the material factor of the naturally aged glass used in this experiment, a Weibull plot was made putting all 345 valid test results into one two-parameter Weibull distribution (Figure 72). This showed that the characteristic strength of this large series is equal to 34.0 MPa. When a material factor of 1.35 is superimposed on this, one arrives at the desirable design strength according to the Eurocode of 25.0 MPa. This indicates that the material factor currently used (1.6 - 1.8) for new glass can be slightly reduced for glass intended for reuse. The previously assumed value of 1.15 was too optimistic, but also the value of 1.35 following from Figure 72, seems more representative than the higher values of 1.6 – 1.8, when considering a large series of tests on used glass.

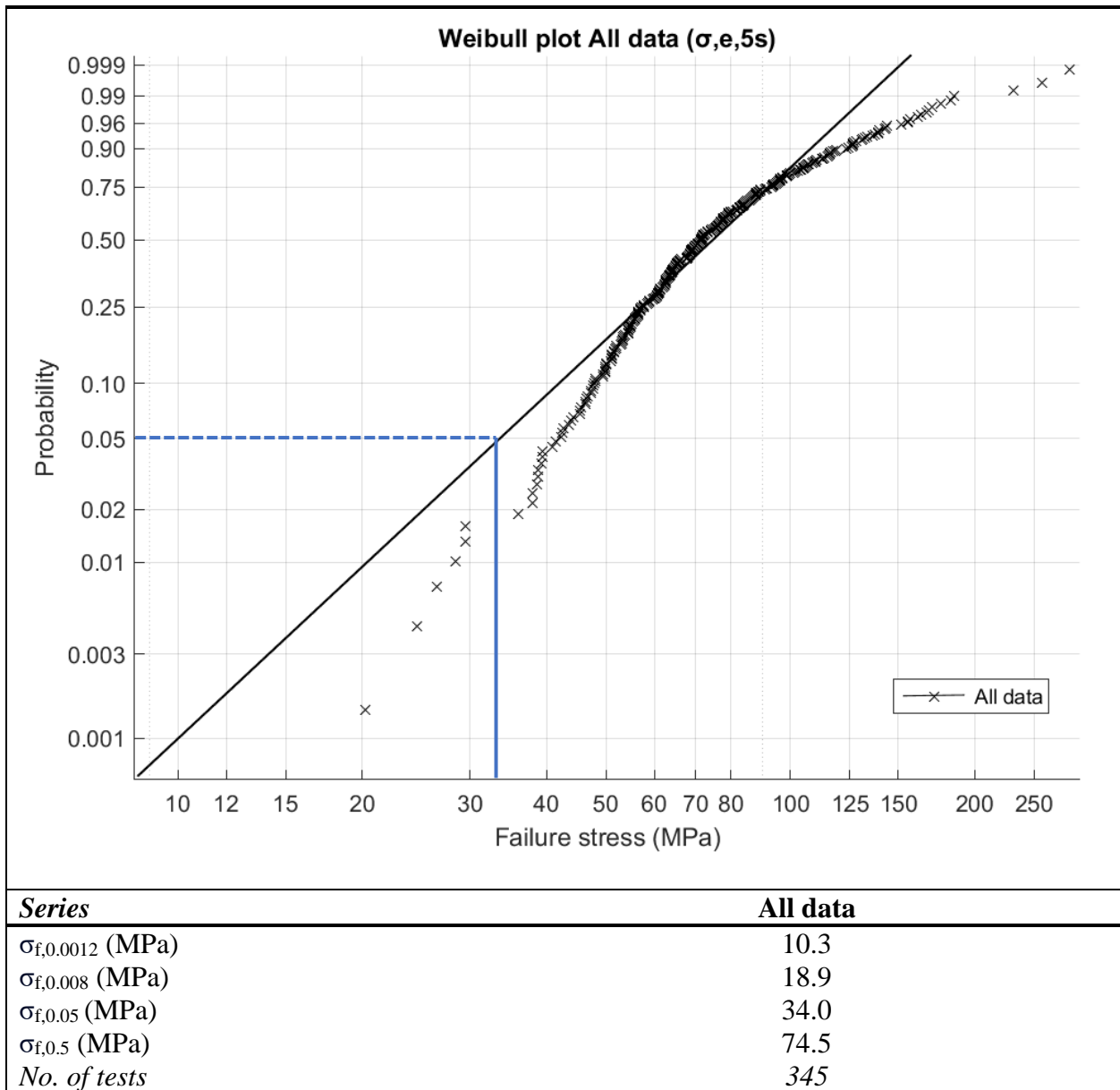


Figure 72. Weibull probability distribution: All data (5 sec)

6.3 Reuse

After comparing the strengths of the tested specimens with the theoretical and required strength according to current standards, options can be discussed on the extent to which reuse is an option. Reusing glass panels from an IGU can be done in several ways. These include separating the two glass panels to obtain two separate panes, or instead leaving the IGU together and reusing it as a whole. Here, the strength values from Section 6.2 can be used to determine the possibilities for reuse when considering strength. Other options may also emerge. These are discussed in this section, distinguishing between five different reuse options. Section 6.3.1 discusses whether it is possible to reuse an entire IGU one-to-one. Another slightly more reliable option beforehand is the solution of a hybrid IGU, discussed in Section 6.3.2. This amounts to an IGU consisting of a used (NA) glass panel and a new (AR) glass panel, making 50% reuse applicable. The use of single glass from used IGUs is also included as an option, in Section 6.3.3. Because Section 5.6.2 looked at the location of the specimens in a particular IGU, the opportunity arose to investigate whether reusing smaller panels sourced from used IGUs is an option. This method of reuse involves identifying the weaknesses of a naturally aged IGU, so that smaller glass panels with higher strength than an entire IGU can be reused. This option is discussed in Section 6.3.4. The last interesting option is laminating old glass from IGUs, possibly in combination with new glass. This is shown in Section 6.3.5.

The purpose of giving all these options for reuse is to reflect whether it is possible to discuss options based on the tests carried out. The results of the tests are compared with the current Dutch and European design standards, which are used as comparators in the case of this study. This will show the possibilities of using 36-year-old glass panels for new purposes in a sustainable way. If the values of the tested IGUs no longer have the strength they should have according to Dutch and European design standards, this does not mean that the glass panels cannot be reused at all. Relatively weaker panels can be reused for other functions and/or locations, where the loads are for instance a lot lower than those assumed by the current standards.

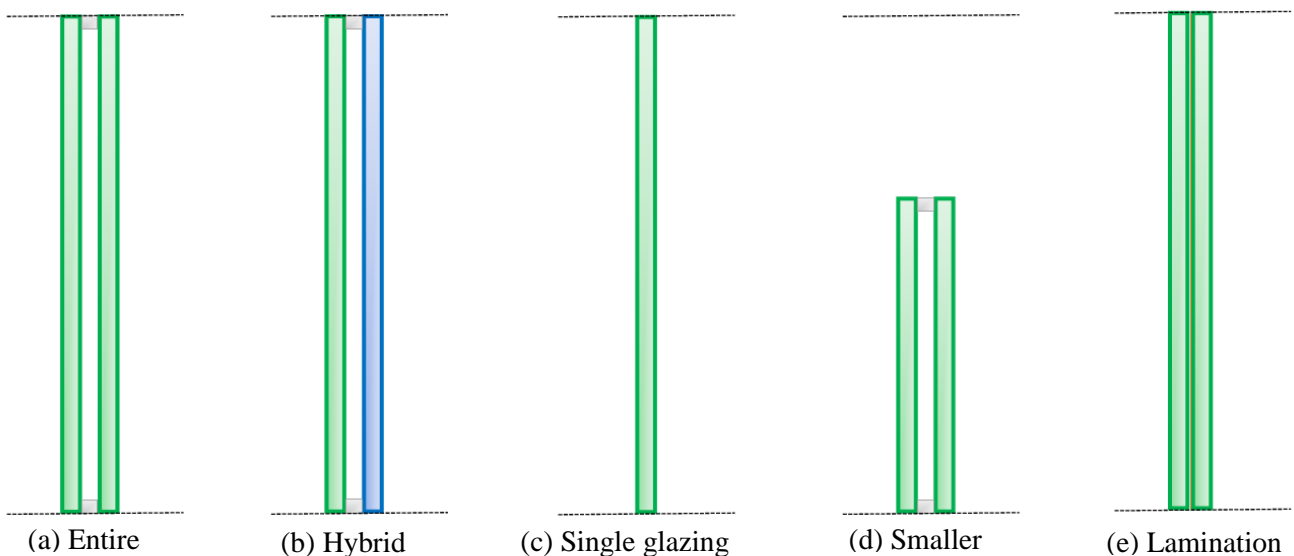


Figure 73. Reuse options.

6.3.1 Entire IGU

The most sustainable reuse option is to maintain the entire IGU. This means reusing 100% of the materials and not using or wasting new materials and raw materials. The question is to what extent it is possible in terms of the remaining strength of old IGUs when compared with current design rules. After all, used glass must still be strong enough to be used for new functions, just as new glass must be. When looking at the tested IGUs individually, only IGU 2 has a higher design strength than the theoretical design strength of the Dutch standard for all four sides tested. This was based on the values read from the Weibull distribution (Figure 68). When looking at the characteristic strength, none of the six IGUs tested has all four sides still stronger than the characteristic strengths of the codes after 36 years of use. In terms of strength, this gives little potential for reuse of an entire IGU, in the same function. Only if the requirements on the IGU differ, such as reducing the stress that occurs on the IGU, are the IGUs as a whole suitable for reuse. Consider a different location, for example, so that the wind load has a different value. There are also other considerations to be considered when reusing an IGU:

- Inspection of condition: It is crucial that the glass panels are in good condition, without cracks, chips or other damage.
- Sealing and insulation: The seals of the IGU must be intact and effective to maintain its insulating properties. If the seals are damaged, this can lead to moisture problems and reduced insulation.
- Compatibility: When reused, the IGU must fit the dimensions and specifications of the new frame or application.
- Safety and conformity: The IGU should comply with local building regulations and safety standards.
- Reuse process: Reusing an IGU requires careful dismantling and possibly repair work. This should be carried out by experienced professionals.

As shown in Figure 68, two of the twelve panels are still compliant according to the design rules of the Dutch code, namely 2-out (#1 and #2) and 2-in (#3 and #4). A combination of panels can also be made to arrive at a 'new' IGU with two panels coming from different IGUs. A caveat to this option is the fact that the sealing and spacer between the two panels must first be removed and then reinstalled. A new spacer and sealing do provide more security in terms of insulation and preventing moisture from forming between the glass panels. As a result, the reuse percentage is slightly less than 100%, but it does give a slightly more reliable construction, because of the new sealing and spacer.

Despite this option, it generally does not seem desirable to reuse an entire IGU in the state as it is after 36 years in a new function. In the case of this study, the IGUs tested often no longer meet the current design standards of the Netherlands and Europe. The IGUs are suitable for reuse only when the load on the IGU is reduced and therefore the requirements are lower. Another function or location is required as a result. The new glass tested by Thijs with the same test conditions still indicates that weathering has a large share in strength reduction, as the new glass has high values for strength and more than meets the design values of the standards.

6.3.2 Hybrid

One option that may offer a little more potential is the option of hybrid construction. This involves using one used glass panel and one new glass panel for an IGU. This provides a reuse rate of 50%. However, a new sealing and spacer will be needed when producing this hybrid construction. Still, the

possibilities are limited. This is because each glass panel of a double-glazed construction generally needs to have the same mechanical strength as single glass of the same thickness. Based on the study, again as mentioned in section 6.3.1, only two of the twelve glass panels tested have the needed strength, according to the Dutch design standard (2-out and 2-in) This ensures that these panels can be used for hybrid construction with a relatively stronger new glass panel. The rest of the tested glass panels have at least one of the two sides that lower strength than the values of the Dutch or European design standard in terms of design strength. Again, giving it a new function or location is an option, resulting in lower requirements and different loads so that relatively weaker glass panels can also be reused. Nevertheless, producing a hybrid double-glazed construction is not a recommended option in practice. There are also other reasons for this:

- **Compatibility of materials:** Used glass panels can vary in composition, quality and strength. It is difficult to guarantee that the used panel has the same properties as the new panel, which can lead to uneven performance and potentially undesirable effects.
- **Wear and age:** Used glass may show signs of wear, scratches or other damage. These defects can affect the overall integrity of the double glazing.
- **Thermal performance:** Double glazing is designed to provide sufficient thermal insulation. If the glass panel used does not meet the required thermal specifications, the insulation value of the double glazing may be reduced.
- **Safety and reliability:** The safety of the final product may be compromised if the glass panel used does not meet safety glass standards.
- **Glass breakage and warranty:** Should a problem occur, it can be difficult to identify the cause of problems if a mix of used and new glass panels is used. Moreover, warranty conditions may not apply.

The bottom line is that hybrid construction is not desirable because of the potentially large differences in performance, in different areas, between the two glass panels. This makes for an unreliable IGU, and the chances of undesirability are considerable. Also, in terms of strength according to the tests carried out, for the IGUs used for this study, reusing the separate glass panels in a hybrid construction is not a suitable solution.

6.3.3 Single glazing

For single-glass strength, the same requirements apply as for the option of reusing whole IGUs and for hybrid construction. Thus, also for this option, there is little possibility of reusing individual glass panels of the tested IGUs as single glass. Only the two aforementioned panels (2-out and 2-in) have still the strength to be reused as single glass, according to Dutch design standards. This amounts to a percentage of 17% of the glass panels tested that are eligible to be reused as single glass. In this case, we are looking at a glass panel removed in its entirety from an IGU, and the dimensions of the panel are maintained. Again, reusing single glass from an IGU is an option when loads and stresses are reduced, by giving a new function to the glass or using it in another location. Other points to consider when using single glass coming from an old IGU:

- **Compatibility of the glass:** The glass panel from the double glazing should be compatible in terms of thickness and dimensions with the opening in which it will be installed.
- **Thermal insulation:** Single glazing has much less thermal insulation than double glazing. If energy efficiency is a crucial factor, using single glass can lead to higher energy costs.
- **Safety and compliance:** Reused glass should comply with local building regulations and safety standards.

- Sealing and finishing: To ensure that the glass is properly sealed, and that the surrounding construction is correctly adjusted to prevent any air leaks.

Even for this option, reuse without modifications to the glass itself, generally seems to be an undesirable solution. Based on the test results of the IGUs, there is too little confidence in the strength of the individual glass panels after the 36-year service life, when it is to be reused with the same strength requirements and occurring loads.

6.3.4 Smaller panels

It is possible to reuse old glass panels by cutting them into smaller glass panels. In this process, old glass panels are collected, cleaned and then cut into smaller sizes suitable for different applications. Because the study looked at the difference in strength between the edge and centre of an IGU, it is possible to detect differences in this. The purpose of this is to see the after 36 years in use to find the strongest areas of a glass panel. Figure 74 shows three images showing the average strengths of the specimens coming from the panels. Because not all panels were the same size, they are divided into IGU 1 & 2 (a), IGU 3 & 4 (b) and IGU 5 & 6 (c). A colour scale shows where in the panel, on average, the strongest specimens were located. This does not consider which side was tested and whether it was an air- or tin-side. This is more about the difference in strength between specimens at the edge and in the centre, as was also compared in Section 5.6.2. Initially, it cannot be seen directly from the figure whether the specimens at the edge of the IGU are clearly stronger or weaker than the specimens in the centre. The average strength (with 60 seconds load duration) of the specimens located in the four corners of the IGU is 58.4 MPa. Relative to the overall average of all specimens, which is 67.5 MPa, this is almost 14% lower than the average strength of the specimens. The method of separating the glass panels with the grinder, which caused additional damage, seems to be the main reason for the lower strength of specimens coming from the corners of an IGU. In Section 5.6.2, it also became further clear that the specimens at the edges are on average slightly weaker than the specimens in the centre. This can be seen from the values in Figure 61 in Section 5.6.2. The mean strength, characteristic strength and design strength of the mid-specimens are 5%, 9% and 27% higher for the edge-specimens, respectively. With the design strength of 14.6 MPa for the edge specimens and 19.9 MPa for the mid-specimens, it can be concluded that when all the mid-specimens are analysed via the Weibull distribution, they have a design strength close to that of new glass according to Dutch and European design standards. Especially the variation in measured values for the edge specimens, accounts for the low design strength for this series. From this, it can be concluded that the mid-specimens are more evenly and homogeneously damaged, which makes for a more reliable series, and subsequently, according to used Weibull theory, a higher design strength.

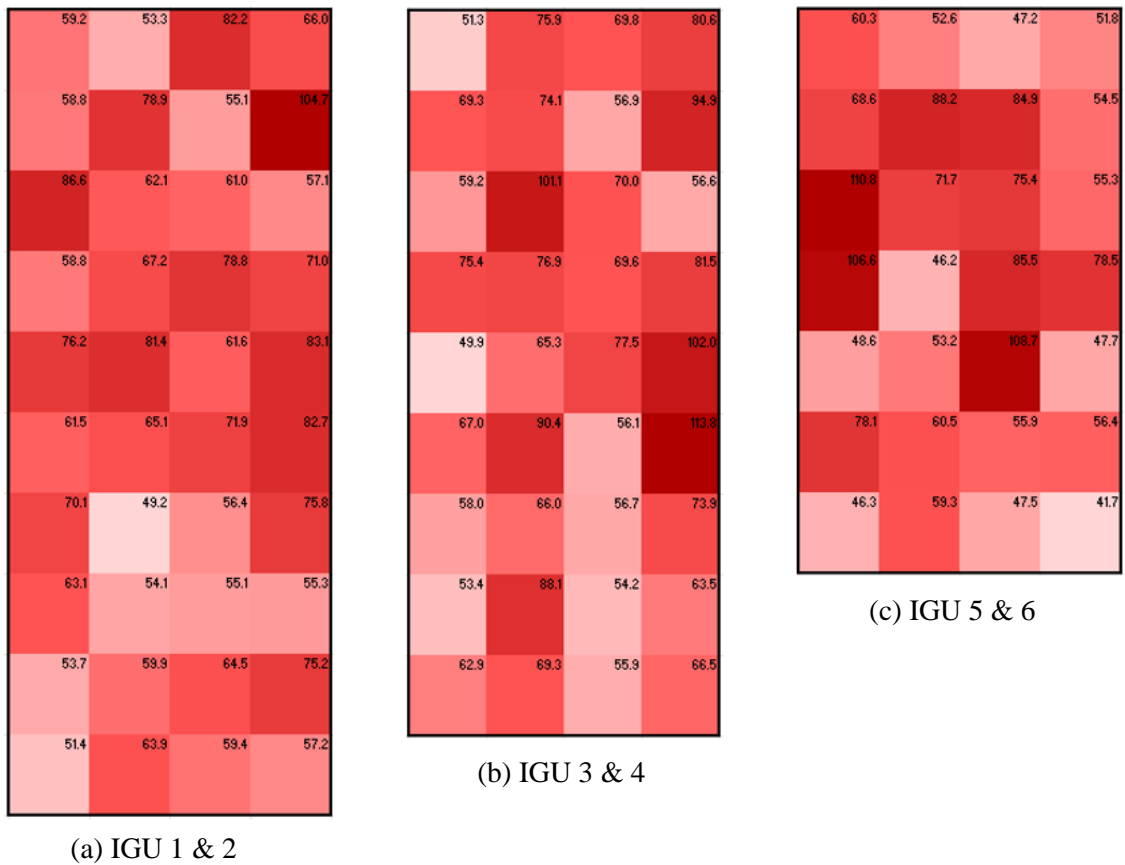


Figure 74. Average strengths of the specimens coming from the panels.

The potential for reuse in this case is greater than if an entire panel has to be used. The strongest spots in a panel can be searched for, increasing the average strength of a smaller panel taken from a larger panel. The challenge of this method of reuse is to search and find the strongest pieces of a glass panel. Further research should be able to develop techniques that use scanning to find the largest damages and then predict the strength with these. In the case of this study, the strength spot is, on average, the centre of a panel. It was not considered separately for each IGU, so there could be distinctions between different IGUs. Using smaller panels for new purposes, could be a solution to effective reuse. Cutting a smaller glass panel of, say, 1000mm x 400mm from the largest glass panel tested of 1509mm x 656mm amounts to a glass reuse rate of more than 40%. This option can be used for either a 'new' IGU with two old glass panels or one old and one new glass panel. It can also be an option that can be used for single glass, for a 'new' smaller IGU or for laminated glass. Sketches of this options of reusing the old glass as smaller glazing can be seen in Figure 75. So, when small glass panels are needed, based on the test results, it is possible to cut them from used glass panels to achieve a sustainable new glass construction.

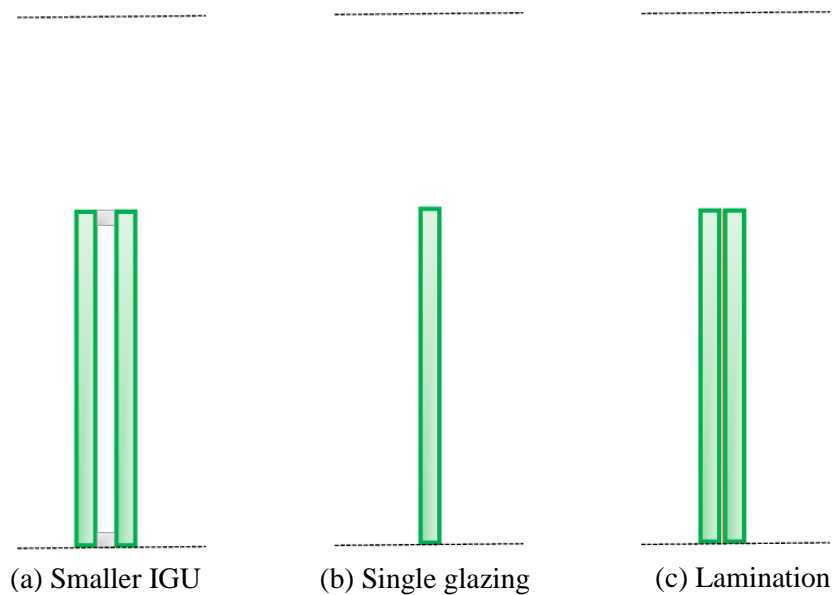


Figure 75. Smaller panel options.

6.3.5 Lamination

The final reuse option discussed is to laminate old panels. Laminated glass consists of at least two sheets of glass with one or more layers of PVB film between them. The glass sheets and film are fused together in the factory under great heat. The foil holds the glass together if the pane breaks. This allows a weaker panel to be laminated with, for example, a new strong panel, giving the entire structure higher strength. This makes it possible to reuse damaged panels. Laminating an old, weak glass panel with a new, strong glass panel can offer some advantages, but there are also some pros and cons to lamination that need to be considered.

Advantages:

- Strengthened strength: The new, strong glass panel can improve the overall strength of the structure because it can compensate for the weakness of the old panel.
- Increased safety: Using a strong new glass panel can increase the overall safety of the laminated glass. Should an incident occur that causes damage to the glass, the combination of layers will be more resistant to further damage.

Considerations:

- Material compatibility: To ensure that the old and new glass panels are compatible in terms of dimensions, thermal expansion coefficients and other material properties. Otherwise, tension may develop between the layers, leading to cracks or other problems.
- Asymmetrical thermal load: If the old and new glass panels have different thermal properties, they may react differently to temperature changes. This can cause tension and lead to problems.
- Cost considerations: In some cases, it may be more economical to invest in a completely new, uniform glass panel rather than trying to laminate an old panel with a new one.

As mentioned under benefits, laminated construction can provide higher strength than the strengths of separate glass posts. There are a number of reasons for this:

- Increased tensile strength: If the new glass panel is significantly stronger than the old panel, it will increase the overall tensile strength of the laminated glass. This means the laminated glass will be more resistant to tensile forces.
- Uniform stress distribution: The new glass panel helps to compensate for any unevenness or weaknesses in the old glass. This leads to a more uniform distribution of stresses throughout the laminated structure.
- Improved breakage resistance: Should the old glass panel crack or break, the new, stronger glass acts as a reinforcing layer that slows or limits the breakage. This reduces the likelihood of complete destruction.

To indicate the extent to which a laminated glass panel handles a load, formulae (21) and (22) are used to calculate how the load is distributed among n different glass panels (Kien Safety Glass Sdn. Bhd., 2000). This formula applies only if there is full shear interaction between the different glass layers.

$$F_i = \left(\frac{t_i^3}{t_1^3 + t_2^3 + \dots + t_n^3} \right) F \quad (21)$$

$$F = F_1 + F_2 + \dots + F_n \quad (22)$$

Where:

- F_i = the load absorbed by the glass with thickness t_i ,
 n = the number of glass layers,
 F = the total load on the laminated glass.

Table 18 shows an example of a laminated glass construction with thicknesses of 4, 5 and 6 mm, to which a total load F is applied. The right-hand column shows how, using formula (21), this load is distributed among the different layers. It is assumed that the interlayer provides full shear interaction.

Table 18. Load distribution example of lamination glass with three layers with different thicknesses.

Layer	Thickness t (mm)	Load
1	4	0.16F
2	5	0.31F
3	6	0.53F

The reason this example is given is to show that a laminated glass panel can very well be made with used glass layers, because the load carried out on the glass panel is distributed across the panels. So, when the load during the service life when reused is little or no different from the load experienced by the glass during the initial life phase, this shows that a 4mm thick glass panel combined with 5mm and 6mm panels will only absorb 16% of the total load. As a result, a glass panel also needs to be less strong. Despite this finding, design codes are a lot stricter and often the weakest panel is considered the norm. Therefore, when this is done, a glass panel that does not meet the strength requirements according to the design standard cannot be reused in a laminated glass construction. If an interlayer is used properly, so that full shear interaction is approached (100% shear interaction is not realistic, due to the finite shear modulus of the material of the interlayer), the assumption that laminated glass is as strong as the weakest layer seems somewhat conservative. The stress distribution across the cross

section of laminated glass looks as shown in Figure 76 (Kuntsche et al., 2019). In practice, the stress often follows the partial shear transfer sequence. When the moment of occurrence is as shown in Figure 76, the upper glass panel is stressed mainly in compression and the lower panel in front in tensile stress. Glass is stronger in compressive stress than in tensile stress, so in theory, the primarily compressively loaded glass panel would require less strength than the panel loaded in tensile stress. With 'full shear transfer', this also applies, and with 'no shear transfer', both panels are loaded on both compression, and tension. As mentioned earlier, in practice, almost only laminated glass occurs where partial shear transfer is an issue. This gives the possibility for glass panels from old IGUs that have lower strength due to weathering to still be reused in a laminated glass construction.

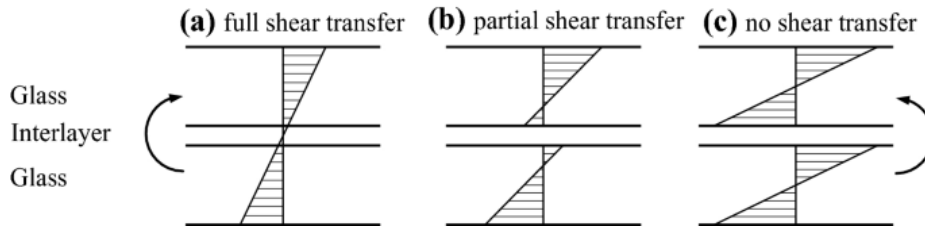


Figure 76. Stress distribution laminated glass (Kuntsche et al., 2019).

In the case of reuse of the tested IGUs, the 2-out and 2-in panels are also suitable for use in a new laminated construction in this case anyway, as these panels separately also have higher design strengths than the theoretical values according to the Dutch standards. If the codes are deviated from for a moment and a laminated construction is considered possible even with weaker panels, a possibility can be found for each tested panel to be used in a laminated glass construction. First, because the load on the construction is distributed over the various layers, and second, in terms of safety, laminated glass ensures that shards stick to the glass through the adhesive interlayer. As a result, in terms of strength and safety, there is sufficient option to reuse the all the panels from the tested IGUs. Laminating is also a reliable option for new functions and other locations, where the option of laminating an IGU can also be considered. In this option, a glass panel is laminated against an IGU, as shown in Figure 77. This can be a used or a new glass panel.

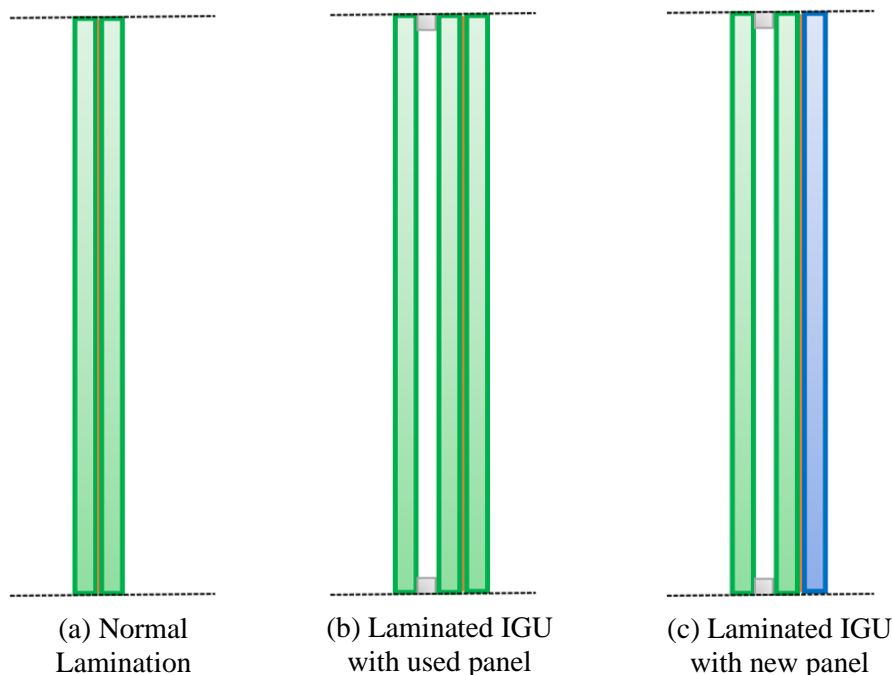


Figure 77. Laminated glass options.

7. Discussion

Due to the many choices that have to be made to conduct the study, generalising the study is an uncertainty. Despite the fairly large number of specimens, it is a limited dataset of specimens from different IGUs in terms of dimensions and location in the building. Also think of the choices for the dimensions of the specimens itself, and for the dimensions of the pressure rings used in the CDR tests. How do results obtained differ from each other when different choices were made here? A question that cannot be answered at the moment based on the results of this study, which makes generalising the results of the tested glass difficult. Apart from certain choices that were made and might be made differently during another study, the reliability of the study in itself is there, due to the large number of tests (406). It can be concluded that enough data was collected to draw certain conclusions. Test conditions were kept the same for each specimen as much as possible. The temperature and relative humidity differed relatively much between, say, two different days, but after analysing whether there was a correlation between the measured strength and temperature and/or humidity, this was found to be hardly there, if at all. The method used to carry out the tests fell back on ASTM C1499-09 (2013), which explained not only the determination of dimensions for the specimens and pressure rings, but also the test procedure. As a result, the testing method can be considered reliable. The process prior to testing, which mainly consisted of separating the glass panels and cutting them into small specimens, is expected to have had more influence on the results obtained. The damages that occur with separation and cutting are not desirable but are impossible to avoid with the way specimens were obtained in this study. This probably has caused more damage on certain specimens than were originally on them, resulting in lower strengths than the strength of the glass actually is after it is removed from a facade. If the separation and cutting is not done by hand but by machine, and in places where damage can be minimised, it gives more representative results. Furthermore, in this study, the prestress of each specimen was included in the calculation of the final failure stress. Because a small compressive stress is present at the glass surface, the measured failure stress is slightly higher than the actual failure stress. Compared to other studies where this was (probably) not considered, one should be aware of this.

When zooming a little deeper into the results, the most striking thing has been that the spread of results greatly affects the course of the distribution line. It was expected beforehand that side #1 and #4 would have lower strengths due to more damage due to weathering. This expectation was partly correct, when looking at the average measured strength, but due to the larger spread in results at side #2 and #3, lower strengths were found here at low failure probabilities. In this study, strengths were searched for low failure probabilities ($P_f = 0.05$, $P_f = 0.008$ or $P_f = 0.0012$) using the linear Weibull distribution (2PW). This method of reading can provide a very conservative approximation of the true strength and is very sensitive to the degree of spread in the data. The bottom line is that a more evenly damaged glass panel often has a higher design strength (low failure probability) than glass panels with less damage, but greater variation in measurements. Thus, in the linear 2PW method, extra uniform damage often results in higher design strength.

Another way of describing the data is the bilinear approximation, where there is a kink, as it were, in the Weibull distribution to better 'follow' the data points and thus describe them (Rodichev et al., 2018). Figure 79 shows an example of a bilinear distribution (BLW) (Ballarini et al., 2016). The occurrence of two separate 2PW distributions in the sample leads to the assumption of two different fracture criteria being present (Berlinger et al., 2021). Determining the different scale and shape parameters of the two parts of a BLW distribution combined with determining the maximum goodness of fit of

several series of data is a difficult process and therefore left out of this study. Another Weibull distribution that could better describe the data is the Bimodal Weibull distribution (BMW). In order to obtain a smooth transition between the data interpolated with two Weibull distributions one can assume that the material has undergone two distinguished and independent failure mechanisms (Ballarini et al., 2016). An example of this distribution can be seen in Figure 78.

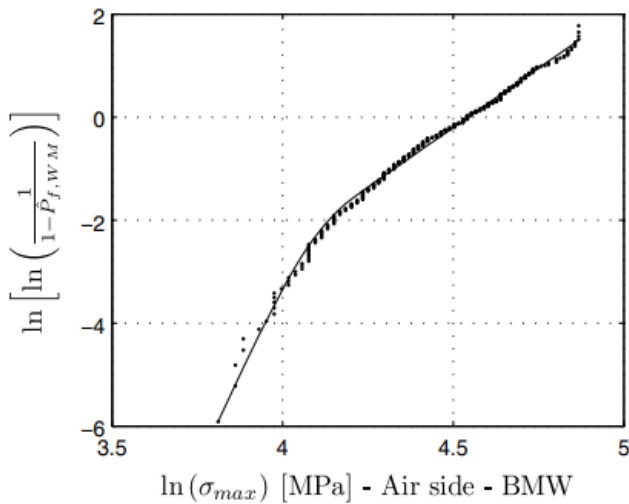


Figure 78. Bimodal Weibull distribution (Ballarini et al., 2016).

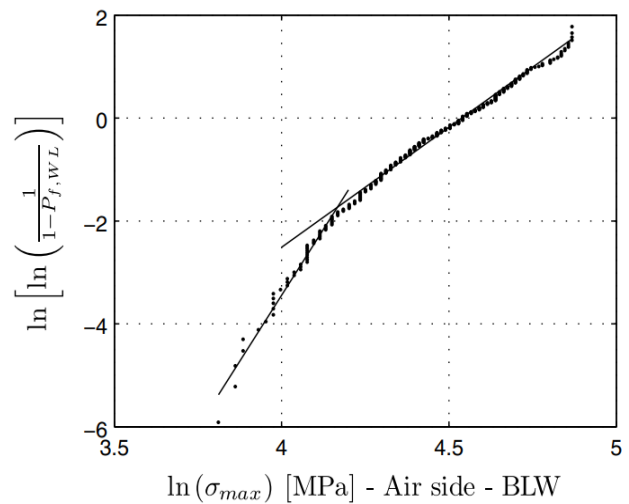


Figure 79. Bilinear Weibull distribution (Ballarini et al., 2016).

A striking gradient occurs when the Weibull distributions are plotted of the air- and tin-sides without 5% or 10% lowest values. Figure 80 shows that the gradient of the air- and tin-sides of used glass actually has an almost perfect bimodal distribution gradient. For the new glass tested by, in this case Thijs, this is less the case, although even here a bimodal distribution seems to better describe the data than a 2PW. Thus, for these plots, the 10% lowest values have been removed from the series. These outliers (10% lowest values) influence the gradient to a large extent, so when these most weak points in a glass panel can be detected and possibly repaired or removed, predicting the strength of a glass panel becomes a lot easier. Appendix F also includes this plot showing Irene's tested new glass and the 2PW gradient of these series.

Also, the data can be described in a very different way than with a Weibull distribution. What is noticeable is that with the 2PW method, the design strength is often lower than the data point with the lowest value of that specific series. When there is a sufficiently large data set, it is also a possibility to equate the overall strength of a glass panel with the strength of the weakest specimen. This gives, as shown in Figure 81, a higher strength for many series than when the strengths are read from the 2PW distribution. The glass may not be as weak at all as it sometimes appeared. The method by which the strength is determined is of great influence for the final conclusion that can be drawn from it.

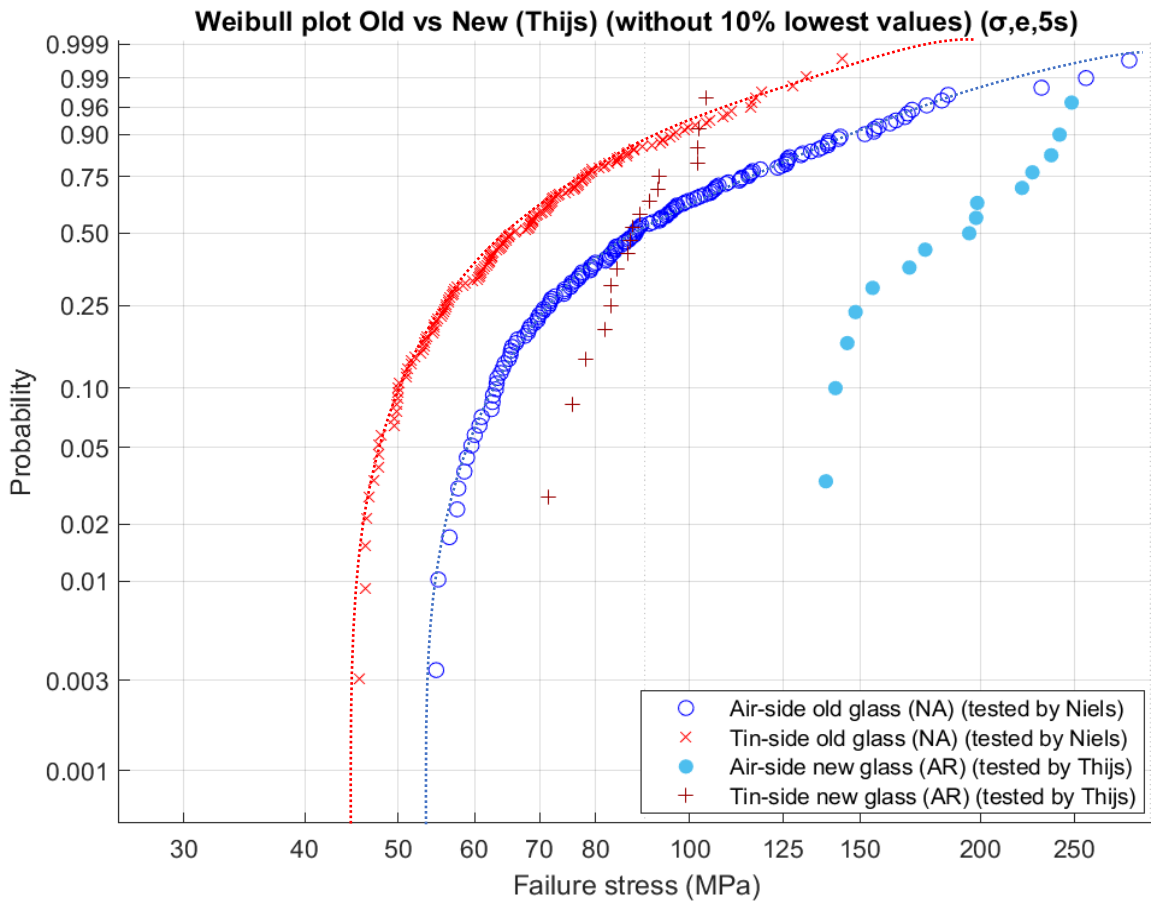


Figure 80. Weibull probability distribution: Old vs New (Thijs) glass (5 sec) – Bimodal flow.

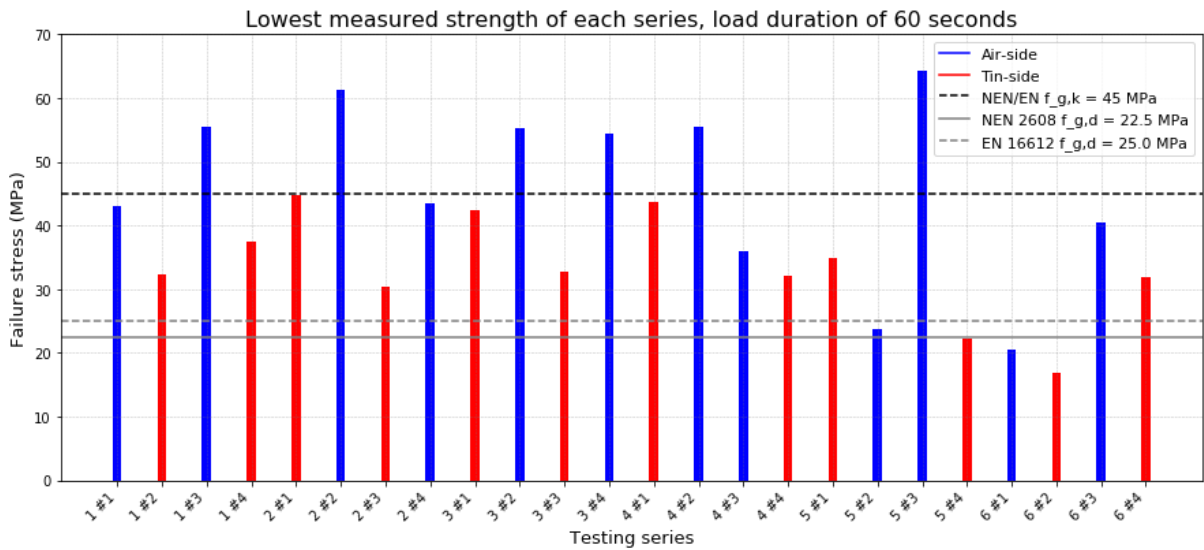


Figure 81. Lowest measured strength of each series, load duration of 60 seconds.

Due to the large variation in results in strength between the different series, it was decided not to link a general strength to the old glass. In the future, it should be possible to do this, as after much research it will be clearer how the glass properties have changed after being in use for a certain number of years. A factor used in current standards to arrive at a design strength is the material factor $\gamma_{m;A}$. This is typically set at 1.6 or 1.8 for glass to ensure safe construction. When assigning a strength value to used glass, the question is whether this factor should be so high, as the glass has already 'proven', so to speak, that it has already performed its function for a certain number of years. So, when old glass is reused, the obvious thing to do is to lower the material factor so that an overly conservative value is not placed on the glass. This also increases the potential for reuse. Figure 72 shows that a value of 1.35 for the material factor results in a design strength of 25.0 MPa. When different series are considered separately, the range of the material factor becomes larger, due to the differences in strength between the different sides or air- and tin-sides.

Finally, there is the clear difference in strength between the air- and tin-sides, which is evident in both new and old glass. One can think of the idea that in double-glazed constructions, air- and tin-sides are handled systematically. Thus, side #2 and #3 can always be a tin-side, leaving the, on average, stronger air-side more exposed to weathering by being side #1 and #4. As a result, both side #2 and #3 are already moderately damaged during the production process, and side #1 and #4 are damaged by weathering during their lifetime. As a result, all sides are expected to be more evenly damaged than if the air- or tin-sides are not considered, making the glass more reliable and making it statistically easier to assign a strength to a glass panel.

The discussion points described above indicate that much can be taken from the study. The way data is analysed, the use of factors according to the codes and the difference between the air- and tin-sides, have proved to be salient issues for this study. The following sections elaborate on the conclusions and make recommendations where future research can be done to create new insights in the field of glass strength.

8. Conclusion

The main research question of this thesis is:

How does weathering of double glazing affect the strength of glass?

Answers to this question were found by conducting CDR tests on 36-year-old double-glazed panels. This testing method combined with statistical analysis of the results gave insights into the strength of used IGU, and how weathering affected the strength over time. Below, the main question is answered based on the drafted sub-questions.

What are the differences in appearance between the different sides of the two panes?

To answer this question, some of the specimens were viewed under the microscope, as described in Section 4.6. Because not all specimens were tested under the microscope, there is a degree of uncertainty in the conclusion below. It was expected that clear differences would be seen between the different sides of the IGU. It was expected that the outside of the outer panel (side #1) would have the most damage, and that side #2 and #3 would have hardly any defects, having not been exposed to weathering during its lifetime. This was partly correct, as side #1, and to a lesser extent side #4, showed fairly homogeneous damage across the specimens viewed. Interestingly, side #2 and #3 also showed quite a lot of damage, but more locally. Local damage is often caused during the production process, by transport or, in this case, during specimen preparation. Theoretically, while performing the function of an IGU, no damage can occur on side #2 and #3, as these sides are not in contact with weather factors or human touch. Based on these results, less variation in strength is expected for side #1 and #4, because the IGUs are damaged fairly homogeneously. For side #2 and #3 this is not the case, and more variation in strength between specimens is expected due to more local damage.

What are the differences between the strengths of the two panes and both sides?

Most of the research was devoted to answering this question. To arrive at strengths, 406 CDR tests were conducted, each testing one side of a specimen for strength. Using Weibull theory, the strength of a tested series of glass specimens was determined statistically. It was expected that side #1 and #4 will be weaker on average than side #2 and #3, due to the weathering that occurs more on these sides. The average strength of all specimens tested on side #1 and #4 are 62.2 and 65.2 MPa, respectively, and those of side #2 and #3 are 71.0 and 72.6 MPa, respectively. Thus, this expectation comes true. What already emerged from the microscopic examination was the fact that the damage on side #1 and #4 was more homogeneous, so less variation in strength was expected. This was confirmed by the course of the Weibull distribution of the four different sides. The greater variation in measured strengths of specimens tested on side #2 or #3 creates a less steep distribution line and therefore less reliable series. As a result, for low failure probabilities, side #2 and #3 are actually weaker than side #1 and #4. For example, for a failure probability of 0.8%, the strength for side #1 and #4 is 22.8 and 16.5 MPa, respectively, while for side #2 and #3 it is 11.9 and 8.4 MPa, respectively. From this, it can be concluded that more homogeneous damage can provide higher design strength (strength at low failure probability) than for average stronger glass panels with more localised damage. The way the linear Weibull distribution is obtained can be questioned, something that has already been discussed in more detail in Section 7.2.

What is the influence of the air- and tin-sides of the glass?

That the manufacturing process already affects difference in strength between the two sides of a glass panel is not something considered in much of the literature. Nevertheless, it was included as a variable in the study, and for valid reason. The damage caused by the tin bath and/or the conveyor belt on which the glass is transported during production greatly affects the strength that glass has, whether it is old or new glass. The influence of the production process as far as the air- or tin-side is concerned affects strength, for example, all specimens tested on the tin-side have an average strength of 57.3 MPa, while for specimens tested on the air-side it is 75.3 MPa. This amounts to a difference of 31%. For new glass tested by Thijs (Van Der Linden, 2023), the average strength of the air-side was even more than twice as high as for the tin-side (172.5 to 82.4 MPa). Side note that his series included only 17 and 20 tests, for the air- and tin-sides, respectively. The tin-side can be seen as the side that is already homogeneously damaged from the start, due to tin residue or micro-damage from the conveyor belt the glass passes over during production. The variation in strength for the specimens tested on the tin-side was almost always smaller than for the air-sides tested. As a result, for low failure probabilities, the tin-side often actually has a higher (design) strength value than the air-side again, just as this was the case when comparing the different sides of an IGU. The conclusion behind this story is that in the future, it should be an option to systematically link the air- and tin-sides to one side, so that it is easier to predict the strength of a side (#1, #2, #3 or #4) in combination with being an air- or tin-side after a certain lifetime.

What are the possibilities of continuing with used glass?

Glass is a special material and research has proven that when a large number of specimens are tested, much variation is found in the results. As a result, glass remains unpredictable, and statistics are needed to relate numbers to a safe strength value. Actually, the answer to this question is simple, but at the same time very complicated. In general, the tested glass panels can all be reused, although it is necessary to consider for each glass panel whether it is possible to do so in the same function, and whether loads do not become higher than the glass can handle. Attaching a strength to an entire glass panel is very difficult based on this research. The reason for this is the fact that there may be different ways how a strength can be linked to the glass. The statistical way of the Weibull distribution often gives conservative values and very low strengths for some glass panels. Using the glass panels in another glass structure, such as in another IGU or as laminated glass, are options that are possible. A broader view should be taken than reusing an entire IGU, especially with the knowledge that machines will soon be available that can separate IGU without bitumen residues or (additional) damage remaining or coming on the glass (Groothoff, 2023). This gives the possibility of being able to test and/or reuse glass panels from an IGU separately. New standards and more testing will have to determine whether a glass panel still meets a certain strength and whether it is eligible for reuse, in the same or different function.

To summarise, the main question is answered:

How does weathering of double glazing affect the strength of glass?

The simple answer to this question is that the sides (#1 and #4) of an IGU that are exposed to weather factors (rain, wind) and/or human or other touches while performing their function have a lower mean strength than the sides of the inside (#2 and #3) of the IGU. This is because this strength depends on the size of the surface flaws. When looking at low failure probabilities, the effect of spreading data is large on the values found for, say, failure stresses at a probability of 0.8% at the 2PW. At these values, side #1 is even stronger than side #2 and #3 and the glass therefore becomes stronger as there is more

(uniform) damage on the glass. Side #1 is for $P_f = 0.008$ 94% and 52% stronger than side #2 and #3, respectively, despite most of the weathering having occurred on this side. Beyond these simple conclusions, there are other things that were involved, such as the effect of the air- and tin-sides. The tin-side is 31% weaker than the air-side when considering $P_f = 0.5$, while at a P_f of 0.008, the tin-side is actually 8% stronger than the air-side at a 2PW. The behaviour between the different sides in terms of strength is thus similar to the results in measured strength between the air and tin sides. It is well known that the 2PW distribution can give conservative strength values for lower failure probabilities. In this study, a bimodal distribution seems to describe the data better for most cases. Since current standards use low failure probabilities for determining design strengths as a starting point, questioning this way of interpreting results is a valid point. It seems more justified to take the lowest value of a series of tests as the design strength of a glass panel, to avoid very conservative values. Taking the measurements and extracting an average value from them gives certain conclusions, but when going deeper into the statistics of the results, there are even more conclusions attached than just those of superficial knowledge. Some of these are described in the discussion and in the answers to the sub-questions. In the future, glass production and use will have to be handled more systematically, consider systematically placing an air-side on side #1, which also makes the air-sides easier to predict in terms of strength, and for the fact that the different sides of an IGU, differ less in terms of strength, should this be desired.

9. Recommendations for further research

Progression of weathering and strength over time

This study tested what the strength is after a certain time, namely 36 years. This strength can therefore be linked to the age of the glass, but what is missing is the strength of the glass when it was new, or what the strength was during these 36 years. It is unclear at what strength the glass started at, so to speak, making it, in this case, impossible to say how much percent the strength has decreased. The effect of weathering over time is unknown, so the question is whether the strength reduction of glass is linear over time, or whether the strength decreases faster or slower, making it a non-linear reduction. This can be investigated, based on consecutive testing on similar glass specimens, by testing the strength several times during their lifetime, so that a correlation between time and strength can be found. Consider a method where a glass panel is removed from a building and tested, then a certain number of years later an adjacent panel with the same conditions, is tested. This can be repeated until a large number of tests have been done. The disadvantage of this method is that it takes many years before results are found.

Other types of glass

Because strengthened glass is often used alongside annealed glass, it is a recommendation for further research to investigate whether strength of this type of glass shows the same behaviour over time as annealed glass. This in turn allows us to investigate in which functions strengthened glass is suitable for reuse. Due to the residual stresses in strengthened glass, a more complicated relationship is expected here, but further research will have to show. Besides strengthened glass, laminated glass is also an option to test for strength. The question here is also whether the interlayer deteriorates as fast as the glass itself. Is it more durable to replace this interlayer at some point, or is that not necessary at all and can this layer also be easily reused? What is a sustainable useful life for the different layers of laminated glass? These questions can be answered if strength tests are done, or if an established method is devised to determine the strength of used glass.

Effect of air- and tin-side

As revealed in the analysis of the results, there is a big difference in strength between the air and tin sides of the glass panels. This applies to both new and old glass. Research will have to show whether systematically placing an air-side on the outside (side #1 and #4) of an IGU and a tin-side on the inside of the IGU (side #2 and #3) provides a more reliable construction in terms of strength. Theoretically, there is more uniform damage on all sides of the IGU, which ensures more predictable strength as a result. Whether this assumption is correct will have to be shown in a follow-up study. For follow-up studies in glass, it has in any case become clear that including and determining the air- and tin-side helps to explain the (differences in) strength of glass.

Size effect

This study worked with specimens that were all 150mm by 150mm. This was deliberately chosen so that, beyond the many variables there were in the IGUs tested, there was no variation in specimen size as well. The question that remains unanswered after this study is whether the size of the loaded area affects the measured strength of weathered glass. Would the strengths have been the same if larger specimens had been used? The size effect and the formula relating the strength of weathered glass to the size of the loaded surface area could be studied. In glass design standards, the strength of large glass elements is extrapolated from that of small elements, according to Weibull theory and the shape parameter β . This gave very conservative values for large specimens, according to Irene's thesis (Sofokleous, 2022). More research on the relationship between specimen sizes and glass strength is needed to obtain less conservative and therefore probably more representative values.

Fractographic analysis

Due to the large number of specimens, in this study only some specimens were viewed under the microscope prior to the destructive tests. To get a better picture of damage to the glass used, all specimens could have been viewed under the microscope to rule out conclusions based on coincidences. Microscopic examination after performing the destructive tests can also be of great value. This allows the fracture pattern to be analysed, where the critical defect of the specimens and the location of this defect can also be determined with more certainty. This requires a close inspection of the fracture surface. The aim of such an examination may be to be able to describe the relationship between the failure stress of the glass and the size of the critical defects.

Relating a strength to defects

One research project that could be of great value in the world of sustainable glass use is to develop a way of detecting the weakest points in a used glass panel. Some kind of scanning machine will have to be developed that can use artificial intelligence to determine what the biggest damages are and where they are located. Once these weaknesses of a glass panel are found, there are then several options for dealing with them. These include 'repairing' the largest defects in the glass, increasing its strength, or removing the least strong part and continuing with a smaller and stronger glass panel. A scanning process, as it were, will have to be developed that, through experience and artificial intelligence, can translate the size and number of defects into a strength corresponding to this degree of damage. The research into 'scanning' glass to then test it for strength will first have to be done separately from each other, to be able to link these results after enough data. When a step in this is taken, predicting strength after a certain period of use will be a lot easier and faster, making glass reuse more accessible.

Non-linear Weibull distribution

As mentioned in the discussion and conclusion, the fact is that a linear 2PW distribution can give very conservative values for strength at low failure probabilities. In particular, the spread in data is something this distribution is very sensitive to. It has also already been briefly described in the discussion that a bilinear or bi-modal Weibull distribution might give a more representative result for the characteristic and design strength of used glass (Ballarini et al., 2016). Thus, to give a better idea about other ways in which the data can be interpreted, consideration can be given to investigating distributions other than a linear 2PW distribution, such as thus the bilinear or a bimodal distribution, as been shown in the discussion. This study can be conducted with the data obtained from this study or can be done with new data. It gives insights into different ways of handling the data obtained, and that the impact of this can be great on final results.

Examination of current design standards

What emerged clearly during this study is the fact that current design standards, in this case the Dutch NEN2608 and the European EN16612:2017 codes, contain little or nothing regarding glass reuse. When design strengths are calculated, the same parameters are adhered to that are used as for new glass. Is this justified? Research will have to show whether the material factor can be brought down to 1.3 – 1.4, for example, or whether other factors should be handled differently when glass has already proven its function with confidence for a certain number of years. It would be useful if research is done on this, and a clearer approach is developed in terms of giving a certain strength value to used glass. In future, design codes will have to pay more attention to this, to avoid confusions and ambiguities regarding the sustainable use of materials.

References

- ASTMC1499-09. (2013). Standard test method for monotonic equibiaxial flexural strength of advanced ceramics at ambient temperature1.
- ASTM-E1300. (1997). Standard practice for determining load resistance of glass in buildings.
- Ballarini, R., Pisano, G., & Royer-Carfagni, G. (2016). The Lower Bound for Glass Strength and Its Interpretation with Generalized Weibull Statistics for Structural Applications. *Journal of Engineering Mechanics-asce*, 142(12). [https://doi.org/10.1061/\(asce\)em.1943-7889.0001151](https://doi.org/10.1061/(asce)em.1943-7889.0001151)
- Barton, K. (2022, September 13). *Insulated Glass Benefits and Types: What You Should Know*. Homedit. <https://www.homedit.com/windows/glass/insulated-glass/>
- Berlinger, M., Kolling, S., & Schneider, J. (2021). A generalized Anderson–Darling test for the goodness-of-fit evaluation of the fracture strain distribution of acrylic glass. *Glass Structures & Engineering*, 6(2), 195–208. <https://doi.org/10.1007/s40940-021-00149-7>
- Brown, W. (1972). A load duration theory for glass design, 75–78.
- Canrinus-Moezelaar, R. (2017, March 17). *Bekijk: Zo hergebruik je glas*. NEMOKennislink. <https://www.nemokennislink.nl/publicaties/zo-hergebruik-je-glas/>
- Charles, R. (1958). Static fatigue of glass. II. *Journal of Applied Physics*, 29(11), 1554–1560
- Cummings, K. M., Lanford, W. A., & Feldmann, M. (1998). Weathering of glass in moist and polluted air. *Nuclear Instruments & Methods in Physics Research Section B-beam Interactions With Materials and Atoms*, 136–138, 858–862. [https://doi.org/10.1016/s0168-583x\(97\)00758-1](https://doi.org/10.1016/s0168-583x(97)00758-1)
- D&O. (2021, March 18). *Hoe wordt glas gemaakt? | Veelgestelde vragen | D&O Bouwglas*. D&O. <https://zichtbaargoed.nl/vraag/hoe-wordt-glas-gemaakt/>
- Datsiou, K. C., & Overend, M. (2017). The strength of aged glass. *Glass Structures & Engineering*, 2(2), 105–120. <https://doi.org/10.1007/s40940-017-0045-6>
- Datsiou, K. C., & Overend, M. (2018). Weibull parameter estimation and goodness-of-fit for glass strength data. *Structural Safety*, 73, 29–41. <https://doi.org/10.1016/j.strusafe.2018.02.002>
- DOE Logo Flatten-2. (n.d.). https://www.energy.gov/sites/prod/files/guide_to_energy_efficient_windows.pdf
- EN1990:2002. (2005). Eurocode - basis of structural design.
- EN16612:2017 (2019). Eurocode - Glass in building - Determination of the lateral load resistance of glass panes by calculation

- Flat Glass Recycling*. (n.d.). Glass Magazine. <https://www.glassmagazine.com/article/flat-glass-recycling>
- Garibaldi Glass. (2021, October 15). *Air Side & Tin Side*. Retrieved February 1, 2023, from <https://www.garibaldiglass.com/air-side-tin-side/>
- Geology Page. (2019, August 17). *Obsidian: What is obsidian? Why obsidian is black?* <https://www.geologypage.com/2019/08/obsidian-what-is-obsidian-why-obsidian-is-black.html>
- Geschiedenis van Glas / Glas*. (2017, April 30). LeerWiki.nl. <https://www.leerwiki.nl/wetenschap/natuurkunde/materiaalkunde/materialen/glas/20371/geschiedenis-van-glas/>
- Glas in beeld. (2012). Hoe groen is glas? In *Glas in Beeld* (pp. 46–49). <https://www.glasinbeeld.nl/wp-content/uploads/2013/01/Hoe-groen-is-glas-3.pdf>
- Glass for Europe. (2023, January 24). Glass for Europe - Trade association of European flat glass value chain -. <https://glassforeurope.com/>
- Glasschades: oppervlaktebeschadigingen, glasbreuk in theorie en praktijk : oorzaken, ontstaan, beoordeling. (2006).
- Glazcon. (2018, May 30). *What is an Insulated Glass Unit?* <https://www.glazcon.com/what-is-an-insulated-glass-unit/>
- Groothoff, M. (2023, January 9). *IG2Pieces: AGC en Hegla ontwikkelen machine voor scheiden isolatieglas • Glas in Beeld*. Glas in Beeld. <https://www.glasinbeeld.nl/23714/ig2pieces-agc-en-hegla-ontwikkelen-machine-voor-scheiden-isolatieglas/>
- Haglin, D. (2021, October 19). *GAS FILL 101: GAS FILL OPTIONS FOR IGUS*. Window+Door. <https://www.windowanddoor.com/article/gas-fill-101-gas-fill-options-igus#:~:text=Typically%2C%20the%20fill%20gases%20used,by%20reducing%20the%20U%2Dfactor>
- Hartwell, R., Macmillan, S., & Overend, M. (2021). Circular economy of façades: Real-world challenges and opportunities. *Resources, Conservation and Recycling*, 175, 105827. <https://doi.org/10.1016/j.resconrec.2021.105827>
- Hasselman, D. P. H., Badaliane, R., McKinney, K. R., & Kim, C. (1976). Failure prediction of the thermal fatigue resistance of a glass. *Journal of Materials Science*, 11(3), 458–464. <https://doi.org/10.1007/bf00540926>
- Hoogerwaard, G. (n.d.). *Structural Glass and Sustainability* [Slide show; Presentation]. Brightspace.
- How Insulated Glass Changed Architecture | All-West Glass*. (2022, September 19). All-West Glass. <https://www.all-westglass.com/post/how-insulated-glass-changed-architecture#:~:text=In%201865%2C%20American%20engineer%20and,insulation%20and%20prevent%20heat%20loss.>

- Infoplaza. (n.d.). *Wind in Nederland*. Weerplaza.
<https://www.weerplaza.nl/weerinhethetnieuws/klimaat/wind-in-nederland/6820/#:~:text=In%20alle%20maanden%20is%20zuidwest,vaak%20voorkomen%20als%20de%20zuidwestenwinden.>
- INSULATED GLASS UNITS -TYPES AND OPTIONS* / *Advanced Window Corp.* (n.d.).
<http://www.advancedwindow.com/other-option/insulated-glass-units--types-and-options>
- Insulating glass spacers – all you wanted to know.* (2020, June 17). glassonweb.com.
<https://www.glassonweb.com/article/insulating-glass-spacers-all-you-wanted-know>
- Ivanovna Min'ko, N., & Mikhailovich Nartsev, V. (2013). Factors Affecting the Strength of the Glass (Review). *Middle-East Journal of Scientific Research*, *ISSN 1990-9233*, 1616–1624.
<https://doi.org/10.5829/idosi.mejsr.2013.18.11.70117>
- iTeh Standards.* (2008, January 7). iTeh Standards.
<https://standards.iteh.ai/catalog/standards/sist/449be4b2-ef32-4688-9af0-%20bff3df157611/iso-16293-1-2008>
- Kien Safety Glass Sdn. Bhd. (2000). Physical Bending Strength of Glass. In *Kien Safety Glass Sdn. Bhd.* (p. 26).
- KL Glass. (2019, July 30). Double Glazed Windows: Argon, Krypton and Xenon Gases. *KL Glass*.
<https://www.klglass.co.uk/blog/double-glazed-windows-argon-krypton-and-xenon-gases/#:~:text=Krypton%20Windows&text=This%20gas%20is%20denser%20than,Krypton%20gas%20used%20in%20windows%3F>
- Kruijs, R. (n.d.). Sterkte van glas. In *Glas in Beeld* (pp. 40–42). <https://www.glasinbeeld.nl/wp-content/uploads/Constructief-glas-Glassterkte-11.pdf>
- Kuntsche, J. K., Schuster, M., & Schneider, J. (2019). Engineering design of laminated safety glass considering the shear coupling: a review. *Glass Structures & Engineering*, *4(2)*, 209–228.
<https://doi.org/10.1007/s40940-019-00097-3>
- MathWorks. (n.d.). *Weibull probability plot*. <https://www.mathworks.com/help/stats/wblplot.html>
- Muller, J. (2015). Evaluation of HCFeMn and SiMn Slag Tapping Flow Behaviour Using Physicochemical Property Modelling and Analytical Flow Modelling.
<https://www.repository.up.ac.za/handle/2263/44429>
- NEN2608. (2014). Glass in building - requirements and determination method.
- Nissink Glass. (2022, November 18). *Glas en zijn geschiedenis*. <https://nissinkglass.com/glas-en-zijn-geschiedenis/>
- Noteboom, C. & TU Delft. (2021). *Structural glass*. Lecture, Delft, Zuid-Holland, Netherlands.
- Nußholz, J. L., Rasmussen, F. N., Whalen, K., & Plepys, A. (2020). Material reuse in buildings: Implications of a circular business model for sustainable value creation. *Journal of Cleaner Production*, *245*, 118546. <https://doi.org/10.1016/j.jclepro.2019.118546>

- Papadopoulos, N., & Drosou, C. A. (2012). INFLUENCE OF WEATHER CONDITIONS ON GLASS PROPERTIES. *Journal of the University of Chemical Technology and Metallurgy*, 429–439.
- Peerless Products Inc. (2020, January 2). *Types of Architectural Glass: Annealed, Laminated, Heat Soaked, Heat-Strengthened, and Tempered Glass*. Peerless Products. <https://www.peerlessproducts.com/media/blog/what-glass-should-you-be-choosing-for-all-over-performance-and-aesthetics>
- prCEN/TC250-1. (2018). Structural glass — design and construction rules — part 1: Basis of design and materials.
- Products, C. G. (2019, February 11). *Understanding the Differences Between Annealed, Tempered, and Heat-Strengthened Glass | Custom Glass Products* |. <https://cgpglass.com/custom-glass-blog/understanding-the-differences-between-annealed-tempered-and-heat-strengthened-glass/>
- Risle, U. (2020). Insulating glass spacers – all you wanted to know. *Glass on Web*. <https://www.glassonweb.com/article/insulating-glass-spacers-all-you-wanted-know>
- Ritzen, M., Oorschot, J. V., Cammans, M., Segers, M., Wieland, T., Scheer, P., Creugers, B., & Abujidi, N. (2019). Circular (de)construction in the Superlocal project. *IOP Conference Series: Earth and Environmental Science*, 225, 012048. <https://doi.org/10.1088/1755-1315/225/1/012048>
- Rodichev, Y., Veer, F., Strizhalo, V., Soroka, E., & Shabetia, A. (2018). Structural Strength of Laminated Glass. *Conference on Architectural and Structural Applications of Glass*. <https://doi.org/10.7480/cgc.6.2168>
- Schenkelberg, F. (2021, October 1). *The 2 Parameter Weibull Distribution 7 Formulas*. Accendo Reliability. <https://accendoreliability.com/2-parameter-weibull-distribution-7-formulas/>
- Shen, X., & WÖRMER, J.-D. (1998). Entwicklung eines bemessungs-und sicherheits-konzeptes für den glasbau. *Bauingenieur*, 73(1), 44–52
- Sir Alastair Pilkington. (n.d.). <https://www.pilkington.com/en/global/knowledge-base/glass-technology/sir-alastair-pilkington>
- Sofokleous, I. (2022). *Methodology for the prediction of the strength of naturally aged glass based on surface flaw characterization* [Master Thesis]. TU Delft.
- Springer Handbook of Glass. (2019). In *Springer handbooks*. Springer International Publishing. <https://doi.org/10.1007/978-3-319-93728-1>
- Stichting Vlakglas Recycling Nederland. (n.d.-a). *Vlakglasrecycling Nederland - Geschiedenis van glas*. Copyright Stichting Vlakglas Recycling. <https://www.vlakglasrecycling.nl/index.php?page=geschiedenis-nl>

- Stichting Vlakglas Recycling Nederland. (n.d.-b). *Vlakglasrecycling Nederland - Productie van floatglas*. Copyright Stichting Vlakglas Recycling.
<https://www.vlakglasrecycling.nl/index.php?page=productie-van-floatglas-nl>
- Taylor, M., & Hill, D. (2011, September). *Glassblowers*. The Glassmakers.
<http://www.theglassmakers.co.uk/archiveromanglassmakers/>
- Tresinie, H. (2023). *'t-Over-leven: duurzame zelfvoorziening*. 't-Over-leven.
<https://toverleven.cultu.be/vlakglas-gieten-of-trekken>
- Van Den Bergh, S. M. G., Hart, R. A., Jelle, B. P., & Gustavsen, A. (2013). Window spacers and edge seals in insulating glass units: A state-of-the-art review and future perspectives. *Energy and Buildings*, 58, 263–280. <https://doi.org/10.1016/j.enbuild.2012.10.006>
- Van Der Linden, T. (2023). *The effectiveness of resin and polishing repairs on glass* [Bachelor Thesis]. TU Delft.
- Vander Werf, B. (n.d.). *IN Compression / modeling with glass*. University of Arizona.
- Veer, F. (2007). The strength of glass, a nontransparent value. *Heron*, 52, 87–104.
<https://research.tudelft.nl/en/publications/the-strength-of-glass-a-nontransparent-value>
- Walters, H. V., & Adams, P. B. (1975). Effects of humidity on the weathering of glass. *Corning Glass Works*, 19, 183–199. [https://doi.org/10.1016/0022-3093\(75\)90084-8](https://doi.org/10.1016/0022-3093(75)90084-8)
- What Is an Insulated Glass Unit or IGU?* (n.d.). Glass Doctor. <https://glassdoctor.com/blog/what-is-an-insulated-glass-unit-or-igu>

Appendix A

SCALP measurements

Using the SCALP-05, prestress was measured on one specimen per glass panel. Using five measurements, the average of these measurements was included in the calculation of the failure stresses for the specimens. The values for the prestresses in the measured specimens can be seen in Table 19.

Table 19. Prestress measurements.

<i>Specimen</i>	Measuring 1 (MPa)	Measuring 2 (MPa)	Measuring 3 (MPa)	Measuring 4 (MPa)	Measuring 5 (MPa)	Average (MPa)
1-out #1 5.3	-4.42	-4.36	-4.40	-4.39	-4.57	-4.43
1-out #2 5.2	-4.32	-4.39	-4.30	-4.53	-4.44	-4.40
1-in #3 5.3	-3.50	-3.64	-3.68	-3.83	-3.39	-3.61
1-in #4 5.2	-3.58	-3.48	-3.16	-3.67	-3.61	-3.50
2-out #1 6.3	-3.21	-3.15	-3.27	-3.17	-3.17	-3.19
2-out #2 6.2	-2.46	-2.61	-2.54	-2.49	-2.55	-2.53
2-in #3 6.3	-3.06	-3.25	-3.25	-3.11	-2.99	-3.13
2-in #4 6.2	-2.78	-2.64	-2.73	-2.49	-2.83	-2.69
3-out #1 5.3	-3.22	-3.08	-2.89	-3.07	-3.60	-3.17
3-out #2 5.2	-3.61	-3.29	-3.24	-3.33	-3.27	-3.35
3-in #3 5.3	-2.90	-2.66	-2.95	-3.07	-2.89	-2.89
3-in #4 5.2	-2.49	-2.67	-2.77	-2.63	-2.92	-2.70
4-out #1 5.3	-3.77	-3.68	-3.71	-3.71	-4.01	-3.78
4-out #2 5.2	-3.62	-3.33	-3.32	-3.64	-3.35	-3.45
4-in #3 5.3	-2.49	-2.50	-2.59	-2.50	-2.60	-2.54
4-in #4 5.2	-2.82	-2.70	-2.41	-2.73	-2.70	-2.68
5-out #1 4.3	-3.46	-3.45	-3.49	-3.38	-3.69	-3.49
5-out #2 4.2	-3.73	-3.71	-3.57	-3.63	-3.70	-3.67
5-in #3 4.3	-2.68	-2.77	-2.79	-2.76	-3.17	-2.83
5-in #4 4.2	-2.83	-2.68	-2.66	-2.65	-2.70	-2.70
6-out #1 4.3	-3.51	-3.42	-3.64	-3.62	-3.63	-3.56
6-out #2 4.2	-3.63	-3.54	-3.58	-3.56	-3.76	-3.62
6-in #3 4.3	-4.54	-4.49	-4.59	-4.49	-4.74	-4.57
6-in #4 4.2	-4.50	-4.55	-4.57	-4.49	-4.41	-4.51

Appendix B

Dimensions measurements

The Table 20 to Table 31 show all the lengths and widths of the specimens, rounded to whole millimetres. The thicknesses of all specimens, which are considered when calculating the equivalent failure stress, are also shown here, rounded to hundredths of millimetres. The thicknesses were measured with a digital caliper on the four edges of a specimen, after which the average thickness can be determined. Sometimes a value was not measured because the edge of the specimen still contained bitumen residue, so the measured thickness was not the exact glass thickness. These cases are indicated in the table with a '-'.

Table 20. Dimensions specimens from panel 1-out.

<i>Panel</i>	1-out						
<i>Specimen</i>	Length (mm)	Width (mm)	d_{egde1} (mm)	d_{egde2} (mm)	d_{egde3} (mm)	d_{egde4} (mm)	d_{mean} (mm)
1-out #1 1.1	151	150	-	7.73	7.73	-	7.73
1-out #1 2.1	148	150	7.74	7.74	7.74	-	7.74
1-out #1 3.1	150	150	7.74	7.74	7.76	-	7.75
1-out #1 4.1	150	150	7.75	7.75	7.76	7.76	7.76
1-out #1 5.1	150	150	7.76	7.77	7.77	7.76	7.77
1-out #1 6.1	145	150	7.77	7.79	7.79	7.78	7.78
1-out #1 7.1	150	150	7.79	7.80	7.81	7.80	7.80
1-out #1 8.1	150	150	7.81	7.83	7.83	7.82	7.82
1-out #1 9.1	150	150	7.83	7.85	7.85	7.84	7.84
1-out #1 10.1	150	150	7.84	7.85	-	7.84	7.84
1-out #2 1.2	151	150	-	7.74	7.74	7.74	7.74
1-out #2 2.2	149	150	7.74	7.74	7.74	7.74	7.74
1-out #2 3.2	150	150	7.74	7.74	7.74	7.74	7.74
1-out #2 4.2	150	150	7.75	7.75	7.75	7.75	7.75
1-out #2 5.2	150	150	7.76	7.76	7.77	7.76	7.76
1-out #2 6.2	145	150	7.77	7.78	7.79	7.78	7.78
1-out #2 7.2	150	150	7.79	7.81	7.82	7.81	7.81
1-out #2 8.2	150	150	7.82	7.83	7.83	7.83	7.83
1-out #2 9.2	150	150	7.85	7.86	7.86	7.85	7.86
1-out #2 10.2	150	150	7.86	7.86	-	7.86	7.86
1-out #1 1.3	150	150	-	7.76	7.76	7.76	7.76
1-out #1 2.3	150	150	7.76	7.76	7.76	7.75	7.76
1-out #1 3.3	150	150	7.75	7.76	7.77	7.76	7.76
1-out #1 4.3	150	150	7.76	7.76	7.77	7.76	7.76
1-out #1 5.3	150	150	7.77	7.78	7.78	7.78	7.78
1-out #1 6.3	145	150	7.78	7.80	7.81	7.79	7.80
1-out #1 7.3	150	150	7.81	7.82	7.83	7.82	7.82
1-out #1 8.3	150	150	7.84	7.84	7.85	7.84	7.84
1-out #1 9.3	150	150	7.85	7.85	7.86	7.86	7.86
1-out #1 10.3	150	150	7.86	7.87	-	7.86	7.86
1-out #2 1.4	148	150	-	7.75	7.75	7.75	7.75
1-out #2 2.4	151	150	7.75	7.75	7.75	7.76	7.75
1-out #2 3.4	150	150	7.76	7.76	7.76	7.76	7.76
1-out #2 4.4	150	150	7.76	7.77	7.79	7.76	7.77
1-out #2 5.4	150	150	7.77	7.77	7.78	7.79	7.78
1-out #2 6.4	145	150	7.78	7.79	7.81	7.80	7.80
1-out #2 7.4	150	150	7.80	7.82	7.83	7.82	7.82
1-out #2 8.4	150	150	7.84	7.85	7.85	7.84	7.85
1-out #2 9.4	150	150	7.84	7.85	7.85	7.86	7.85
1-out #2 10.4	150	150	7.85	7.85	7.88	7.87	7.86

Table 21. Dimensions specimens from panel 1-in.

<i>Panel</i>	1-in						
<i>Specimen</i>	Length (mm)	Width (mm)	d_{egde1} (mm)	d_{egde2} (mm)	d_{egde3} (mm)	d_{egde4} (mm)	d_{mean} (mm)
1-in #3 1.1	147	150	-	5.88	5.88	5.88	5.88
1-in #3 2.1	150	150	5.88	5.88	5.87	5.88	5.88
1-in #3 3.1	150	150	5.87	5.87	5.86	5.87	5.87
1-in #3 4.1	150	150	5.86	5.85	5.86	5.86	5.86
1-in #3 5.1	150	150	5.86	5.85	5.84	5.85	5.85
1-in #3 6.1	150	150	5.85	5.84	5.84	5.84	5.84
1-in #3 7.1	149	150	5.83	5.83	5.83	5.84	5.83
1-in #3 8.1	150	150	5.83	5.83	5.82	5.83	5.83
1-in #3 9.1	150	150	5.83	5.83	5.82	5.82	5.83
1-in #3 10.1	150	150	5.82	5.82	-	5.82	5.82
1-in #4 1.2	149	150	-	5.88	5.88	5.88	5.88
1-in #4 2.2	150	150	5.88	5.88	5.87	5.88	5.88
1-in #4 3.2	150	150	5.87	5.87	5.86	5.87	5.87
1-in #4 4.2	150	150	5.87	5.85	5.85	5.85	5.86
1-in #4 5.2	150	150	5.85	5.84	5.86	5.85	5.85
1-in #4 6.2	150	150	5.84	5.84	5.83	5.84	5.84
1-in #4 7.2	149	150	5.84	5.83	5.83	5.84	5.84
1-in #4 8.2	150	150	5.84	5.83	5.82	5.83	5.83
1-in #4 9.2	150	150	5.84	5.83	5.83	5.83	5.83
1-in #4 10.2	150	150	5.82	5.82	-	5.82	5.82
1-in #3 1.3	152	150	-	5.88	5.88	5.89	5.88
1-in #3 2.3	150	150	5.87	5.88	5.87	5.88	5.88
1-in #3 3.3	150	150	5.87	5.86	5.87	5.87	5.87
1-in #3 4.3	150	150	5.87	5.85	5.86	5.86	5.86
1-in #3 5.3	150	150	5.85	5.85	5.85	5.85	5.85
1-in #3 6.3	150	150	5.83	5.84	5.84	5.83	5.84
1-in #3 7.3	150	150	5.83	5.83	5.83	5.83	5.83
1-in #3 8.3	150	150	5.83	5.83	5.83	5.83	5.83
1-in #3 9.3	150	150	5.82	5.82	5.82	5.82	5.82
1-in #3 10.3	156	150	5.83	5.82	-	5.82	5.82
1-in #4 1.4	154	150	-	5.87	5.88	5.88	5.88
1-in #4 2.4	150	150	5.88	5.88	5.88	5.88	5.88
1-in #4 3.4	151	150	5.87	5.87	5.86	5.87	5.87
1-in #4 4.4	151	150	5.86	5.86	5.85	5.85	5.86
1-in #4 5.4	150	150	5.85	5.85	5.85	5.85	5.85
1-in #4 6.4	150	150	5.84	5.84	5.85	5.83	5.84
1-in #4 7.4	150	150	5.84	5.84	5.83	5.83	5.84
1-in #4 8.4	150	150	5.83	5.83	5.82	5.83	5.83
1-in #4 9.4	150	150	5.83	5.82	5.83	5.83	5.83
1-in #4 10.4	152	150	5.82	5.82	-	5.82	5.82

Table 22. Dimensions specimens from panel 2-out.

<i>Panel</i>	2-out						
<i>Specimen</i>	Length (mm)	Width (mm)	d_{egde1} (mm)	d_{egde2} (mm)	d_{egde3} (mm)	d_{egde4} (mm)	d_{mean} (mm)
2-out #1 1.1	150	150	-	4.79	4.78	4.77	4.78
2-out #1 2.1	151	150	4.79	4.78	4.79	4.81	4.79
2-out #1 3.1	150	150	4.79	4.79	4.79	4.78	4.79
2-out #1 4.1	150	150	4.79	4.78	4.79	4.80	4.79
2-out #1 5.1	150	150	4.79	4.78	4.79	4.78	4.79
2-out #1 6.1	150	150	4.78	4.78	4.77	4.78	4.78
2-out #1 7.1	150	150	4.78	4.79	4.79	4.80	4.79
2-out #1 8.1	149	150	4.77	4.79	4.79	4.80	4.79
2-out #1 9.1	150	150	4.79	4.78	4.79	4.80	4.79
2-out #1 10.1	150	150	4.77	4.78	-	4.80	4.78
2-out #2 1.2	150	150	-	4.79	4.77	4.79	4.78
2-out #2 2.2	150	150	4.79	4.79	4.81	4.81	4.80
2-out #2 3.2	150	150	4.80	4.80	4.80	4.78	4.80
2-out #2 4.2	150	150	4.79	4.80	4.79	4.80	4.80
2-out #2 5.2	150	150	4.79	4.79	4.79	4.80	4.79
2-out #2 6.2	150	150	4.79	4.79	4.79	4.79	4.79
2-out #2 7.2	150	150	4.78	4.77	4.79	4.79	4.78
2-out #2 8.2	149	150	4.79	4.79	4.80	4.79	4.79
2-out #2 9.2	150	150	4.79	4.79	4.80	4.80	4.80
2-out #2 10.2	150	150	4.79	4.79	-	4.80	4.79
2-out #1 1.3	150	150	-	4.79	4.79	4.80	4.79
2-out #1 2.3	150	150	4.79	4.79	4.80	4.80	4.80
2-out #1 3.3	150	150	4.79	4.80	4.79	4.79	4.79
2-out #1 4.3	150	150	4.80	4.80	4.80	4.79	4.80
2-out #1 5.3	150	150	4.80	4.80	4.79	4.80	4.80
2-out #1 6.3	150	150	4.79	4.80	4.80	4.80	4.80
2-out #1 7.3	150	150	4.79	4.80	4.80	4.79	4.80
2-out #1 8.3	149	150	4.80	4.80	4.80	4.80	4.80
2-out #1 9.3	150	150	4.79	4.80	4.81	4.80	4.80
2-out #1 10.3	150	150	4.80	4.80	-	4.79	4.80
2-out #2 1.4	150	150	-	4.80	4.80	4.79	4.80
2-out #2 2.4	150	150	4.80	4.80	4.80	4.80	4.80
2-out #2 3.4	150	150	4.80	4.80	4.80	4.80	4.80
2-out #2 4.4	149	150	4.80	4.80	4.80	4.80	4.80
2-out #2 5.4	150	150	4.78	4.80	4.80	4.80	4.80
2-out #2 6.4	150	150	4.79	4.79	4.80	4.80	4.80
2-out #2 7.4	150	150	4.79	4.80	4.80	4.80	4.80
2-out #2 8.4	149	150	4.80	4.80	4.80	4.80	4.80
2-out #2 9.4	150	150	4.80	4.80	4.80	4.80	4.80
2-out #2 10.4	150	150	4.79	4.80	-	4.80	4.80

Table 23. Dimensions specimens from panel 2-in.

<i>Panel</i>	2-in						
<i>Specimen</i>	Length (mm)	Width (mm)	d_{egde1} (mm)	d_{egde2} (mm)	d_{egde3} (mm)	d_{egde4} (mm)	d_{mean} (mm)
2-in #3 1.1	149	150	-	3.86	3.88	3.84	3.86
2-in #3 2.1	150	150	3.86	3.86	3.84	3.84	3.85
2-in #3 3.1	149	150	3.87	3.87	3.84	3.84	3.86
2-in #3 4.1	150	150	3.84	3.85	3.84	3.83	3.84
2-in #3 5.1	150	150	3.83	3.85	3.86	3.83	3.84
2-in #3 6.1	150	150	3.83	3.84	3.84	3.84	3.84
2-in #3 7.1	150	150	3.83	3.84	3.83	3.84	3.84
2-in #3 8.1	150	150	3.83	3.85	3.84	3.84	3.84
2-in #3 9.1	149	150	3.84	3.84	3.83	3.83	3.84
2-in #3 10.1	150	150	3.84	3.85	-	3.85	3.85
2-in #4 1.2	150	151	-	3.83	3.82	3.82	3.82
2-in #4 2.2	150	150	3.83	3.84	3.84	3.84	3.84
2-in #4 3.2	150	150	3.82	3.84	3.84	3.82	3.83
2-in #4 4.2	150	150	3.83	3.84	3.83	3.83	3.83
2-in #4 5.2	150	150	3.83	3.83	3.83	3.82	3.83
2-in #4 6.2	150	150	3.82	3.83	3.83	3.82	3.83
2-in #4 7.2	150	150	3.82	3.82	3.82	3.82	3.82
2-in #4 8.2	150	150	3.82	3.82	3.82	3.82	3.82
2-in #4 9.2	150	150	3.82	3.83	3.83	3.83	3.83
2-in #4 10.2	150	150	3.82	3.84	-	3.84	3.83
2-in #3 1.3	150	150	-	3.82	3.82	3.81	3.82
2-in #3 2.3	150	150	3.82	3.82	3.82	3.81	3.82
2-in #3 3.3	150	150	3.82	3.81	3.82	3.82	3.82
2-in #3 4.3	150	150	3.82	3.82	3.82	3.81	3.82
2-in #3 5.3	150	150	3.83	3.82	3.81	3.82	3.82
2-in #3 6.3	150	150	3.81	3.82	3.82	3.81	3.82
2-in #3 7.3	150	150	3.81	3.82	3.81	3.82	3.82
2-in #3 8.3	150	150	3.82	3.81	3.81	3.81	3.81
2-in #3 9.3	150	150	3.81	3.82	3.83	3.82	3.82
2-in #3 10.3	150	150	3.82	3.83	-	3.81	3.82
2-in #4 1.4	151	150	-	3.82	3.82	3.83	3.82
2-in #4 2.4	150	150	3.81	3.82	3.82	3.82	3.82
2-in #4 3.4	150	150	3.82	3.82	3.82	3.82	3.82
2-in #4 4.4	150	150	3.82	3.82	3.82	3.82	3.82
2-in #4 5.4	150	150	3.82	3.83	3.82	3.81	3.82
2-in #4 6.4	150	150	3.82	3.83	3.82	3.82	3.82
2-in #4 7.4	150	150	3.82	3.82	3.82	3.81	3.82
2-in #4 8.4	150	150	3.82	3.82	3.82	3.82	3.82
2-in #4 9.4	150	150	3.82	3.83	3.82	3.82	3.82
2-in #4 10.4	150	150	3.83	3.83	-	3.84	3.83

Table 24. Dimensions specimens from panel 3-out.

<i>Panel</i>	3-out						
<i>Specimen</i>	Length (mm)	Width (mm)	d_{egde1} (mm)	d_{egde2} (mm)	d_{egde3} (mm)	d_{egde4} (mm)	d_{mean} (mm)
3-out #1 1.1	150	150	4.87	4.89	4.88	4.86	4.88
3-out #1 2.1	149	150	4.87	4.88	4.87	4.85	4.87
3-out #1 3.1	150	150	4.87	4.88	4.86	4.86	4.87
3-out #1 4.1	150	150	4.87	4.88	4.86	4.85	4.87
3-out #1 5.1	150	150	4.87	4.88	4.87	4.85	4.87
3-out #1 6.1	150	150	4.87	4.88	4.87	4.85	4.87
3-out #1 7.1	150	150	4.87	4.88	4.87	4.85	4.87
3-out #1 8.1	150	150	4.87	4.88	4.87	4.85	4.87
3-out #1 9.1	150	150	4.86	4.87	4.87	4.85	4.86
3-out #2 1.2	150	150	4.84	4.85	4.84	4.84	4.84
3-out #2 2.2	150	150	4.85	4.85	4.84	4.83	4.84
3-out #2 3.2	150	150	4.85	4.84	4.86	4.85	4.85
3-out #2 4.2	150	150	4.84	4.85	4.84	4.84	4.84
3-out #2 5.2	150	150	4.85	4.85	4.85	4.84	4.85
3-out #2 6.2	151	150	4.85	4.85	4.84	4.83	4.84
3-out #2 7.2	150	150	4.84	4.85	4.84	4.83	4.84
3-out #2 8.2	150	150	4.85	4.85	4.85	4.83	4.85
3-out #2 9.2	150	150	4.85	4.87	4.84	4.84	4.85
3-out #1 1.3	150	150	4.82	4.83	4.82	4.82	4.82
3-out #1 2.3	150	150	4.82	4.83	4.82	4.81	4.82
3-out #1 3.3	150	150	4.82	4.83	4.83	4.82	4.83
3-out #1 4.3	150	150	4.82	4.83	4.82	4.81	4.82
3-out #1 5.3	150	150	4.82	4.83	4.82	4.81	4.82
3-out #1 6.3	151	150	4.82	4.83	4.82	4.81	4.82
3-out #1 7.3	150	150	4.82	4.83	4.82	4.82	4.82
3-out #1 8.3	150	150	4.83	4.83	4.82	4.82	4.83
3-out #1 9.3	150	150	4.84	4.84	4.83	4.82	4.83
3-out #2 1.4	150	150	4.82	4.81	4.81	4.82	4.82
3-out #2 2.4	150	150	4.81	4.81	4.81	4.81	4.81
3-out #2 3.4	151	150	4.81	4.81	4.81	4.81	4.81
3-out #2 4.4	150	150	4.81	4.81	4.81	4.81	4.81
3-out #2 5.4	150	150	4.81	4.81	4.81	4.81	4.81
3-out #2 6.4	151	150	4.81	4.82	4.81	4.81	4.81
3-out #2 7.4	150	150	4.81	4.82	4.81	4.81	4.81
3-out #2 8.4	150	150	4.81	4.82	4.81	4.81	4.81
3-out #2 9.4	150	150	4.81	4.82	4.81	4.81	4.81

Table 25. Dimensions specimens from panel 3-in.

<i>Panel</i>	3-in						
<i>Specimen</i>	Length (mm)	Width (mm)	d_{egde1} (mm)	d_{egde2} (mm)	d_{egde3} (mm)	d_{egde4} (mm)	d_{mean} (mm)
3-in #3 1.1	150	150	3.79	3.80	3.79	3.79	3.79
3-in #3 2.1	151	150	3.79	3.80	3.79	3.79	3.79
3-in #3 3.1	151	150	3.79	3.79	3.80	3.79	3.79
3-in #3 4.1	150	150	3.80	3.80	3.79	3.80	3.80
3-in #3 5.1	150	150	3.79	3.80	3.80	3.79	3.80
3-in #3 6.1	150	150	3.80	3.80	3.80	3.80	3.80
3-in #3 7.1	150	150	3.80	3.81	3.81	3.81	3.81
3-in #3 8.1	150	150	3.82	3.82	3.83	3.82	3.82
3-in #4 1.2	150	150	3.79	3.79	3.79	3.79	3.79
3-in #4 2.2	150	150	3.79	3.79	3.79	3.79	3.79
3-in #4 3.2	150	150	3.79	3.80	3.79	3.79	3.79
3-in #4 4.2	150	150	3.79	3.80	3.80	3.80	3.80
3-in #4 5.2	150	150	3.80	3.80	3.80	3.80	3.80
3-in #4 6.2	150	150	3.80	3.80	3.81	3.80	3.80
3-in #4 7.2	150	150	3.81	3.81	3.81	3.81	3.81
3-in #4 8.2	150	150	3.81	3.81	3.82	3.82	3.82
3-in #3 1.3	150	150	3.79	3.79	3.79	3.79	3.79
3-in #3 2.3	150	150	3.79	3.79	3.79	3.79	3.79
3-in #3 3.3	150	150	3.79	3.79	3.79	3.79	3.79
3-in #3 4.3	149	150	3.79	3.80	3.80	3.79	3.80
3-in #3 5.3	150	150	3.80	3.80	3.80	3.80	3.80
3-in #3 6.3	150	150	3.80	3.80	3.80	3.80	3.80
3-in #3 7.3	150	150	3.81	3.81	3.81	3.81	3.81
3-in #3 8.3	150	150	3.81	3.82	3.82	3.85	3.83
3-in #4 1.4	149	150	3.80	3.79	3.79	3.79	3.79
3-in #4 2.4	149	150	3.78	3.79	3.79	3.79	3.79
3-in #4 3.4	149	150	3.79	3.79	3.79	3.79	3.79
3-in #4 4.4	149	150	3.79	3.79	3.80	3.80	3.80
3-in #4 5.4	150	150	3.80	3.79	3.80	3.80	3.80
3-in #4 6.4	151	150	3.80	3.80	3.81	3.80	3.80
3-in #4 7.4	150	150	3.81	3.81	3.81	3.81	3.81
3-in #4 8.4	151	150	3.81	3.82	3.82	3.82	3.82

Table 26. Dimensions specimens from panel 4-out.

<i>Panel</i>	4-out						
<i>Specimen</i>	Length (mm)	Width (mm)	d_{egde1} (mm)	d_{egde2} (mm)	d_{egde3} (mm)	d_{egde4} (mm)	d_{mean} (mm)
4-out #1 1.1	150	150	5.79	5.81	5.82	5.81	5.81
4-out #1 2.1	146	150	5.82	5.82	5.82	5.82	5.82
4-out #1 3.1	151	150	5.82	5.82	5.82	5.82	5.82
4-out #1 4.1	150	150	5.82	5.83	5.83	5.83	5.83
4-out #1 5.1	150	150	5.83	5.84	5.83	5.83	5.83
4-out #1 6.1	150	150	5.83	5.84	5.83	5.83	5.83
4-out #1 7.1	150	150	5.84	5.85	5.85	5.85	5.85
4-out #1 8.1	149	150	5.85	5.86	5.86	5.86	5.86
4-out #1 9.1	150	150	5.86	5.87	5.86	5.87	5.87
4-out #2 1.2	150	150	5.80	5.80	5.81	5.81	5.81
4-out #2 2.2	146	150	5.81	5.81	5.81	5.81	5.81
4-out #2 3.2	151	150	5.81	5.82	5.82	5.82	5.82
4-out #2 4.2	150	150	5.82	5.83	5.83	5.82	5.83
4-out #2 5.2	150	150	5.82	5.82	5.83	5.83	5.83
4-out #2 6.2	150	150	5.83	5.84	5.84	5.84	5.84
4-out #2 7.2	150	150	5.84	5.85	5.85	5.85	5.85
4-out #2 8.2	149	150	5.85	5.86	5.87	5.86	5.86
4-out #2 9.2	150	150	5.86	5.87	5.86	5.87	5.87
4-out #1 1.3	150	150	5.80	5.81	5.81	5.81	5.81
4-out #1 2.3	145	150	5.81	5.81	5.81	5.81	5.81
4-out #1 3.3	151	150	5.81	5.82	5.82	5.81	5.82
4-out #1 4.3	149	150	5.82	5.82	5.83	5.83	5.83
4-out #1 5.3	150	150	5.82	5.82	5.83	5.83	5.83
4-out #1 6.3	150	150	5.83	5.83	5.84	5.84	5.84
4-out #1 7.3	150	150	5.84	5.85	5.85	5.85	5.85
4-out #1 8.3	149	150	5.85	5.86	5.86	5.86	5.86
4-out #1 9.3	150	150	5.86	5.87	5.86	5.87	5.87
4-out #2 1.4	150	150	5.81	5.81	5.81	5.81	5.81
4-out #2 2.4	144	150	5.81	5.82	5.82	5.82	5.82
4-out #2 3.4	150	150	5.82	5.82	5.82	5.82	5.82
4-out #2 4.4	150	150	5.82	5.83	5.83	5.83	5.83
4-out #2 5.4	150	150	5.83	5.83	5.83	5.83	5.83
4-out #2 6.4	150	150	5.84	5.84	5.85	5.84	5.84
4-out #2 7.4	150	150	5.84	5.85	5.85	5.85	5.85
4-out #2 8.4	150	150	5.85	5.86	5.87	5.86	5.86
4-out #2 9.4	150	150	5.86	5.87	5.86	5.87	5.87

Table 27. Dimensions specimens from panel 4-in.

<i>Panel</i>	4-in						
<i>Specimen</i>	Length (mm)	Width (mm)	d_{egde1} (mm)	d_{egde2} (mm)	d_{egde3} (mm)	d_{egde4} (mm)	d_{mean} (mm)
4-in #3 1.1	150	150	3.85	3.86	3.86	3.86	3.86
4-in #3 2.1	150	150	3.86	3.86	3.86	3.85	3.86
4-in #3 3.1	150	150	3.85	3.85	3.85	3.86	3.85
4-in #3 4.1	149	150	3.86	3.85	3.86	3.86	3.86
4-in #3 5.1	144	150	3.85	3.86	3.86	3.86	3.86
4-in #3 6.1	145	150	3.86	3.86	3.86	3.86	3.86
4-in #3 7.1	145	150	3.86	3.86	3.86	3.86	3.86
4-in #3 8.1	-	-	-	-	-	-	-
4-in #3 9.1	-	-	-	-	-	-	-
4-in #4 1.2	150	150	3.85	3.85	3.85	3.85	3.85
4-in #4 2.2	150	150	3.85	3.85	3.86	3.85	3.85
4-in #4 3.2	150	150	3.85	3.85	3.85	3.85	3.85
4-in #4 4.2	149	150	3.85	3.85	3.85	3.85	3.85
4-in #4 5.2	144	150	3.86	3.86	3.86	3.86	3.86
4-in #4 6.2	144	150	3.86	3.87	3.86	3.86	3.86
4-in #4 7.2	-	-	-	-	-	-	-
4-in #4 8.2	150	150	3.87	3.87	3.86	3.86	3.87
4-in #4 9.2	145	150	3.86	3.86	-	3.86	3.86
4-in #3 1.3	-	-	-	-	-	-	-
4-in #3 2.3	150	150	3.86	3.86	3.86	3.85	3.86
4-in #3 3.3	150	150	3.86	3.86	3.86	3.86	3.86
4-in #3 4.3	150	150	3.85	3.86	3.86	3.86	3.86
4-in #3 5.3	144	150	3.86	3.86	3.86	3.86	3.86
4-in #3 6.3	-	-	-	-	-	-	-
4-in #3 7.3	149	150	3.86	3.86	3.86	3.85	3.86
4-in #3 8.3	150	150	3.86	3.87	3.88	3.86	3.87
4-in #3 9.3	145	150	3.86	3.86	-	3.86	3.86
4-in #4 1.4	150	150	3.88	3.87	3.85	-	3.87
4-in #4 2.4	150	150	3.86	3.86	3.86	3.85	3.86
4-in #4 3.4	150	150	3.85	3.84	3.85	3.85	3.85
4-in #4 4.4	150	150	3.85	3.85	3.84	3.84	3.85
4-in #4 5.4	-	-	-	-	-	-	-
4-in #4 6.4	150	150	3.85	3.85	3.85	3.84	3.85
4-in #4 7.4	150	150	3.86	3.85	3.86	3.84	3.85
4-in #4 8.4	150	150	3.84	3.85	3.86	3.84	3.85
4-in #4 9.4	144	150	3.84	3.85	-	3.86	3.85

Table 28. Dimensions specimens from panel 5-out.

<i>Panel</i>	5-out						
<i>Specimen</i>	Length (mm)	Width (mm)	d_{egde1} (mm)	d_{egde2} (mm)	d_{egde3} (mm)	d_{egde4} (mm)	d_{mean} (mm)
5-out #1 1.1	153	150	-	5.88	5.87	-	5.88
5-out #1 2.1	148	150	5.87	5.86	5.86	-	5.86
5-out #1 3.1	150	150	5.86	5.85	5.85	-	5.85
5-out #1 4.1	150	150	5.85	5.85	5.85	-	5.85
5-out #1 5.1	150	149	5.83	5.84	5.84	-	5.84
5-out #1 6.1	150	149	5.83	5.83	5.83	-	5.83
5-out #1 7.1	150	149	5.81	5.83	5.83	-	5.82
5-out #2 1.2	151	150	-	5.87	5.86	5.87	5.87
5-out #2 2.2	150	150	5.86	5.85	5.85	5.86	5.86
5-out #2 3.2	150	150	5.85	5.84	5.84	5.84	5.84
5-out #2 4.2	150	150	5.85	5.85	5.83	5.84	5.84
5-out #2 5.2	149	150	5.83	5.83	5.83	5.83	5.83
5-out #2 6.2	150	150	5.83	5.83	5.82	5.82	5.83
5-out #2 7.2	150	150	5.82	5.82	5.81	5.81	5.82
5-out #1 1.3	150	150	-	5.87	5.87	5.87	5.87
5-out #1 2.3	150	150	5.86	5.85	5.85	5.85	5.85
5-out #1 3.3	150	150	5.85	5.84	5.84	5.84	5.84
5-out #1 4.3	150	150	5.84	5.83	5.83	5.83	5.83
5-out #1 5.3	150	150	5.83	5.82	5.83	5.82	5.83
5-out #1 6.3	150	150	5.82	5.82	5.82	5.82	5.82
5-out #1 7.3	150	150	5.82	5.82	5.82	5.82	5.82
5-out #2 1.4	149	150	-	-	5.86	5.87	5.87
5-out #2 2.4	151	150	5.87	-	5.85	5.86	5.86
5-out #2 3.4	150	150	5.85	-	5.85	5.85	5.85
5-out #2 4.4	150	150	5.84	-	5.84	5.84	5.84
5-out #2 5.4	150	150	5.84	-	5.84	5.84	5.84
5-out #2 6.4	149	150	5.83	-	5.82	5.83	5.83
5-out #2 7.4	150	150	5.81	-	5.83	5.82	5.82

Table 29. Dimensions specimens from panel 5-in.

<i>Panel</i>	5-in						
<i>Specimen</i>	Length (mm)	Width (mm)	d_{egde1} (mm)	d_{egde2} (mm)	d_{egde3} (mm)	d_{egde4} (mm)	d_{mean} (mm)
5-in #3 1.1	150	150	-	-	3.85	3.85	3.85
5-in #3 2.1	151	150	3.85	-	3.85	3.85	3.85
5-in #3 3.1	150	150	3.85	-	3.85	3.86	3.85
5-in #3 4.1	150	150	3.85	-	3.85	3.85	3.85
5-in #3 5.1	150	150	3.86	-	3.85	3.86	3.86
5-in #3 6.1	150	150	3.86	-	3.85	3.86	3.86
5-in #3 7.1	150	150	3.86	-	3.86	3.86	3.86
5-in #4 1.2	150	150	-	3.85	3.85	3.86	3.85
5-in #4 2.2	151	150	3.86	3.85	3.85	3.86	3.86
5-in #4 3.2	151	150	3.85	3.85	3.86	3.86	3.86
5-in #4 4.2	150	150	3.85	3.85	3.86	3.86	3.86
5-in #4 5.2	150	150	3.86	3.86	3.86	3.86	3.86
5-in #4 6.2	150	150	3.87	3.86	3.86	3.86	3.86
5-in #4 7.2	150	150	3.86	3.86	3.86	3.86	3.86
5-in #3 1.3	150	151	-	3.86	3.87	3.87	3.87
5-in #3 2.3	151	150	3.86	3.86	3.87	3.87	3.87
5-in #3 3.3	151	150	3.87	3.86	3.86	3.86	3.86
5-in #3 4.3	150	150	3.86	3.86	3.86	3.86	3.86
5-in #3 5.3	150	150	3.86	3.86	3.86	3.86	3.86
5-in #3 6.3	150	150	3.86	3.86	3.87	3.86	3.86
5-in #3 7.3	150	150	3.86	3.86	3.86	3.86	3.86
5-in #4 1.4	150	150	-	3.86	3.86	-	3.86
5-in #4 2.4	151	150	3.86	3.87	3.87	-	3.87
5-in #4 3.4	151	150	3.86	3.86	3.87	-	3.86
5-in #4 4.4	150	150	3.86	3.86	3.86	-	3.86
5-in #4 5.4	150	150	3.86	3.86	3.87	-	3.86
5-in #4 6.4	150	150	3.86	3.87	3.86	-	3.86
5-in #4 7.4	150	150	3.87	3.87	3.88	-	3.87

Table 30. Dimensions specimens from panel 6-out.

<i>Panel</i>	6-out						
<i>Specimen</i>	Length (mm)	Width (mm)	d_{egde1} (mm)	d_{egde2} (mm)	d_{egde3} (mm)	d_{egde4} (mm)	d_{mean} (mm)
6-out #1 1.1	150	150	5.90	5.89	5.89	-	5.89
6-out #1 2.1	151	150	5.89	5.89	5.89	-	5.89
6-out #1 3.1	151	150	5.89	5.89	5.89	-	5.89
6-out #1 4.1	150	150	5.89	5.89	5.90	-	5.89
6-out #1 5.1	150	150	5.89	5.89	5.89	-	5.89
6-out #1 6.1	151	150	5.89	5.89	5.89	-	5.89
6-out #1 7.1	150	150	5.89	5.89	-	-	5.89
6-out #2 1.2	150	150	-	5.88	5.88	5.89	5.88
6-out #2 2.2	151	150	5.88	5.88	5.89	5.89	5.89
6-out #2 3.2	151	150	5.88	5.87	5.88	5.89	5.88
6-out #2 4.2	150	150	5.88	5.88	5.88	5.89	5.88
6-out #2 5.2	151	150	5.88	5.87	5.88	5.89	5.88
6-out #2 6.2	150	150	5.88	5.88	5.88	5.89	5.88
6-out #2 7.2	150	150	5.88	5.88	5.89	-	5.88
6-out #1 1.3	150	150	-	5.87	5.88	5.88	5.88
6-out #1 2.3	151	150	5.87	5.86	5.87	5.88	5.87
6-out #1 3.3	151	150	5.88	5.87	5.87	5.87	5.87
6-out #1 4.3	150	150	5.87	5.86	5.87	5.87	5.87
6-out #1 5.3	149	150	5.87	5.86	5.87	5.87	5.87
6-out #1 6.3	151	150	5.87	5.86	5.87	5.87	5.87
6-out #1 7.3	150	149	5.87	5.86	5.86	-	5.86
6-out #2 1.4	150	150	-	-	5.86	5.87	5.87
6-out #2 2.4	151	150	5.86	-	5.86	5.87	5.86
6-out #2 3.4	152	150	5.86	-	5.86	5.86	5.86
6-out #2 4.4	151	150	5.86	-	5.86	5.86	5.86
6-out #2 5.4	160	150	5.86	-	5.86	5.86	5.86
6-out #2 6.4	140	150	5.86	-	5.86	5.86	5.86
6-out #2 7.4	150	150	5.86	-	5.86	5.86	5.86

Table 31. Dimensions specimens from panel 6-in.

<i>Panel</i>	6-in						
<i>Specimen</i>	Length (mm)	Width (mm)	d_{egde1} (mm)	d_{egde2} (mm)	d_{egde3} (mm)	d_{egde4} (mm)	d_{mean} (mm)
6-in #3 1.1	150	155	7.82	7.86	7.89	-	7.86
6-in #3 2.1	151	157	7.89	7.90	7.91	-	7.90
6-in #3 3.1	150	156	7.89	7.89	7.89	-	7.89
6-in #3 4.1	151	157	7.89	7.88	7.87	-	7.88
6-in #3 5.1	150	157	7.86	7.86	7.86	-	7.86
6-in #3 6.1	150	157	7.84	7.85	7.84	-	7.84
6-in #3 7.1	155	156	7.84	7.82	-	-	7.83
6-in #4 1.2	151	150	7.82	7.87	7.89	7.86	7.86
6-in #4 2.2	150	150	7.89	7.90	7.90	7.90	7.90
6-in #4 3.2	150	150	7.90	7.90	7.89	7.90	7.90
6-in #4 4.2	150	150	7.89	7.88	7.87	7.88	7.88
6-in #4 5.2	150	150	7.87	7.86	7.86	7.86	7.86
6-in #4 6.2	151	150	7.85	7.85	7.84	7.85	7.85
6-in #4 7.2	155	149	7.84	7.84	-	7.84	7.84
6-in #3 1.3	150	150	7.84	7.87	7.89	7.87	7.87
6-in #3 2.3	150	150	7.89	7.90	7.90	7.90	7.90
6-in #3 3.3	150	150	7.90	7.90	7.89	7.90	7.90
6-in #3 4.3	150	150	7.89	7.88	7.88	7.89	7.89
6-in #3 5.3	150	150	7.87	7.87	7.86	7.87	7.87
6-in #3 6.3	151	150	7.85	7.84	7.84	7.85	7.85
6-in #3 7.3	155	150	7.84	7.84	-	7.84	7.84
6-in #4 1.4	150	157	7.82	-	7.89	7.87	7.86
6-in #4 2.4	150	155	7.87	-	7.90	7.89	7.89
6-in #4 3.4	150	157	7.90	-	7.89	7.90	7.90
6-in #4 4.4	150	156	7.89	-	7.89	7.88	7.89
6-in #4 5.4	150	155	7.87	-	7.85	7.87	7.86
6-in #4 6.4	150	156	7.85	-	7.83	7.85	7.84
6-in #4 7.4	155	156	7.85	-	-	7.83	7.84

Appendix C

Microscopy examination photos

Figure 82 to Figure 89 show pictures taken with the microscope during the microscopic examination. A distinction has been made between the different sides (#1, #2, #3 and #4) and different magnifications (20x and 50x).

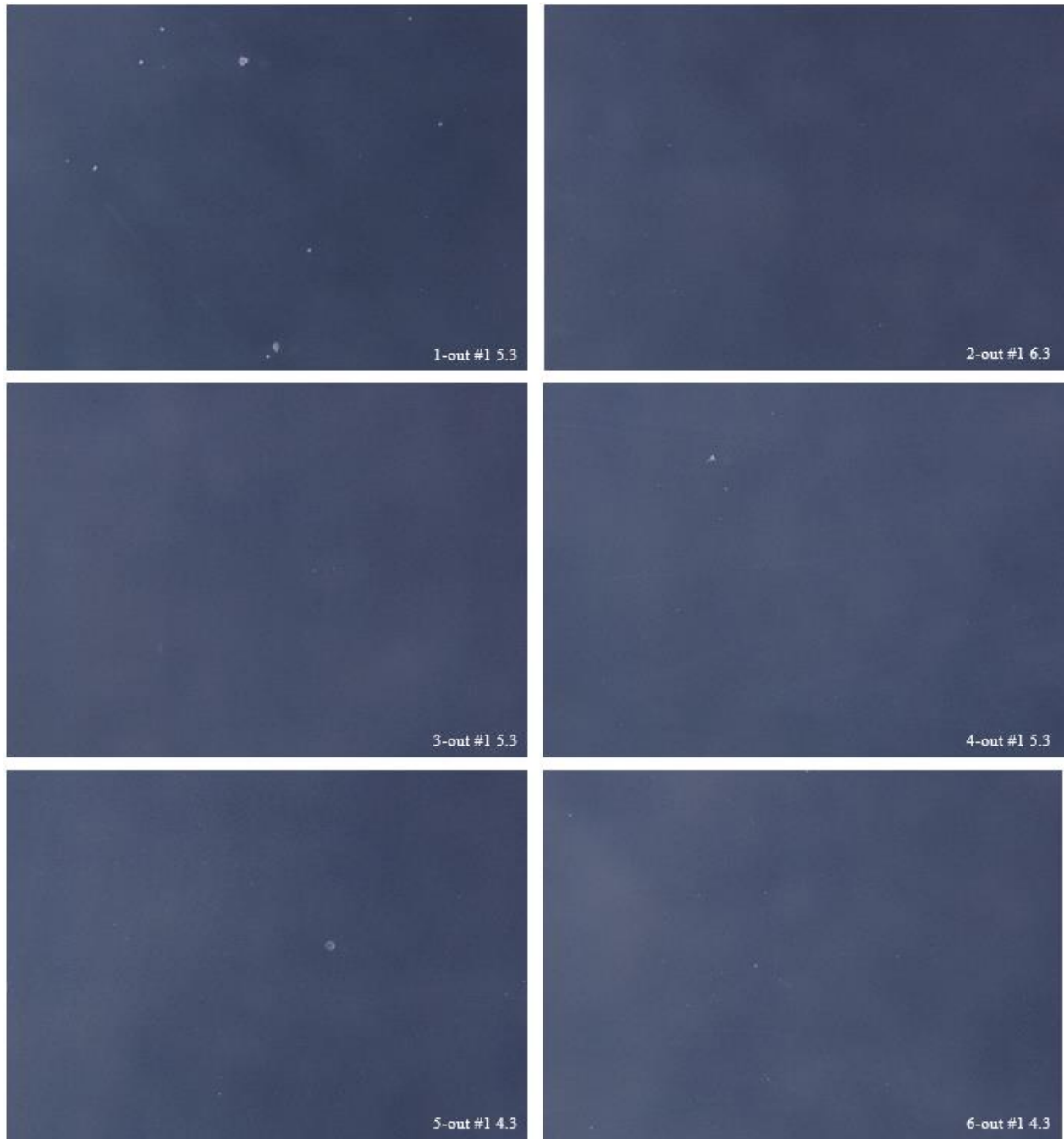


Figure 82. Microscopic photos side #1, magnification 20x.



Figure 83. Microscopic photos side #1, magnification 50x.

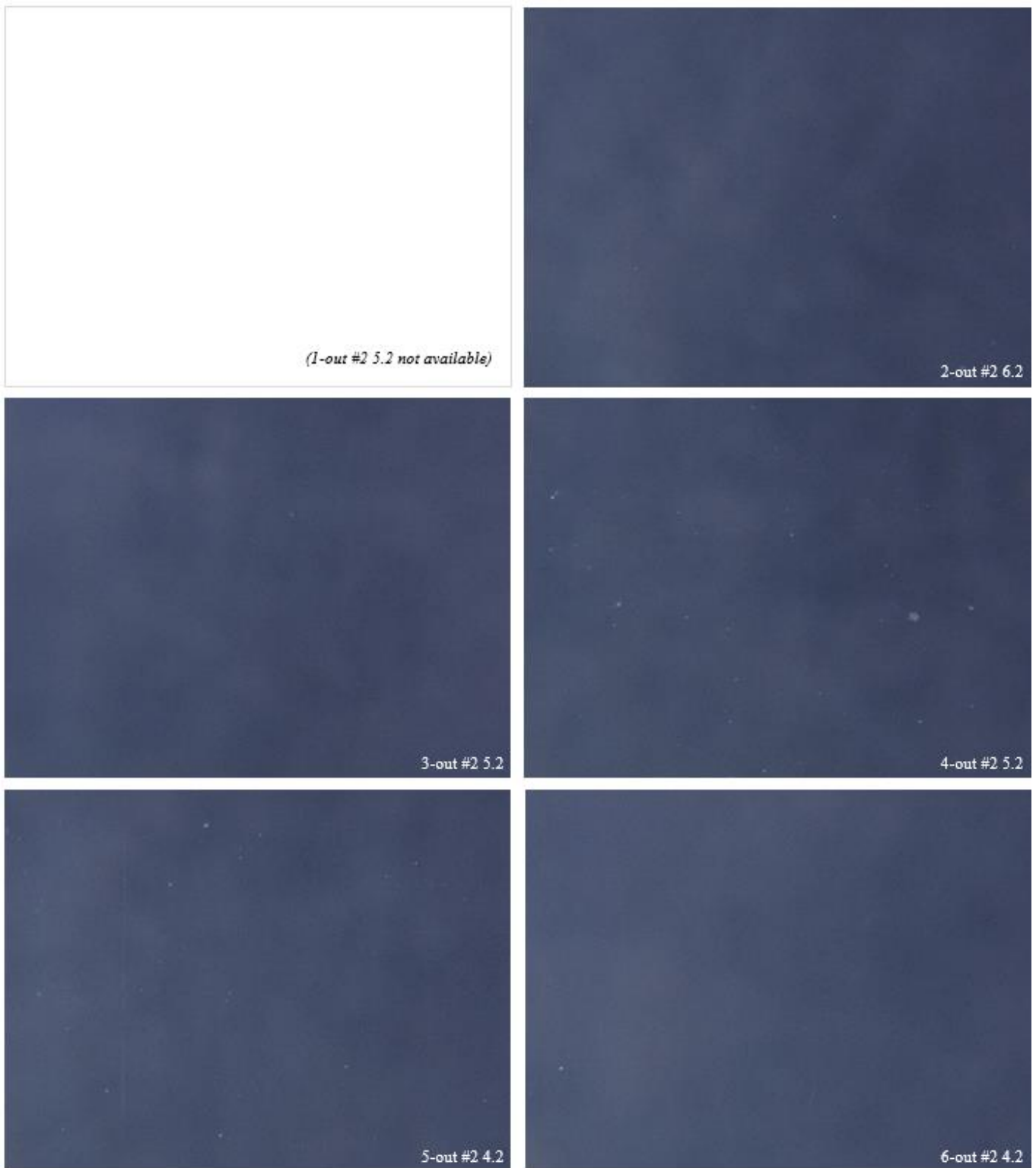


Figure 84. Microscopic photos side #2, magnification 20x.



Figure 85. Microscopic photos side #2, magnification 50x.

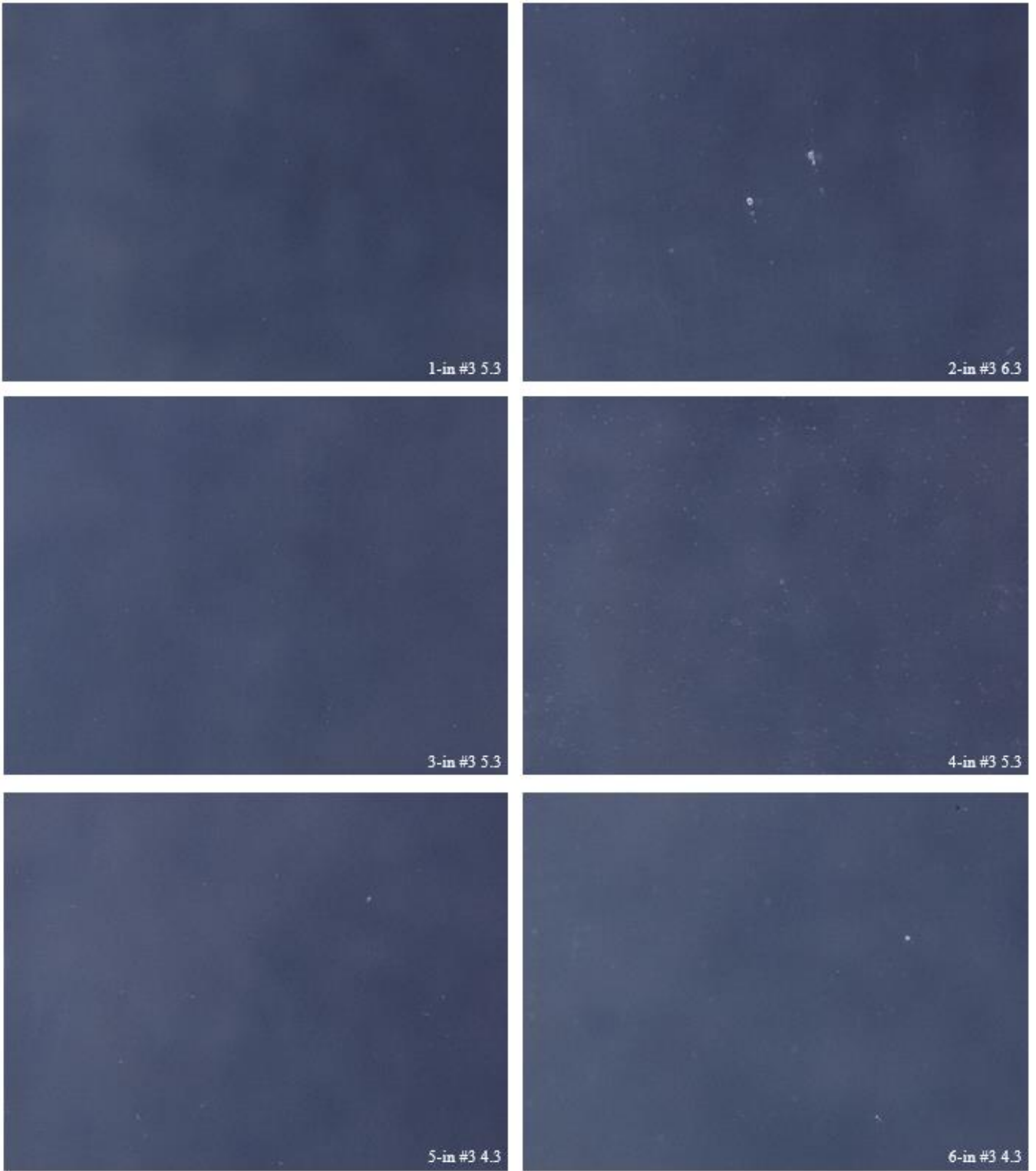


Figure 86. Microscopic photos side #3, magnification 20x.

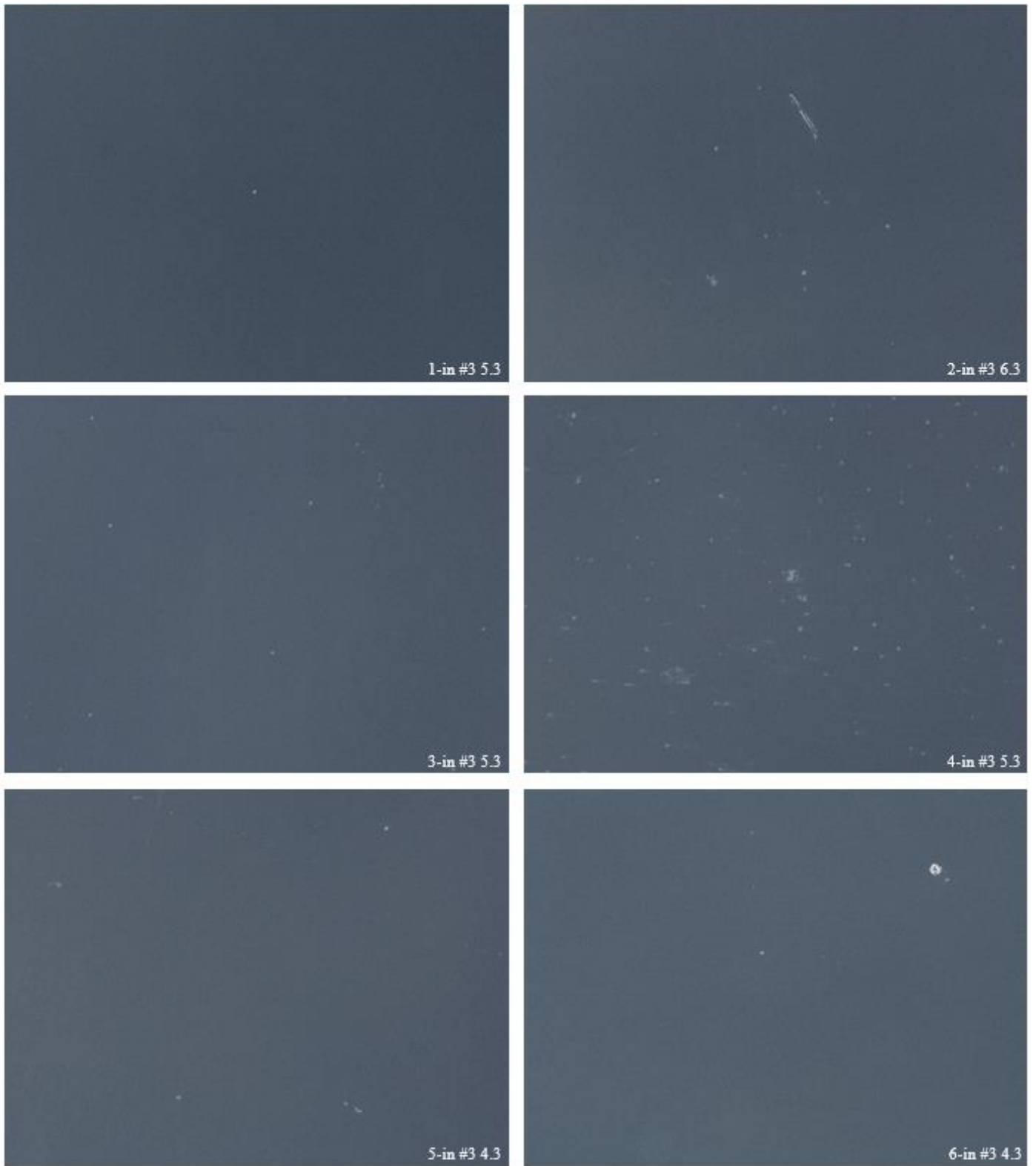


Figure 87. Microscopic photos side #3, magnification 50x.

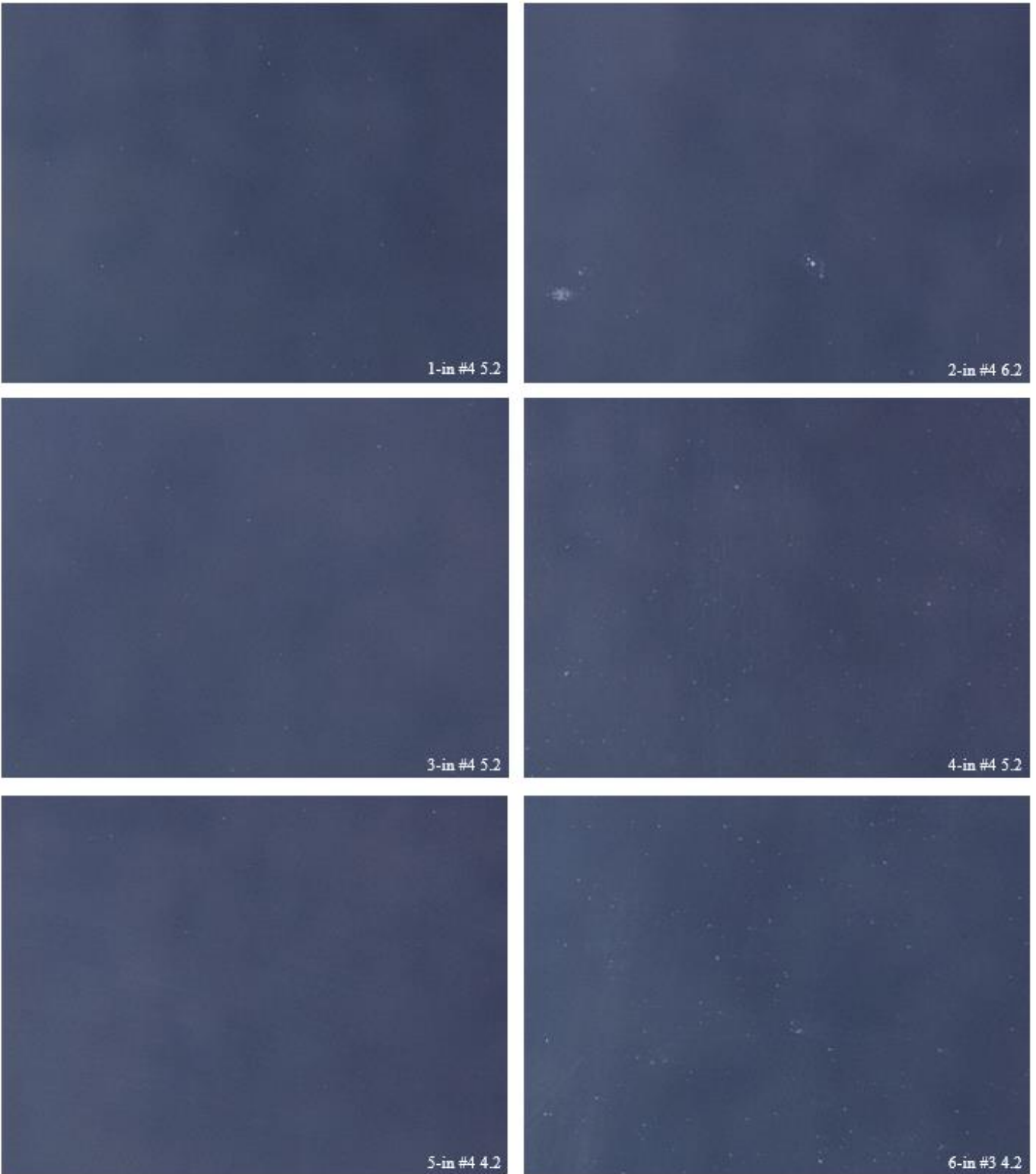


Figure 88. Microscopic photos side #4, magnification 20x.

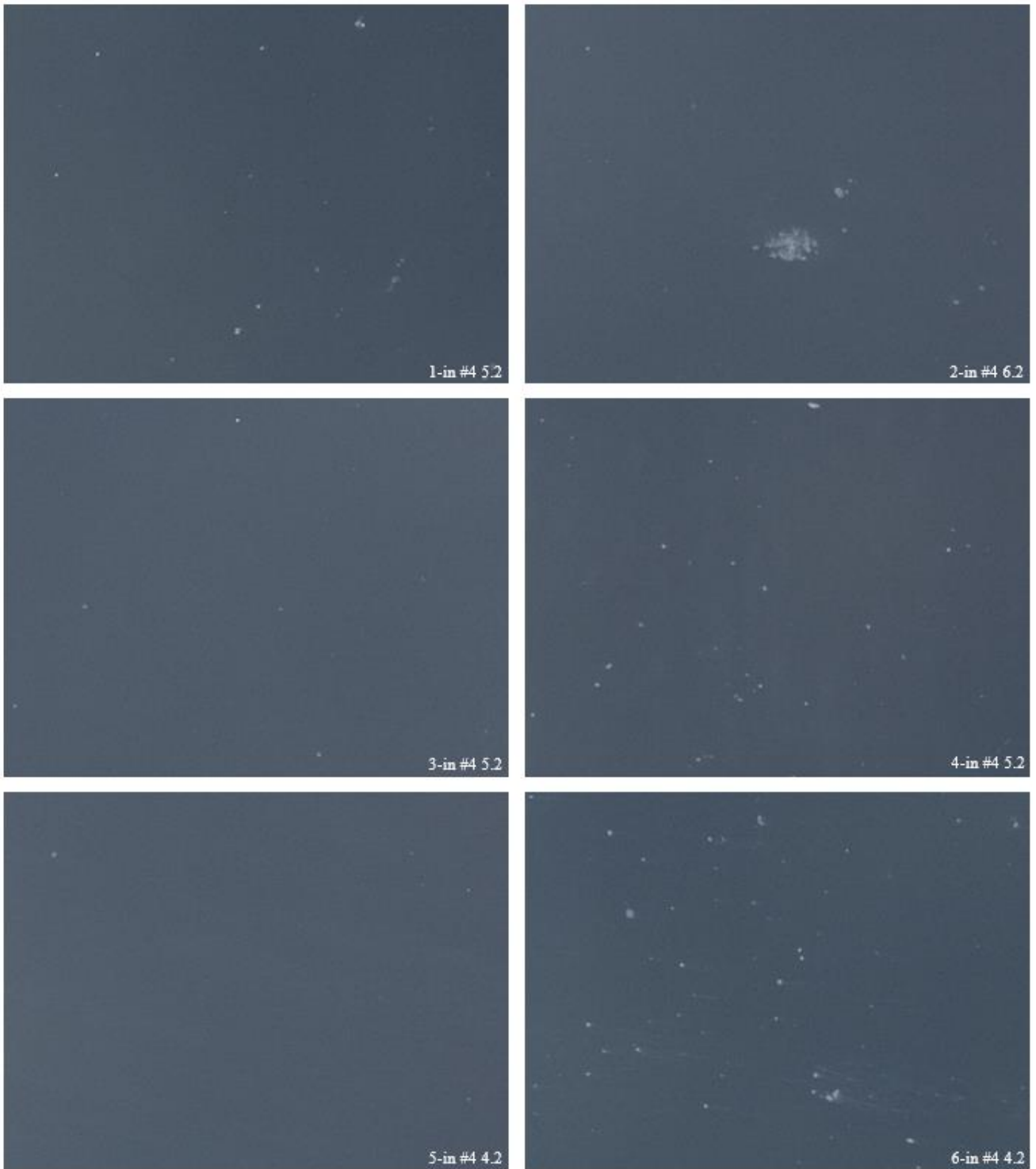


Figure 89. Microscopic photos side #4, magnification 50x.

Appendix D

Overview CDR test results

Table 32 to Table 37 show the results of the different IGUs distinguishing between the four sides. Shown here are:

- the maximum failure stress measured;
- the minimum failure stress measured;
- the mean failure stress value;
- the standard deviation;
- the mean time until a specimen failed.

Table 32. Characteristic values IGU 1.

IGU	1			
Series	#1	#2	#3	#4
$\sigma_{f,max}$ (MPa)	90.5	101.0	158.0	122.5
$\sigma_{f,min}$ (MPa)	43.0	32.4	37.4	38.5
$\sigma_{f,mean}$ (MPa)	65.2	52.1	93.3	64.7
Standard deviation	14.3	19.6	36.9	23.3
$t_{f,mean}$ (s)	9.6	7.9	8.4	6.3

Table 33. Characteristic values IGU 2.

IGU	2			
Series	#1	#2	#3	#4
$\sigma_{f,max}$ (MPa)	99.9	119.0	64.8	116.0
$\sigma_{f,min}$ (MPa)	44.7	61.3	30.3	43.4
$\sigma_{f,mean}$ (MPa)	66.0	83.6	48.1	71.7
Standard deviation	15.7	18.3	7.7	17.9
$t_{f,mean}$ (s)	5.4	6.4	3.5	4.8

Table 34. Characteristic values IGU 3.

IGU	3			
Series	#1	#2	#3	#4
$\sigma_{f,max}$ (MPa)	71.7	143.5	73.3	145.1
$\sigma_{f,min}$ (MPa)	42.3	55.2	32.7	54.5
$\sigma_{f,mean}$ (MPa)	58.3	98.4	49.7	80.3
Standard deviation	9.4	32.3	11.0	26.0
$t_{f,mean}$ (s)	5.0	7.5	3.5	5.2

Table 35. Characteristic values IGU 4.

IGU	4			
Series	#1	#2	#3	#4
$\sigma_{f,max}$ (MPa)	81.8	142.5	121.8	109.2
$\sigma_{f,min}$ (MPa)	43.6	55.6	35.9	32.1
$\sigma_{f,mean}$ (MPa)	61.2	80.8	76.6	61.1
Standard deviation	12.4	23.5	33.1	22.5
$t_{f,mean}$ (s)	6.5	7.8	5.1	4.3

Table 36. Characteristic values IGU 5.

IGU	5			
Series	#1	#2	#3	#4
$\sigma_{f,max}$ (MPa)	73.4	129.5	243.7	112.7
$\sigma_{f,min}$ (MPa)	35.0	23.8	64.3	22.2
$\sigma_{f,mean}$ (MPa)	54.5	63.6	133.8	60.4
Standard deviation	11.9	29.5	64.3	25.3
$t_{f,mean}$ (s)	5.8	6.6	7.5	4.5

Table 37. Characteristic values IGU 6.

IGU	6			
Series	#1	#2	#3	#4
$\sigma_{f,max}$ (MPa)	132.4	66.0	75.1	93.9
$\sigma_{f,min}$ (MPa)	20.5	16.8	40.4	31.8
$\sigma_{f,mean}$ (MPa)	66.0	51.5	53.6	54.1
Standard deviation	32.8	14.5	10.2	18.2
$t_{f,mean}$ (s)	6.8	5.8	8.8	8.7

Appendix E

Python script

Figure 90 shows the python script used to extract key information from the datasets obtained from the CDR tests. Values extracted from this were:

- the time to failure;
- the force required to achieve failure;
- the deflection of the specimen during failure;
- temperature;
- relative humidity.

```
%matplotlib inline
import numpy as np
import matplotlib.pyplot as plt
import pandas as pd
from IPython.display import display
df = pd.read_csv(r'C:\Users\nstuu\Documents\Master BE\Afstuderen Glass Reuse\Test results\All csv files\
                \Niels_2023-05-03_1-out #1 1.1.csv', delimiter=';')

w0=df.iloc[0,7] #displacement at t=0

df.drop(df[df['F'] <= (df.iloc[0,6])].index, inplace = True) #remove every value smaller dan 1st value
df.drop(df[df['F'] <= (df.iloc[1,6])].index, inplace = True) #remove every value smaller dan 2nd value
df.drop(df[df['F'] <= (df.iloc[2,6])].index, inplace = True) #remove every value smaller dan 3rd value

df.drop(df[df['F'] <= (df.iloc[0,6])+0.075].index, inplace = True)
#start timing when steps of load are 75 N
#display(df)

m_loadring = 0.9509 #kg
t = df.iloc[:,2]
F = df.iloc[:,6]
F_breakage = df.loc[df.F.idxmax()].F*1000
w_breakage = df.loc[df.F.idxmax()].S
t_end = df.loc[df.F.idxmax()].Time
t_start = df.iloc[0,1]
t_breakage = (t_end-t_start).round(2)
print('Time it takes for sample to break =',t_breakage,'seconds')
print('Load at breakage =',(F_breakage+m_loadring*9.81).round(2),'N')
print('Displacement at breakage =',(w_breakage-w0).round(4),'mm')
print('Temperature during test =',df.iloc[0,7], '°C')
print('Relative humidity during test =',df.iloc[0,8], '%')
plt.plot(t,F)
plt.ylabel('Force in kN')
plt.xlabel('time in seconds');
```

Figure 90. Python script to extract information from Excel data.

Appendix F

Additional Weibull plots

Figure 91 to Figure 101 show some additional Weibull plots. These include the Weibull distributions of the individual IGUs where the four sides are compared, and two Weibull plots where edge- and mid-specimens are compared in combination with being an air- or tin-side. Values for characteristic points and number of tests are also indicated here. Also, the plots with new versus old glass are presented here, where the difference between the BMW and the 2PW can be seen.

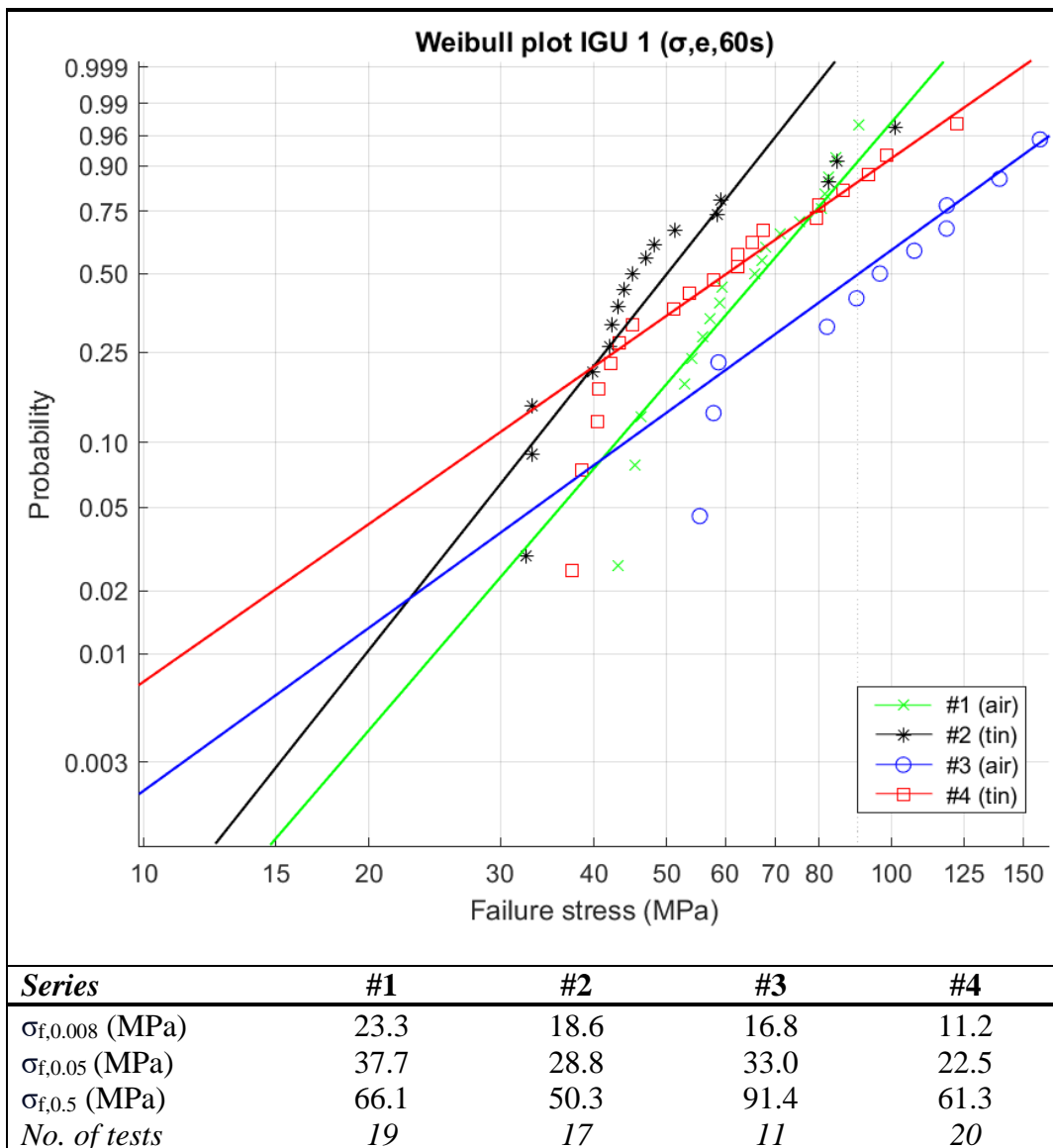


Figure 91. Weibull probability distribution: All sides IGU 1.

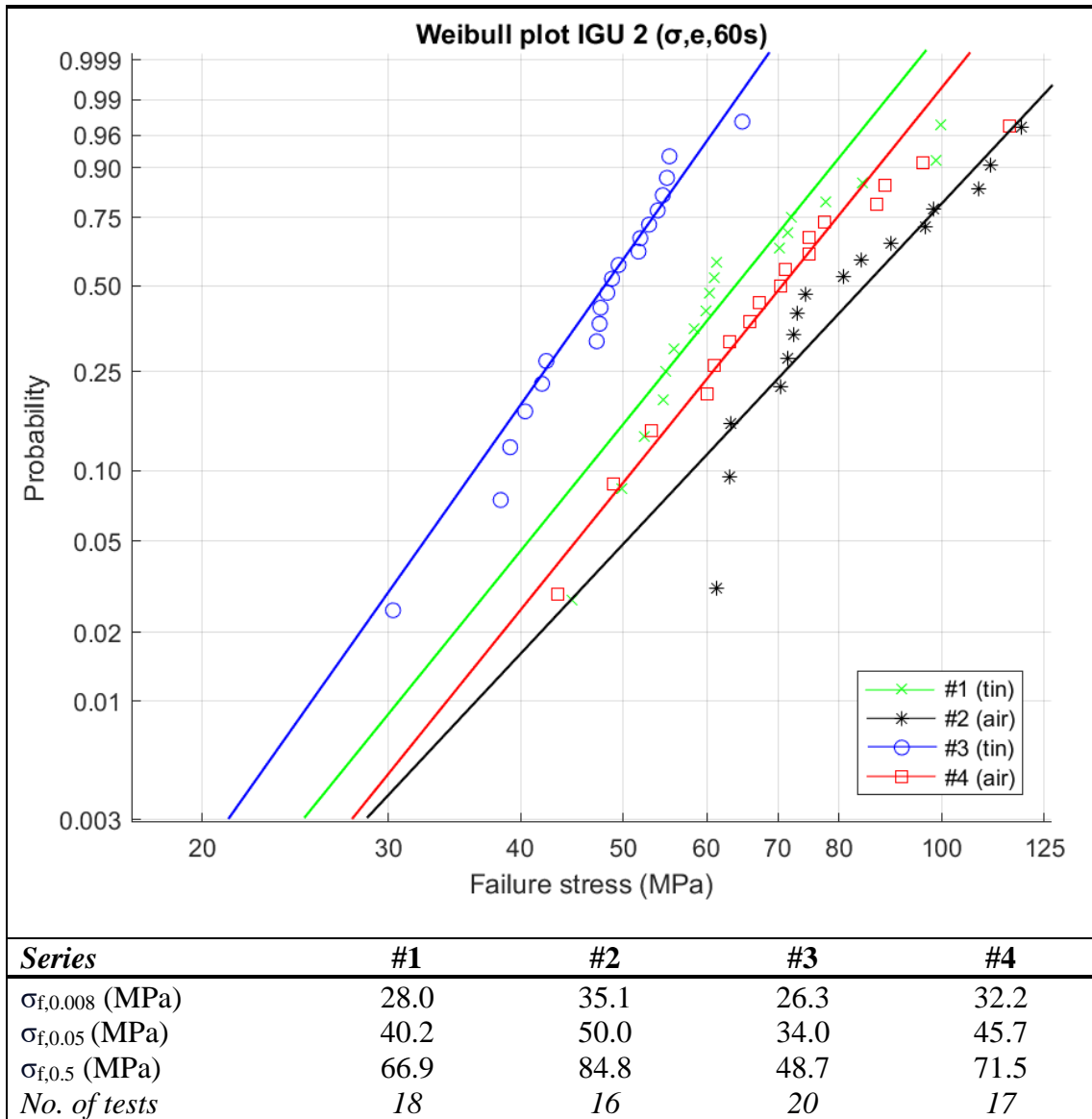


Figure 92. Weibull probability distribution: All sides IGU 2.

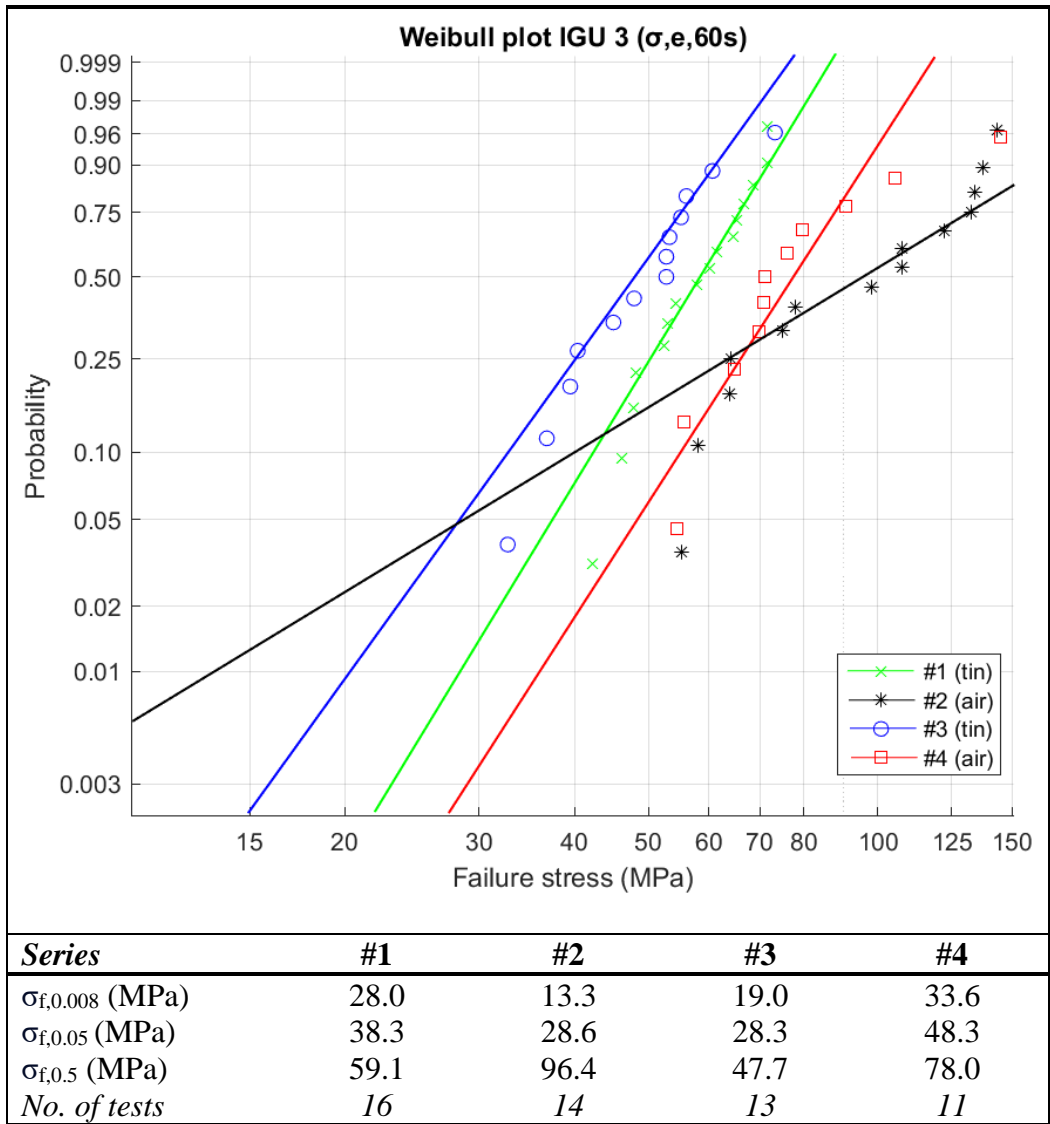


Figure 93. Weibull probability distribution: All sides IGU 3.

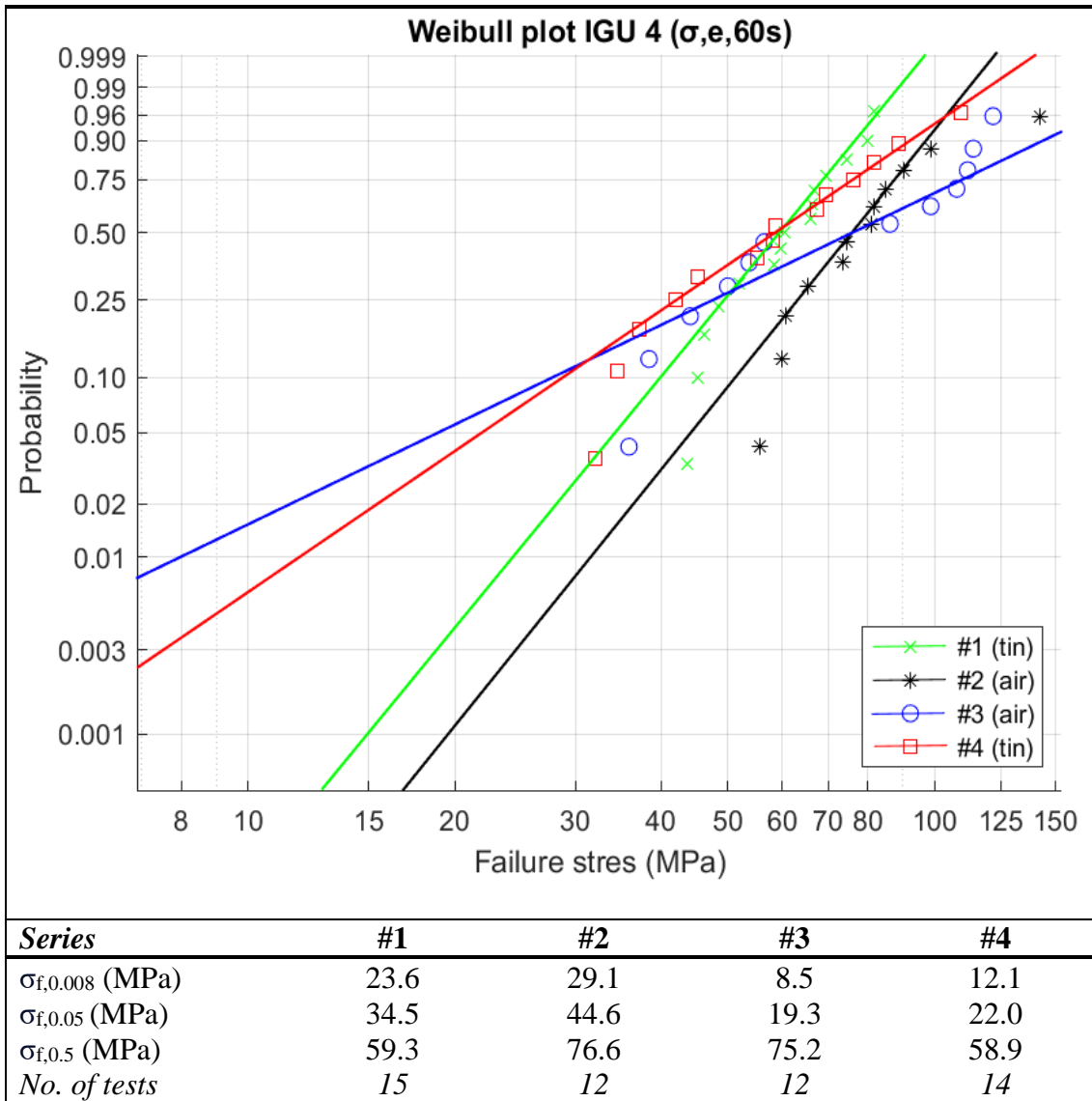


Figure 94. Weibull probability distribution: All sides IGU 4.

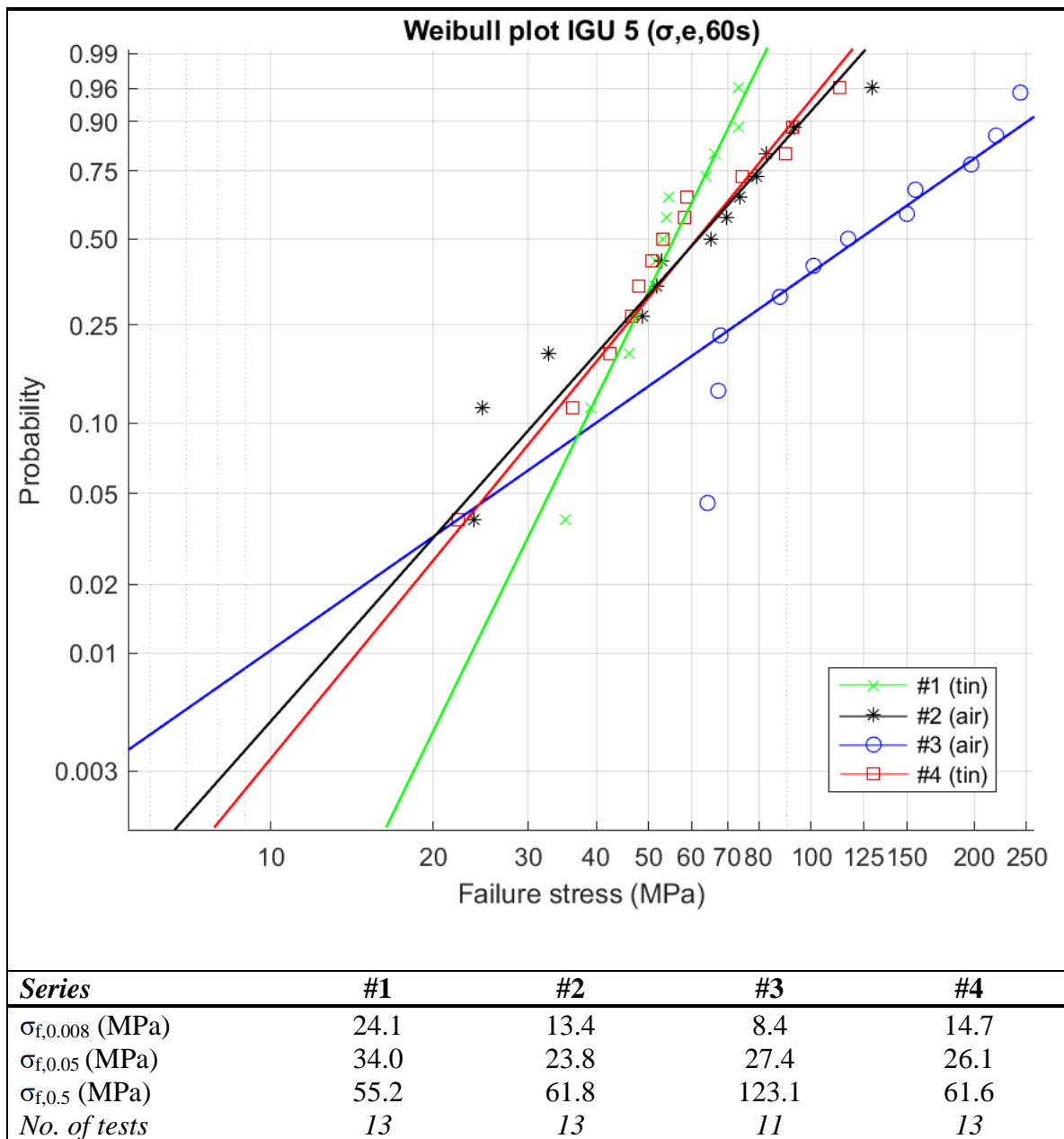


Figure 95. Weibull probability distribution: All sides IGU 5.

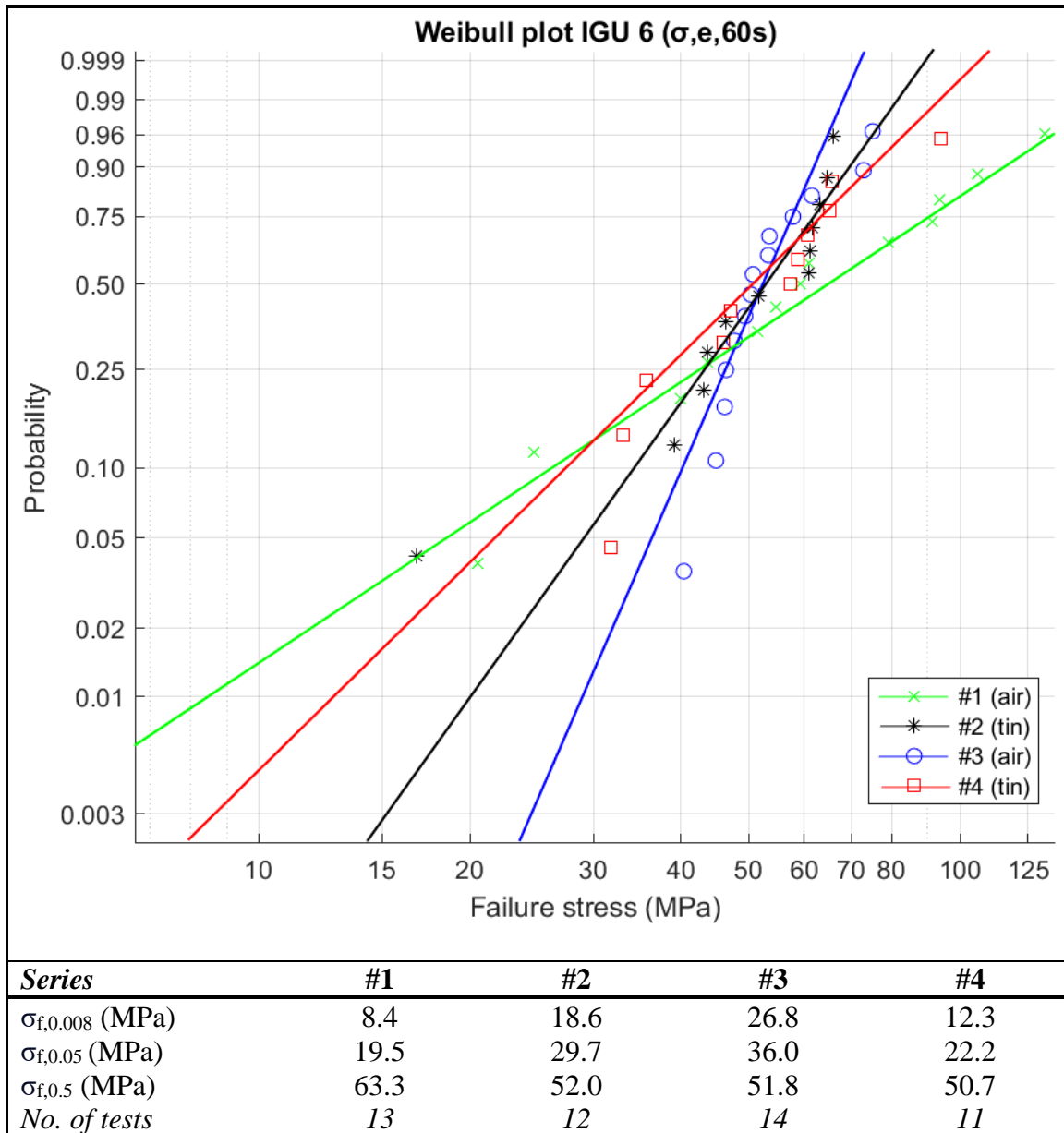


Figure 96. Weibull probability distribution: All sides IGU 6.

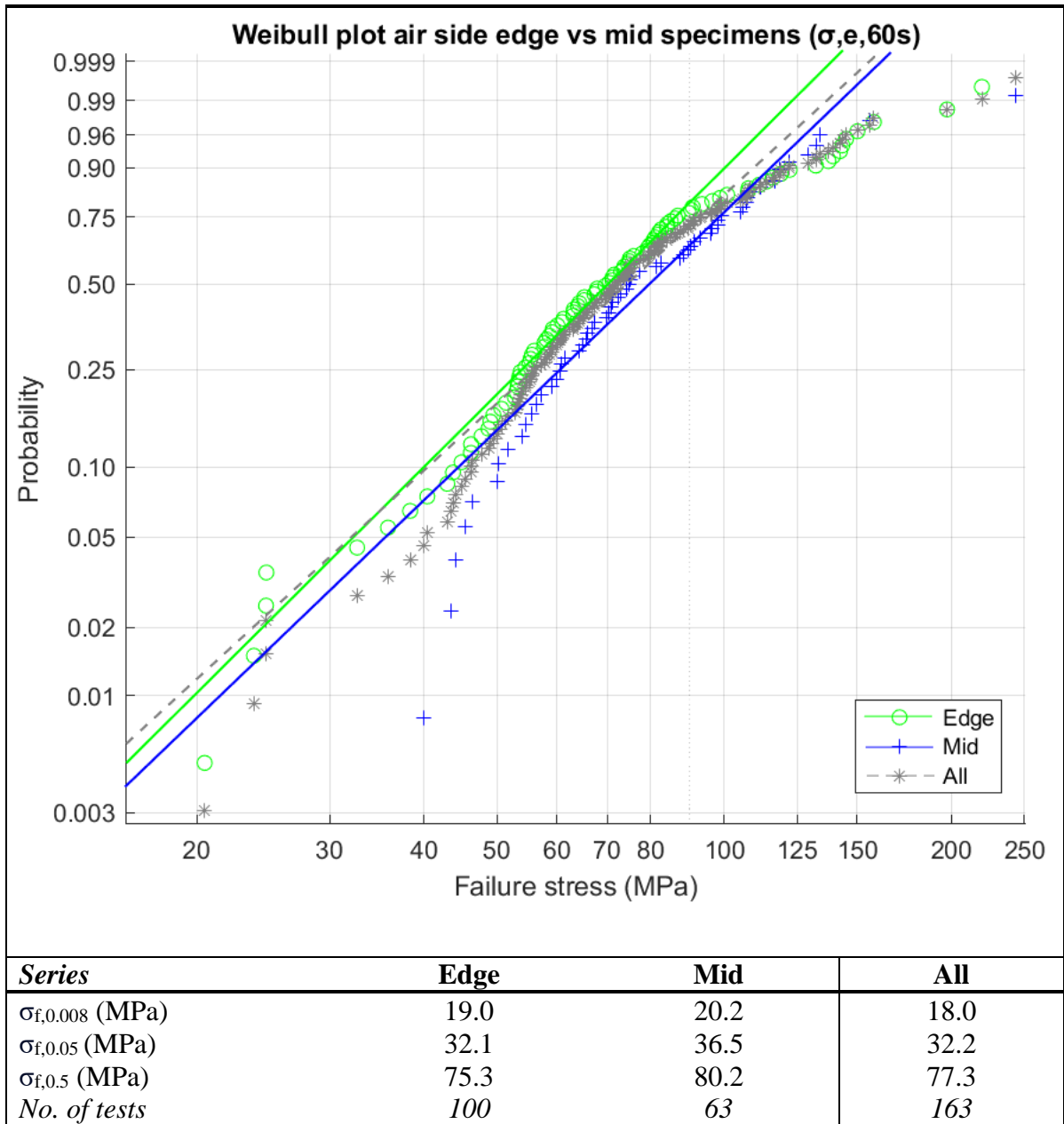
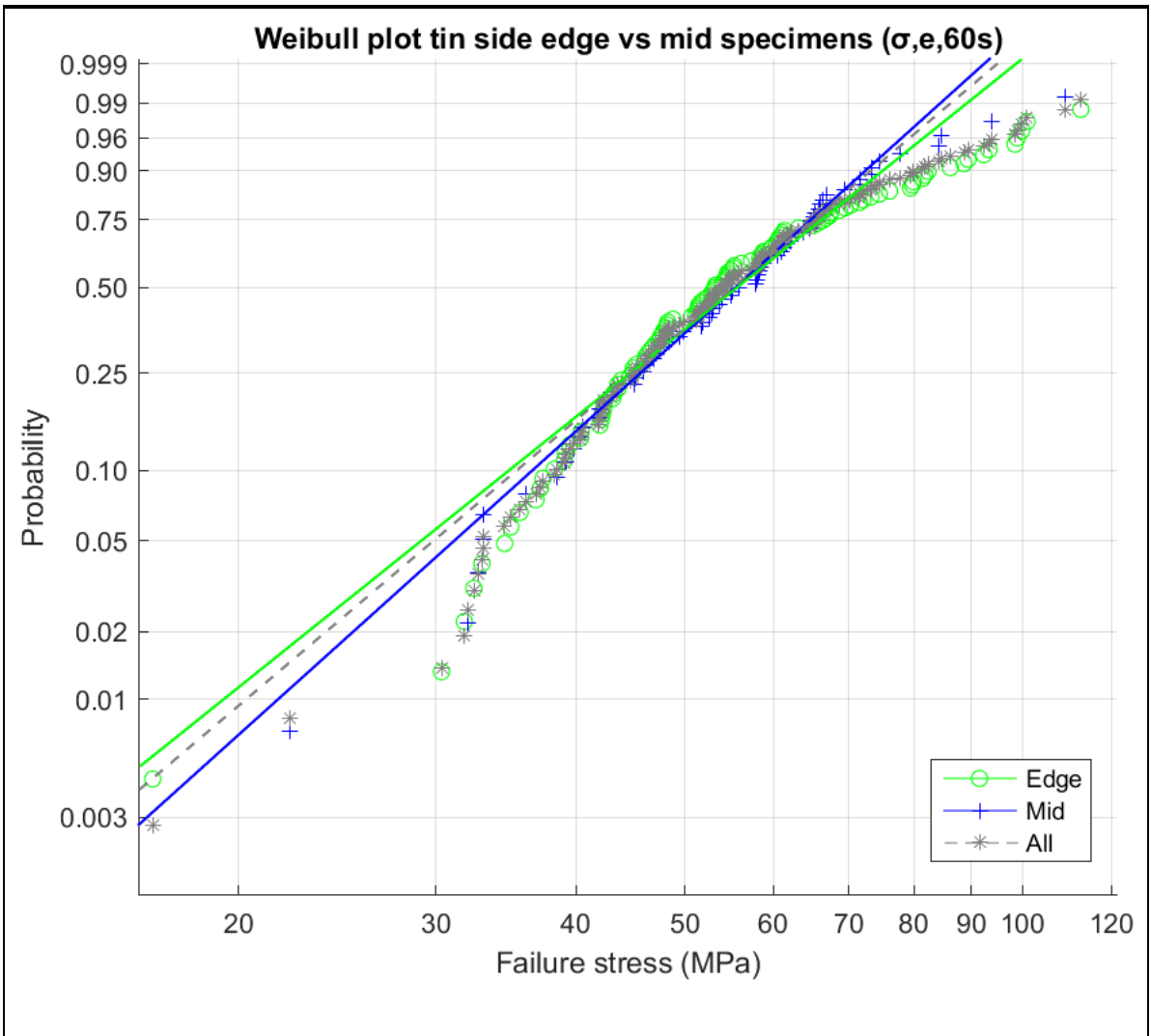


Figure 97. Weibull probability distribution: Edge- vs mid-specimens air-side.



<i>Series</i>	Edge	Mid	All
$\sigma_{f,0.008}$ (MPa)	18.3	21.1	19.5
$\sigma_{f,0.05}$ (MPa)	29.5	31.8	30.5
$\sigma_{f,0.5}$ (MPa)	57.6	56.7	57.3
<i>No. of tests</i>	113	69	182

Figure 98. Weibull probability distribution: Edge- vs mid-specimens tin-side.

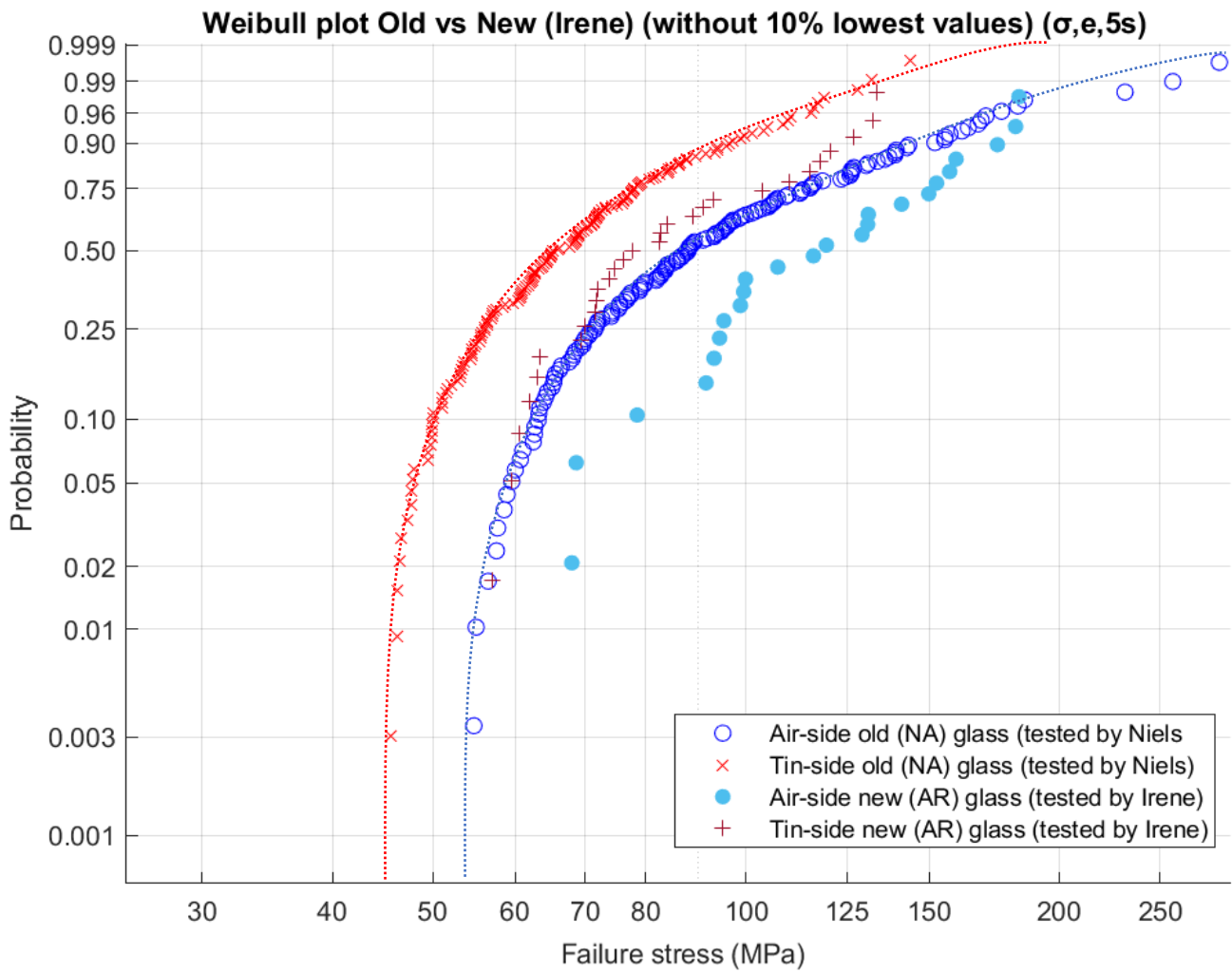


Figure 99. Weibull probability distribution: Old vs New (Irene) glass (5 sec) – Bimodal flow.

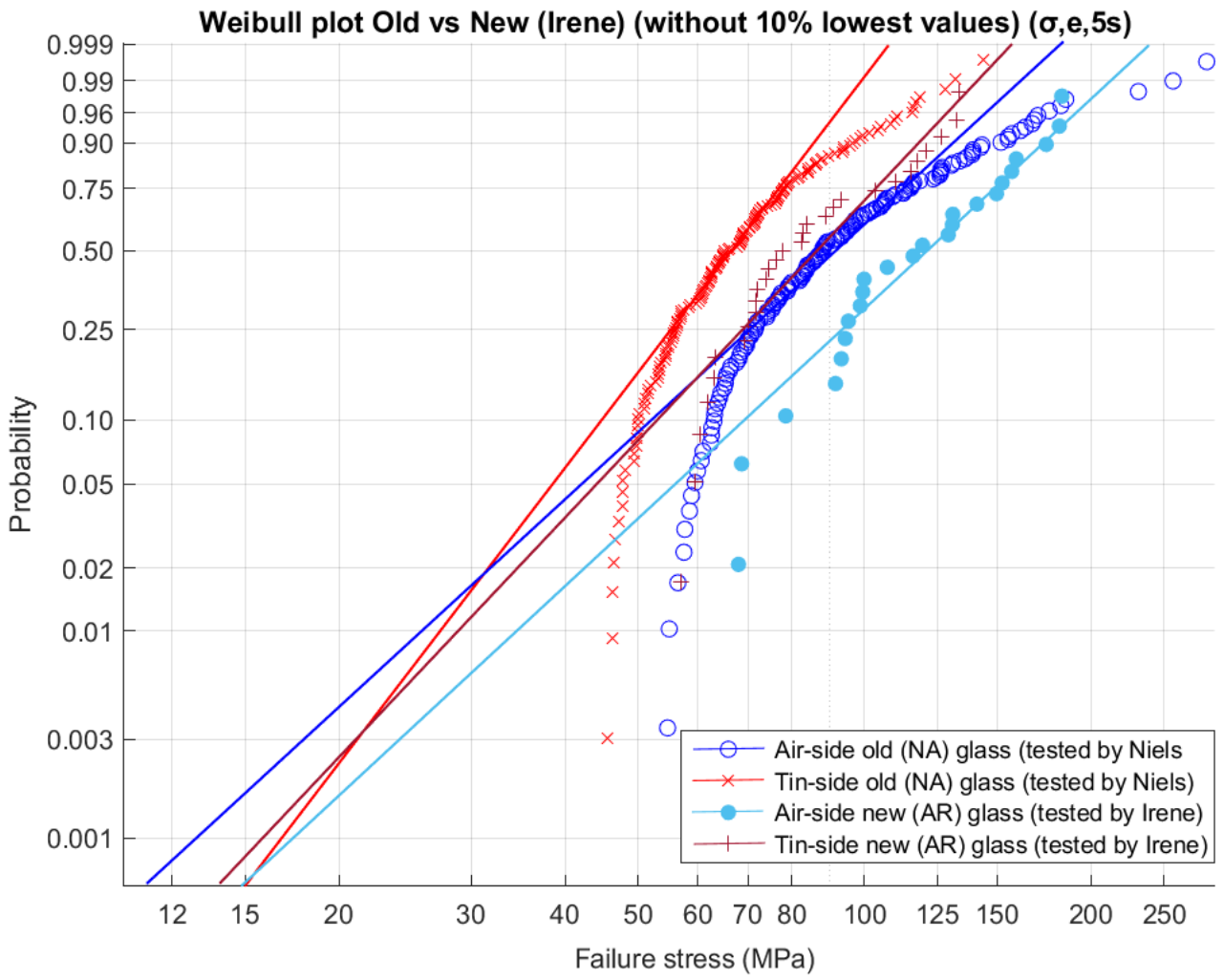


Figure 100. Weibull probability distribution: Old vs New (Irene) glass (5 sec) – 2PW.

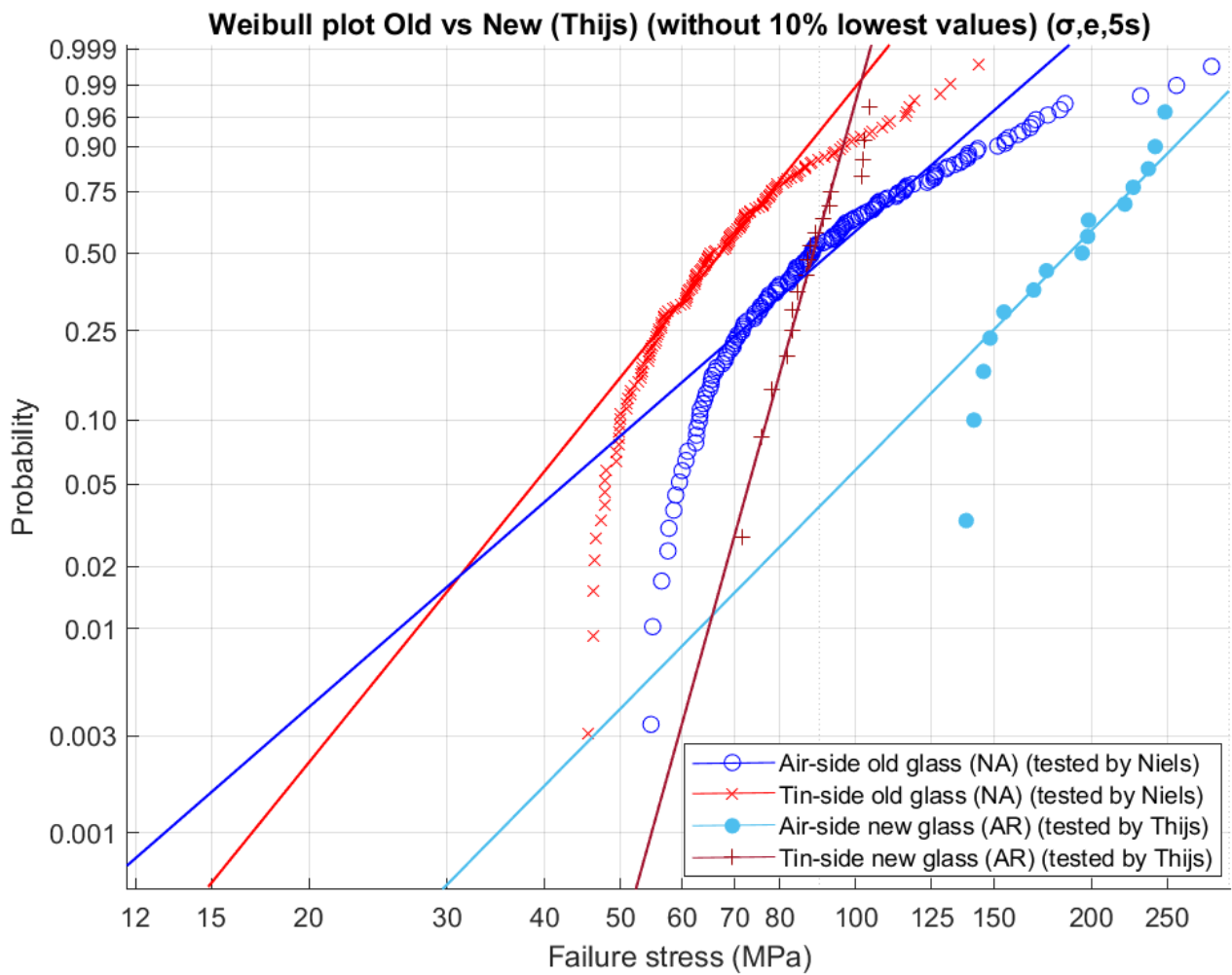


Figure 101. Weibull probability distribution: Old vs New (Thijs) glass (5 sec) – 2PW.

Appendix G

All CDR test results

In Table 38, the results of the CDR tests on weathered glass are reported. The data for each specimen which are included in the table are:

- the load at breakage F_{breakage} in N;
- the displacement at breakage in mm;
- the failure stress σ_f in MPa;
- the time to failure in seconds;
- the normalised failure stress $\sigma_{e,60s}$ for a reference period of 60 seconds;
- the location of the fracture origin in relation to the loading ring, IR (inside), LR (on), OR (outside) or ND (not detectable).

Table 38. All test results.

<i>Specimen</i>	F_{breakage} (N)	δ_{failure} (mm)	σ_f (MPa)	t_{failure} (s)	$\sigma_{f,\text{eq}}$ (MPa)	<i>Origin</i>
1-out #1 1.1	14077.25	0.51	113.5	10.10	80.6	IR
1-out #1 2.1	12468.99	0.55	100.3	11.03	71.1	IR
1-out #1 3.1	12007.20	0.41	96.4	10.03	67.8	IR
1-out #1 4.1	14663.80	0.48	117.5	11.08	84.1	IR
1-out #1 5.1	15684.12	0.59	125.3	11.92	90.5	IR
1-out #1 6.1	14428.30	0.63	114.8	12.02	82.5	LR
1-out #1 7.1	10758.02	0.39	85.2	9.82	59.3	IR
1-out #1 8.1	9857.11	0.38	77.6	7.79	52.8	IR
1-out #1 9.1	8791.67	0.33	68.9	7.35	46.2	LR
1-out #1 10.1	8201.45	0.44	64.2	7.88	43.0	IR
1-out #2 1.2	7890.57	0.28	63.5	6.82	42.0	LR
1-out #2 2.2	10592.63	0.49	85.2	9.22	59.1	LR
1-out #2 3.2	10483.32	0.46	84.3	9.10	58.4	LR
1-out #2 4.2	6432.58	0.36	51.6	6.08	33.1	IR
1-out #2 5.2	14808.45	0.54	118.4	10.60	84.6	LR
1-out #2 6.2	10414.80	0.50	82.9	10.11	57.7	OR
1-out #2 7.2	8165.79	0.48	64.5	7.40	43.0	IR
1-out #2 8.2	8953.41	0.31	70.4	6.42	46.9	IR
1-out #2 9.2	7749.55	0.33	60.5	6.65	39.8	LR
1-out #2 10.2	9180.14	0.29	71.6	7.16	48.1	IR
1-out #1 1.3	10130.56	0.52	81.0	9.32	56.0	IR
1-out #1 2.3	8421.30	0.42	67.4	7.94	45.3	IR
1-out #1 3.3	14232.66	0.59	113.9	11.01	81.4	IR
1-out #1 4.3	11899.61	0.46	95.1	10.36	67.0	IR
1-out #1 5.3	13391.88	0.52	106.7	9.90	75.4	IR
1-out #1 6.3	10747.49	0.41	85.2	9.12	59.0	LR
1-out #1 7.3	11865.36	0.53	93.5	10.22	65.7	IR
1-out #1 8.3	10633.99	0.42	83.3	8.21	57.2	LR
1-out #1 9.3	10138.32	0.44	79.2	7.91	54.0	IR
1-out #1 10.3	11681.15	0.51	91.0	9.28	63.4	OR
1-out #2 1.4	6368.86	0.30	51.1	6.86	33.0	IR
1-out #2 2.4	8914.71	0.36	71.5	7.26	48.1	OR
1-out #2 3.4	7915.83	0.37	63.3	7.62	42.2	IR
1-out #2 4.4	6384.54	0.27	50.9	5.67	32.4	IR
1-out #2 5.4	14553.79	0.54	115.9	9.94	82.4	LR
1-out #2 6.4	8434.67	0.40	66.9	7.96	45.0	IR
1-out #2 7.4	17636.64	0.62	139.0	12.06	101.0	LR
1-out #2 8.4	8425.21	0.48	66.0	7.00	43.9	IR
1-out #2 9.4	9477.45	0.41	74.1	8.25	50.4	OR
1-out #2 10.4	9696.15	0.42	75.6	7.95	51.4	IR
1-in #3 1.1	6155.62	0.58	85.7	6.20	58.7	IR
1-in #3 2.1	16106.46	1.13	224.5	12.25	166.7	ND
1-in #3 3.1	13551.68	0.88	189.5	11.37	139.5	IR
1-in #3 4.1	16686.30	1.13	234.2	13.88	175.4	ND
1-in #3 5.1	9562.23	0.59	134.5	9.00	96.5	LR
1-in #3 6.1	8806.30	0.60	124.2	8.50	88.5	OR
1-in #3 7.1	8233.17	0.53	116.5	7.36	82.0	IR
1-in #3 8.1	8938.11	0.65	126.7	7.70	89.8	LR
1-in #3 9.1	6719.08	0.53	95.4	7.18	66.3	OR
1-in #3 10.1	5680.54	0.39	80.8	6.74	55.4	IR
1-in #4 1.2	4817.41	0.44	67.1	5.64	45.0	IR
1-in #4 2.2	6516.98	0.48	90.8	5.70	62.2	IR

Specimen	F_{breakage} (N)	δ_{failure} (mm)	σ_f (MPa)	t_{failure} (s)	σ_{f,eq} (MPa)	Origin
1-in #4 3.2	4404.46	0.26	61.6	4.44	40.4	IR
1-in #4 4.2	6069.64	0.48	85.3	5.16	57.8	IR
1-in #4 5.2	6442.52	0.38	90.6	5.92	62.2	LR
1-in #4 6.2	5627.14	0.37	79.5	5.16	53.6	LR
1-in #4 7.2	4179.65	0.31	59.1	4.30	38.5	LR
1-in #4 8.2	4382.78	0.26	62.1	4.22	40.6	IR
1-in #4 9.2	11443.37	0.81	162.0	9.88	117.7	OR
1-in #4 10.2	8533.23	0.56	121.3	8.22	86.2	IR
1-in #3 1.3	15373.36	0.91	213.9	11.52	158.0	LR
1-in #3 2.3	13859.85	0.82	193.4	11.62	142.6	OR
1-in #3 3.3	15531.70	1.09	217.2	12.76	161.6	ND
1-in #3 4.3	11572.11	0.71	162.3	10.90	118.6	LR
1-in #4 5.3	4026.64	0.22	56.7	5.50	37.4	IR
1-in #3 6.3	11612.02	0.79	164.2	8.92	118.5	IR
1-in #3 7.3	13836.42	0.88	196.0	11.74	144.7	ND
1-in #3 8.3	12337.19	0.88	174.8	11.24	128.3	OR
1-in #3 9.3	10427.69	0.82	148.2	9.77	107.3	IR
1-in #3 10.3	5939.94	0.38	84.3	6.30	57.8	IR
1-in #4 1.4	9850.09	0.65	137.3	8.70	98.5	LR
1-in #4 2.4	9443.56	0.66	131.5	7.61	93.3	IR
1-in #4 3.4	4520.58	0.40	63.2	5.54	42.1	IR
1-in #4 4.4	8074.92	0.62	113.4	6.82	79.4	IR
1-in #4 5.4	6890.87	0.52	97.0	6.73	67.3	IR
1-in #4 6.4	11907.60	0.74	168.1	10.14	122.5	LR
1-in #4 7.4	4553.34	0.50	64.4	6.02	43.2	IR
1-in #4 8.4	5320.70	0.45	75.4	5.84	51.1	IR
1-in #4 9.4	8020.50	0.59	113.7	7.16	79.9	LR
1-in #4 10.4	6598.31	0.52	93.8	6.82	65.1	IR
2-out #1 1.1	4104.25	0.49	86.5	6.07	59.6	OR
2-out #1 2.1	3723.23	0.46	78.0	4.46	52.4	IR
2-out #1 3.1	6653.24	0.75	139.7	6.76	98.9	IR
2-out #1 4.1	3209.89	0.40	67.3	4.36	44.7	IR
2-out #1 5.1	4842.44	0.64	101.8	5.46	70.2	IR
2-out #1 6.1	4898.79	0.65	103.3	5.70	71.5	LR
2-out #1 7.1	6693.68	0.82	140.4	7.20	99.9	LR
2-out #1 8.1	3828.36	0.57	80.4	5.02	54.5	IR
2-out #1 9.1	4224.85	0.54	88.6	4.98	60.4	LR
2-out #1 10.1	4091.45	0.64	86.1	4.74	58.3	IR
2-out #2 1.2	4969.36	0.68	104.6	5.63	73.0	IR
2-out #2 2.2	6569.33	0.87	137.3	7.26	98.2	IR
2-out #2 3.2	4942.94	0.64	103.5	5.78	72.4	IR
2-out #2 4.2	6019.14	0.77	126.0	6.79	89.6	IR
2-out #2 5.2	7193.34	0.87	150.8	7.38	108.3	IR
2-out #2 6.2	5052.30	0.71	106.0	6.00	74.4	LR
2-out #2 7.2	8652.96	0.97	182.1	8.68	132.7	OR
2-out #2 8.2	6756.80	0.84	141.6	7.72	101.8	OR
2-out #2 9.2	6457.33	0.89	135.2	6.90	96.4	LR
2-out #2 10.2	4219.62	0.65	88.4	5.54	61.3	IR
2-out #1 1.3	4189.87	0.57	87.8	5.09	59.8	LR
2-out #1 2.3	4554.87	0.65	95.4	5.46	65.6	OR
2-out #1 3.3	3538.21	0.64	74.2	4.72	49.8	IR
2-out #1 4.3	5345.19	0.70	111.8	5.80	77.7	IR
2-out #1 5.3	5727.19	0.74	119.8	6.48	84.1	IR

<i>Specimen</i>	F_{breakage} (N)	δ_{failure} (mm)	σ_f (MPa)	t_{failure} (s)	$\sigma_{f,\text{eq}}$ (MPa)	<i>Origin</i>
2-out #1 6.3	3937.85	0.61	82.4	5.08	55.9	IR
2-out #1 7.3	4294.51	0.62	89.9	5.02	61.3	IR
2-out #1 8.3	4266.63	0.61	89.1	5.32	61.0	IR
2-out #1 9.3	3900.85	0.54	81.5	4.58	54.9	IR
2-out #1 10.3	4989.40	0.65	104.4	5.46	72.1	IR
2-out #2 1.4	4903.62	0.67	102.6	5.54	71.5	IR
2-out #2 2.4	7678.83	0.89	160.4	7.90	115.9	OR
2-out #2 3.4	8716.64	1.10	182.1	9.26	133.2	OR
2-out #2 4.4	7845.34	1.03	163.9	8.46	119.0	IR
2-out #2 5.4	7361.34	1.00	154.1	8.03	111.3	IR
2-out #2 6.4	5441.81	0.69	113.9	6.66	80.7	IR
2-out #2 7.4	5657.52	0.72	118.3	6.82	84.0	IR
2-out #2 8.4	4384.74	0.56	91.6	4.94	63.1	LR
2-out #2 9.4	4849.07	0.60	101.3	5.42	70.5	IR
2-out #2 10.4	4353.95	0.65	91.1	5.53	63.2	IR
2-in #3 1.1	1830.02	0.42	59.1	3.42	38.3	IR
2-in #3 2.1	2467.64	0.56	80.1	3.33	52.9	IR
2-in #3 3.1	1920.35	0.49	62.2	3.36	40.4	IR
2-in #3 4.1	2236.57	0.53	73.0	2.89	47.5	LR
2-in #3 5.1	2228.62	0.59	72.6	3.22	47.6	IR
2-in #3 6.1	1479.50	0.42	48.4	2.84	30.3	IR
2-in #3 7.1	1888.34	0.47	61.8	2.33	39.1	LR
2-in #3 8.1	2537.65	0.59	82.8	3.88	55.3	IR
2-in #3 9.1	2487.46	0.59	81.4	4.04	54.5	IR
2-in #3 10.1	2252.46	0.73	73.3	4.15	48.8	IR
2-in #4 1.2	3077.55	0.69	101.3	4.22	69.2	OR
2-in #4 2.2	4170.50	0.92	136.3	5.88	96.1	IR
2-in #4 3.2	3394.35	0.79	111.4	5.23	77.4	LR
2-in #4 4.2	3856.96	0.90	126.4	5.46	88.5	LR
2-in #4 5.2	3105.09	0.73	102.0	4.94	70.4	IR
2-in #4 6.2	2985.14	0.74	98.2	4.56	67.3	IR
2-in #4 7.2	2889.82	0.70	95.3	5.32	65.9	IR
2-in #4 8.2	3296.65	0.72	108.7	4.66	74.9	LR
2-in #4 9.2	2013.25	0.50	66.1	3.14	43.4	LR
2-in #4 10.2	2702.23	0.77	88.5	4.24	60.1	IR
2-in #3 1.3	2490.46	0.58	82.3	3.88	55.0	IR
2-in #3 2.3	2916.07	0.64	96.3	3.82	64.8	LR
2-in #3 3.3	2362.68	0.61	78.0	3.84	51.9	IR
2-in #3 4.3	2360.73	0.57	78.0	3.68	51.7	IR
2-in #3 5.3	2274.39	0.55	75.0	3.50	49.5	LR
2-in #3 6.3	2439.49	0.64	80.7	4.02	53.9	IR
2-in #3 7.3	1984.39	0.51	65.6	2.80	42.3	IR
2-in #3 8.3	2156.26	0.73	71.4	3.76	47.2	IR
2-in #3 9.3	1953.41	0.48	64.4	3.30	41.9	IR
2-in #3 10.3	2227.74	0.64	73.5	3.38	48.3	LR
2-in #4 1.4	2733.20	0.61	90.0	4.04	61.0	IR
2-in #4 2.4	4938.55	1.06	163.1	6.30	116.0	IR
2-in #4 3.4	3767.99	0.86	124.3	5.38	86.9	IR
2-in #4 4.4	2406.50	0.61	79.4	3.78	53.2	IR
2-in #4 5.4	3111.87	0.73	102.6	5.28	71.2	IR
2-in #4 6.4	4123.73	0.90	135.8	6.04	95.9	OR
2-in #4 7.4	3294.42	0.70	108.8	4.60	74.9	LR
2-in #4 8.4	2805.87	0.67	92.5	4.38	63.1	IR

Specimen	F_{breakage} (N)	δ_{failure} (mm)	σ_f (MPa)	t_{failure} (s)	σ_{f,eq} (MPa)	Origin
2-in #4 9.4	2255.94	0.49	74.3	3.36	49.3	OR
2-in #4 10.4	2249.55	0.55	73.7	3.51	49.0	IR
3-out #1 1.1	3170.05	0.38	64.2	4.14	42.3	IR
3-out #1 2.1	3965.92	0.56	80.6	4.54	54.3	IR
3-out #1 3.1	4789.97	0.65	97.3	4.98	66.6	OR
3-out #1 4.1	4594.13	0.69	93.4	5.40	64.2	OR
3-out #1 5.1	4902.64	0.61	99.6	5.39	68.6	IR
3-out #1 6.1	4345.36	0.65	88.3	5.24	60.3	LR
3-out #1 7.1	3546.68	0.56	72.1	4.56	48.2	IR
3-out #1 8.1	4390.53	0.72	89.2	5.74	61.4	IR
3-out #1 9.1	3409.88	0.42	69.4	4.24	46.1	IR
3-out #2 1.2	7351.08	0.80	150.9	7.40	107.6	IR
3-out #2 2.2	10972.84	1.30	225.3	10.96	166.3	OR
3-out #2 3.2	8898.00	1.03	182.1	9.37	132.5	LR
3-out #2 4.2	7303.85	0.96	149.9	8.30	107.6	IR
3-out #2 5.2	6748.63	0.83	138.3	7.42	98.3	IR
3-out #2 6.2	8976.69	1.05	184.3	9.18	133.9	IR
3-out #2 7.2	11388.52	1.25	234.0	10.86	172.8	OR
3-out #2 8.2	4532.03	0.68	92.9	6.20	64.2	LR
3-out #2 9.2	4556.06	0.69	93.2	5.64	64.0	IR
3-out #1 1.3	4681.16	0.65	96.9	5.62	66.8	LR
3-out #1 2.3	4967.56	0.74	102.9	6.16	71.6	IR
3-out #1 3.3	3801.29	0.55	78.6	4.78	53.0	LR
3-out #1 4.3	4531.65	0.65	93.9	5.52	64.6	IR
3-out #1 5.3	4112.89	0.67	85.2	4.98	57.9	IR
3-out #1 6.3	3758.86	0.53	77.9	4.78	52.5	IR
3-out #1 7.3	5003.52	0.81	103.6	5.66	71.7	IR
3-out #1 8.3	4629.84	0.57	95.7	4.75	65.3	LR
3-out #1 9.3	3474.38	0.47	71.6	4.36	47.8	IR
3-out #2 1.4	4124.53	0.55	85.6	5.14	58.2	IR
3-out #2 2.4	9097.88	1.08	189.3	9.06	137.6	IR
3-out #2 3.4	10878.11	1.18	226.3	10.86	167.0	OR
3-out #2 4.4	8617.95	1.01	179.3	9.12	130.2	OR
3-out #2 5.4	8102.08	0.99	168.6	9.12	122.2	LR
3-out #2 6.4	9444.69	1.07	196.3	9.84	143.5	IR
3-out #2 7.4	5363.46	0.72	111.5	6.60	78.0	IR
3-out #2 8.4	5164.74	0.75	107.4	6.62	75.0	IR
3-out #2 9.4	3930.08	0.55	81.7	4.96	55.2	IR
3-in #3 1.1	3168.69	0.75	106.0	5.12	73.3	IR
3-in #3 2.1	1817.07	0.55	60.8	3.16	39.5	IR
3-in #3 3.1	2175.65	0.56	72.8	3.18	47.9	IR
3-in #3 4.1	2664.10	0.65	88.9	4.14	60.1	OR
3-in #3 5.1	1728.66	0.41	57.8	2.55	36.8	IR
3-in #3 6.1	1885.62	0.51	62.8	2.64	40.4	IR
3-in #3 7.1	2530.86	0.60	84.0	3.60	56.1	LR
3-in #3 8.1	2393.78	0.69	78.8	3.94	52.8	IR
3-in #4 1.2	2426.09	0.65	81.3	3.72	54.5	IR
3-in #4 2.2	2840.06	0.73	95.2	4.34	64.9	IR
3-in #4 3.2	3024.21	0.76	101.2	4.92	69.8	LR
3-in #4 4.2	3083.02	0.75	102.9	4.67	70.8	IR
3-in #4 5.2	2464.81	0.73	82.2	4.21	55.6	IR
3-in #4 6.2	4451.40	1.02	148.2	6.42	105.2	IR
3-in #4 7.2	3123.62	0.67	103.6	4.61	71.2	IR

<i>Specimen</i>	F_{breakage} (N)	δ_{failure} (mm)	σ_f (MPa)	t_{failure} (s)	σ_{f,eq} (MPa)	Origin
3-in #4 8.2	3926.68	0.94	129.8	5.41	90.9	IR
3-in #3 1.3	2671.56	0.69	89.5	4.30	60.7	IR
3-in #3 2.3	1544.97	0.44	51.8	2.54	32.7	IR
3-in #3 3.3	3118.91	0.81	104.5	4.52	71.6	OR
3-in #3 4.3	3365.71	0.88	112.5	4.84	77.6	OR
3-in #3 5.3	2362.32	0.78	78.7	3.98	52.8	IR
3-in #3 6.3	2479.65	0.68	82.6	3.60	55.2	IR
3-in #3 7.3	2075.24	0.64	68.8	3.13	45.0	IR
3-in #3 8.3	2434.86	0.65	80.1	3.48	53.3	IR
3-in #4 1.4	6007.22	1.33	201.0	7.48	145.1	LR
3-in #4 2.4	3393.02	0.85	113.8	5.80	79.7	LR
3-in #4 3.4	3271.51	0.85	109.6	5.04	76.0	IR
3-in #4 4.4	2945.81	0.76	98.4	5.02	67.9	OR
3-in #4 5.4	6259.23	1.31	208.9	8.00	151.6	OR
3-in #4 6.4	8189.99	1.60	272.6	9.83	201.3	ND
3-in #4 7.4	7199.07	1.46	238.7	9.04	174.9	OR
3-in #4 8.4	4655.35	1.09	153.7	7.26	110.2	OR
4-out #1 1.1	5395.99	0.60	77.0	5.59	51.9	OR
4-out #1 2.1	5156.86	0.51	73.3	5.64	49.2	OR
4-out #1 3.1	4616.66	0.55	65.6	5.51	43.6	IR
4-out #1 4.1	5427.55	0.53	77.0	5.90	52.0	IR
4-out #1 5.1	6037.91	0.57	85.5	6.27	58.4	IR
4-out #1 6.1	6129.09	0.65	86.8	6.72	59.6	IR
4-out #1 7.1	7068.00	0.73	99.5	7.58	69.5	IR
4-out #1 8.1	4910.02	0.46	68.9	5.72	46.1	IR
4-out #1 9.1	8070.79	0.69	113.0	8.18	79.8	IR
4-out #2 1.2	6574.41	0.66	93.9	6.86	65.3	IR
4-out #2 2.2	9651.95	0.84	137.7	9.12	99.1	IR
4-out #2 3.2	9467.59	1.44	134.7	10.42	97.7	OR
4-out #2 4.2	6128.90	0.55	87.0	6.43	59.9	LR
4-out #2 5.2	10060.03	0.81	142.8	9.50	103.1	OR
4-out #2 6.2	8967.35	0.78	126.7	8.13	90.2	LR
4-out #2 7.2	6244.45	0.57	87.9	6.60	60.7	IR
4-out #2 8.2	7822.76	0.74	109.7	7.69	77.4	OR
4-out #2 9.2	7561.29	0.77	105.8	7.85	74.6	IR
4-out #1 1.3	8138.05	0.70	116.2	7.69	81.8	IR
4-out #1 2.3	6798.34	0.61	97.0	6.56	67.0	IR
4-out #1 3.3	4788.58	0.58	68.2	5.20	45.2	IR
4-out #1 4.3	7538.77	0.74	107.0	6.93	74.5	IR
4-out #1 5.3	8213.65	0.81	116.6	8.60	82.7	OR
4-out #1 6.3	6247.78	0.54	88.4	6.36	60.6	LR
4-out #1 7.3	6761.67	0.57	95.2	6.83	65.9	IR
4-out #1 8.3	5159.22	0.52	72.4	5.35	48.4	IR
4-out #1 9.3	6836.67	0.70	95.7	6.97	66.3	IR
4-out #2 1.4	7366.58	0.68	105.1	7.18	73.6	LR
4-out #2 2.4	12341.82	1.04	175.6	10.71	128.6	OR
4-out #2 3.4	12036.53	0.96	171.1	10.82	125.3	OR
4-out #2 4.4	10492.21	0.86	148.8	9.86	107.9	OR
4-out #2 5.4	8183.34	0.74	115.9	7.35	81.7	LR
4-out #2 6.4	13704.74	1.01	193.3	11.41	142.5	IR
4-out #2 7.4	8466.64	0.81	119.2	8.58	85.0	IR
4-out #2 8.4	8145.76	0.79	114.2	8.21	81.1	IR
4-out #2 9.4	5813.71	0.54	81.4	6.07	55.6	IR

Specimen	F_{breakage} (N)	δ_{failure} (mm)	σ_f (MPa)	t_{failure} (s)	σ_{f,eq} (MPa)	Origin
4-in #3 1.1	1808.10	0.54	58.5	3.34	38.4	IR
4-in #3 2.1	4948.67	1.03	160.1	6.40	114.0	LR
4-in #3 3.1	3783.29	0.91	122.7	5.69	86.2	IR
4-in #3 4.1	4307.80	1.00	139.3	6.28	98.8	LR
4-in #3 5.1	1705.81	0.52	55.2	3.08	35.9	IR
4-in #3 6.1	4682.34	1.12	151.2	6.52	107.8	IR
4-in #3 7.1	5096.06	1.25	164.6	7.46	118.5	OR
4-in #3 8.1			<i>Not available</i>			
4-in #3 9.1			<i>Not available</i>			
4-in #4 1.2	3370.83	0.83	109.5	5.31	76.1	IR
4-in #4 2.2	2648.56	0.77	85.9	4.24	58.3	IR
4-in #4 3.2	4128.53	1.08	134.1	5.96	94.5	OR
4-in #4 4.2	3091.58	0.91	100.4	5.04	69.4	IR
4-in #4 5.2	1968.58	0.63	63.6	3.55	42.0	IR
4-in #4 6.2	1560.51	0.49	50.3	2.72	32.1	IR
4-in #4 7.2			<i>Not available</i>			
4-in #4 8.2	4754.82	1.14	153.2	6.70	109.2	IR
4-in #4 9.2	4445.96	1.02	143.6	6.46	102.0	OR
4-in #3 1.3			<i>Not available</i>			
4-in #3 2.3	2568.89	0.70	83.1	4.31	56.5	IR
4-in #3 3.3	4850.46	1.12	156.7	6.59	111.8	IR
4-in #3 4.3	6530.19	1.43	211.2	8.60	154.2	OR
4-in #3 5.3	5222.78	1.35	168.7	7.74	121.8	IR
4-in #3 6.3			<i>Not available</i>			
4-in #3 7.3	2046.77	0.58	66.2	3.76	44.1	IR
4-in #3 8.3	2311.97	0.71	74.4	3.96	50.0	IR
4-in #3 9.3	2469.61	0.56	79.8	3.84	53.7	IR
4-in #4 1.4	2125.18	0.62	68.4	3.48	45.3	IR
4-in #4 2.4	3040.07	0.74	98.3	4.51	67.4	IR
4-in #4 3.4	1759.42	0.50	57.2	3.13	37.2	LR
4-in #4 4.4	3587.72	0.96	116.8	5.36	81.5	IR
4-in #4 5.4			<i>Not available</i>			
4-in #4 6.4	2507.17	0.73	81.5	4.32	55.3	IR
4-in #4 7.4	2670.11	0.77	86.6	4.06	58.6	IR
4-in #4 8.4	1646.83	0.44	53.5	3.04	34.5	IR
4-in #4 9.4	3899.95	1.03	126.6	5.50	88.7	IR
5-out #1 1.1	5463.90	0.52	76.2	5.38	51.4	IR
5-out #1 2.1	3851.01	0.50	53.9	4.58	35.0	IR
5-out #1 3.1	7077.97	0.71	99.5	6.63	69.1	OR
5-out #1 4.1	4951.84	0.59	69.7	5.66	46.9	IR
5-out #1 5.1	5363.21	0.65	75.8	5.70	51.3	IR
5-out #1 6.1	5511.58	0.63	78.1	5.83	53.1	IR
5-out #1 7.1	4200.04	0.47	59.6	4.59	39.1	IR
5-out #2 1.2	5609.07	0.62	78.5	5.66	53.0	LR
5-out #2 2.2	8288.32	1.24	116.4	8.23	82.5	IR
5-out #2 3.2	12514.14	1.04	176.5	11.22	129.5	IR
5-out #2 4.2	5390.27	0.57	76.0	6.35	51.7	IR
5-out #2 5.2	11537.60	0.89	163.5	9.80	118.6	OR
5-out #2 6.2	9143.82	0.88	129.8	8.97	92.9	IR
5-out #2 7.2	7022.57	0.73	100.0	7.12	69.7	IR
5-out #1 1.3	5678.16	0.57	79.3	5.92	54.0	IR
5-out #1 2.3	4949.42	0.82	69.6	4.36	46.0	IR
5-out #1 3.3	7443.77	0.67	105.0	6.98	73.4	IR

Specimen	F_{breakage} (N)	δ_{failure} (mm)	σ_f (MPa)	t_{failure} (s)	σ_{f,eq} (MPa)	Origin
5-out #1 4.3	7377.60	0.81	104.4	7.49	73.3	LR
5-out #1 5.3	6510.16	0.62	92.4	6.40	63.8	IR
5-out #1 6.3	6708.64	0.80	95.4	6.93	66.3	IR
5-out #1 7.3	5653.87	0.73	80.4	5.65	54.6	IR
5-out #2 1.4	5175.57	0.65	72.4	5.71	48.7	IR
5-out #2 2.4	6729.01	0.73	94.4	6.76	65.3	IR
5-out #2 3.4	7524.31	0.78	105.9	6.83	73.8	IR
5-out #2 4.4	7987.54	0.72	112.8	7.50	79.3	IR
5-out #2 5.4	2752.75	0.58	38.9	3.98	23.8	IR
5-out #2 6.4	3644.26	0.55	51.7	3.57	32.6	IR
5-out #2 7.4	2850.64	0.43	40.5	3.46	24.7	IR
5-in #3 1.1	2911.56	0.82	94.5	4.24	64.3	IR
5-in #3 2.1	4398.80	1.16	142.8	6.18	101.0	IR
5-in #3 3.1	9127.24	1.85	295.9	10.75	219.8	IR
5-in #3 4.1	8227.89	1.68	267.2	10.29	197.6	IR
5-in #3 5.1	5964.46	1.33	193.0	8.08	139.8	OR
5-in #3 6.1	6392.82	1.37	206.9	8.27	150.3	IR
5-in #3 7.1	3060.97	0.82	98.9	4.80	67.9	IR
5-in #4 1.2	2402.90	0.75	77.9	5.00	53.2	LR
5-in #4 2.2	3677.16	1.01	119.1	5.30	83.0	OR
5-in #4 3.2	2645.31	0.84	85.7	4.34	58.2	IR
5-in #4 4.2	2224.24	0.70	72.0	3.62	47.9	IR
5-in #4 5.2	1715.97	0.76	55.4	3.40	36.1	IR
5-in #4 6.2	1138.81	0.29	36.7	2.08	22.2	IR
5-in #4 7.2	3334.84	0.91	107.7	4.98	74.5	IR
5-in #3 1.3	4839.00	1.20	155.8	6.91	111.2	OR
5-in #3 2.3	6640.32	1.48	213.9	8.52	155.8	IR
5-in #3 3.3	5067.30	1.24	163.5	7.06	117.0	IR
5-in #3 4.3	3870.79	1.17	125.0	5.62	87.5	IR
5-in #3 5.3	10095.29	1.92	326.1	11.58	243.7	IR
5-in #3 6.3	5939.07	1.33	191.6	8.44	139.2	OR
5-in #3 7.3	3023.91	0.95	97.7	5.12	67.3	IR
5-in #4 1.4	2166.50	0.77	70.0	3.76	46.6	IR
5-in #4 2.4	1995.48	0.75	64.2	3.50	42.4	IR
5-in #4 3.4	2322.77	0.89	74.9	4.58	50.7	IR
5-in #4 4.4	4898.23	1.15	158.2	6.56	112.7	LR
5-in #4 5.4	3944.75	0.99	127.2	5.84	89.4	IR
5-in #4 6.4	4055.99	1.12	130.8	6.18	92.4	IR
5-in #4 7.4	2690.22	0.85	86.3	4.46	58.8	IR
6-out #1 1.1	8108.37	0.84	112.4	7.66	79.2	LR
6-out #1 2.1	9393.35	0.90	130.4	8.99	93.4	IR
6-out #1 3.1	6186.69	0.70	85.9	6.76	59.2	IR
6-out #1 4.1	12983.31	1.12	180.0	11.40	132.4	IR
6-out #1 5.1	4723.00	0.52	65.6	5.47	43.7	IR
6-out #1 6.1	5482.32	0.62	76.1	5.62	51.4	IR
6-out #1 7.1	2909.27	0.38	40.4	3.39	24.7	IR
6-out #2 1.2	5524.12	0.64	76.8	5.22	51.6	IR
6-out #2 2.2	7617.68	0.88	105.9	7.03	74.0	OR
6-out #2 3.2	6829.96	0.70	95.1	6.91	66.0	IR
6-out #2 4.2	4268.94	0.60	59.4	5.41	39.2	IR
6-out #2 5.2	6728.61	0.71	93.7	6.52	64.7	IR
6-out #2 6.2	6445.63	0.71	89.7	6.33	61.7	IR
6-out #2 7.2	6390.19	0.69	88.9	6.44	61.2	IR

<i>Specimen</i>	F_{breakage} (N)	δ_{failure} (mm)	σ_f (MPa)	t_{failure} (s)	σ_{f,eq} (MPa)	Origin
6-out #1 1.3	10113.08	0.95	141.0	9.32	101.6	OR
6-out #1 2.3	9125.34	0.88	127.5	8.92	91.3	IR
6-out #1 3.3	6343.64	0.67	88.6	6.42	61.0	IR
6-out #1 4.3	10525.48	0.93	147.2	9.17	106.1	IR
6-out #1 5.3	5718.89	0.69	80.0	6.28	54.6	IR
6-out #1 6.3	4352.66	0.49	60.9	4.77	40.0	IR
6-out #1 7.3	2435.68	0.49	34.1	3.78	20.5	IR
6-out #2 1.4	4968.60	0.65	69.6	5.15	46.4	IR
6-out #2 2.4	6520.04	0.78	91.3	6.77	63.1	IR
6-out #2 3.4	6282.00	0.84	88.1	7.16	61.0	LR
6-out #2 4.4	4650.03	0.69	65.2	5.79	43.6	LR
6-out #2 5.4	2095.68	0.42	29.4	2.95	16.8	IR
6-out #2 6.4	4652.65	0.64	65.2	4.94	43.1	LR
6-out #2 7.4	4521.24	0.60	63.4	5.57	42.2	OR
6-in #3 1.1	8815.35	0.51	68.8	7.87	46.2	IR
6-in #3 2.1	8684.42	0.57	67.0	7.83	44.9	IR
6-in #3 3.1	10094.40	0.56	78.1	8.49	53.3	IR
6-in #3 4.1	9387.58	0.56	72.8	8.54	49.4	IR
6-in #3 5.1	9589.01	0.55	74.8	8.08	50.7	LR
6-in #3 6.1	10670.53	0.67	83.6	9.40	57.8	LR
6-in #3 7.1	9891.30	0.65	77.7	9.70	53.5	IR
6-in #4 1.2	12450.86	0.64	97.1	10.27	68.3	OR
6-in #4 2.2	16813.88	0.75	129.9	12.04	93.9	LR
6-in #4 3.2	6673.86	0.48	51.6	6.56	33.1	IR
6-in #4 4.2	8782.09	0.53	68.1	8.35	46.0	LR
6-in #4 5.2	10961.31	0.61	85.4	8.45	58.8	IR
6-in #4 6.2	11884.50	0.62	93.0	10.14	65.2	IR
6-in #4 7.2	6360.54	0.42	49.9	6.40	31.8	IR
6-in #3 1.3	7911.44	0.47	61.6	6.73	40.4	IR
6-in #3 2.3	8912.25	0.61	68.8	8.40	46.4	IR
6-in #3 3.3	9543.00	0.62	73.7	9.05	50.3	IR
6-in #3 4.3	13715.65	0.69	106.3	10.20	75.1	IR
6-in #3 5.3	13197.77	0.67	102.7	11.11	72.9	IR
6-in #3 6.3	11282.70	0.67	88.3	9.92	61.5	LR
6-in #3 7.3	9034.05	0.55	70.8	7.91	47.7	IR
6-in #4 1.4	12060.50	0.61	94.1	9.39	65.7	IR
6-in #4 2.4	8995.00	0.59	69.7	8.45	47.1	IR
6-in #4 3.4	7102.40	0.52	54.9	6.94	35.7	IR
6-in #4 4.4	11057.16	0.63	85.6	8.72	59.1	OR
6-in #4 5.4	11206.09	0.63	87.3	9.35	60.6	LR
6-in #4 6.4	10579.45	0.58	82.9	9.46	57.3	IR
6-in #4 7.4	13200.84	0.60	103.5	9.36	72.7	OR

Appendix H

Characteristic and design strengths (load duration of 5 seconds)

Figure 102 to Figure 107 show some additional graphs where the characteristic and design strength is determined for a load duration of 5 seconds, instead of the commonly used 60 seconds.

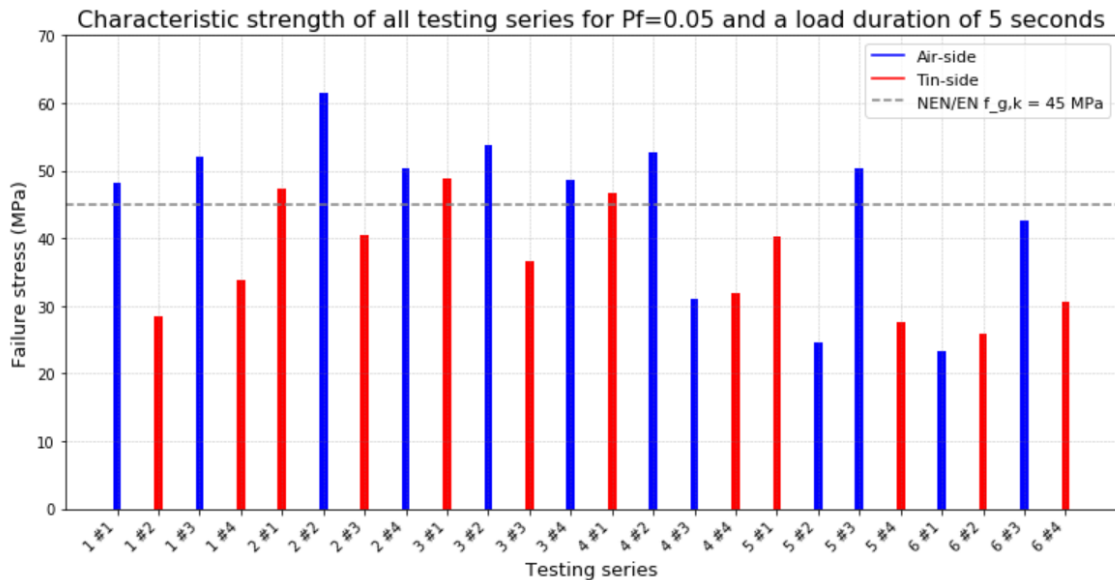


Figure 102. Characteristic strength of all series for $P_f=0.05$ and load duration of 5 seconds.

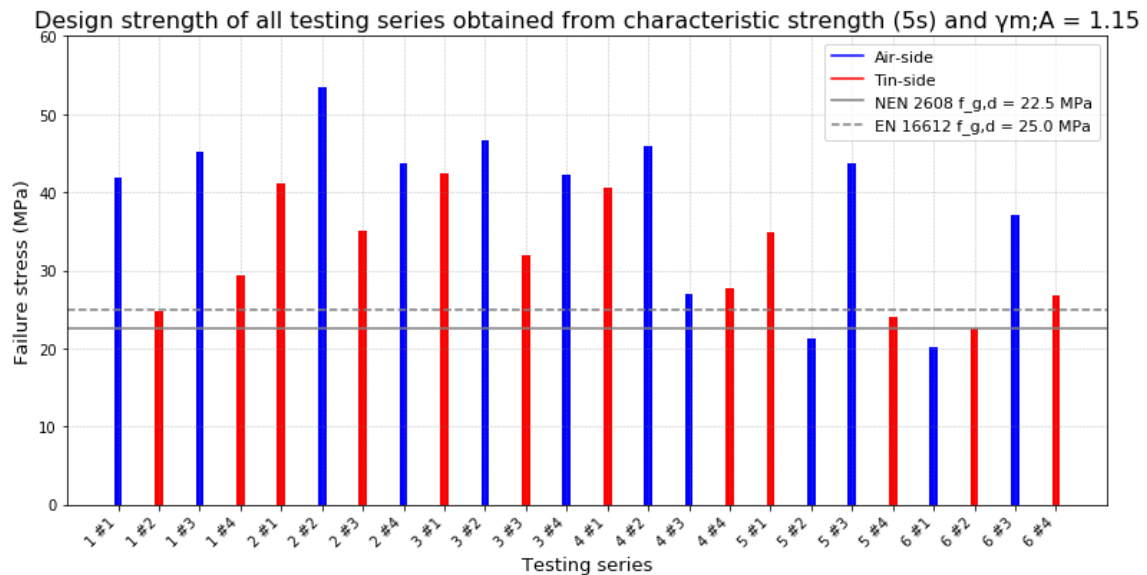


Figure 103. Design strength of all series obtained from the characteristic strength with $\gamma_{m;A} = 1.15$ and load duration of 5 seconds.

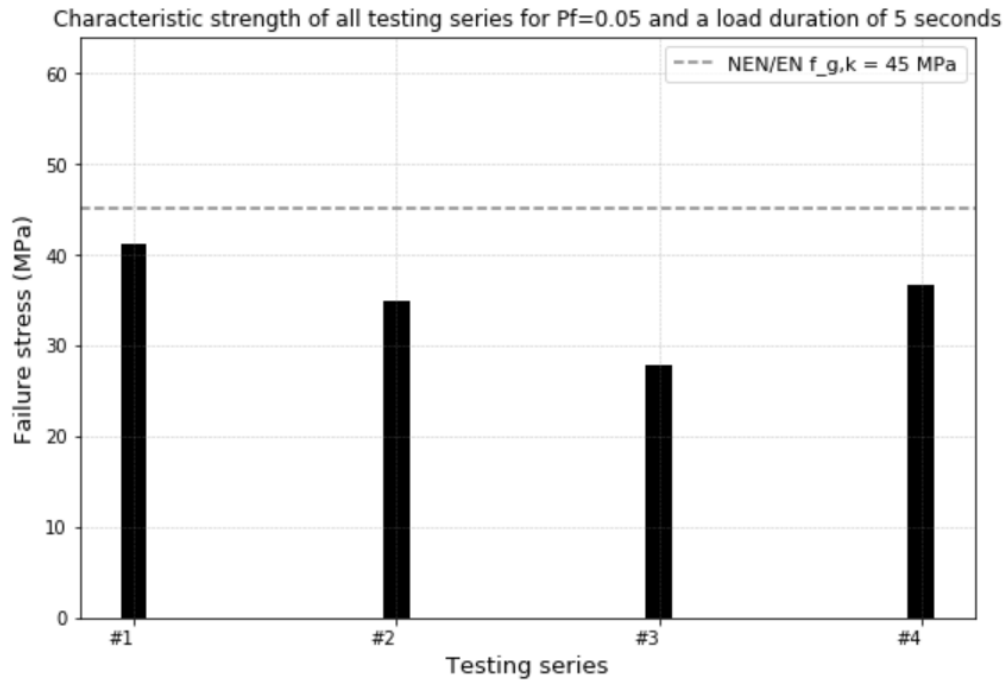


Figure 104. Characteristic strength of all sides for $P_f=0.05$ and load duration of 5 seconds.

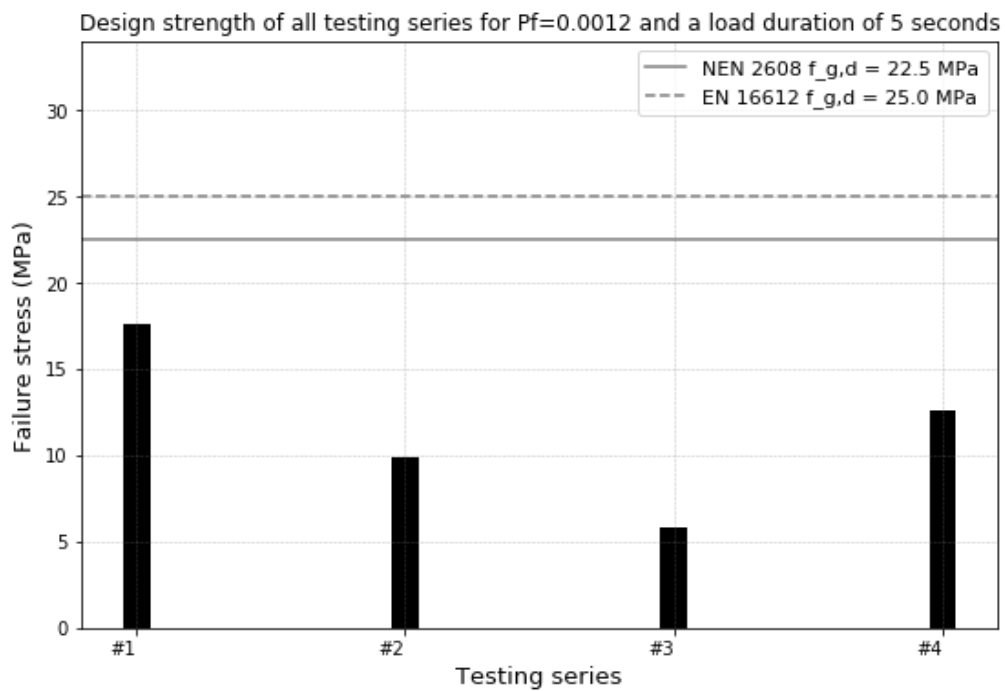


Figure 105. Design strength of all sides for $P_f=0.0012$ and load duration of 5 seconds.

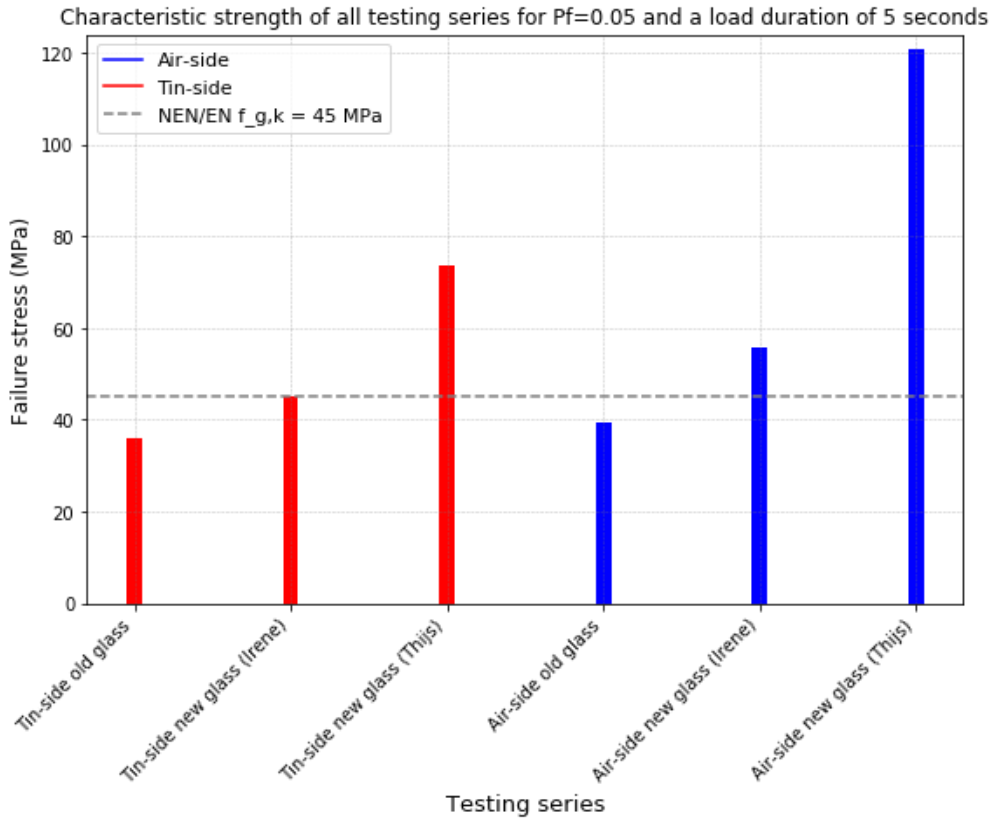


Figure 106. Characteristic strength new and old glass for $P_f=0.05$ and load duration of 5 seconds.

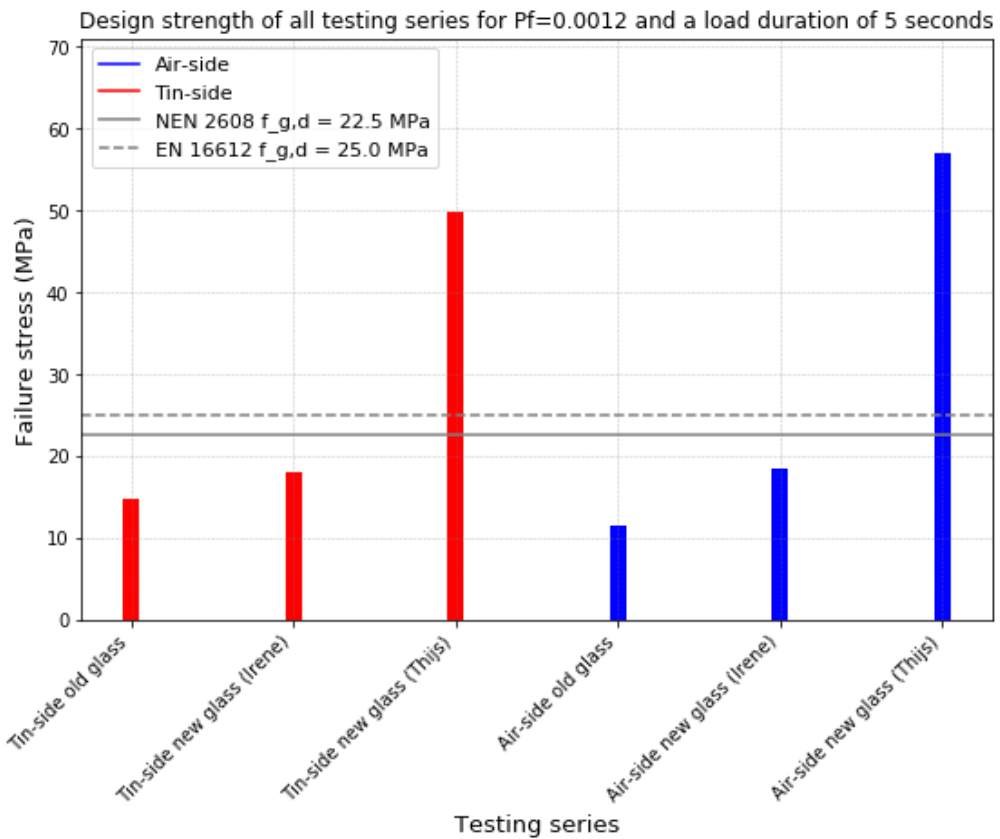


Figure 107. Design strength new and old glass for $P_f=0.0012$ and load duration of 5 seconds.

Appendix I

Normal distribution values

Table 39 to Table 42 shows for the four different sides what the values of $\sigma_{f,0.008}$, $\sigma_{f,0.05}$ and $\sigma_{f,0.5}$ of both the 2PW distribution and the normal distribution are. A distinction was also made between all specimens, those tested on air-side, and those tested on tin-side. All values were determined with a load duration of 60 seconds.

Table 39. 2PW and Normal distribution – Side #1

<i>Side</i>		#1		
		$\sigma_{f,0.008}$ (MPa)	$\sigma_{f,0.05}$ (MPa)	$\sigma_{f,0.5}$ (MPa)
All specimens	2PW	24.1	34.7	62.7
	Normal	20.8	33.9	62.2
Air-side specimens	2PW	18.3	32.0	67.3
	Normal	10.6	28.0	65.5
Tin-side specimens	2PW	27.2	38.0	61.2
	Normal	29.1	39.0	60.4

Table 40. 2PW and Normal distribution – Side #2

<i>Side</i>		#2		
		$\sigma_{f,0.008}$ (MPa)	$\sigma_{f,0.05}$ (MPa)	$\sigma_{f,0.5}$ (MPa)
All specimens	2PW	12.4	23.7	69.7
	Normal	-0.6	22.1	71.0
Air-side specimens	2PW	15.1	30.6	81.3
	Normal	8.8	31.7	81.1
Tin-side specimens	2PW	17.5	28.2	52.0
	Normal	10.7	23.7	51.9

Table 41. 2PW and Normal distribution – Side #3

<i>Side</i>		#3		
		$\sigma_{f,0.008}$ (MPa)	$\sigma_{f,0.05}$ (MPa)	$\sigma_{f,0.5}$ (MPa)
All specimens	2PW	15.9	27.0	65.5
	Normal	-26.2	5.2	72.6
Air-side specimens	2PW	14.6	29.1	80.7
	Normal	-21.9	13.3	89.0
Tin-side specimens	2PW	23.9	31.7	49.4
	Normal	27.3	34.1	48.7

Table 42. 2PW and Normal distribution – Side #4

<i>Side</i>		#4		
		$\sigma_{f,0.008}$ (MPa)	$\sigma_{f,0.05}$ (MPa)	$\sigma_{f,0.5}$ (MPa)
All specimens	2PW	16.8	27.2	63.1
	Normal	9.9	27.5	65.2
Air-side specimens	2PW	31.3	45.6	73.9
	Normal	24.4	40.5	75.1
Tin-side specimens	2PW	11.8	24.0	59.1
	Normal	6.8	23.8	60.4